

2018

THE DEVELOPMENT AND MECHANISTIC STUDY OF DUAL H-BONDING ORGANIC CATALYSTS FOR THE ROP OF CYCLIC ESTERS

Kurt Fastnacht
University of Rhode Island, fastnachtk@uri.edu

Follow this and additional works at: https://digitalcommons.uri.edu/oa_diss

Terms of Use

All rights reserved under copyright.

Recommended Citation

Fastnacht, Kurt, "THE DEVELOPMENT AND MECHANISTIC STUDY OF DUAL H-BONDING ORGANIC CATALYSTS FOR THE ROP OF CYCLIC ESTERS" (2018). *Open Access Dissertations*. Paper 784.
https://digitalcommons.uri.edu/oa_diss/784

This Dissertation is brought to you by the University of Rhode Island. It has been accepted for inclusion in Open Access Dissertations by an authorized administrator of DigitalCommons@URI. For more information, please contact digitalcommons-group@uri.edu. For permission to reuse copyrighted content, contact the author directly.

THE DEVELOPMENT AND MECHANISTIC STUDY OF DUAL H-BONDING
ORGANIC CATALYSTS FOR THE ROP OF CYCLIC ESTERS

BY:

KURT V. FASTNACHT

A DISSERTATION IN PARTIAL FULFILLMENT OF THE REQUIREMENTS FOR

THE DEGREE OF DOCTOR OF PHILOSOPHY

IN

ORGANIC CHEMISTRY

UNIVERSITY OF RHODE ISLAND

2018

DOCTOR OF PHILOSOPHY DISSERTATION

OF

KURT FASTNACHT

APPROVED:

Dissertation Committee:

Major Professor Matthew Kiesewetter

Brenton Deboef

Bongsup Cho

Stephen Kennedy

Jason Dwyer

Nasser Z. Zawia

DEAN OF THE GRADUATE SCHOOL

UNIVERSITY OF RHODE ISLAND

2018

ABSTRACT

Organic catalysis for the Ring Opening Polymerization (ROP) of cyclic monomers is a rapidly emerging field of study that gained interest in 2005 with the advent of dual H-bonding catalysts. Synthesizing catalysts that produce fast reaction rates with superior reaction control over molecular weight (M_n) and molecular weight distributions (M_w/M_n) are of great interest for material applications. Current organic catalysts do not have the capabilities to satisfy these requirements, limiting the feasibility to pursue commercial scale applications.

Analysis of polymerizations is done using a number of techniques. Nuclear Magnetic Resonance (NMR) is a power spectroscopy technique used to evaluate reaction progression for polymerization reactions. Through reaction conversions, the kinetics of each catalyst can be measured and compared with one another. Through NMR titration experiments, binding studies were used to compare and in some cases quantify the interactions between monomer and alcohol/chain end with the catalyst and cocatalysts respectively.

Gel Permeation Chromatography (GPC) is another technique used for the analysis of polymers, which allows for the determination of the polymer molecular weight (M_n) and molecular weight distribution (M_w/M_n). The catalyst chosen to perform the ROP of monomer has a large impact on the control over the M_n and M_w/M_n . This method allows for the determination of polymer M_n and M_w/M_n , which translate to reaction control.

Organic catalysis for the Ring Opening Polymerization (ROP) of cyclic monomers is a rapidly emerging field of study that gained interest in 2005 with the

advent of dual H-bonding catalysts. Synthesizing catalysts that produce fast reaction rates with superior reaction control over M_n and M_w/M_n are of great interest for material applications. Current organic catalysts do not have the capabilities to satisfy both requirements limiting the feasibility to pursue commercial scale applications. First, a review of H-bonding organic catalysts and their relative reactivity will be discussed.

The polymerization of cyclic esters by H-bonding (thio)urea has greatly increased since the first iterations of catalyst scaffolds. The incorporation of multi-armed H-bond donating species saw drastic increases in reaction rate. The incorporation of an oxygen (urea) in substitution of a sulfur (thiourea) saw an increase for all H-bond donors tested. These reactions also remained well controlled.

These catalysts have been shown to be tolerant of solvent free polymerizations. The adoption of solvent free reactions is greatly valued by the commercial industry. Solvent free conditions allowed for the polymerization of several copolymers that were not possible through reactions within solvent.

H-bonding (thio)urea catalysts used for the ROP of caprolactone were subjected to elevated temperatures (22-110°C). **1-O** and **2-O** produced linear Eyring plots out to 110°C (highest temperature evaluated). All other catalysts deviated from linearity at 80°C, due to decomposition of the H-bonding species. A switch to polar solvent alleviated decomposition for some H-bond donors while other remained curved. A mechanistic reasoning will be discussed.

The introduction of a chiral architecture into the catalyst scaffold made kinetic resolution of racemic lactide possible. This chiral scaffold was responsible for an increase in isotacticity (P_m) of the resulting polymer. Multi armed chiral H-bond donors saw

increase reaction rates but only small increase in P_m value versus mono-armed H-bond donors. A decrease in reaction temperature produced enhanced the P_m values.

A new class of bifunctional, quinone derived catalyst was developed for the ring-opening polymerization (ROP) of lactone monomers. Similar in architecture to other bifunctional catalysts, the quinone catalyst can activate monomer and alcohol/chain simultaneously. Attempts at ROP of both δ -valerolactone and L-lactide were unsuccessful. A mechanistic explanation is discussed.

H-bonding urea or thiourea catalyst paired with a base cocatalyst have been employed for organocatalytic ring-opening polymerization (ROP) of aliphatic lactones (TOSUO, 4-MCL, 3,5-MCL and 6-MCL). Random copolymers with low dispersities were synthesized. A series of copolymers of CL and 3,5-MCL were produced and evaluated using TGA and DSC. Variation of the substituent along with its position on the monomer resulted in a different reaction rates. The relative rates of ROP for functionalized ϵ -caprolactone (4-MCL, 3,5-MCL, 6-MCL, and TOSUO) by H-bonding organic catalysts have been evaluated and a mechanistic reasoning discussed. H-bonding organic catalysts saw increased reaction rates and control for all monomers versus both metal and enzymatic catalysts.

ACKNOWLEDGEMENTS

I would like to thank my Ph.D. advisor, Dr. Matthew Kieseewetter, for all his support, time and wisdom. You have really made my time at the University of Rhode Island worth more than just a degree. I would also like to thank my committee members for their support through this process.

I would also like to thank the chemistry graduate community at the University of Rhode Island for all the support.

I would like to thank my mentors from before my time at URI who encouraged me to pursue a Ph.D.

I would also like to thank my family and friends who have supported me during this process.

-Kurt Fastnacht

PREFACE

This dissertation is written in Manuscript Format.

Chapter 1 presents a literature chapter pertaining to the field of H-bonding organic catalysts used for the ring-opening polymerization of cyclic esters. This chapter evaluates the many types, both dual and bifunctional systems, for reaction kinetics and control. This chapter was written as part of a submitted book chapter. (Publishing, expected 2018, Fastnacht, K.V.; Datta, P.P.; Kieseewetter, M.K. *Supramolecular Catalysts Organic Catalysis for Polymerisation*, Eds. Andrew Dove, Haritz Sardon, Stefan Naumann. RSC).

Chapter 2 explores the catalyst structure and heteroatom significance on polymerization rates and control. The development of multi H-bonding (thio)ureas paired with strong organic bases resulted in the rapid turnover of δ -valerolactone and ϵ -caprolactone. Sam Spink preformed all experiments on ϵ -caprolactone. Nayanthara U. Dharmaratne and Jinal U. Pothupitiya performed the transesterification experiments. Partha P. Datta was responsible for binding studies. (See publication: Fastnacht, K. V.; Spink, S. S.; Dharmaratne, N. U.; Pothupitiya, J. U.; Datta, P. P.; Kieseewetter, E. T.; Kieseewetter, M. K. “Bis- and Tris-Urea H-Bond Donors for Ring-Opening Polymerization: Unprecedented Activity and Control from an Organocatalyst” *ACS Macro Lett.* **2016**, *5*, 982–986).

Chapter 3 probes the possibility of the kinetic resolution of racemic lactide using chiral H-bonding catalysts paired with an alkyl amine base. This work details the development of chiral multi H-bond donors to control the resulting microstructure of the

polymer chain. All synthesis and experiments were performed by myself. This chapter includes unpublished results.

Chapter 4 examines the solvent free polymerization of δ -valerolactone and L-lactide. Through bulk conditions we were able to produce copolymers not accessible in solution and produce high isotactic PLA. This chapter highlights the effectiveness of a commercially available H-bond donor. Danielle N. Coderre and I are responsible for the polymerization reactions in solvent. Nayanthara U. Dharmaratne, Jinal U. Pothupitiya and Terra M. Jouaneh are responsible for solvent free polymerizations and other experiments. (See publication. Jinal U. Pothupitiya, Nayanthara U. Dharmaratne, Terra Marie M. Jouaneh, Kurt V. Fastnacht, Danielle N. Coderre, and Matthew K. Kiesewetter. “H-Bonding Organocatalysts for the Living, Solvent-Free Ring-Opening Polymerization of Lactones: Toward an All-Lactones, All-Conditions Approach” *Macromolecules* **2017** 50 (22), 8948-8954)

Chapter 5 explores higher temperature reactions for H-bonding organic catalysts. The work evaluates a host of donors and reports their relative Arrhenius behavior. Transition state thermodynamic values were calculated. A mechanistic evaluation of the results has been discussed. Thomas Wright helped with polymerizations in polar solvent. Danielle N. Coderre and I are responsible for all polymerizations in non-polar and some in polar solvents. All other experiments were done by us as well. This chapter includes unpublished results.

Chapter 6 indicates the possibility of a new type of bifunctional catalyst derived from a quinoidal (thio)urea. This chapter evaluates the interactions between catalyst and monomer/chain end. All synthesis and binding experiments were done by myself.

Danielle N. Coderre and I are responsible for the polymerization reactions. This chapter includes unpublished results.

Chapter 7 assesses the catalytic activity of (thio)urea H-bonding catalysts for the ring-opening polymerization of aliphatic cyclic esters. All monomers are derived from ϵ -caprolactone but produce vastly different reaction kinetics. A mechanistic discussion will elucidate the variation in kinetics and control of each monomer and their substitutions. Thomas Wright performed polymerizations for molecular weight data. Danielle N. Coderre and I performed all polymerization reactions and all other experiments. This chapter includes unpublished results.

TABLE OF CONTENTS

ABSTRACT.....	ii
ACKNOWLEDGEMENTS.....	v
PREFACE.....	vi
TABLE OF CONTENTS.....	ix
LIST OF TABLE.....	x
LIST OF FIGURES.....	xii
LIST OF SCHEMES.....	xxvi
CHAPTER 1.....	1
CHAPTER 2.....	51
CHAPTER 3.....	107
CHAPTER 4.....	133
CHAPTER 5.....	180
CHAPTER 6.....	227
CHAPTER 7.....	259

LIST OF TABLES

Table	Page
Table 2.1. MTBD and bis- or tris thiourea Catalyzed ROP of VL and CL.....	72
Table 2.2. Bis- and Tris-urea Cocatalyzed ROP of Lactones.....	73
Table 2.3. Transesterification of Ethyl Acetate.....	74
Table 2.4. Low 3-O /MTBD Cocatalyst Loadings in the ROP of VL.....	74
Table 2.5. Solvent Screen in the 3-O /MTBD Cocatalyzed ROP of VL.....	75
Table 2.6. Post-polymerization Transesterification in 3-O /MTBD Cocatalyzed ROP....	75
Table 3.1. Mono-chiral thioureas for the kinetic resolution ROP of <i>rac</i> -lactide.....	123
Table 3.2. Chiral multi-H-bond donor catalysts used for the stereocontrolled ROP of <i>rac</i> -lactide.....	124
Table 4.1. TCC plus base cocatalyzed ROP of VL.....	157
Table 4.2. H-bond Donor Plus Base Cocatalyzed ROP of VL.....	158
Table 4.3. TCC plus base cocatalyzed ROP of macrolactones.....	159
Table 4.4. H-bond Mediated Solvent-free ROP of L-LA.....	160
Table 4.5. Solvent free ROP of VL with TCC/BEMP.....	161
Table 4.6. TCC plus MTBD or BEMP cocatalyzed ROP of CL.....	162
Table 4.7. Base Screen in the 2-S Mediated ROP of L-LA.....	163
Table 5.1. Activation Parameters for H-bond Donor/MTBD Cocatalyzed ROP of CL.....	197
Table 5.2. Thermal decomposition of H-bond donors with and without MTBD.	198
Table 6.1. Table shows the results of various polymerization attempts using 5b for δ -VL and L-LA.....	245
Table 7.1. Cocatalysts for the ROP of functionalized ϵ -Caprolactone.....	275

Table 7.2. Decomposition onset temperatures for homo and copolymers.....276

LIST OF FIGURES

FIGURE	PAGE
Figure 1.1. The Takemoto catalyst was the inspiration for the popular thiourea plus base catalyst system. Weaker base cocatalysts effect the ROP of lactide, while stronger bases open other monomers.....	45
Figure 1.2. Functionalizable monomers which undergo controlled ROP by 2 /base.....	45
Figure 1.3. Squaramide H-bond Donors for ROP of Lactide.	46
Figure 1.4. Internal Lewis Acid Stabilized (Thio)ureas for ROP.	46
Figure 1.5. Sulfonamide H-bonding Catalysts.....	46
Figure 1.6. Diphenyl Phosphate, Phosphoramidic and Imidodiphosphoric Acid Catalyzed ROP.....	47
Figure 1.7. Phenol and Benzylic Alcohol H-bond Donors for ROP.....	47
Figure 1.8. Azaphosphatrane H-bond Donor.....	47
Figure 1.9. Electrophilic Monomer Activation by Stable Cations.....	48
Figure 1.10. Bronsted Acid and Base Cocatalysts for ROP.....	48
Figure 1.11. Ammonium Betaine Mediated ROP.....	48
Figure 1.12. Thiazoline and Oxazoline Bifunctional Catalysts.....	49
Figure 2.1. Base and (thio)urea cocatalysts evaluated for ROP.....	78
Figure 2.2. M_n vs conversion for the 2-S /MTBD catalyzed ROP of VL.....	78
Figure 2.3. First order evolution of [VL] vs time for the 2-S /MTBD catalyzed ROP of VL.....	79
Figure 2.4. M_n vs $[VL]_0/[I]_0$ for the 2-S /MTBD catalyzed ROP of VL.....	79

Figure 2.5. GPC traces of the polymer resulting from the 2-S /MTBD (5 mol% each, 0.0499 mmol) cocatalyzed ROP and subsequent chain extension of VL (0.999 mmol, then 0.999 mmol more) from 1-pyrenebutanol (0.0199 mmol) in C ₆ D ₆ (999 μL).....	80
Figure 2.6. Observed rate constant (k_{obs} , min ⁻¹) vs [MTBD] in the 2-S /MTBD catalyzed ROP of VL.....	80
Figure 2.7. Observed rate constant (k_{obs} , h ⁻¹) vs [2-S] in the 2-S /MTBD catalyzed ROP of CL.....	81
Figure 2.8. M_n vs conversion of VL for the 3-O /MTBD catalyzed ROP of VL.....	81
Figure 2.9. First order evolution of [VL] vs time for the 3-O /MTBD catalyzed ROP of VL.....	82
Figure 2.10. M_n vs conversion for the 3-O /MTBD catalyzed ROP of CL.....	82
Figure 2.11. First order evolution of [CL] vs time for the 3-O /MTBD catalyzed ROP of CL.....	83
Figure 2.12. First order evolution of [CL] and [VL] vs time for the 3-O /MTBD catalyzed copolymerization of CL.....	83
Figure 2.13. GPC traces of the polymer resulting from the 3-O /MTBD (1.67 mol% each, 0.015 mmol) cocatalyzed ROP and subsequent chain extension of CL (0.876 mmol, then 1.1723 mmol more) from 1-pyrenebutanol (0.035 mmol) in C ₆ D ₆ (219 μL)	84
Figure 2.14. Observed rate constant (k_{obs} , min ⁻¹) vs [3-O] in the 3-O /MTBD catalyzed ROP of VL.....	84
Figure 2.15. DFT B3LYP//6-31G** geometry optimized structures of 3-S	85

Figure 2.16. DFT B3LYP//6-31G** geometry optimized structures of 3-O	85
Figure 2.17. MALDI-TOF of the PLA resulting from the 3-O /(tris[2-(dimethylamino)ethyl]amine) catalyzed ROP of L-LA.....	86
Figure 2.18. Downfield half of the ¹ H NMR spectra (acetone + trace benzene-d ₆ (lock), 400 MHz) of (upper) 1-O , (middle) 2-O , and (lower) 3-O . The progressive downfield shift of the NH protons is indicative of increased (2-O vs 3-O) intramolecular H-bonding.....	87
Figure 2.19. ¹ H NMR (300 MHz, DMSO-d ₆) of 2-O	88
Figure 2.20. ¹³ C NMR (75 MHz, DMSO-d ₆) of 2-O	89
Figure 2.21. ¹ H NMR (300 MHz, DMSO-d ₆) of 1-[3,5-bis(trifluoromethyl)phenyl thiourea]-3-aminopropane.....	90
Figure 2.22. ¹ H NMR (300 MHz, DMSO-d ₆) of 2-OS	91
Figure 2.23. ¹³ C NMR (75 MHz, acetone-d ₆) of 2-OS	92
Figure 2.24. ¹ H NMR (300 MHz, acetone-d ₆) of 3-O	93
Figure 2.25. ¹³ C NMR (75 MHz, acetone-d ₆) of 3-O	94
Figure 2.26. ¹ H NMR (300 MHz, acetone-d ₆) of 3-S	95
Figure 2.27. ¹³ C NMR (75 MHz, acetone-d ₆) of 3-S	96
Figure 3.1. Example of selectively decoupled ¹ H NMR of methine region of PLA. Left is before and right is after the selectively decoupled ¹ H NMR. (top image, 300MHz, CDCl ₃). Example curve fitting for stereo sequenced peaks (bottom image, 500MHz, CDCl ₃)	125
Figure 3.2. Chiral H-bonding catalysts developed for the kinetic resolution of <i>rac</i> -LA.....	126

Figure 3.3. ^1H NMR (300 MHz, CDCl_3) of <i>tert</i> -butyl-bis(2-aminoethyl)carbamate.....	127
Figure 3.4. ^1H NMR (300 MHz, $\text{DMSO}-d_6$) of 1,1'-(azanediylbis(ethane-2,1-diyl))bis(3-(3,5-bis(trifluoromethyl)phenyl)thiourea)	128
Figure 3.5. ^1H NMR (300 MHz, $\text{DMSO}-d_6$) of 1,1'-(azanediylbis(ethane-2,1-diyl))bis(3-(3,5-bis(trifluoromethyl)phenyl)urea)	129
Figure 3.6. ^1H NMR (300 MHz, C_6D_6) of 4	130
Figure 3.7. ^1H NMR (300 MHz, $\text{DMSO}-d_6$) of 5	131
Figure 4.1. (upper) First order evolution of [monomer] vs time and (lower) M_n and M_w/M_n vs conversion for the TCC/MTBD cocatalyzed ROP of VL.....	165
Figure 4.2. RI and UV GPC traces of the ROP initiated from pyrenebutanol for (top) PVL (TCC/BEMP) and (bottom) PLA (2-S /PMDTA)	166
Figure 4.3. (upper) First order evolution of [monomer] vs time; and (lower) M_n and M_w/M_n vs conversion for the TCC/BEMP cocatalyzed ROP of VL.....	167
Figure 4.4. (upper) First order evolution of [monomer] vs time and (lower) M_n and M_w/M_n vs conversion for the TCC/BEMP cocatalyzed ROP of CL.....	168
Figure 4.5. Percent conversion to polymer of VL solutions of MTBD, BEMP and TCC plus benzyl alcohol (0.5 mol%, 0.02 mmol for all catalysts) at (upper) - 10°C and (lower) room temperature. Conversions were determined via aliquot by ^1H NMR (CDCl_3)	169
Figure 4.6. Solvent-free ROP allows for the direct-from-monomer creation of a negative mold in seconds. Above, the hollow, PVL negative mold is of a polypropylene reaction vial.....	170

Figure 4.7. 400 MHz ^1H NOESY in acetone- d_6 of (upper) TCC/MTBD (0.05 mmol each), and (lower) TCC/BEMP (0.05 mmol each). 1-S /MTBD show no cross peaks in acetone- d_6 or C_6D_6 at 0.05 mmol.....	171
Figure 4.8. M_n and M_w/M_n vs conversion for the TCC/BEMP cocatalyzed ROP of EB.....	172
Figure 4.9. (upper) First order evolution of [LA] vs time, and (lower) M_n and M_w/M_n vs conversion.....	173
Figure 4.10. First order evolution of [LA] vs time for the 2-S /PMDTA (2.5 mol% each) cocatalyzed ROP from benzyl alcohol (1 mol%) in (upper) toluene at 50°C (0.25 M, 0.694 mmol), and (lower) CDCl_3 at 40°C (1 M, 0.694 mmol)	174
Figure 4.11. First order evolution of [VL] and [CL] vs time for the one-pot copolymerization catalyzed by TCC/BEMP.....	175
Figure 4.12. First order evolution of [monomer] vs time for the copolymerization of: (upper) VL and EB. (middle) CL and EB. (lower) VL and LA.....	176
Figure 4.13. ^1H and ^{13}C NMR (400 MHz ^1H , CDCl_3) of the poly(VL-co-CL-co-EB). ^1H NMR suggests a mole ratio of the monomers in the polymer to be 1:1 (VL+CL:EB)	177
Figure 4.14. First order evolution of [monomer] vs time for the copolymerization of VL and L-LA.....	178
Figure 4.15. Percentage conversion of EB vs time for the copolymerization of: VL, CL and EB.....	178
Figure 5.1. H-bonding and imidate mediated ROP of CL.....	199

Figure 5.2. Example Eyring plots for the ROP of CL from benzyl alcohol in toluene catalyzed by (upper) TCC /MTBD, and (lower) 2-O /MTBD.....	200
Figure 5.3. Eyring plot constructed from the observed first order rate constants for the 1-O /MTBD (0.0438 mmol each) cocatalyzed ROP of CL (0.876 mmol, 2M) from benzyl alcohol (0.00876 mmol) in toluene.....	201
Figure 5.4. Eyring plot constructed from the observed first order rate constants for the 1-S /MTBD (0.0438 mmol each) cocatalyzed ROP of CL (0.876 mmol, 2M) from benzyl alcohol (0.00876 mmol) in toluene.....	201
Figure 5.5. Eyring plot constructed from the observed first order rate constants for the 3-S /MTBD (0.0146 mmol each) cocatalyzed ROP of CL (0.876 mmol, 2M) from benzyl alcohol (0.00876 mmol) in toluene.....	202
Figure 5.6. Eyring plot constructed from the observed first order rate constants for the 3-O /MTBD (0.0146 mmol each) cocatalyzed ROP of CL (0.876 mmol, 2M) from benzyl alcohol (0.00876 mmol) in toluene.....	202
Figure 5.7. Eyring plot constructed from the linear portion of the observed first order rate constants for the 2-S /MTBD (0.0219 mmol each) cocatalyzed ROP of CL (0.876 mmol, 2M) from benzyl alcohol (0.00876 mmol) in toluene.....	203
Figure 5.8. (upper) Temperature drop ROP of CL (2M, 0.876 mmol) in toluene. (lower) ¹ H NMR (400 MHz, benzene- <i>d</i> ₆) of the ROP of CL (0.876 mmol, 2M), benzyl alcohol (0.00876 mmol), 1-S /MTBD (0.0438 mmol each)	204
Figure 5.9. Eyring plot constructed from the observed first order rate constants for the TCC /DBU (0.0438 mmol each) cocatalyzed ROP of CL (0.876 mmol, 2M) from benzyl alcohol (0.00876 mmol) in toluene.....	205

Figure 5.10. Eyring plot for the TCC/MTBD (0.0438 mmol) cocatalyzed ROP of CL (2M, 0.876 mmol) from benzyl alcohol (0.00876 mmol) in toluene and MIBK solvent.....	205
Figure 5.11. Eyring plot constructed from the observed first order rate constants for the 1-S /MTBD (0.0438 mmol each) cocatalyzed ROP of CL (0.876 mmol) from benzyl alcohol (0.00876 mmol) in methyl isobutyl ketone.....	206
Figure 5.12. Eyring plot constructed from the observed first order rate constants for the 1-O /MTBD (0.0438 mmol each) cocatalyzed ROP of CL (0.876 mmol) from benzyl alcohol (0.00876 mmol) in methyl isobutyl ketone.....	206
Figure 5.13. Eyring plot constructed from the observed first order rate constants for the 2-O /MTBD (0.0219 mmol each) cocatalyzed ROP of CL (0.876 mmol) from benzyl alcohol (0.00876 mmol) in methyl isobutyl ketone.....	207
Figure 5.14. Eyring plot constructed from the observed first order rate constants for the 2-S /MTBD (0.0219 mmol each) cocatalyzed ROP of CL (0.876 mmol) from benzyl alcohol (0.00876 mmol) in methyl isobutyl ketone.....	207
Figure 5.15. Eyring plot constructed from the observed first order rate constants for the 3-O /MTBD (0.0146 mmol each) cocatalyzed ROP of CL (0.876 mmol) from benzyl alcohol (0.00876 mmol) in methyl isobutyl ketone.....	208
Figure 5.16. ¹ H NMR spectra of TCC/MTBD (0.00438 mmol each) cocatalyst in the presence of varying [CL] (0.25-2M) in CDCl ₃	208
Figure 5.17. Eyring plot constructed from the observed first order rate constants for the 2-S /PMDETA (0.0219 mmol each) cocatalyzed ROP of L-LA (0.876 mmol) from benzyl alcohol (0.00876 mmol) in methyl isobutyl ketone.....	209

Figure 5.18. M_n and M_w/M_n Versus Conversion plot for 2-O at 110°C.....	209
Figure 5.19. M_n and M_w/M_n versus conversion plot for the 3-O /MTBD cocatalyzed ROP of CL from benzyl alcohol in toluene at 110°C.....	210
Figure 5.20. M_n and M_w/M_n versus conversion plot for 1-S at 80°C.....	210
Figure 5.21. M_n and M_w/M_n versus conversion plot for 1-S at 110°C.....	211
Figure 5.22. M_n and M_w/M_n versus conversion plot for 1-S at 110°C.....	211
Figure 5.23. M_n and M_w/M_n Versus Conversion plot for 2-O at 90°C.....	212
Figure 5.24. M_n and M_w/M_n versus conversion plot for 2-O at 90°C.....	212
Figure 5.25. Eyring plot constructed from the observed first order rate constants for the TCC/MTBD (0.0438 mmol each) cocatalyzed ROP of CL (0.876 mmol, 1M) from benzyl alcohol (0.00876 mmol) in toluene.....	213
Figure 5.26. Eyring plot constructed from the observed first order rate constants for the 2- O /MTBD (0.0219 mmol each) cocatalyzed ROP of CL (0.876 mmol, 1M) from benzyl alcohol (0.00876 mmol) in toluene.....	213
Figure 5.27. Eyring plot constructed from the observed first order rate constants for the 1- S /MTBD (0.0438 mmol each) cocatalyzed ROP of CL (0.876 mmol) from benzyl alcohol (0.00876 mmol) at 1M, 2M and 3M concentrations in toluene.....	214
Figure 5.28. Eyring plot constructed from the observed first order rate constants for the TCC/MTBD (0.0438 mmol each) cocatalyzed ROP of CL (0.876 mmol) from benzyl alcohol (0.00876 mmol) in benzene.....	214
Figure 5.29. First order evolution of [CL] versus time for the TCC/MTBD (0.0438 mmol each) cocatalyzed ROP of CL (2M, 0.876 mmol) from benzyl alcohol (0.00876 mmol) in toluene.....	215

Figure 5.30. First order evolution of [CL] versus time for the 1-O /MTBD (0.0438 mmol each) cocatalyzed ROP of CL (2M, 0.876 mmol) from benzyl alcohol (0.00876 mmol) in toluene.....	215
Figure 5.31. First order evolution of [CL] versus time for the 1-S /MTBD (0.0438 mmol each) cocatalyzed ROP of CL (2M, 0.876 mmol) from benzyl alcohol (0.00876 mmol) in toluene.....	216
Figure 5.32. First order evolution of [CL] versus time for the 2-S /MTBD (0.0219 mmol each) cocatalyzed ROP of CL (2M, 0.876 mmol) from benzyl alcohol (0.00876 mmol) in toluene.....	216
Figure 5.33. First order evolution of [CL] versus time for the 3-S /MTBD (0.0146 mmol each) cocatalyzed ROP of CL (2M, 0.876 mmol) from benzyl alcohol (0.00876 mmol) in toluene.....	217
Figure 5.34. First order evolution of [CL] versus time for the 2-O /MTBD (0.0219 mmol each) cocatalyzed ROP of CL (2M, 0.876 mmol) from benzyl alcohol (0.00876 mmol) in toluene.....	217
Figure 5.35. First order evolution of [CL] versus time for the 3-O /MTBD (0.0146 mmol each) cocatalyzed ROP of CL (2M, 0.876 mmol) from benzyl alcohol (0.00876 mmol) in toluene.....	218
Figure 5.36. First order evolution of [CL] versus time for the TCC/DBU (0.0438 mmol each) cocatalyzed ROP of CL (2M, 0.876 mmol) from benzyl alcohol (0.00876 mmol) in toluene.....	218

Figure 5.37. First order evolution of [CL] versus time for the TCC/MTBD (0.0438 mmol each) cocatalyzed ROP of CL (1M, 0.876 mmol) from benzyl alcohol (0.00876 mmol) in toluene.....	219
Figure 5.38. First order evolution of [CL] versus time for the 2-O /MTBD (0.0219 mmol each) cocatalyzed ROP of CL (1M, 0.876 mmol) from benzyl alcohol (0.00876 mmol) in toluene.....	219
Figure 5.39. First order evolution of [CL] versus time for the 1-S /MTBD (0.0438 mmol each) cocatalyzed ROP of CL (1M, 0.876 mmol) from benzyl alcohol (0.00876 mmol) in toluene.....	220
Figure 5.40. First order evolution of [CL] versus time for the 1-S /MTBD (0.0438 mmol each) cocatalyzed ROP of CL (3M, 0.876 mmol) from benzyl alcohol (0.00876 mmol) in toluene.....	220
Figure 5.41. First order evolution of [CL] versus time for the 1-S /MTBD (0.0438 mmol each) cocatalyzed ROP of CL (2M, 0.876 mmol) from benzyl alcohol (0.00876 mmol) in methyl isobutyl ketone.....	221
Figure 5.42. First order evolution of [CL] versus time for the TCC/MTBD (0.0438 mmol each) cocatalyzed ROP of CL (2M, 0.876 mmol) from benzyl alcohol (0.00876 mmol) in methyl isobutyl ketone.....	221
Figure 5.43. First order evolution of [CL] versus time for the 2-S /MTBD (0.0219 mmol each) cocatalyzed ROP of CL (2M, 0.876 mmol) from benzyl alcohol (0.00876 mmol) in methyl isobutyl ketone.....	222

Figure 5.44. First order evolution of [CL] versus time for the 1-O /MTBD (0.0438 mmol each) cocatalyzed ROP of CL (2M, 0.876 mmol) from benzyl alcohol (0.00876 mmol) in methyl isobutyl ketone.....	222
Figure 5.45. First order evolution of [CL] versus time for the 2-O /MTBD (0.0219 mmol each) cocatalyzed ROP of CL (2M, 0.876 mmol) from benzyl alcohol (0.00876 mmol) in methyl isobutyl ketone.....	223
Figure 5.46. First order evolution of [CL] versus time for the 3-O /MTBD (0.0146 mmol each) cocatalyzed ROP of CL (2M, 0.876 mmol) from benzyl alcohol (0.00876 mmol) in methyl isobutyl ketone.....	223
Figure 5.47. First order evolution of [CL] versus time for the TCC/MTBD (0.0438 mmol each) cocatalyzed ROP of CL (2M, 0.876 mmol) from benzyl alcohol (0.00876 mmol) in benzene.....	224
Figure 5.48. Eyring plot for the solvent-free ROP of LA (1.380 mmol) from benzyl alcohol (0.014 mmol) catalyzed by 2-S /PMDETA (0.007 mmol each)	225
Figure 6.1. Bifunctional catalysts a and b have both been employed for the ROP of cyclic esters. Catalyst c is proposed to be active for the ROP of cyclic esters.....	246
Figure 6.2. Synthesis of hydroquinone derived compounds through click style reaction between 4-aminophenol and the corresponding iso(thio)cyanate.....	246
Figure 6.3. Oxidation of hydroquinone species was done in acetic acid as solvent at 0°C and quenched using Et(OH) ₂	247
Figure 6.4. Decomposition of 2b . Top spectra shows the ¹ H NMR of the isolated product and the bottom spectra is the same product after 24 hrs.....	247

Figure 6.5. Decomposition of 4b . Top spectra shows isolated product, bottom spectra shows the same product after 24 hrs.....	248
Figure 6.6. ¹ H NMR spectra taken for the polymerization of L-LA by 5b	249
Figure 6.7. ¹ H NMR (400 MHz, C ₆ D ₆) analysis of binding interaction between 5b and VL.....	250
Figure 6.8. Both images show ¹ H NMR (400 MHz, C ₆ D ₆) analysis of binding interaction between 5b and BnOH (5b and benzyl alcohol at 50 mM each)	251
Figure 6.9. ¹ H NMR (300 MHz, DMSO- <i>d</i> ₆) of 2	252
Figure 6.10. ¹ H NMR (300 MHz, DMSO- <i>d</i> ₆) of 5	253
Figure 6.11. ¹ H NMR (300 MHz, DMSO- <i>d</i> ₆) of 1	254
Figure 6.12. ¹ H NMR (300 MHz, DMSO- <i>d</i> ₆) of 4	255
Figure 6.13. ¹ H NMR (300 MHz, DMSO- <i>d</i> ₆) of 3	256
Figure 6.14. ¹ H NMR (300 MHz, DMSO- <i>d</i> ₆) of 5b	257
Figure 7.1. Dual catalyst species consisting of an H-bond donor and base cocatalyst used for the ROP of functionalized ε-Caprolactone.....	278
Figure 7.2. Example ¹ H NMR (300 MHz, CDCl ₃) of 3,5-MCL monomer (red), conversion to polymer (blue)	279
Figure 7.3. First order evolution of [TOSUO] versus time for the 3-O /MTBD (0.0145 mmol each) cocatalyzed ROP of TOSUO (2M, 0.871 mmol) from benzyl alcohol (0.017) mmol) in C ₆ D ₆	280
Figure 7.4. First order evolution of [TOSUO] versus time for the 3-O /BEMP (0.0145 mmol each) cocatalyzed ROP of TOSUO (2M, 0.871 mmol) from benzyl alcohol (0.017) mmol) in C ₆ D ₆	280

Figure 7.5. First order evolution of [TOSUO] versus time for the 3-O /DBU (0.0145 mmol each) cocatalyzed ROP of TOSUO (2M, 0.871 mmol) from benzyl alcohol (0.017) mmol) in C ₆ D ₆	281
Figure 7.6. First order evolution of [TOSUO] versus time for the 3-O /MTBD (0.0145 mmol each) cocatalyzed ROP of TOSUO (2M, 0.871 mmol) from benzyl alcohol (0.017) mmol) in acetone- <i>d</i> ₆	281
Figure 7.7. First order evolution of [TOSUO] versus time for the TBD (0.0436 mmol each) catalyzed ROP of TOSUO (2M, 0.871 mmol) from benzyl alcohol (0.017) mmol) in acetone- <i>d</i> ₆	282
Figure 7.8. First order evolution of [3,5-MCL] versus time for the 3-O /MTBD (0.0155 mmol each) cocatalyzed ROP of 3,5-MCL (2M, 0.936 mmol) from benzyl alcohol (0.019) mmol) in C ₆ D ₆	282
Figure 7.9. First order evolution of [3,5-MCL] versus time for the 3-O /MTBD (0.0155 mmol each) cocatalyzed ROP of 3,5-MCL (2M, 0.936 mmol) from benzyl alcohol (0.019) mmol) in acetone- <i>d</i> ₆	283
Figure 7.10. First order evolution of [6-MCL] versus time for the 3-O /BEMP (0.0963 mmol each) cocatalyzed ROP of 6-MCL (2M, 0.936 mmol) from benzyl alcohol (0.019) mmol) in acetone- <i>d</i> ₆	283
Figure 7.11. First order evolution of [6-MCL] versus time for the TBD (0.0468 mmol each) catalyzed ROP of [6-MCL] (2M, 0.936 mmol) from benzyl alcohol (0.019) mmol) in acetone- <i>d</i> ₆	284
Figure 7.12. The H-bonding and imidate mediated ROP of cyclic esters.....	284

Figure 7.13. Conversion vs time (top) and first order evolution (bottom) of [TOSUO] and [CL] versus time for the 3-O /MTBD (0.0166 mmol each) cocatalyzed ROP of TOSUO and CL (2M, 0.50 mmol each) from benzyl alcohol (0.02 mmol) in C ₆ D ₆	285
Figure 7.14. ¹ H NMR (300 MHz, CDCl ₃). Random copolymerization of CL and 3,5-MCL.....	286
Figure 7.15. DSC of PCL (M _n = 8,800; M _w /M _n = 1.08)	287
Figure 7.16. DSC of copolymer of 3,5-MCL and CL (25% 3,5-MCL) (M _n = 10,500; M _w /M _n = 1.07)	287

LIST OF SCHEMES

SCHEME	PAGE
Scheme 1.1. Dual catalyst (bimolecular) mediated ROP of δ -valerolactone. Thiourea and MTBD are exemplary H-bond donors (HBDs) and H-bond acceptors (HBAs), respectively.....	39
Scheme 1.2. DMAP catalyzed ROP of lactide has been proposed to proceed via nucleophilic (upper) and H-bond mediated (lower) pathways.....	39
Scheme 1.3. Azobenzene-based Switchable Thiourea.	40
Scheme 1.4. Cinchona Alkaloid-based H-bond Donors for the Stereoselective ROP of <i>rac</i> -Lactide.....	40
Scheme 1.5. Multi-(thio)urea H-bond Donors for ROP.	41
Scheme 1.6. Urea Anion Mediated ROP.	42
Scheme 1.7. Cyclodextrin Promoted ROP of Lactones.	43
Scheme 1.8. Evolution of Dual Catalysts for ROP.	44
Scheme 2.1. Highly Active and Highly Selective H-bond Donor 3-O	77
Scheme 2.2. Proposed Mechanism for 3-O /MTBD Catalyzed ROP.....	77
Scheme 4.1. Mechanism for the urea or thiourea plus base cocatalyzed ROP.....	164
Scheme 7.1. Example equilibrium reaction illustrating binding between H-bond donor and monomer.....	277

MANUSCRIPT – I

Submitted for publication in Organic Catalysts for Polymerization

Bifunctional and Supramolecular Organocatalysts for Polymerization

Kurt V. Fastnacht, Partha P. Datta and Matthew K. Kiesewetter

Chemistry, University of Rhode Island, Kingston, RI, USA

Corresponding Author: Matthew Kiesewetter, Ph.D.
Chemistry
University of Rhode Island
140 Flagg Road
Kingston, RI, 02881, USA
Email address: mkiesewetter@chm.uri.edu

ABSTRACT

Bimolecular, H-bond mediated catalysts for ROP—thiourea or urea plus base, squaramides, and protic acid/base pairs, among others—are unified in a conceptual approach of applying a mild Lewis acid plus mild Lewis base to effect ROP. The bimolecular, and other supramolecular catalysts for ROP, produce among the best-defined materials available via synthetic chemistry through a delicately balanced series of competing chemical reactions by interacting with substrate at an energy of <4 kcal/mol. These catalysts are among the most controlled available for ROP. Part of this arises from the modular, highly-tunable nature of dual catalysts, which effect extremely controlled ROP of a host of cyclic monomers. The broader field of organocatalytic polymerization is a bridge between the disparate worlds of materials chemist (ease of use) and synthetic polymer chemist (mechanistic interest). The cooperative and collegial nature of the organocatalysis for ROP community has facilitated the synergistic evolution of new mechanism to new abilities – in monomer scope, polymer architecture and level of reaction control.

INTRODUCTION

The catalysts in this chapter conduct polymerization via non-nucleophilic, H-bond mediated pathways. These catalysts include thiourea or urea plus base, squaramides, and protic acid/base pairs—which are unified in a conceptual approach of applying a mild Lewis acid plus Lewis base to effect ring-opening polymerization (ROP)—as well as other supramolecular catalysis. This class of catalyst produces among the best-defined materials available via synthetic chemistry through a delicately balanced series of competing chemical reactions by interacting with substrate at an energy of <4 kcal/mol.^{1,2} Indeed, the multitude of simultaneous chemical reactions in a typical supramolecular polymerization is as much awe-inspiring as it is difficult to comprehend, and changing any one factor (H-bond donor, H-bond acceptor, reagent, solvent, temperature, etc.) impacts all the interactions in solution. The polymerization catalysis community has been building an understanding of these systems incrementally over the last decade, and our understanding and abilities in rate, selectivity, diversity of polymer architectures available and reaction control continue to evolve.

The purview of the catalysts in this chapter is ring-opening polymerization (ROP), especially of cyclic esters and carbonates. Conceptually, the catalysts in this chapter are ideally suited to effect highly controlled polymerizations. Catalysts for the ROP of lactones and carbonates effect polymerization by 1) activating the chain-end, 2) activating the monomer, or 3) activating both. By separating the roles of monomer and chain-end activation into discrete functions, the dual catalysts can be separately tuned to effect enchainment and thus minimize side reactions. Conceptually, a dual catalyst consists of both a hydrogen bond donor (HBD) (e.g. urea or thiourea) for monomer

activation and a hydrogen bond acceptor (HBA) (e.g. tertiary amines) for chain-end activation. Such dual catalysts may be a single molecule, but in common practice, bimolecular cocatalysts are employed to activate monomer and initiator alcohol/chain end separately, Scheme 1.1.

The fountainhead of dual catalysis is undoubtedly the 2005 manuscript and its follow-up from Hedrick and Waymouth.^{3,4} The roots of organocatalysis reach back more than 100 years to synthesis of quinine alkaloids,⁵ and, in fact, organocatalysts were among the earliest catalysts for the synthesis of polyesters.⁶ The renaissance of organocatalysis *circa* 2000 saw the application of supramolecular catalysts for small molecule synthesis.⁷ However, it was the veritable Johnny Appleseeds of organocatalytic polymerization that disclosed supramolecular catalysts for ROP along their continuing journey of discovery and subsequently nurtured field such that it now encompasses many branches of questioning by several research groups.⁴ The first supramolecular catalyst for ROP (the Takemoto catalyst, **1**, Figure 1.1) was adapted from the work of Takemoto, who used chiral H-bonding catalysts for asymmetric Michael reactions.⁸ The thiourea/amine base catalyst **1** was introduced into the polymerization community for the organocatalytic ROP of lactide.⁴ The inspired (and somewhat miraculous) step of separating the roles of HBD and HBA into discrete cocatalysts facilitated modulation of the individual cocatalysts leading to the ROP of other monomers and launched a field, Figure 1.1.^{3,4}

The class of organic molecules that effects catalysis via supramolecular interactions are among the most controlled catalysts available for ROP. Part of this is due to the modular, highly-tunable nature of dual catalysts, which effect extremely controlled

ROP ($\text{PDI} = \mathcal{D} = D_m = M_w/M_n < 1.1$) of a host of different cyclic monomers.^{9,10} Most of the research in the field of dual catalysis for organic polymerizations has been dedicated to the ROP of cyclic esters and carbonates; however, other monomers will be mentioned. Dual catalysts effect *living polymerizations*, which is a type of *chain growth polymerization* that proceeds without chain-transfer or termination.¹¹ This is ultimately a kinetic distinction, and it is often said that a polymerization exhibits the characteristics of a ‘living’ polymerization: molecular weights (M_n) are predictable from $[M]_0/[I]_0$, linear evolution of M_n with conversion, first order consumption of monomer and narrow weight distributions (M_w/M_n).¹¹ In practice, these conditions arise when a polymerization has a fast initiation rate relative to propagation rate and few to no side reactions. We shall refrain from pointing out when a catalyst (system) exhibits the characteristics of a ‘living’ polymerization, and rather point out when it is either especially well-controlled or exhibits low levels of control. Several, thorough reviews have been conducted in the wider field,¹²⁻²¹ but not with quite the level of focus that the current platform provides. Hence, we will attempt to emphasize the virtues and deficits of the various catalysts, especially as they contrast to other organic catalysts for polymerization.

DUAL CATALYSTS

The dual catalysts for polymerization are a logical mechanistic conclusion of early organocatalysts for ROP, and H-bond mediated (supramolecular) polymerization mechanisms have been implicated for catalysts in a host of architectures.^{2,22-24} For example, the pyridine bases 4-(dimethylamino)pyridine (DMAP) and 4-pyrrolidinopyridine (PPY) have been proposed to effect the zwitterionic ROP of lactones.²⁵⁻²⁸ However, subsequent mechanistic studies suggest that the nucleophilic and H-bonding pathways are both accessible with the hydrogen-bonded pathway being energetically favorable.²⁹⁻³² An alcohol-activated mechanism of enchainment has been proposed for the phosphazene bases (e.g. P₁-*t*Bu, P₂-*t*Bu, *t*-BuP₄, BEMP in Figure 1.1), which have been shown to effect the ROP of lactones in the presence of alcohols.^{24,33-36} A similar pathway can be envisaged for the guanidine and amidine bases, 7-methyl-1,5,7-triazabicyclo[4.4.0]dec-5-ene (MTBD) and 1,8-diazabicyclo[5.4.0]undec-7-ene (DBU).^{2,23} The dual catalysis conceptual approach of separately activating the monomer and propagating chain end arises from these early organocatalysts which often suffered from low activity or reaction control.^{4,22,23} By separately activating both reactive species, greater specificity and control can be achieved.

Thiourea H-bond Donors

As with many organocatalysts for polymerization, thiourea/base mediated ROP has its roots in small molecule transformations where Jacobsen *et al.* had shown that an array of ureas and thioureas were effective catalysts for Mannich, Strecker, Pictet-Spengler, and hydrophosphonylation reactions,³⁷⁻⁴⁴ among others.⁷ Indeed, the parent dual catalyst, **1**, for ROP was used by Takemoto *et al.* for enantioselective aza-Henry and

Michael additions.^{8,45,46} In the seminal polymerization work, **1** was shown to effect the ROP of lactide with, at the time, remarkably living behavior.⁴ Incredibly, failure to quench the reaction after full conversion to polymer did not result in broadening of molecular weight distribution, signifying very minimal transesterification, and minimal racemization was observed.⁴ When the HBD and HBA roles of **1** were divided into separate HBD (**2**) and HBA (*N,N*-dimethylcyclohexylamine) molecules, a field of research was born, Figure 1.1. Polylactide formation was only successful when both **2** and *N,N*-dimethylcyclohexylamine were applied simultaneously, and a range of non-H-bonding solvents were found to facilitate ROP (e.g. chloroform, dichloromethane and toluene), while THF and DMF failed.⁴ A host of alkylamine cocatalysts (with **2**) has been shown to be effective for the ROP of lactide.^{3,47} Strong bases – MTBD, DBU and later BEMP – are effective cocatalysts with **2** for the ROP of other monomers: δ -valerolactone (VL), ϵ -caprolactone (CL), trimethylene carbonate (TMC), MTC and others, Figures 1.1 and 1.2.^{2,48} The stronger bases will effect a less-controlled ROP of lactide in the absence of thiourea, but thiourea plus strong base is necessary to open other lactones and carbonates with reasonable rates.² The ROP of β -butyrolactone (BL) is not easily performed with most organocatalysts.^{2,49} A common red herring in the ROP literature will attribute unexplainable and otherwise ‘spooky’ observations to *ring strain*. Indeed, it is often observed for organocatalytic ROP that enchainment rates ($k_{LA} > k_{VL} \gg k_{CL} \gg k_{BL}$)^{50,51} have no correlation to *ring strain* as measured by equilibrium monomer concentration, $[M]_{eq}$: $[VL]_{eq}$ (low strain) $\gg [CL]_{eq} \sim [LA]_{eq} \gg [BL]_{eq}$ (high strain).^{50,51}

The origin of the high selectivity for monomer is thought to arise from selective binding of thiourea to monomer versus polymer. The binding constants of lactones (*s-cis*

esters) and open *s*-trans esters to **2** were measured by ¹H NMR titration.² The *s*-trans ester (ethyl acetate) exhibited minimal binding while binding constants of $K_{eq} \sim 40$ were observed between VL or CL and thioureas.² Thiourea H-bond donors have subsequently been shown to bind much more strongly to base cocatalyst, where the nature of the cocatalyst binding constant is a better indicator of co-catalytic activity than monomer binding.^{48,52-54} The cocatalyst binding can be inhibitory to catalysis under the proper circumstances.^{48,52-55} However, the rapid, reversible and promiscuous binding of thiourea to several reagents in solution appears to reduce the overall order of the transformation ($\text{Rate} = k[M][I]_o[\text{cocatalysts}]_o$),^{48,53,54} and the notion of thiourea as an entropy trap prior to enchainment has been repeatedly reinforced.^{56,57} Indeed, our understanding of the multitude of interrelated interactions that occur during a (thio)urea/base mediated ROP continues to unfold.⁵⁸⁻⁶⁰ The theme of competitive binding repeats throughout the literature, including the amide and indole H-bond donor catalysts applied to the ROP of LA which are structurally reminiscent to (thio)ureas.^{52,61,62} The major take-away message is that the high selectivity of H-bonding catalysts appears to rise from two sources, 1) selective binding of thiourea to monomer versus polymer, and 2) strong binding ($K_{eq} = 100 - 4,200$) of thiourea to base cocatalysts which reduces their relative affinity to other reagents and can become an inhibitory interaction.^{48,52} The high selectivity for *s*-cis esters and carbonates has been used to great effect for the generation of classes of functionalizable monomers, Figure 1.2.⁶³⁻⁶⁸

Thiourea-mediated Stereoselective ROP

The stereoselective ROP of *rac*-lactide is an attractive method for the generation of polylactides (PLAs) with highly regular or novel stereosequences, and the modular

scaffold and rich diversity of chiral thiourea H-bond donors has proved an enticing target for several groups. The ROP of *rac*- or *meso*-lactide to generate highly tactic PLA has been well documented.⁶⁹⁻⁷¹ Briefly, stereoselective enchainment of the chiral monomer onto the chiral chain end can occur via control rendered by 1) the propagating chain end, 2) a chiral catalyst or 3) a mixed mechanism.^{69,72,73} For the ROP of *rac*-LA, a high probability of propagating with retention of stereochemistry (P_m = probability of *meso* enchainment) will result in a highly isotactic PLA.^{3,69} Waymouth and Hedrick reported the (**R,R**)-**1** mediated ROP of *rac*-lactide to proceed with modest selectivity (P_m = 0.76); however, **2**/(-)-sparteine catalyzed ROP of *rac*-LA rendered similar selectivity (P_m = 0.77).³ The polymers did not display a melting point, suggesting low stereoregularity.³ Exceeding these P_m values has become a benchmark of sorts for the stereoselective ROP of *rac*-lactide by H-bonding catalysts. Despite its successes, (-)-sparteine itself fell out of favor as an organocatalyst when it became scarce *circa* 2010, but a replacement base, benzyl bispidine, was disclosed which renders similar reaction rates and selectivity in the ROP of *rac*-lactide with **2**, P_m = 0.74.^{47,74}

Recent research into photoresponsive azobenzene-based thiourea, **3**, for the ROP of *rac*-lactide suggests a conceptual approach to switchable organocatalysts for ROP.^{75,76} Catalysts that are switchable by external stimuli (i.e. redox pathways, lights, coordination chemistry etc.)⁷⁶⁻⁹⁴ offer an attractive route to advanced catalyst structures and, presumably, polymer architectures. Thiourea **3** is based on the classic photoswitchable azobenzene moiety, Scheme 1.3. The *trans*-**3** isomer contains an open active site for coordination of lactide by H-bonding whereas *cis*-**3** is blocked by intramolecular H-bonding to the nitro group. The **3**/PMDETA (Scheme 1.3) cocatalyzed ROP of *rac*-LA

proceeded with moderate isoselectivities ($P_m \sim 0.74$) at room temperature.⁷⁵ The ROP was proposed to proceed from the *trans*-isomer, presumably via a chain-end control mechanism.^{3,75} We make the safe prediction that switchable organic catalysts for ROP will play an important role in the next decade.^{76,91}

A thiourea with pendant cinchona alkaloid, **5** in Scheme 1.4, provided the first example of isotactic-rich, stereogradient PLA via kinetic resolution polymerization with organocatalysts. The bifunctional **4** (internal nitrogen base) effected the ROP of *rac*-LA to generate isotactic-rich PLA, $P_m = 0.69$.⁹⁵ No transesterification was observed in MALDI-TOF MS, and almost no epimerization was observed. Polymerization experiments, isolation of residual monomer and analysis by chiral HPLC suggest that the stereoselectivity in the **4**-catalyzed polymerization of *rac*-LA arises from the kinetic resolution by the catalyst/initiator to produce enantioenriched (stereogradient) PLAs. This motif was later incorporated into a thiourea/BINAM-containing organocatalyst, **5** (Scheme 1.4), for the kinetic resolution ROP of lactide.⁹⁶ This stereoselective ROP scheme – arguably the current gold standard – used an epimerization catalyst to transform *meso*- to *rac*-LA which **5** was able to enchain to isotactic poly(l-lactide) with high selectivity, $k_S/k_R = 53$.⁹⁶ Not surprisingly, solvent (and other reaction conditions) dramatically perturb the selectivity.⁹⁶ It should also be noted that structurally similar H-bond donors failed to produce ROP with appreciable rates or selectivities,^{95,96} which highlights a challenge of stereoselective, organocatalytic ROP. Indeed, a significant amount of inspiring ground work exists upon which to build highly successful stereoselective catalysts for ROP, and the field *could* proceed along this trial and error

pathway. However, more fundamental information that might provide a solid mechanistic basis for a path forward may save a tremendous amount of effort.

Squaramides

The squaramide H-bond donor scaffold has been used to great success in small molecule catalysis⁹⁷ and may represent an underexplored opportunity for polymer synthesis. Guo *et al.* examined squaramides for the ROP of l-lactide in dichloromethane at room temperature, initiated from benzyl alcohol.⁹⁸ Squaramide **6** was unable to effect polymerization alone but was active with tertiary amine, (–)-sparteine, cocatalyst, Figure 1.3. H-bond donor **6** plus sparteine exhibits similar activity for ROP of lactide versus thiourea **2**, and squaramides with no electron withdrawing substituents saw less conversion than their electron-deficient counterparts.⁹⁸ A slate of bifunctional squaramide catalysts, **7**, was also evaluated for ROP, Figure 1.3.^{99,100} The bifunctional catalyst **7-Me** displayed reduced activity versus pentyl groups on the amine motif **7**, which was the only one of the examined structures to achieve full conversion in 24 h.⁹⁹ No epimerization was observed during polymerization. A classic H-bond mediated mechanism of enchainment was corroborated by NMR titration studies.⁹⁹ The H-bonding ability of squaramides is perturbed versus that of thioureas,⁹⁹ but they have approximately the same acidity (Schreiner's thiourea (**8**) $pK_a = 8.5$; **6** $pK_a = 8.4$; both in DMSO).^{101,102} The altered structures possessing minimally altered pK_a may have unseen implications for nascent imidate-mediated ROP, see below.

RATE-ACCELERATED DUAL CATALYSIS

From the very early days of the field, thiourea/base cocatalysts exhibited remarkably controlled ROP, so remarkable that the poor activity and productivity of the catalysts could be justified. However, with the application of *N*-heterocyclic carbene (NHC) and TBD organocatalysts to ROP, it became very clear that organocatalysts could possess activity to rival that of metal catalysts.^{16,23,49} The dream of combining the rate of NHCs or TBD with the high selectivity of thiourea/base systems became an alluring research goal for several groups. One route that can be envisaged uses internal Lewis acids to stabilize the (thio)urea as it binds to monomer. The challenge became finding synthetically accessible (thio)ureas with Lewis acids that are compatible with ROP.

Internal Lewis Acid Enhanced H-Bond Donors

A urea H-bond donating catalyst with an internal boronate ester, **9**, displayed enhanced activity versus its parent urea, **10** (Figure 1.4). HBD **9** was applied with sparteine cocatalyst for the ROP of LA at room temperature ($k_2/k_9 \sim 1$).¹⁰³ Importantly, the ROP of LA with **9**/sparteine showed good control and maintained a narrow molecular weight distribution ($M_w/M_n \sim 1.18$) for days after the reaction had finished (initial $M_w/M_n \sim 1.16$), indicating minor transesterification. This motif is an extreme example of the internal H-bond stabilization that is thought to be present in all (thio)ureas bearing electron deficient aryl rings.¹⁰⁴

Multi (thio)urea Catalysts

Mechanistic studies on **2**/base cocatalyzed ROP led to the development of highly effective bis- and tris-(thio)urea H-bond donors.^{53,105} In general, urea HBDs are more active than thioureas, and tris-donors are more active than bis- which are more active

than mono-; although tris-thiourea (**14**) is markedly inactive, Scheme 1.5.^{53,105} These general trends hold for most monomers that have been examined, but the rate accelerations are most dramatic for the slower monomers (i.e. CL).^{53,105} Just as with **2**, weak alkylamine base cocatalysts are required for the ROP of lactide with **11-15**,^{4,47,53} but strong base cocatalysts are required for VL, CL and carbonate monomers.^{2,105} For the trisurea (**15**)/BEMP cocatalyzed ROP of CL, a ~500 times increase in rate is observed versus **2**/BEMP, and the reaction is more controlled.^{48,105} A typical (thio)urea/base cocatalyzed ROP is run ~2M monomer and displays good control for M_n from $[M]_0/[I]_0 = \sim 20-500$,^{2,53,105} although enhanced (vs **2**) weight control is observed for **13** and **15** at higher $[M]_0/[I]_0$.¹⁰⁵ The comparisons above are controlled for mol percent (thio)urea moiety in the ROP; typical catalyst loadings are 5 mol% mono-(thio)urea/base; 2.5 mol% bis-donor/base; 1.67 mol% tris-donor/base.^{2,105}

An *activated-(thio)urea* mechanism is proposed for multi-H-bond donor mediated ROP in non-polar solvent, but urea H-bond donors remain highly-active in polar solvent. Kinetic studies on the several systems in benzene- d_6 reveal the (thio)urea ROPs to be first order in monomer, initiator, and cocatalysts, suggesting one mono-/bis-/tris-H-bond donor acting at one monomer in the transition state.^{48,53,54,105} H-bonds are electrostatic in nature and have low directionality,¹⁰⁶ which allows for the possibility of multi-(thio)ureas directly activating monomer in a multi-activation mechanism. Computational models suggest that tris-thiourea **14** is C3 symmetric (all H-bonded),¹⁰⁵ and an analogue of **15** with n-propyl (versus ethyl) linking arms is highly inactive for ROP,¹⁰⁷ suggesting that the (thio)urea moieties prefer to bind to themselves. These experiments, along with computational studies, suggest an *activated-(thio)urea* mechanism is operative in non-

polar solvent.¹⁰⁵ Traditional H-bonding catalysts (e.g. **2**/base) become very inactive in polar solvent, which limits their utility.³ The urea HBDs, however, remain highly active in polar solvents (e.g. acetone and THF).^{105,108} Recent, and still-evolving, studies suggest that a different mechanism involving urea anions is operative in polar solvent.^{58–60}

Urea and Thiourea Anions

The deprotonation of urea or thiourea with strong bases (alkoxides or metal hydrides) has been shown to produce the corresponding urea anion or thiourea anion (also: imidate or thioimidate) which are incredibly active for the ROP of lactones.^{59,60} An active catalyst system generated by the treatment of urea **17** with potassium methoxide (KOMe) in THF results in the extremely active ROP of l-lactide at room temperature, Scheme 1.6.^{59,60} The same ROP with KOMe alone slowed almost 200 times while broadening M_w/M_n (2.22 versus 1.06), and the **17**/KOMe cocatalyst system is ~25 times more active than thiourea anion motif.^{59,60} Polymerizations with VL and CL were also completed within seconds.⁵⁹ An ROP with similar activity can be achieved by a urea (e.g. **16**) plus strong organic base (e.g. MTBD, DBU, BEMP) cocatalyzed ROP.¹⁰⁸ The latter method may be operationally simpler, and urea plus organic base cocatalyzed ROP *may* be more controlled, especially post polymerization.¹⁰⁸ The rates of the two methods appear to be very similar and mark a departure from early H-bond mediated ROP: seconds instead of hours or days! Remarkably, the ROPs remain highly controlled.

The urea/base cocatalyst systems operate by a different mechanism than classic H-bond mediated ROP. For the urea/alkali base cocatalyzed ROP, the proton transfer to form the ‘hyperactive’ (thio)imidate is largely irreversible. Hence, more acidic (thio)ureas are thought to generate more basic (thio)imidates, resulting in faster catalysis.

Indeed, there is a negative linear correlation between $\ln(k_p)$ against number of CF_3 substituents,^{59,108} and Schreiner *et al.* reported a linear reduction in $\text{p}K_a$ with number of CF_3 substituents on the diaryl ureas and thioureas in DMSO.^{102,109} This mechanism is reminiscent of a bifunctional TBD-mediated ROP of lactones,^{23,59} where the imidate can serve as both H-bond donor and acceptor. This same mechanism is believed to be operative for bis- and tris-urea H-bond donors in polar solvent as well.^{48,53,105,108}

An antibacterial compound, triclocarban (TCC, Scheme 1.6), was shown to be a very effective H-bond donating catalyst for the ROP of lactones when used with organic base cocatalysts.¹⁰⁸ It was proposed that this compound effects ROP through the same mechanism as other urea/strong base mediated polymerizations, and TCC/BEMP displays the same approximate rate and control behavior as trisurea (**15**)/BEMP, although the trisurea is more active ($k_{15}/k_{\text{TCC}} \sim 4$, VL).^{105,108} We anticipate that the movement towards readily available reagents will prompt wider adoption of organocatalysts and facilitate new applications; the success of TBD may be due, at least in part, to its commercial availability. To demonstrate this point, TCC/base cocatalyzed ROP was applied to the solvent-free polymerization of several lactones, which was previously limited due to 1) the presumed inactivity of urea HBDs in polar (monomer) solvent, and 2) the large amounts of catalyst required for neat conditions.⁵⁸ Solvent-free ROP catalyzed by TCC/base allowed for the one-pot synthesis of di- and tri-block copolymers, and TCC/alkylamines were effective for the solvent-free ROP of LA,⁵⁸ a longstanding challenge.¹¹⁰ The reactions remained highly controlled and ‘living’ in nature despite solidifying prior to full conversion.

NON-(THIO)UREA LEWIS ACID/BASE CATALYSIS

Sulfonamides, Phosphoric and Phosphoramidic H-bond Donor/Acceptors

A selection of mono- and bis-sulfonamide HBDs which have been applied with base cocatalysts for the ROP of LA are shown in Figure 1.5. The **18**/DMAP cocatalysts produced the most rapid ROP of LA of the HBDs examined, and it was well-controlled.¹¹¹ Structurally similar catalysts, **19** and **20**, were less active, and no monosulfonamide/base cocatalyzed ROPs of LA have been shown to reach full conversion in 24 h. Neither mono- nor bis-sulfonamides promoted the ring opening of LA in the absence of an amine cocatalyst. For the monosulfonamides, it was suggested that low catalyst activity might arise from reduced H-bond donation versus the bis donors.¹¹¹ This account is consistent with observations for the mono-, bis- and tris-(thio)urea H-bond donors.¹⁰⁵

Phosphoric and phosphoramidic acids, the weak acidity of which contrasts with strong acids used for electrophilic monomer activated ROP,¹³ can act as bifunctional organocatalysts for ROP.¹¹²⁻¹¹⁷ Diphenyl phosphate (**21**), phosphoramidic (**22**) and imidodiphosphoric (**23**) acids were used for the ROP of cyclic esters and carbonates, Figure 1.6. Catalysts **21** and **22** were found to be active towards the ROP of CL, yielding conversion to polymer in 5.5 and 1.5 h, respectively.¹¹² Catalyst **23** is also active for the ROP of VL, CL or TMC monomers, albeit sluggish.¹¹⁴⁻¹¹⁶ The reactions are well-controlled ($M_w/M_n < 1.2$). Binding studies between catalyst and monomer or benzyl alcohol (initiator) suggest H-bonding, which have previously been observed with these catalyst motifs (e.g. P=O and P-NH).¹¹⁸ Computational studies on **21** and **22** indicate the possibility of bifunctional activation.¹¹² Solvent screens performed on **22** and **23** (ROP of

TMC) show dramatic slowing of reaction rate in THF (versus CH₂Cl₂ or toluene), corroborating an H-bond mediated mechanism. These systems are part of the vast underpinning of mechanistic studies that have propelled this field forward, and these systems are advantageous in their synthetic modularity and highly controlled nature. This work has roots in the methyl sulfonic acid and triflic acid catalyzed ROP of lactones, which have been proposed to operate through both electrophilic monomer activated and bifunctional H-bond activated mechanisms.¹¹³

Phenol and Benzyl Alcohol H-bond Donors

Considering their efficacy for the ROP of several monomers, electron deficient alcoholic H-bond donors may constitute an underdeveloped class of H-bond donating catalyst. Bibal *et al.* evaluated certain *o*-,*m*-,*p*- substituted phenols **24** for their catalytic activity towards the ROP of LA (Figure 1.7).¹¹⁹ Full conversion of lactide initiated from 4-biphenylmethanol (a fluorescent alcohol) was observed in 24 h for all phenol/sparteine cocatalyst systems except for *o*- and *p*-OMe-phenol, and the fastest reaction rates were produced from phenols with electron withdrawing groups. MALDI-TOF MS indicated the presence of polymer chains initiated from phenols, an inherent liability with using alcoholic catalysts for organocatalytic ROP of esters and carbonates. Bis-donor catalysts (**24**, *o*-diphenol and *m*-diphenol; Figure 1.7) plus DBU cocatalyst are effective for the ROP of VL from 4-biphenylmethanol.¹²⁰ The electron rich diols gave high conversions while the electron poor H-bond donors had lower conversions. Strong binding between cocatalysts has been shown to be inhibitory under some circumstances.^{48,52} However, Hedrick *et al.* suggested that steric bulk surrounding the catalytic alcohol would limit initiation from catalyst, producing more controlled reactions (Figure 1.7).¹²¹ The

hexafluoroalcohol (**26**, R=H) plus sparteine cocatalyzed ROP of LA initiated from benzyl alcohol resulted in full conversion of monomer in 23 h, but the bulky H-bond donor **26** (R=CF₃) showed no conversion, which may be due to its high acidity (pK_a^{DMSO} (CF₃)₃COH = 10.7)¹²². In a rare display by H-bond mediated ROP, even β -BL was polymerized by **25** (R=methacryloyl)/sparteine to 71% conv. in 138 h.¹²¹

Experimental and computational data suggest the H-bond mediated ROP is mechanistically similar to those previously described. Only minimal binding between phenol and VL was observed, but this important observation reinforces early conclusions that weak binding between catalysts and monomer is not vital to catalysis.⁴⁸ Rather, a larger picture approach considering all reagent bindings, especially cocatalyst bindings, must be considered.^{15,48,52} However, binding measurements on the more effective H-bond donors, **25** (R=methacryloyl) and **26** (R=Me) indicate H-bonding to VL.

Certainly, structural modulation of the established thiourea and urea scaffolds will continue to offer new catalysts – especially if mechanistic advances like the urea anions continue to appear. These changes may occur through the application of these catalysts in new roles. For examples, thioureas have recently been applied as additives in the strong acid mediated ROP of lactones. Guo *et al.* found that thioureas when added to a trifluoroacetic acid (TFA) catalyzed ROP of VL or CL increased the reaction rate by up to 3 times in an electrophilic monomer activation mechanism; the M_w/M_n was reduced and higher conversions were achieved than with TFA alone.^{123,124} However, the drastic departures from the conventional offer a good chance for truly new and exciting developments. The azaphosphatrane (**27**) cocatalyzed (with sparteine) ROP of cyclic esters is the perfect example, Figure 1.8.¹²⁵ These structures suggest a new catalytic

handle to provide monomer activation with attenuated cocatalyst binding.^{125,126} Further, they are highly modular and have multiple sites available for optimization.¹²⁵

Electrostatic Monomer Activation by Cations

H-bonds – a very poor name for the phenomenon – require no orbital overlap and are a type of electrostatic interaction.¹⁰⁶ Bibal *et al.* have demonstrated electrostatic activation of monomer by cationic species along with base cocatalysts to effect the ROP of LA, VL and CL; both tertiary alkyl ammonium salts and alkali metal cations encapsulated in crown ethers have been successfully applied, Figure 1.9.¹²⁷ The fastest ROP rates for LA were observed with [15-c-5]Na and sparteine, where full conversion was achieved in 2 h. However, full conversions of LA and VL to polymer were achieved for all cocatalyst systems within 24 h (sparteine for LA; DBU for VL and CL). As usual, the ROP of CL was the slowest, achieving only 53% conversion in 120 h with [15-c-5]Na/sparteine. For the ammonium salt mediated ROPs, exchanging NTf₂ for a BARF counterion (Figure 1.9) resulted in a slight increase in reaction rate for all catalytic systems, which is likely attributed to the increased solubility of BARF versus NTf₂.¹²⁷ The ammonium species do not polymerize cyclic esters in the absence of a base cocatalyst, which suggests that the native counter-anion is insufficient for alcohol activation. DFT calculations reinforce activation of monomer by the electrophilic portions of the alkylammonium (i.e. the methyl groups) and activation of alcohol end group by base cocatalyst, Figure 1.9.¹²⁷ Further exploration of this interesting class of catalysts may provide new reactivity and synthetic possibilities.

BRONSTED ACID/BASE PAIRS

The accepted mechanism for the dual organocatalytic ROP of cyclic esters relies on two factors when promoting polymerization: the activation of monomer and initiator/chain end with a Lewis acid (HBD) and Lewis base (HBA), respectively. One can imagine employing a protic acid in place of a thiourea (e.g.) which would result in proton transfer to base cocatalyst, generating a new cocatalyst system where the activation of monomer may occur by base- H^+ and activation of chain end may occur by acid. Indeed, the previously discussed ‘hyperactive’ urea anions may operate by this mode when a strong organic base (e.g. BEMP) is employed.^{58,108} Practically, catalysts of this type are employed by reacting organic bases – many of which are themselves organic catalysts for ROP – with a protic acid to form an acid/base pair. One representative pair, DBU plus benzoic acid (Figure 1.10), was derived serendipitously by incompletely quenching a DBU-catalyzed ROP of lactide.

Benzoic acid, which is widely used to quench organic catalysts by protonating amine bases,² forms an active ROP cocatalyst when mixed 1:1 with DBU.¹²⁸ Hedrick *et al.* found that a 1:1 ratio of DBU to benzoic acid produced well controlled PLA ($M_w/M_n \sim 1.06$) to full conversion in 24 h. When the ratio [benzoic acid]/[DBU] increased to 1.5 and 2, the polymerization rate decreased and stopped, respectively. At lower than 1 equivalence of acid (to DBU), the reaction was faster and less controlled due to free DBU.^{2,129} Molecular modeling of the acid/base pair with LA and methanol suggests a catalytic ion pair where DBU- H^+ activates monomer and the benzoate anion (BA^-) activates chain end. The acid/base pairs of DBU with HCl, acetic acid (AcOH) or *p*-toluenesulfonic acid (TsOH) were also evaluated for catalytic activity. No catalytic

activity was found after 48 h using HCl. However, the resonance stabilized AcO^- and TsO^- anions both were able to polymerize LA with DBU-H^+ cocatalyst, providing controlled molecular weights and narrow M_w/M_n .¹²⁸ On a superficial level, these results provide a clear rationale for using two equivalents of benzoic acid with respect to base to quench an ROP (co)mediated by organic bases.

Several conjugate acid/base pairs have also been applied for organocatalytic ROP.¹³⁰ An exemplary pair consisting of 1 eq. DMAP and 1 eq. $\text{DMAP}\cdot\text{HX}$ ($X = \text{Cl}$, MSA , TfOH) was used as a catalyst for the ROP of LA in solution, and it exhibited augmented rates versus DMAP alone. The conjugate pair with triflate counterion was found to be the most active catalyst, although full conversion to polymer was not achieved in 24 h. The ideal ratio of DMAP to $\text{DMAP}\cdot\text{HX}$ is 1:1. The same group of conjugate acid/base pairs were also evaluated for the ROP of LA, VL and CL in bulk conditions at 100°C .¹³¹ For LA, the same trend was found in the bulk as was found in solution, with the conjugate pair $\text{DMAP}/\text{DMAP-H}^+/\text{TfO}^-$ system having the highest rate and full conversion in 1 h. $\text{DMAP}/\text{DMAP-H}^+/\text{TfO}^-$ was the only catalyst system effective for the ROP of VL and CL, but full conversions were not achieved within 24 h. VL and CL were not as controlled as LA, giving $M_w/M_n > 1.3$, for reactions with degree of polymerization (DP) ~ 100 . For all ROPs, side reactions that are likely to broaden M_w/M_n often occur at long reactions times. As with many acid mediated ROP, water impurities complicated mechanistic analysis. Several other advancements on this theme have been explored by applying known H-bond acceptors with acids for ROP.¹³²⁻¹³⁶ Conceptually interesting, increased synthetic effort may be able to transition this scheme from concept to practice.

SUPRAMOLECULAR CATALYSTS

Betaines

Narrow polydispersity and high molecular weights are possible with ammonium betaine catalysts. Coulembier *et al.* demonstrated that ammonium betaines, used as bifunctional organic catalysts, H-bond with initiating/propagating alcohols at the phenoxide, Figure 1.11.¹³⁷ ROP of l-lactide was performed with *m*-(trimethylammonio)phenolate betaine (**27**) producing a living and controlled polymerization, with minimal transesterification and high isotacticity.^{137,138} Faster rates are seen in chloroform versus THF, which was taken to suggest that the ionic catalyst acts via a H-bonding mechanism.¹³⁷ Computational studies suggest that strong interactions are seen between 1-pyrenemethanol and the phenolate anion of *m*-betaine (relative to the other isomers), which is consistent with the rapid ROP with *m*-betaine versus the *p*- and *o*-isomers.¹³⁷

Amino-Oxazoline

The structures of amino-oxazolines and thiazolines are analogous to that of TBD. An initial screening of the thiazoline catalyzed ROP of LA determined that thiazolines with electron withdrawing groups resulted in reduced ROP activity and produced atactic PLA.¹³⁹ Amino-thiazolines with electron donating alkyl groups are more active, and amino-thiazoline with cyclohexyl groups demonstrated the fastest rates for ROP of LA, Figure 1.12; however, this catalyst is much less active than the ‘parent’ TBD catalyst.¹³⁹ Elevated temperatures indicated little to no rate enhancement, which could arise from weaker supramolecular interactions during the enchainment transition state. ¹H NMR binding experiments demonstrate the more electron-deficient compounds have stronger

interactions with cyclic esters and conversely have weaker interactions with initiating alcohol. These experiments corroborate the presumption that both the H-bond accepting and donating sites are necessary for effective catalysis.¹³⁹ These catalysts are notable because they are mechanistically similar to TBD but far more modular synthetically. With the rising interest in specialized catalyst architectures, these motifs may prove highly useful.

Cyclodextrins

Cyclodextrins (CDs) have garnered interest due to their selective inclusion properties and reactivities,^{140–142} and they constitute an example of extremely mild supramolecular catalyst for ROP.^{143,144} The ability of CDs to catalyze the hydrolysis of polyesters in water was thought to proceed via a polymer inclusion complex with CDs.¹⁴¹ In the absence of water, CDs catalyze the ROP of lactone monomers.¹⁴¹ Further, CDs can create selective inclusion complexes with some lactones where the size of a CD can promote or suppress the transesterification of lactones. The inclusion of lactones in the hydrophobic CD cavity is believed to be the driving force to yield polyesters,¹⁴⁰ and the existence of hydrophobic, catalytic pockets has been proposed for other organocatalysts for ROP.^{56,105,140} Accordingly, the ROPs catalyzed by the CD with a smaller cavity (i.e. α -CD in Scheme 1.7) produce the highest yields of β -butyrolactone (β -BL) under solvent-free conditions at 100°C, while the larger lactones, VL and CL, experience higher yields with the larger γ -CD (Scheme 1.7).¹⁴⁰ Solvent-free copolymerizations of VL and LA were also performed.¹⁴⁰

Mechanistic studies suggest that ROP is initiated from the CD and that the lactone/CD inclusion complex is vital to catalysis. When ROP is attempted using an

acylated CD (no free hydroxyls), no conversion to polylactone is observed, which suggests that CDs are covalently attached to the polylactone chain end in a normal CD-catalyzed ROP.¹⁴⁰ Further, suppression of the ROP of VL was noted with a β -CD/adamantane inclusion complex catalyst system. The adamantane guest is strongly inserted in the β -CD cavity, which excludes VL, suggesting that lactone/CD inclusion complexes are essential for ROP.¹⁴⁰ The mechanistic picture that emerges suggests that, initially, a complex is formed between lactone and CD at a ratio of 1:1, and a hydroxyl group at the C₂-position attacks the monomer to begin enchainment. Further development of these or similar extremely mild catalysts for ROP could provide new and exciting methods of ultra-controlled ROP.

CONCLUSION

The narrative of this chapter can be summarized by following the circular evolution of dual catalysts away from and back towards the popular organocatalyst, TBD. When the TBD catalyzed ROP of lactones was disclosed in 2006,²³ it was the perfect storm of a successful catalyst. It is easy to use, readily available, highly active and exhibits decent selectivity for monomer and control ($M_w/M_n \sim 1.2$). While TBD was originally proposed to operate via a nucleophilic mechanism of enchainment, an H-bond mediated, bifunctional, mechanism was also envisaged.²³ This mechanism has been much debated, and it is not entirely certain which mechanism is operative and when.^{32,145,146} Conceptually, a thiourea/base mediated ROP can be viewed as separating the H-bond donating and accepting roles of TBD into separate cocatalyst moieties. This approach, while highly-tunable and beneficial for the reasons described above, required sacrificing reaction rate. The various efforts to increase reaction rate without sacrificing control (serendipitously?) brought the community back to an active catalyst which bears a strong structural resemblance to TBD, urea plus strong base mediated ROP. Far from ending up in the same place, the numerous studies that brought us ‘full circle’ have greatly enriched our understanding of how these catalysts operate and have largely mitigated the activity versus selectivity problem of organocatalytic ROP, Scheme 1.8. By no means is this story complete, and as of January 2018 our mechanistic understanding of nascent urea/strong base mediated ROP is still evolving. Indeed, the broader field of organocatalytic polymerization is a bridge between the disparate worlds of materials chemist (ease of use) and synthetic polymer chemist (mechanistic interest). We assert that the cooperative and collegial nature of our community has facilitated the

synergistic evolution of new mechanism to new abilities – in monomer scope, polymer architecture and level of reaction control. We hope that this will continue.

LIST OF REFERENCES

- (1) Anslyn, E. V.; Dougherty, D. A. In *Modern Physical Organic Chemistry*; 2006; pp 162–194.
- (2) Lohmeijer, B. G. G.; Pratt, R. C.; Leibfarth, F.; Logan, J. W.; Long, D. A.; Dove, A. P.; Nederberg, F.; Choi, J.; Wade, C.; Waymouth, R. M.; Hedrick, J. L. *Macromolecules* **2006**, *39* (25), 8574–8583.
- (3) Pratt, R. C.; Lohmeijer, B. G. G.; Long, D. A.; Lundberg, P. N. P.; Dove, A. P.; Li, H.; Wade, C. G.; Waymouth, R. M.; Hedrick, J. L. *Macromolecules* **2006**, *39* (23), 7863–7871.
- (4) Dove, A. P.; Pratt, R. C.; Lohmeijer, B. G. G.; Waymouth, R. M.; Hedrick, J. L.; V, S. U. *J. Am. Chem. Soc.* **2005**, *127*, 13798–13799.
- (5) Bredig, G.; Fiske, P. S. *Biochem. Z.* **1912**, *46*, 7.
- (6) Flory, P. J. *J. Am. Chem. Soc.* **1940**, *62* (9), 2261–2264.
- (7) Doyle, A. G.; Jacobsen, E. N. *Chem. Rev.* **2007**, *107* (12), 5713–5743.
- (8) Okino, T.; Hoashi, Y.; Takemoto, Y. *J. Am. Chem. Soc.* **2003**, *125* (42), 12672–12673.
- (9) \mathcal{D} , like PDI (polydispersity index), is sufficiently incoherent to the novice, yet \mathcal{D} features the added deficit of being nearly impossible to google.
- (10) Stepto, R. F. T. *Pure Appl. Chem.* **2009**, *81* (2), 351–353.
- (11) Odian, G. In *Principles of Polymerization*; New York, 1991; pp 532–603.
- (12) Kiesewetter, M. K.; Shin, E. J.; Hedrick, J. L.; Waymouth, R. M. *Macromolecules* **2010**, *43* (5), 2093–2107.
- (13) Kamber, N. E.; Jeong, W.; Waymouth, R. M.; Pratt, R. C.; Lohmeijer, B. G. G.;

- Hedrick, J. L. *Chem. Rev.* **2007**, *107* (12), 5813–5840.
- (14) Dove, A. P. In *Handbook of Ring-Opening Polymerization*; Dubois, P., Coulembier, O., Raquez, J.-M., Eds.; Wiley-VCH: Federal Republic of Germany, 2009; pp 357–378.
- (15) Thomas, C.; Bibal, B. *Green Chem.* **2014**, *16* (4), 1687–1699.
- (16) Dove, A. P. *ACS Macro Lett.* **2012**, *1* (12), 1409–1412.
- (17) Zhang, X.; Fevre, M.; Jones, G. O.; Waymouth, R. M. *Chem. Rev.* **2017**, acs.chemrev.7b00329.
- (18) Byers, J. A.; Biernesser, A. B.; Delle Chiaie, K. R.; Kaur, A.; Kehl, J. A. In *Synthesis, Structure and Properties of Poly(lactic acid)*; Di Lorenzo, M. L., Androsch, R., Eds.; Springer International Publishing: Cham, 2018; pp 67–118.
- (19) Grubbs, R. B.; Grubbs, R. H. *Macromolecules* **2017**, No. X, acs.macromol.7b01440.
- (20) Hu, S.; Zhao, J.; Zhang, G.; Schlaad, H. *Prog. Polym. Sci.* **2017**, *74*, 34–77.
- (21) Song, Q.-L.; Hu, S.-Y.; Zhao, J.-P.; Zhang, G.-Z. *Chinese J. Polym. Sci.* *581–601* *Chinese J. Polym. Sci.* **2017**, *35* (5), 581–601.
- (22) Jeong, W.; Shin, E. J.; Culkin, D. A.; Hedrick, J. L.; Waymouth, R. M. *J. Am. Chem. Soc.* **2009**, *131* (13), 4884–4891.
- (23) Pratt, R. C.; Lohmeijer, B. G. G.; Long, D. A.; Waymouth, R. M.; Hedrick, J. L. *J. Am. Chem. Soc.* **2006**, *128* (14), 4556–4557.
- (24) Zhang, L.; Nederberg, F.; Pratt, R. C.; Waymouth, R. M.; Hedrick, J. L.; Wade, C. G. *Macromolecules* **2007**, *40* (12), 4154–4158.
- (25) Nederberg, F.; Connor, E. F.; Glausser, T.; Hedrick, J. L. *Chem. Commun.* **2001**,

No. 20, 2066–2067.

- (26) Nederberg, F.; Connor, E. F.; Möller, M.; Glauser, T.; Hedrick, J. L. *Angew. Chem. Int. Ed. Engl.* **2001**, *40*, 2712–2715.
- (27) Kricheldorf, H. R.; Lomadze, N.; Schwarz, G. *Macromolecules* **2008**, *41* (21), 7812–7816.
- (28) Kricheldorf, H. R.; Lossow, C. Von; Schwarz, G. *J. Polym. Sci. Part A Polym. Chem.* **2006**, *44* (15), 4680–4695.
- (29) Bonduelle, C.; Martín-Vaca, B.; Cossío, F. P. P.; Bourissou, D. *Chem. – A Eur. J.* **2008**, *14* (17), 5304–5312.
- (30) Chuma, A.; Horn, H. W.; Swope, W. C.; Pratt, R. C.; Zhang, L.; Lohmeijer, B. G. G.; Wade, C. G.; Waymouth, R. M.; Hedrick, J. L.; Rice, J. E. *J. Am. Chem. Soc.* **2008**, *130* (21), 6749–6754.
- (31) Lai, C.-L. L.; Lee, H. M.; Hu, C.-H. H. *Tetrahedron Lett.* **2005**, *46* (37), 6265–6270.
- (32) Simón, L.; Goodman, J. M. *J. Org. Chem.* **2007**, *72* (25), 9656–9662.
- (33) Schwesinger, R.; Schlemper, H. *Angew. Chemie Int. Ed. English* **1987**, *26* (11), 1167–1169.
- (34) Molenberg, A.; Möller, M. *Macromol. Rapid Commun.* **1995**, *16* (6), 449–453.
- (35) Kaljurand, I.; Kütt, A.; Sooväli, L.; Rodima, T.; Mäemets, V.; Leito, I.; Koppel, I. *A. J. Org. Chem.* **2005**, *70* (3), 1019–1028.
- (36) Schlaad, H.; Kukula, H.; Rudloff, J.; Below, I. *Macromolecules* **2001**, *34* (13), 4302–4304.
- (37) Sigman, M. S.; Vachal, P.; Jacobsen, E. N. *Angew. Chemie - Int. Ed.* **2000**, *39* (7),

1279–1281.

- (38) Vachal, P.; Jacobsen, E. N. *Org. Lett.* **2000**, *2* (6), 867–870.
- (39) Vachal, P.; Jacobsen, E. N. *J. Am. Chem. Soc.* **2002**, *124* (34), 10012–10014.
- (40) Wenzel, A. G.; Jacobsen, E. N. *J. Am. Chem. Soc.* **2002**, *124* (44), 12964–12965.
- (41) Taylor, M. S.; Jacobsen, E. N. *J. Am. Chem. Soc.* **2004**, *126* (34), 10558–10559.
- (42) Yoon, T. P.; Jacobsen, E. N. *Angew. Chemie - Int. Ed.* **2005**, *44* (3), 466–468.
- (43) Joly, G. D.; Jacobsen, E. N. *J. Am. Chem. Soc.* **2004**, *126* (13), 4102–4103.
- (44) Fuerst, D. E.; Jacobsen, E. N. *J. Am. Chem. Soc.* **2005**, *127* (25), 8964–8965.
- (45) Okino, T.; Nakamura, S.; Furukawa, T.; Takemoto, Y. *Org. Lett.* **2004**, *6* (4), 625–627.
- (46) Hoashi, Y.; Okino, T.; Takemoto, Y. *Angew. Chemie - Int. Ed.* **2005**, *44* (26), 4032–4035.
- (47) Coady, D. J.; Engler, A. C.; Horn, H. W.; Bajjuri, K. M.; Fukushima, K.; Jones, G. O.; Nelson, A.; Rice, J. E.; Hedrick, J. L. *ACS Macro Lett.* **2012**, *1* (1), 19–22.
- (48) Kazakov, O. I.; Datta, P. P.; Isajani, M.; Kiesewetter, E. T.; Kiesewetter, M. K. *Macromolecules* **2014**, *47*, 7463–7468.
- (49) Jeong, W.; Hedrick, J. L.; Waymouth, R. M. *J. Am. Chem. Soc.* **2007**, *129* (27), 8414–8415.
- (50) Duda, A.; Kowalski, A. In *Handbook of Ring-Opening Polymerization*; Dubois, P., Coulembier, O., Raquez, J.-M., Eds.; Wiley-VCH Verlag GmbH & Co. KGaA, 2009; pp 1–52.
- (51) Olsén, P.; Odélius, K.; Albertsson, A. C. *Biomacromolecules* **2016**, *17* (3), 699–709.

- (52) Koeller, S.; Kadota, J.; Peruch, F.; Deffieux, A.; Pinaud, N.; Pianet, I.; Massip, S.; Léger, J.-M.; Desvergne, J.-P.; Bibal, B. *Chem. Eur. J.* **2010**, *16* (14), 4196–4205.
- (53) Spink, S. S.; Kazakov, O. I.; Kieseewetter, E. T.; Kieseewetter, M. K. *Macromolecules* **2015**, *48* (17), 6127–6131.
- (54) Kazakov, O. I.; Kieseewetter, M. K. *Macromolecules* **2015**, *48* (17), 6121–6126.
- (55) Thomas, C.; Peruch, F.; Bibal, B. *RSC Adv.* **2012**, *2* (33), 12851.
- (56) Datta, P. P.; Pothupitiya, J. U.; Kieseewetter, E. T.; Kieseewetter, M. K. *Eur. Polym. J.* **2017**, *95* (May), 671–677.
- (57) Lippert, K. M.; Hof, K.; Gerbig, D.; Ley, D.; Hausmann, H.; Guenther, S.; Schreiner, P. R. *European J. Org. Chem.* **2012**, *2012* (30), 5919–5927.
- (58) Pothupitiya, J. U.; Dharmaratne, N. U.; Jouaneh, T. M. M.; Fastnacht, K. V.; Coderre, D. N.; Kieseewetter, M. K. *Macromolecules* **2017**, *50* (22), 8948–8954.
- (59) Lin, B.; Waymouth, R. M. *J. Am. Chem. Soc.* **2017**, *139* (4), 1645–1652.
- (60) Zhang, X.; Jones, G. O.; Hedrick, J. L.; Waymouth, R. M. *Nat. Chem.* **2016**, *8* (11), 1047–1053.
- (61) Koeller, S.; Thomas, C.; Peruch, F.; Deffieux, A.; Massip, S.; Léger, J. M.; Desvergne, J. P.; Milet, A.; Bibal, B. *Chemistry* **2014**, *20* (10), 2849–2859.
- (62) Koeller, S.; Kadota, J.; Deffieux, A.; Peruch, F.; Massip, S.; Léger, J. M.; Desvergne, J. P.; Bibal, B. *J. Am. Chem. Soc.* **2009**, *131* (42), 15088–15089.
- (63) Blake, T. R.; Waymouth, R. M. *J. Am. Chem. Soc.* **2014**, *136* (26), 9252–9255.
- (64) Engler, A. C.; Chan, J. M. W.; Coady, D. J.; O'Brien, J. M.; Sardon, H.; Nelson, A.; Sanders, D. P.; Yang, Y. Y.; Hedrick, J. L. *Macromolecules* **2013**, *46* (4), 1283–1290.

- (65) Chang, Y. A.; Rudenko, A. E.; Waymouth, R. M. *ACS Macro Lett.* **2016**, *5* (10), 1162–1166.
- (66) Venkataraman, S.; Ng, V. W. L.; Coady, D. J.; Horn, H. W.; Jones, G. O.; Fung, T. S.; Sardon, H.; Waymouth, R. M.; Hedrick, J. L.; Yang, Y. Y. *J. Am. Chem. Soc.* **2015**, *137* (43), 13851–13860.
- (67) McKinlay, C. J.; Waymouth, R. M.; Wender, P. A. *J. Am. Chem. Soc.* **2016**, *138* (10), 3510–3517.
- (68) Sanders, D. P.; Fukushima, K.; Coady, D. J.; Nelson, A.; Fujiwara, M.; Yasumoto, M.; Hedrick, J. L. *J. Am. Chem. Soc.* **2010**, *132* (42), 14724–14726.
- (69) Ovitt, T. M.; Coates, G. W. *J. Am. Chem. Soc.* **2002**, *124* (7), 1316–1326.
- (70) Chamberlain, B. M.; Cheng, M.; Moore, D. R.; Ovitt, T. M.; Lobkovsky, E. B.; Coates, G. W. *J. Am. Chem. Soc.* **2001**, *123* (14), 3229–3238.
- (71) Bakewell, C.; Cao, T. P. A.; Long, N.; Le Goff, X. F.; Auffrant, A.; Williams, C. K. *J. Am. Chem. Soc.* **2012**, *134* (51), 20577–20580.
- (72) Zell, M. T.; Padden, B. E.; Paterick, A. J.; Thakur, K. A. M.; Kean, R. T.; Hillmyer, M. A.; Munson, E. J. *Macromolecules* **2002**, *35*, 7700–7707.
- (73) Thakur, K. a M.; Kean, R. T.; Hall, E. S.; Kolstad, J. J.; Lindgren, T. a; Doscotch, M. a; Siepmann, J. I.; Munson, E. J. *Macromolecules* **1997**, *30* (8), 2422–2428.
- (74) Todd, R.; Rubio, G.; Hall, D. J.; Tempelaar, S.; Dove, A. P. *Chem. Sci.* **2013**, *4* (3).
- (75) Dai, Z.; Cui, Y.; Chen, C.; Wu, J. *Chem. Commun.* **2016**, *52* (57), 8826–8829.
- (76) Guillaume, S. M.; Kirillov, E.; Sarazin, Y.; Carpentier, J.-F. *Chem. – A Eur. J.* **2015**, *21* (22), 7988–8003.

- (77) Cacciapaglia, R.; Di Stefano, S.; Mandolini, L. *J. Am. Chem. Soc.* **2003**, *125* (8), 2224–2227.
- (78) Beswick, J.; Blanco, V.; De Bo, G.; Leigh, D. A.; Lewandowska, U.; Lewandowski, B.; Mishiro, K. *Chem. Sci.* **2015**, *6* (1), 140–143.
- (79) Wang, J.; Feringa, B. L. *Science (80-.)*. **2011**, *331* (6023), 1429–1432.
- (80) Sud, D.; Norsten, T. B.; Branda, N. R. *Angew. Chemie Int. Ed.* **2005**, *44* (13), 2019–2021.
- (81) Neilson, B. M.; Bielawski, C. W. *J. Am. Chem. Soc.* **2012**, *134* (30), 12693–12699.
- (82) Samanta, M.; Siva Rama Krishna, V.; Bandyopadhyay, S. *Chem. Commun.* **2014**, *50* (73), 10577–10579.
- (83) Imahori, T.; Yamaguchi, R.; Kurihara, S. *Chem. – A Eur. J.* **2012**, *18* (35), 10802–10807.
- (84) Gregson, C. K. A.; Gibson, V. C.; Long, N. J.; Marshall, E. L.; Oxford, P. J.; White, A. J. P. *J. Am. Chem. Soc.* **2006**, *128* (23), 7410–7411.
- (85) Broderick, E. M.; Guo, N.; Wu, T.; Vogel, C. S.; Xu, C.; Sutter, J.; Miller, J. T.; Meyer, K.; Cantat, T.; Diaconescu, P. L. *Chem. Commun.* **2011**, *47* (35), 9897–9899.
- (86) Yoon, H. J.; Kuwabara, J.; Kim, J.-H.; Mirkin, C. A. *Science (80-.)*. **2010**, *330* (6000), 66–69.
- (87) Broderick, E. M.; Guo, N.; Vogel, C. S.; Xu, C.; Sutter, J.; Miller, J. T.; Meyer, K.; Mehrkhodavandi, P.; Diaconescu, P. L. *J. Am. Chem. Soc.* **2011**, *133* (24), 9278–9281.
- (88) Romain, C.; Williams, C. K. *Angew. Chemie Int. Ed.* **2014**, *53* (6), 1607–1610.

- (89) Sohtome, Y.; Tanaka, S.; Takada, K.; Yamaguchi, T.; Nagasawa, K. *Angew. Chemie Int. Ed.* **2010**, *49* (48), 9254–9257.
- (90) Piermattei, A.; Karthikeyan, S.; Sijbesma, R. P. *Nat. Chem.* **2009**, *1*, 133–137.
- (91) Coulembier, O.; Moins, S.; Todd, R.; Dubois, P. *Macromolecules* **2014**, *47* (2), 486–491.
- (92) Tian, X.; Cassani, C.; Liu, Y.; Moran, A.; Urakawa, A.; Galzerano, P.; Arceo, E.; Melchiorre, P. *J. Am. Chem. Soc.* **2011**, *133* (44), 17934–17941.
- (93) Blanco, V.; Leigh, D. A.; Marcos, V.; Morales-Serna, J. A.; Nussbaumer, A. L. *J. Am. Chem. Soc.* **2014**, *136* (13), 4905–4908.
- (94) Broderick, E. M.; Thuy-Boun, P. S.; Guo, N.; Vogel, C. S.; Sutter, J.; Miller, J. T.; Meyer, K.; Diaconescu, P. L. *Inorg. Chem.* **2011**, *50* (7), 2870–2877.
- (95) Miyake, G. M.; Chen, E. Y. X. *Macromolecules* **2011**, *44* (11), 4116–4124.
- (96) Zhu, J.-B.; Chen, E. Y.-X. *J. Am. Chem. Soc.* **2015**, *137* (39), 12506–12509.
- (97) Banik, S. M.; Levina, A.; Hyde, A. M.; Jacobsen, E. N. *Science* (80-.). **2017**, *358* (6364), 761–764.
- (98) Liu, J.; Chen, C.; Li, Z.; Wu, W.; Zhi, X.; Zhang, Q.; Wu, H.; Wang, X.; Cui, S.; Guo, K. *Polym. Chem.* **2015**, *6* (20), 3754–3757.
- (99) Rostami, A.; Sadeh, E.; Ahmadi, S. *J. Polym. Sci. Part A Polym. Chem.* **2017**, *55*, 2483–2493.
- (100) Liu, J.; Xu, J.; Li, Z.; Xu, S.; Wang, X.; Wang, H.; Guo, T.; Gao, Y.; Zhang, L.; Guo, K. *Polym. Chem.* **2017**, *8*, 7054–7068.
- (101) Ni, X.; Li, X.; Wang, Z.; Cheng, J. P. *Org. Lett.* **2014**, *16* (6), 1786–1789.
- (102) Jakab, G.; Tancon, C.; Zhang, Z.; Lippert, K. M.; Schreiner, P. R. *Org. Lett.* **2012**,

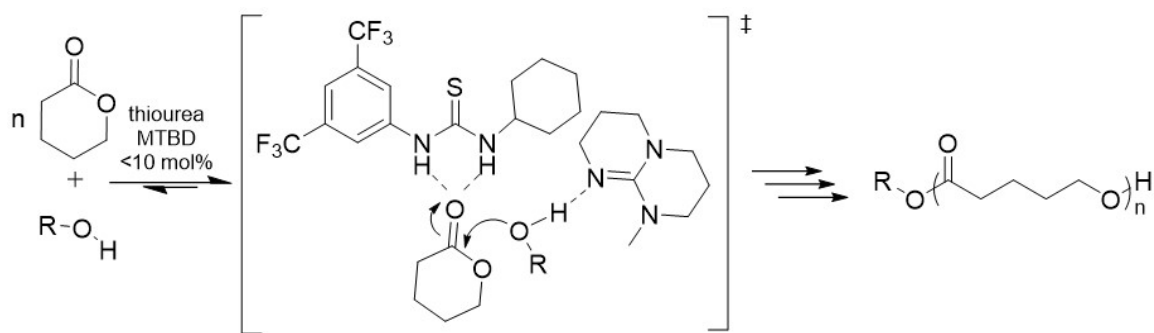
14 (7), 1724–1727.

- (103) Xu, S.; Sun, H.; Liu, J.; Xu, J.; Pan, X.; Dong, H.; Liu, Y.; Li, Z.; Guo, K. *Polym. Chem.* **2016**, 7 (44), 6843–6853.
- (104) Wittkopp, A.; Schreiner, P. R. *Chem. - A Eur. J.* **2003**, 9 (2), 407–414.
- (105) Fastnacht, K. V.; Spink, S. S.; Dharmaratne, N. U.; Pothupitiya, J. U.; Datta, P. P.; Kiesewetter, E. T.; Kiesewetter, M. K. *ACS Macro Lett.* **2016**, 5 (8), 982–986.
- (106) Anslyn, E. V.; Dougherty, D. A. In *Modern Physical Organic Chemistry*; University Science, 2006; pp 145–222.
- (107) Fastnacht, K. V.; Dharmaratne, N. U.; Kiesewetter, M. K. *Unpubl. results*.
- (108) Dharmaratne, N. U.; Pothupitiya, J. U.; Bannin, T. J.; Kazakov, O. I.; Kiesewetter, M. K. *ACS Macro Lett.* **2017**, 6 (4), 421–425.
- (109) Blain, M.; Yau, H.; Jean-Gérard, L.; Auvergne, R.; Benazet, D.; Schreiner, P. R.; Caillol, S.; Andrioletti, B. *ChemSusChem* **2016**, 9 (16), 2269–2272.
- (110) Mezzasalma, L.; Dove, A. P.; Coulembier, O. *Eur. Polym. J.* **2017**, 95 (May), 628–634.
- (111) Alba, A.; Schopp, A.; De Sousa Delgado, A.-P.; Cherif-Cheikh, R.; Martín-Vaca, B.; Bourissou, D. *J. Polym. Sci. Part A Polym. Chem.* **2010**, 48 (4), 959–965.
- (112) Delcroix, D.; Couffin, A.; Susperregui, N.; Navarro, C.; Maron, L.; Martín-Vaca, B.; Bourissou, D. *Polym. Chem.* **2011**, 2 (10), 2249–2256.
- (113) Susperregui, N.; Delcroix, D.; Martín-Vaca, B.; Bourissou, D.; Maron, L. *J. Org. Chem.* **2010**, 75 (19), 6581–6587.
- (114) Kan, S.; Jin, Y.; He, X.; Chen, J.; Wu, H.; Ouyang, P.; Guo, K.; Li, Z. *Polym. Chem.* **2013**, 4 (21), 5432.

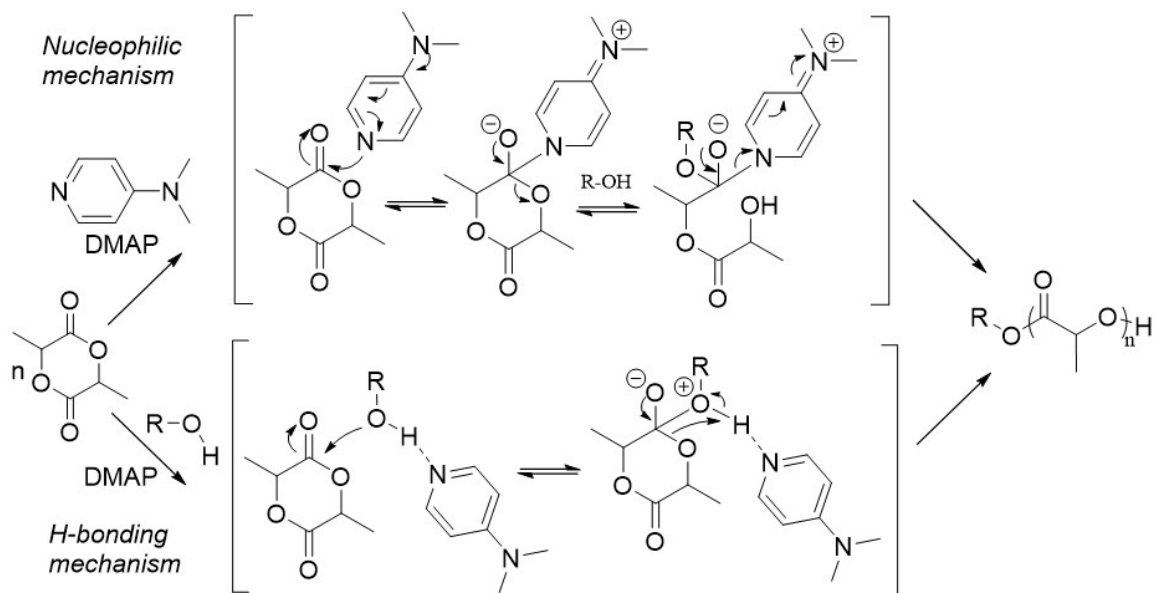
- (115) He, X.; Ji, Y.; Jin, Y.; Kan, S.; Xia, H.; Chen, J.; Liang, B.; Wu, H.; Guo, K.; Li, Z. *J. Polym. Sci. Part A Polym. Chem.* **2014**, *52* (7), 1009–1019.
- (116) Chen, J.; Kan, S.; Xia, H.; Zhou, F.; Chen, X.; Jiang, X.; Guo, K.; Li, Z. *Polym. (United Kingdom)* **2013**, *54* (16), 4177–4182.
- (117) Macdonald, E. K.; Shaver, M. P. *Eur. Polym. J.* **2017**, *95* (April), 702–710.
- (118) Akiyama, T. *Chem. Rev.* **2007**, *107* (12), 5744–5758.
- (119) Thomas, C.; Peruch, F.; Deffieux, A.; Milet, A.; Desvergne, J. P.; Bibal, B. *Adv. Synth. Catal.* **2011**, *353* (7), 1049–1054.
- (120) Thomas, C.; Peruch, F.; Bibal, B. *All Res. J. Chem.* **2012**, *3*, 7–11.
- (121) Coulembier, O.; Sanders, D. P.; Nelson, A.; Hollenbeck, A. N.; Horn, H. W.; Rice, J. E.; Fujiwara, M.; Dubois, P.; Hedrick, J. L. *Angew. Chemie - Int. Ed.* **2009**, *48* (28), 5170–5173.
- (122) Taft, R. W.; Bordwell, F. G. *Acc. Chem. Res.* **1988**, *21* (12), 463–469.
- (123) Li, X.; Zhang, Q.; Li, Z.; Wang, X.; Liu, J.; Cui, S.; Xu, S.; Zhao, C.; Chen, C.; Guo, K. *Polym. (United Kingdom)* **2016**, *84*, 293–303.
- (124) Li, X.; Zhang, Q.; Li, Z.; Xu, S.; Zhao, C.; Chen, C.; Zhi, X.; Wang, H.; Zhu, N.; Guo, K. *Polym. Chem.* **2016**, *7* (7), 1368–1374.
- (125) Zhang, D.; Jardel, D.; Peruch, F.; Calin, N.; Dufaud, V.; Dutasta, J. P.; Martinez, A.; Bibal, B. *European J. Org. Chem.* **2016**, *2016* (8), 1619–1624.
- (126) Sun, H.; Xu, S.; Li, Z.; Xu, J.; Liu, J.; Wang, X.; Wang, H.; Dong, H.; Liu, Y.; Guo, K. *Polym. Chem.* **2017**, *1*, 5570–5579.
- (127) Thomas, C.; Milet, A.; Peruch, F.; Bibal, B. *Polym. Chem.* **2013**, *4* (12), 3491–3498.

- (128) Coady, D. J.; Fukushima, K.; Horn, H. W.; Rice, J. E.; Hedrick, J. L. *Chem. Commun.* **2011**, 47 (47), 3105–3107.
- (129) Brown, H. A.; De Crisci, A. G.; Hedrick, J. L.; Waymouth, R. M. *ACS Macro Lett.* **2012**, 1 (9), 1113–1115.
- (130) Kadota, J.; Pavlović, D.; Desvergne, J. P.; Bibal, B.; Peruch, F.; Deffieux, A. *Macromolecules* **2010**, 43 (21), 8874–8879.
- (131) Kadota, J.; Pavlović, D.; Hirano, H.; Okada, A.; Agari, Y.; Bibal, B.; Deffieux, A.; Peruch, F. *RSC Adv.* **2014**, 4 (28), 14725.
- (132) Gontard, G.; Amgoune, A.; Bourissou, D. *J. Polym. Sci. Part A Polym. Chem.* **2016**, 54 (20), 3253–3256.
- (133) Wang, X.; Cui, S.; Li, Z.; Kan, S.; Zhang, Q.; Zhao, C.; Wu, H.; Liu, J.; Wu, W.; Guo, K. *Polym. Chem.* **2014**, 5 (20), 6051–6059.
- (134) Coulembier, O.; Josse, T.; Guillerm, B.; Gerbaux, P.; Dubois, P. *Chem. Commun.* **2012**, 48 (95), 11695.
- (135) Zhi, X.; Liu, J.; Li, Z.; Wang, H.; Wang, X.; Cui, S.; Chen, C.; Zhao, C.; Li, X.; Guo, K. *Polym. Chem.* **2016**, 7 (2), 339–349.
- (136) Chen, S.; Liu, Y.; Li, Z.; Wang, X.; Dong, H.; Sun, H.; Yang, K.; Gebru, H.; Guo, K. *Eur. Polym. J.* **2017**, 97 (November), 389–396.
- (137) Guillerm, B.; Lemaure, V.; Cornil, J.; Lazzaroni, R.; Dubois, P.; Coulembier, O. *Chem. Commun. (Camb)*. **2014**, 50 (70), 10098–10101.
- (138) Tsutsumi, Y.; Yamakawa, K.; Yoshida, M.; Ema, T.; Sakai, T. *Org. Lett.* **2010**, 12 (24), 5728–5731.
- (139) Becker, J. M.; Tempelaar, S.; Stanford, M. J.; Pounder, R. J.; Covington, J. A.;

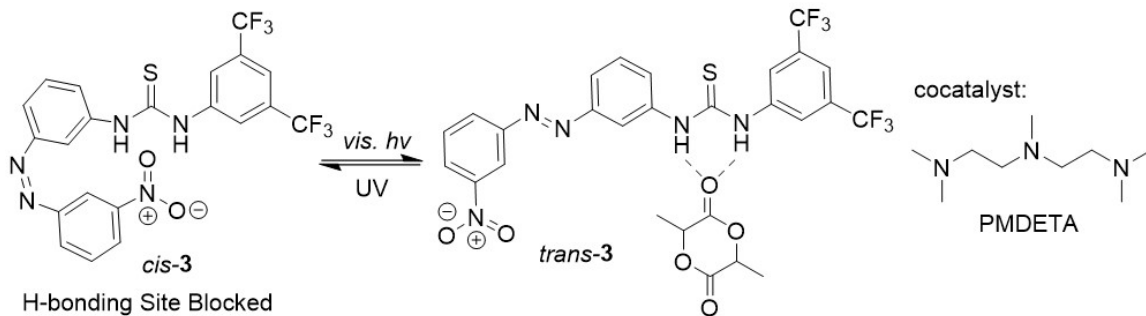
- Dove, A. P. *Chem. - A Eur. J.* **2010**, *16* (20), 6099–6105.
- (140) Harada, A.; Osaki, M.; Takashima, Y.; Yamaguchi, H. *Acc. Chem. Res.* **2008**, *41* (9), 1143–1152.
- (141) Takashima, Y.; Osaki, M.; Harada, A. *J. Am. Chem. Soc.* **2004**, *126* (42), 13588–13589.
- (142) Osaki, M.; Takashima, Y.; Yamaguchi, H.; Harada, A. *Macromolecules* **2007**, *40* (9), 3154–3158.
- (143) Glockner, P.; Ritter, H. *Macromol. Chem. Phys.* **2000**, *201* (17), 2455–2457.
- (144) Takayanagi, M.; Ito, S.; Matsumoto, K.; Nagaoka, M. *J. Phys. Chem. B* **2016**, *120* (29), 7174–7181.
- (145) Kieseewetter, M. K.; Scholten, M. D.; Kirn, N.; Weber, R. L.; Hedrick, J. L.; Waymouth, R. M. *J. Org. Chem.* **2009**, *74* (24), 9490–9496.
- (146) Horn, H. W.; Jones, G. O.; Wei, D. S.; Fukushima, K.; Lecuyer, J. M.; Coady, D. J.; Hedrick, J. L.; Rice, J. E. *J. Phys. Chem. A* **2012**, *116* (51), 12389–12398.



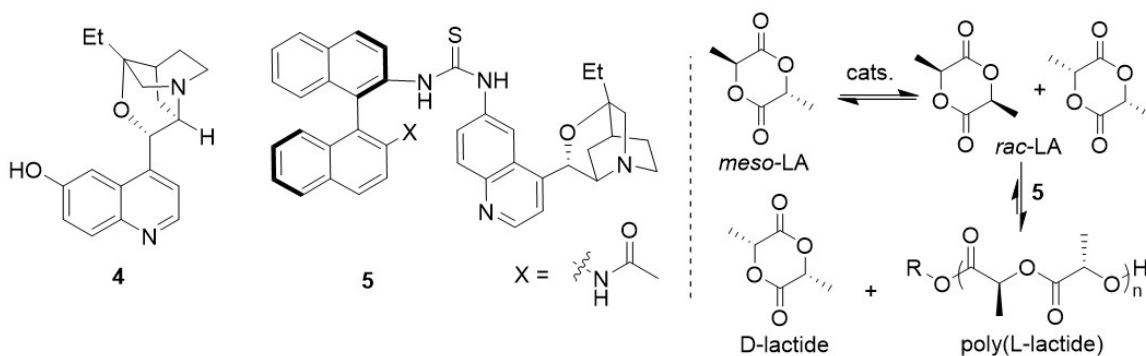
Scheme 1.1. Dual catalyst (bimolecular) mediated ROP of δ -valerolactone. Thiourea and MTBD are exemplary H-bond donors (HBDs) and H-bond acceptors (HBAs), respectively.



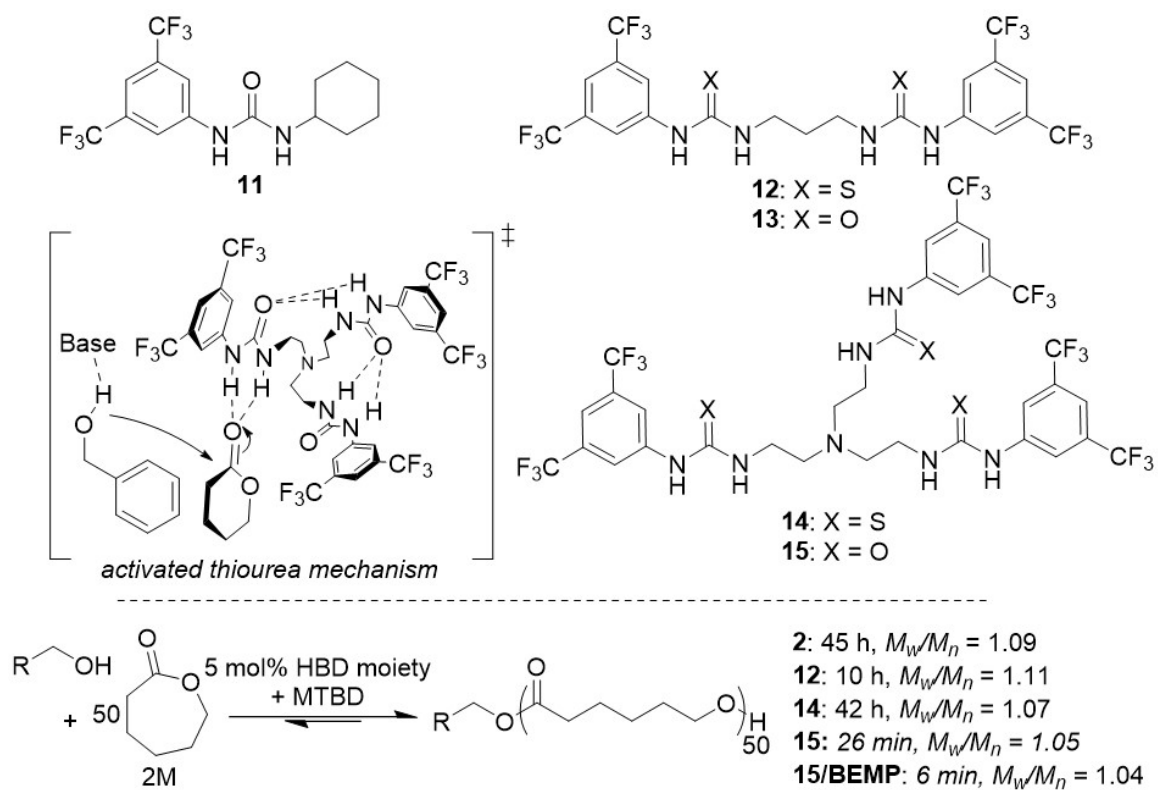
Scheme 1.2. DMAP catalyzed ROP of lactide has been proposed to proceed via nucleophilic (upper) and H-bond mediated (lower) pathways.



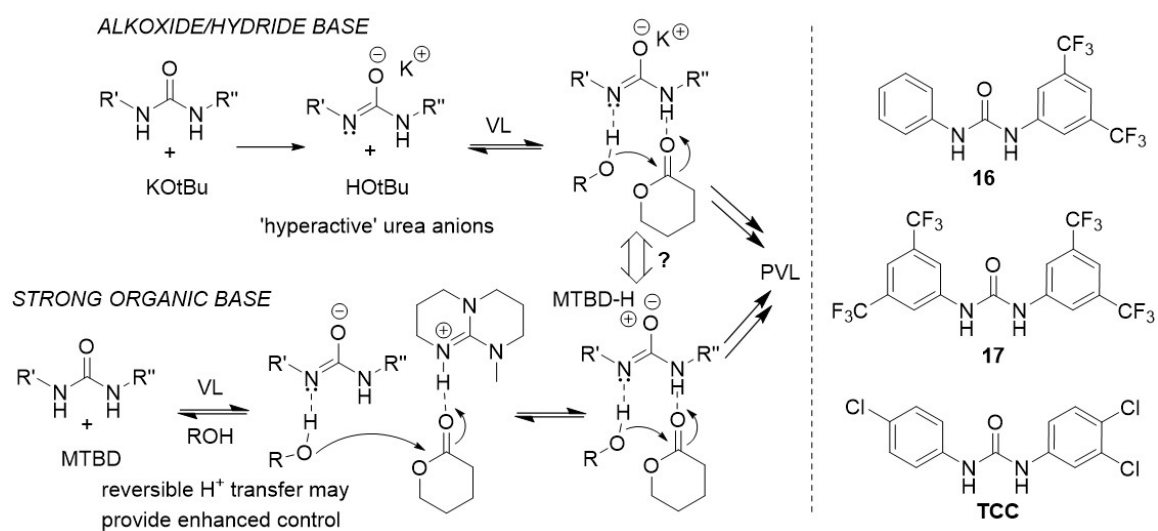
Scheme 1.3. Azobenzene-based switchable thiourea.



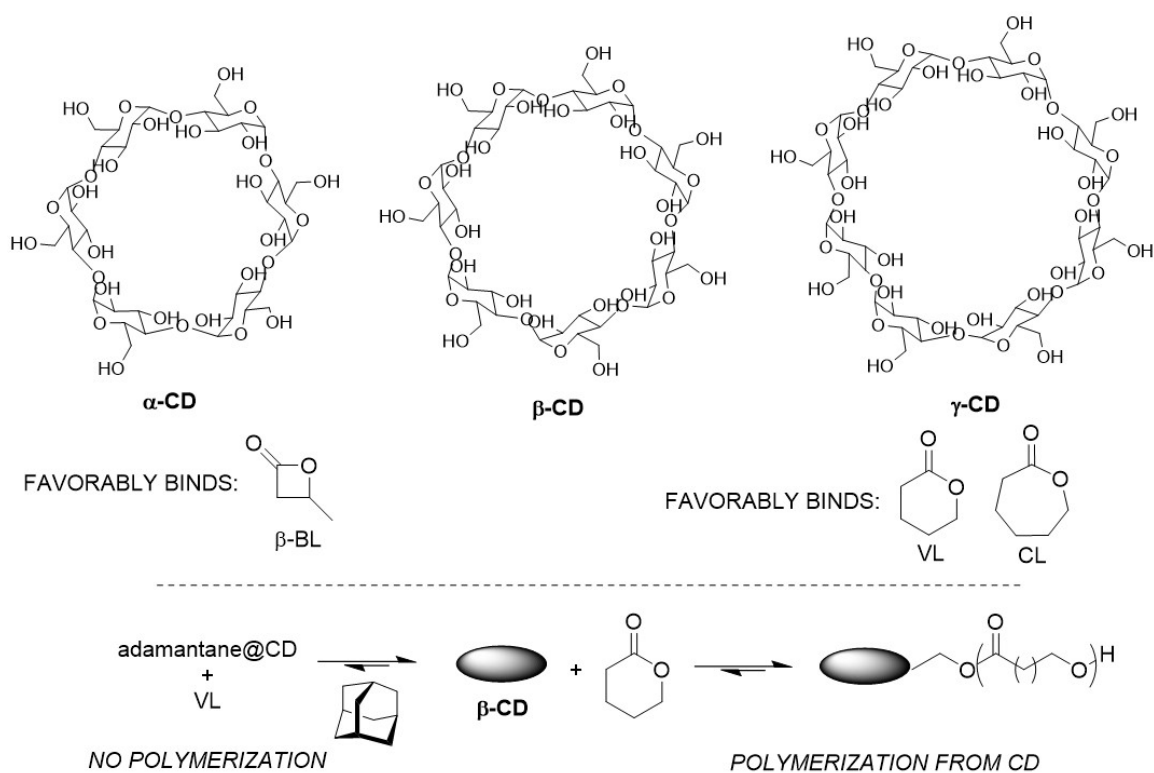
Scheme 1.4. Cinchona alkaloid-based H-bond donors for the stereoselective ROP of *rac*-lactide.



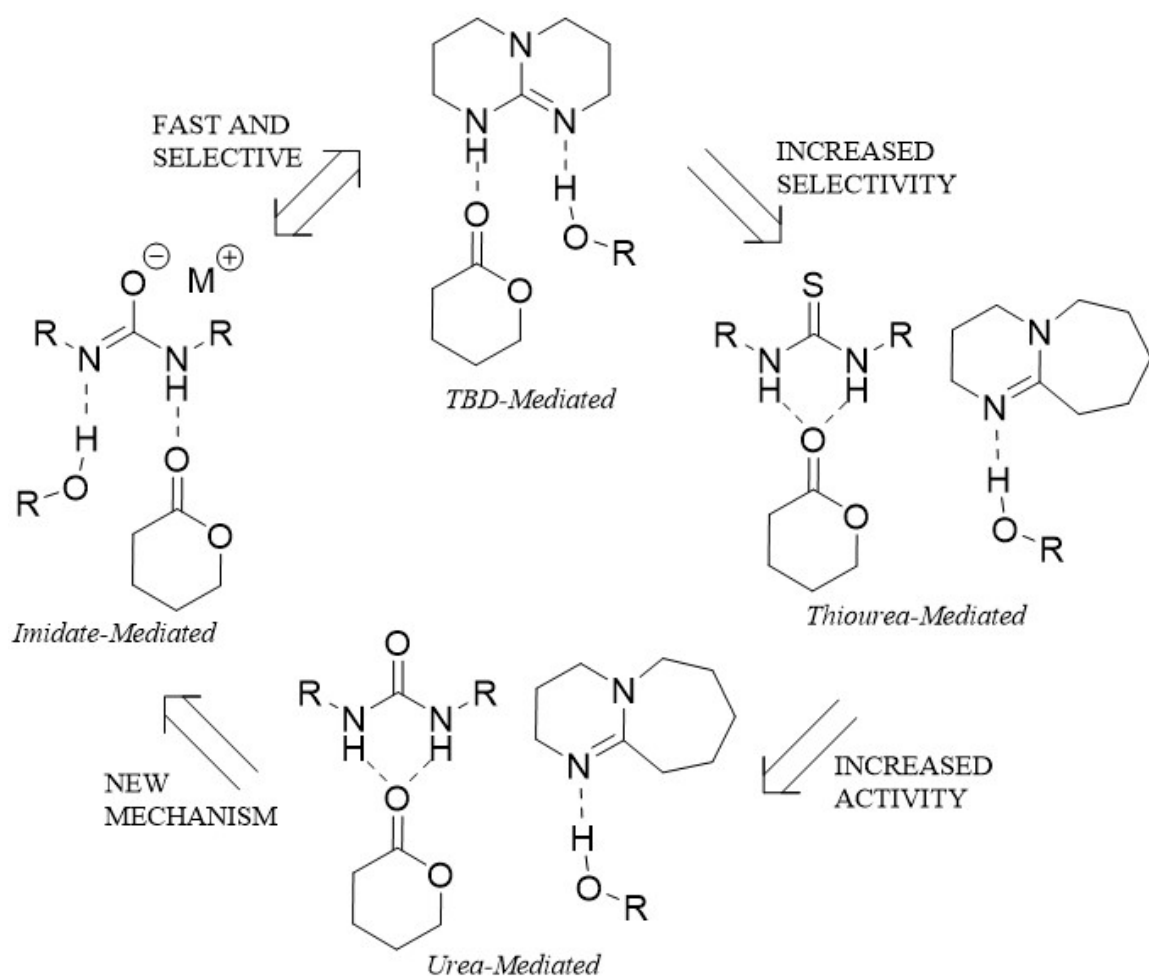
Scheme 1.5. Multi-(thio)urea H-bond donors for ROP.



Scheme 1.6. Urea anion mediated ROP.



Scheme 1.7. Cyclodextrin promoted ROP of lactones.



Scheme 1.8. Evolution of dual catalysts for ROP.

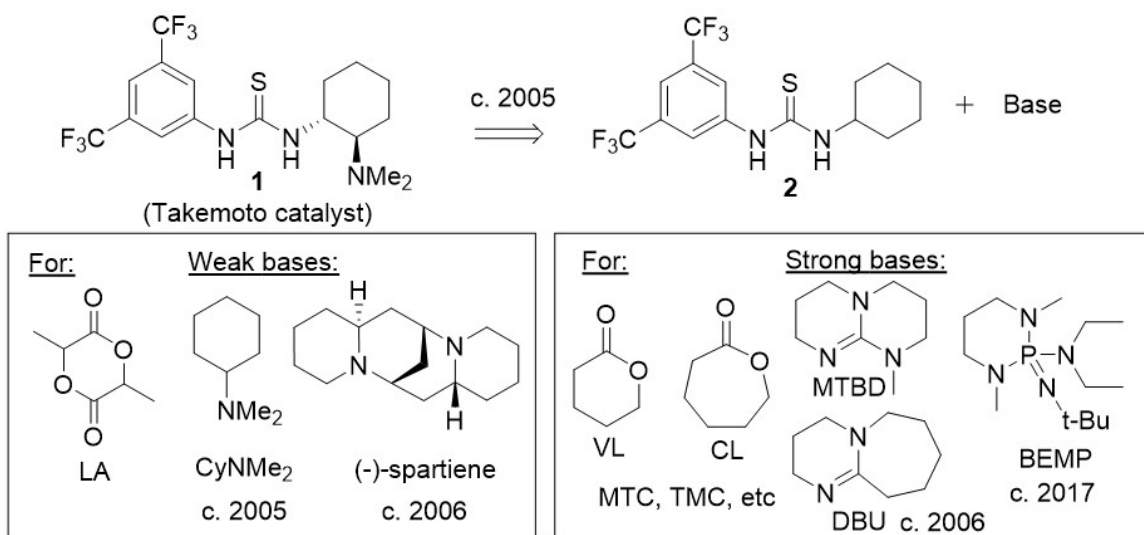


Figure 1.1. The Takemoto catalyst was the inspiration for the popular thiourea plus base catalyst system. Weaker base cocatalysts effect the ROP of lactide, while stronger bases open other monomers.

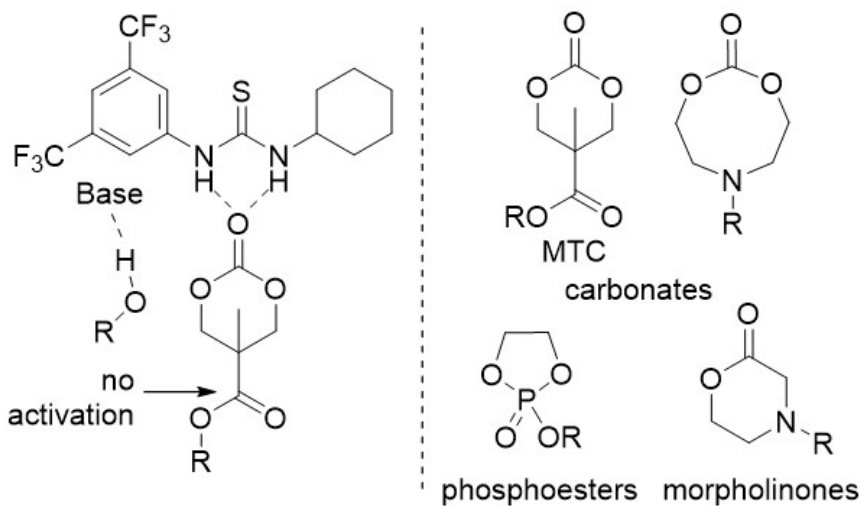


Figure 1.2. Functionalizable monomers which undergo controlled ROP by **2**/base.

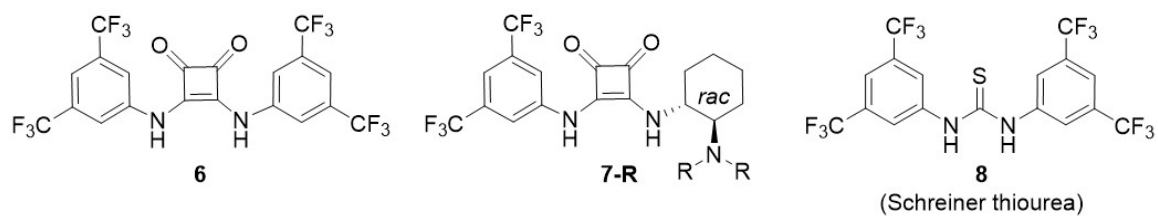


Figure 1.3. Squaramide H-bond donors for ROP of lactide.

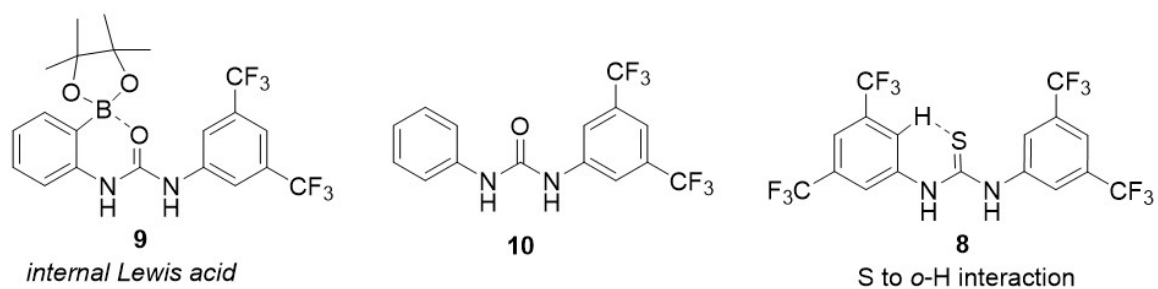


Figure 1.4. Internal Lewis acid stabilized (thio)ureas for ROP.

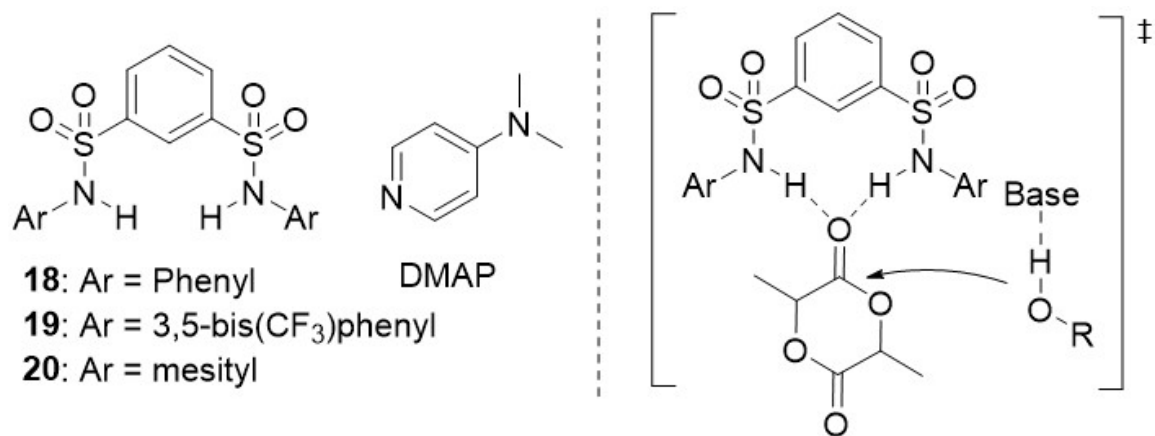


Figure 1.5. Sulfonamide H-bonding catalysts.

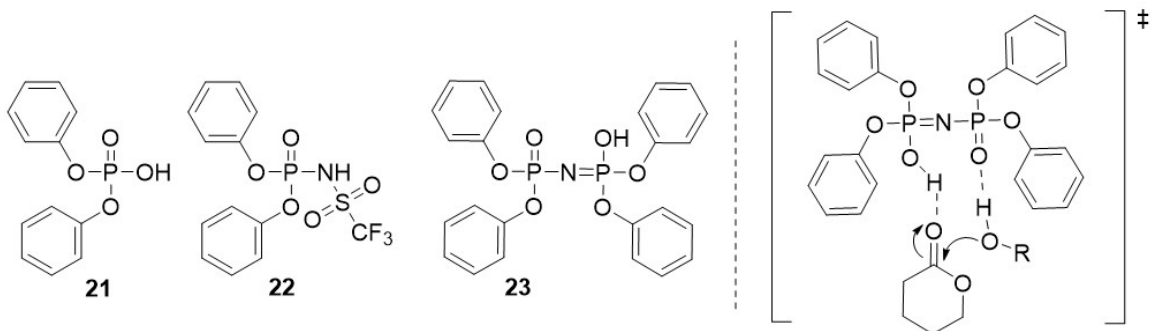


Figure 1.6. Diphenyl phosphate, phosphoramidic and imidodiphosphoric acid catalyzed ROP.

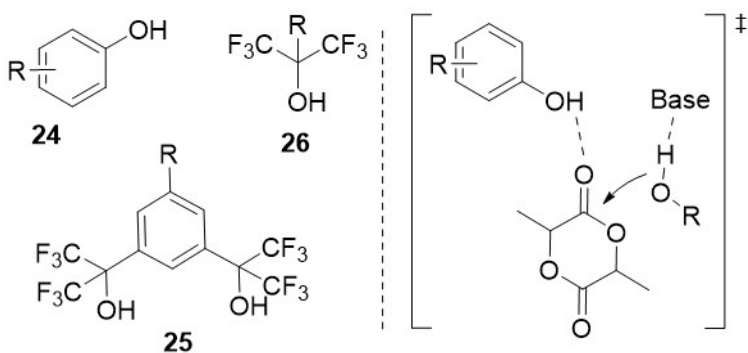


Figure 1.7. Phenol and benzylic alcohol H-bond donors for ROP.

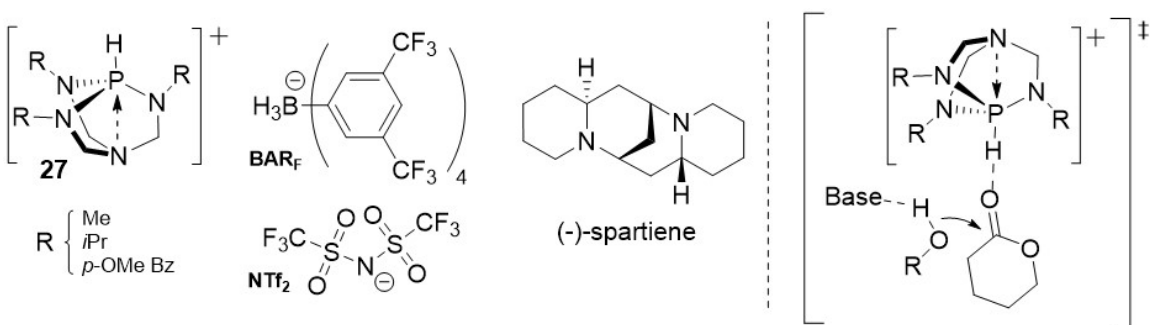


Figure 1.8. Azaphosphatrane H-bond donor.

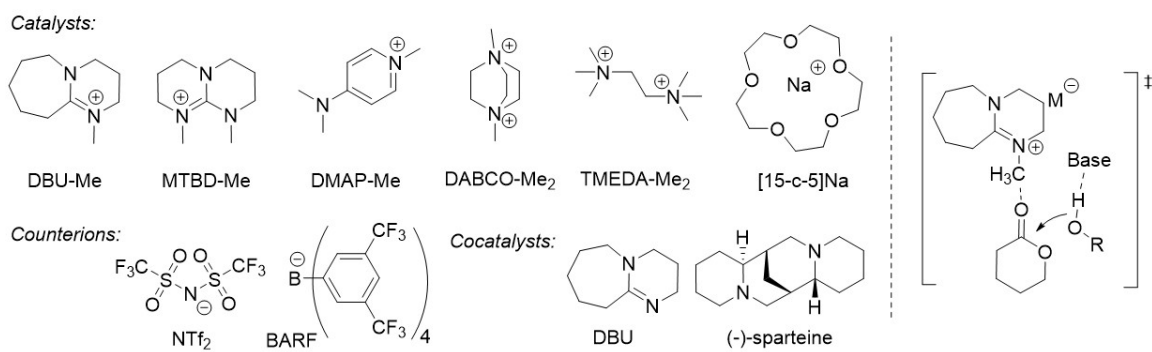


Figure 1.9. Electrophilic monomer activation by stable cations.

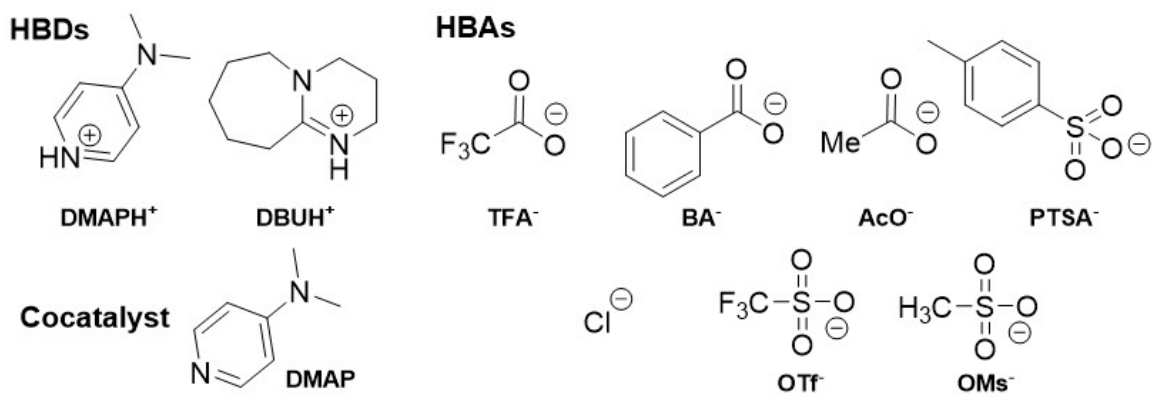


Figure 1.10. Bronsted acid and base cocatalysts for ROP.

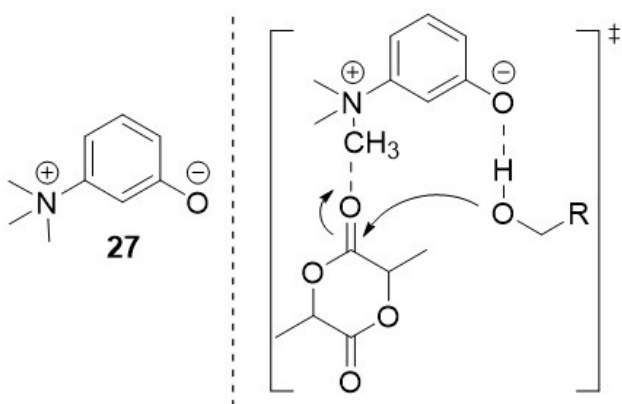


Figure 1.11. Ammonium betaine mediated ROP.

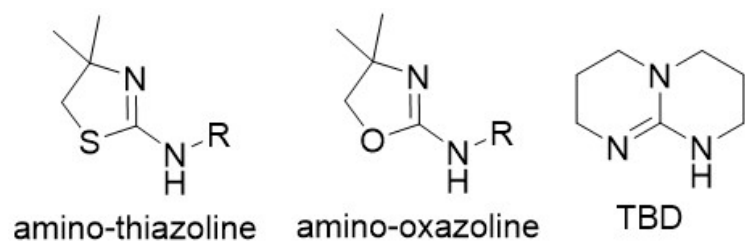


Figure 1.12. Thiazoline and oxazoline bifunctional catalysts.

INTENTIONALLY BLANK PAGE

MANUSCRIPT – II

Published in ACS Macro Letters

**Bis- and Tris-Urea H-Bond Donors for Ring-Opening Polymerization:
Unprecedented Activity and Control from an Organocatalyst**

Kurt V. Fastnacht, Samuel S. Spink, Nayanthara U. Dharmaratne, Jinal U. Pothupitiya,
Partha P. Datta, Elizabeth T. Kiesewetter and Matthew K. Kiesewetter
Chemistry, University of Rhode Island, Kingston, RI, USA

Corresponding Author: Matthew Kiesewetter, Ph.D.
Chemistry
University of Rhode Island
140 Flagg Road
Kingston, RI, 02881, USA
Email address: mkiesewetter@chm.uri.edu

ABSTRACT

A new class of H-bond donating ureas was developed for the ring-opening polymerization (ROP) of lactone monomers, and they exhibit dramatic rate acceleration versus previous H-bond mediated polymerization catalysts. The most active of these new catalysts, a tris-urea H-bond donor, is among the most active organocatalysts known for ROP, yet it retains the high selectivity of H-bond mediated organocatalysts. The urea cocatalyst, along with an H-bond accepting base, exhibits the characteristics of a “living” ROP, is highly active, in one case, accelerating a reaction from days to minutes, and remains active at low catalyst loadings. The rate acceleration exhibited by this H-bond donor occurs for all base cocatalysts examined. A mechanism of action is proposed, and the new catalysts are shown to accelerate small molecule transesterifications versus currently known mono-thiourea catalysts. It is no longer necessary to choose between a highly active or highly selective organocatalyst for ROP.

INTRODUCTION

The H-bonding catalysts for ring-opening polymerization (ROP) stand out among the highly controlled polymerization methods for their ability to tolerate functional groups while precisely controlling molecular weight and polydispersity.¹⁻⁷ H-bond donating cocatalysts are believed to effect a “living” ROP via dual activation of monomer by a H-bond donor, usually a thiourea (TU), and activation of alcohol chain end by base cocatalyst.^{8,9} The exquisite and remarkable combination of rate and selectivity present in other fields (e.g., olefin polymerization catalysis)^{10,11} has yet to be paralleled in organocatalytic ROP, especially H-bond mediated transformations. The development of organocatalysts for polymerization has largely proceeded along divergent pathways toward highly selective^{1,9,12-15} or highly active¹⁶⁻¹⁹ catalysts. Indeed, the low activity of organocatalysts for ROP has been specifically identified as a shortcoming of the field, whereas highly active metal-containing catalysts for ROP are well-known.^{20,21} We recently disclosed a bithiourea (bisTU) H-bond donating cocatalyst, **2-S** in Figure 2.1, for the ROP of L-lactide (LA), which displayed enhanced catalytic activity (over mono-TU), but no reduction in reaction control.²² During the process of extending the utility of this system to other lactone monomers, we developed a trisurea (trisU, **3-O** in Figure 2.1) H-bond donor featuring remarkable activity for the ROP of lactones. Not only does this cocatalyst demonstrate the utility of the under-explored urea motif (c.f. thiourea) of H-bond donors, but when applied with a H-bond accepting cocatalyst, it is the most active ROP organocatalyst known, and one whose enhanced rate does not come at the expense of reaction control, Scheme 2.1.

EXPERIMENTAL SECTION

General Considerations. All manipulations were performed in an MBRAUN stainless steel glovebox equipped with a gas purification system or using Schlenk technique under a nitrogen atmosphere. All chemicals were purchased from Fisher Scientific and used as received unless stated otherwise. Tetrahydrofuran and dichloromethane were dried on an Innovative Technologies solvent purification system with alumina columns and nitrogen working gas. Benzene- d_6 and chloroform- d were purchased from Cambridge Isotope Laboratories and distilled from CaH_2 under a nitrogen atmosphere. δ -valerolactone (VL; 99%), ϵ -caprolactone (CL; 99%) and benzyl alcohol were distilled from CaH_2 under reduced pressure. 1,3-diaminopropane, 3,5-bis(trifluoromethyl)phenyl isocyanate and cyclohexylamine were purchased from Acros Organics. 3,5-bis(trifluoromethyl)phenyl isothiocyanate was purchased from Oakwood Products. 7-methyl-1,5,7-triazabicyclo[4.4.0]dec-5-ene (MTBD) was purchased from TCI. Tris(2-aminoethyl)amine was purchased from Alpha Aesar. The H-bond donors **1-S**, **1-O** and **2-S** were prepared according to published procedures.^{23–25} NMR experiments were performed on Bruker Avance III 300 MHz or 400 MHz spectrometers. Size exclusion chromatography (SEC) was performed at 40 °C using dichloromethane eluent on an Agilent Infinity GPC system equipped with three Agilent PLGel columns 7.5 mm \times 300 mm (5 μm , pore sizes: 103, 104, 105 Å). M_n and M_w/M_n were determined versus PS standards (500 g/mol–3150 kg/mol, Polymer Laboratories). Water and acetonitrile were all Optima HPLC grade solvents from Fisher Chemical (Fair Lawn, NJ, USA).

Mass spectrometry was performed using a Thermo Electron (San Jose, CA, USA) LTQ Orbitrap XL mass spectrometer affixed with either an atmospheric-pressure

chemical ionization (APCI) or electrospray ionization (ESI) interface, positive ions were produced and introduced into the instrument. Tune conditions for infusion experiments (10 $\mu\text{L}/\text{min}$ flow, sample concentration $<20 \mu\text{g}/\text{mL}$ in 50/50 v/v water/acetonitrile) were as follows: ionspray voltage, 5,000 V; capillary temperature, 275 $^{\circ}\text{C}$; sheath gas (N_2 , arbitrary units), 8; auxiliary gas (N_2 , arbitrary units), 0; capillary voltage, 35 V; and tube lens, 110 V. Prior to analysis, the instrument was calibrated for positive ions using Pierce LTQ ESI positive ion calibration solution (lot #PC197784). Ion trap experiments used N_2 as a collision gas with normalized collision energies (NCE) between 10-25 eV for multistage fragmentation. High-energy collision (HCD) experiments were performed with He as the collision gas with a NCE of 25 eV.

Computational Details. The Spartan '14 package for Windows 7 was used for all computations. Computed structures were geometry optimized at the B3LYP/6-31G* level of theory. Reported energies were calculated in CH_2Cl_2 solvent and were calculated at the B3LYP/6-31G** level of theory from the DFT-optimized structures. Energies, structures and coordinates are given below.

Synthesis of 1-[3,5-bis(trifluoromethyl)phenyl thiourea]-3-aminopropane. A dried 50 mL Schlenk flask was charged with a stir bar, dichloromethane (15.0 mL) and 1,3-diaminopropane (0.45 mL, 5.40 mmol). 3,5-bis(trifluoromethyl)phenyl isothiocyanate (1.00 mL, 5.495 mmol) was added dropwise to the round bottom flask. The solution was stirred for 24 hours, and the solvent was removed under reduced pressure. The resulting solid was purified via silica gel column chromatography with 90 : 10, dichloromethane : methanol mobile phase. Yield: 21%. ^1H NMR (300 MHz, DMSO) spectrum below.

Product was carried on without full characterization. ^1H NMR (300 MHz, $\text{C}_2\text{D}_6\text{OS}$) δ 1.6 (p, $J = 6$, 2H) 2.65 (t, $J = 6$, 2H) 3.54 (br, 2H) 7.69 (s, 1H) 8.23 (s, 2H).

Synthesis of 2-OS. 1-[3,5-bis(trifluoromethyl)phenyl thiourea]-3-aminopropane (100.8 mg, 0.292 mmol) was added to a dried 10 mL Schlenk flask containing dichloromethane (1 mL), 3,5-bis(trifluoromethyl)phenyl isocyanate (74.0 mL, 0.290 mmol). Product precipitated from solution and was isolated by decanting the solvent. Solid was recrystallized from dichloromethane and dried under high vacuum overnight. Yield: 70%. HRMS m/z calcd ($\text{C}_{21}\text{H}_{16}\text{F}_{12}\text{N}_4\text{OS} + \text{H}^+$) 601.0926, found 601.0893. ^1H NMR (300 MHz, DMSO-d_6) δ 1.74 (p, $J = 6$, 2H) 3.19 (q, $J = 6$, 2H) 3.55 (br, 2H) 6.75 (t, $J = 6$, 1H) 7.53 (s, 1H) 7.73 (s, 1H) 8.08 (s, 2H) 8.24 (s, 2H) 9.33 (s, 1H) 10.15 (s, 1H). ^{13}C NMR (75 MHz, acetone- d_6) δ 29.0, 36.8, 41.4, 113.0, 115.7, 116.8, 121.1, 121.5, 123.0 (q), 124.8, 130.2 (q), 141.5, 142.2, 154.5, 180.1.

Synthesis of 2-O. A dried 10 mL Schlenk flask was charged with a stir bar, dichloromethane (7 mL), 1,3-diaminopropane (35.9 μL , 0.43 mmol). 3,5-bis(trifluoromethyl)phenyl isocyanate (148.6 μL , 0.86 mmol) was added dropwise to the round bottom flask. The resulting slurry was stirred for 1 hr, filtered and washed with cold dichloromethane. Yield: 97%. HRMS m/z calcd ($\text{C}_{21}\text{H}_{16}\text{F}_{12}\text{N}_4\text{O}_2 + \text{H}^+$) 585.1154, found 585.1100. ^1H NMR (300 MHz, DMSO-d_6) δ 1.68 (p, $J = 6$ Hz, 2H) 3.22 (q, $J = 6$ Hz, 4H) 6.59 (t, $J = 6$, 2H) 7.58 (s, 2H) 8.14 (s, 4H) 9.39 (s, 2H). ^{13}C NMR (75 MHz, DMSO-d_6) δ 30.3, 36.6, 113.3, 117.1, 123.3 (q), 130.5 (q), 142.6, 154.9.

Synthesis of 3-S. A dried 100 mL Schlenk flask was charged with a stir bar, tetrahydrofuran (50 mL), tris(2-aminoethyl) amine (1.05 mL, 6.84 mmol), 3,5-bis(trifluoromethyl)phenyl isocyanate (3.90 mL, 21.20 mmol). The solution was left to

stir for 24 hrs and the solvent was subsequently removed in vacuo. The resulting solid product was purified using a silica gel column with a 90 : 10, hexanes : ethyl acetate mobile phase. Product was removed of volatiles under high vacuum overnight. Yield: 87%. HRMS m/z calcd ($C_{33}H_{27}F_{18}N_7S_3 + H^+$) 960.1275, found 960.1262. 1H NMR (300 MHz, acetone- d_6) δ 2.82 (t, $J = 6$, 6H) 3.68 (m, 6H) 7.44 (s, 3H) 7.71 (br, 2H) 8.04 (s, 6H) 9.40 (br, 2H). ^{13}C NMR (75 MHz, acetone- d_6) δ 43.7, 53.7, 117.6, 123.3, 124.2 (q), 131.8 (q), 142.5, 182.1.

Synthesis of 3-O. A dried 100 mL Schlenk flask was charged with a stir bar, tetrahydrofuran (50 mL), tris(2-aminoethyl) amine (1.03 mL, 6.84 mmol), 3,5-bis(trifluoromethyl)phenylisocyanate (3.6 mL, 21.20 mmol). The solution was stirred for 24 hrs. The solvent was removed in vacuo. Resulting solid was purified using a silica gel column with a 96:4 dichloromethane:methanol mobile phase. Yield: 88%. HRMS m/z calcd ($C_{33}H_{27}F_{18}N_7O_3 + H^+$) 912.1961, found 912.1933. 1H NMR (300 MHz, acetone- d_6) δ 2.58 (t, $J = 3$, 6H) 3.21 (m, 6H) 6.32 (m, 2 H) 7.29 (s, 3H) 7.86 (s, 6H) 8.58 (s, 2H). ^{13}C NMR (75 MHz, acetone- d_6) δ 39.3, 55.8, 114.9, 118.3, 124.4 (q), 132.3 (q), 143.3, 156.3.

Example VL Polymerization Experiment. A 7 mL vial was charged with **3-O** (15.2 mg, 0.0167 mmol), MTBD (2.4 μ L, 0.0167 mmol), benzyl alcohol (2.08 μ L, 0.01999 mmol) and C_6D_6 (250 μ L). In a second 7 mL vial, VL (0.100 g, 0.999 mmol) was dissolved in C_6D_6 (249 μ L). The contents of the second vial were transferred to the first via pipette and stirred until homogenous, approximately 1 min. The contents were transferred to an NMR tube via pipette, and the reaction was monitored by 1H NMR. The reaction was quenched using benzoic acid (4.06 mg, 0.0333 mmol). Polymer was

precipitated with the addition of hexanes. Supernatant was decanted and solid PVL was dried in vacuo. Yield: 89%, $M_n = 7,500$, $M_w/M_n = 1.07$.

Chain Extension Experiment. A 7 mL vial was loaded with **3-O** (13.3 mg, 0.015 mmol), MTBD (2.2 mg, 0.015 mmol), 1-pyrenebutanol (9.6 mg, 0.035 mmol), and C_6D_6 (219 μ L). In a second 7mL vial, CL (100 mg, 0.876 mmol) and C_6D_6 (219 μ L) were loaded. The contents of the second vial were added to the first and stirred. After 15 min, a 150 μ L aliquot was taken from the reaction vial, quenched with benzoic acid (1.2mg, 0.010 mmol), and additional CL (197.3 mg, 1.723 mmol) was added to the reaction vial. After another 50 min, a second aliquot was quenched with benzoic acid (1.2 mg, 0.010 mmol). Samples from both the first and second aliquots were then transferred to NMR tubes and conversion was determined via 1H NMR analysis. The remainder of the aliquots was precipitated with the addition of hexane, and the supernatants were decanted. Each solid PCL sample was dried in vacuo, and GPC analysis was performed.

Example Copolymerization Experiment. A 7 mL vial was charged with **3-O** (15.2 mg, 0.0167 mmol), MTBD (2.4 μ L, 0.0167 mmol), benzyl alcohol (1.04 μ L, 0.00999 mmol) and C_6D_6 (250 μ L). In a second 7 mL vial, VL (0.100 g, 0.999 mmol) and CL (0.144 g, 0.999 mmol) were dissolved in C_6D_6 (249 μ L). The contents of vial 2 were transferred to the first via pipette and stirred until homogenous, approximately 5 sec. The contents were transferred to an NMR tube via pipette, and the reaction was monitored by 1H NMR. The reaction was quenched using benzoic acid (4.06 mg, 0.0333 mmol). Polymer was precipitated with the addition of hexanes. Supernatant was decanted and solid polymer was dried in vacuo, 91% yield (196 mg), $M_n = 21,400$; $M_w/M_n = 1.21$.

Example ROP of Lactide. L-lactide (72 mg, 0.5 mmol) and *o*-dichlorobenzene (0.5 mL) were added into a 7 mL vial and stirred until a homogenous solution was obtained. To a second 7 mL vial, benzyl alcohol (2.163 mg, 0.02 mmol), Me₆TREN (0.008 mmol) and **3-O** (0.008 mmol) were added. Contents from the first vial were transferred into vial 2 via Pasteur pipette. The contents were mixed and transferred to an NMR tube. Reaction progression was monitored by ¹H NMR. After 30 min, the reaction had reached 55% conversion and was quenched with benzoic acid. The reaction was removed of volatiles and treated with hexanes/isopropanol (1:1) to dissolve monomer. The residual polymer was subjected to dialysis in DCM against methanol. Yield: 38 mg, 52%; M_n = 2,700; M_w/M_n = 1.11.

Example Transesterification Experiment. Ethyl acetate (100 mg, 1.14 mmol), **1-S** (0.057 mmol) and C₆D₆ (0.22 mL) were added to a 7 mL glass vial. To a second 7 mL glass vial, benzyl alcohol (122.7 mg, 1.14 mmol), MTBD (0.057 mmol) and C₆D₆ (0.22 mL) were added. The contents of vial 2 were transferred via Pasteur pipette to vial 1, and the solution was stirred until homogeneous (1 min). The solution was transferred to an NMR tube, and reaction progression was monitored by ¹H NMR.

RESULTS AND DISCUSSION

The effects of bisTU on the ROP of δ -valerolactone (VL) and ϵ -caprolactone (CL) were evaluated, and the rate acceleration in the presence of **2-S** versus **1-S** is general to both lactone monomers. For the ROP of either VL or CL (2 M, 100 mg) from benzyl alcohol in C_6D_6 , the application of **2-S**/MTBD (2.5 mol % each) produces a rate acceleration over the traditional monothiourea (**1-S**/MTBD 5 mol % each) that is not associated with loss of reaction control, Table 2.1. The reactions retain the characteristics of “living” polymerizations, exhibiting a linear evolution of M_n versus conversion, first order consumption of monomer, M_n that is predictable by $[M]_0/[I]_0$ and a living chain end that is susceptible to chain extension, see Figures 2.2-7. The imine base, DBU, and phosphazene base, BEMP, are also effective cocatalysts for the ROP of lactones (with **2-S**), but the reaction is more active with MTBD cocatalyst, Table 2.1.

ROP involving **2-S** is suggested to proceed through an activated-TU mechanism, whereby one TU moiety activates the other, which in turn activates the monomer. The ROPs of VL and CL are first order in the consumption of monomer (Figure 2.3 and 2.10), which suggests one bisTU (**2-S**) molecule activating one monomer in the transition state. This is consistent with previous suggestions that H-bond-mediated ROP operates via dual activation of monomer by **1** and of alcohol chain end by base.¹ Because H-bonds require no orbital overlap and are electrostatic in nature,²⁶ we cannot rule out a dual-thiourea activated mechanism, Eq. 2.1. However, computational studies for the activation of lactones by **2-S** suggest an activated-TU mechanism is preferred over a dual-thiourea activation mechanism, Eq. 2.1; this assertion is also supported by the **2-S**/alkylamine cocatalyzed ROP of lactide.^{22,27}

The series of thiourea H-bond donating catalysts was extended to a trisTU H-bond donor, **3-S**, but this catalyst exhibits significantly reduced activity versus **1-S** or **2-S** in the TU/base cocatalyzed ROP of lactones, Table 2.1. This suggests that simply adding TU moieties does not result in faster ROP. Geometry optimized DFT computations suggest that a stable conformation of **3-S** is the C3 symmetric structure, see Figure 2.15 and 2.16. This calculated structure features a cyclic arrangement of the three TU moieties, each serving as a H-bond donor and a H-bond acceptor to each of the adjacent TU moieties with H-bond lengths of 2.61 ± 0.07 Å. We hypothesize that the added stability due to the three intramolecular H-bonds attenuates the activity of **3-S** (versus **2-S**). In contrast, the intramolecular H-bond activation in **2-S** leaves a TU moiety available for catalysis. Additive effects from multiple TU moieties are found in nature,²⁸ and such constructs have been observed to be beneficial to catalysis,^{22,29,30} although not universally so.^{24,31} Interested in extending the suite of H-bond-mediated catalysts, we noted that changing the C=S to the shorter C=O bond would be expected to disrupt the intramolecular H-bond network, freeing one urea moiety for catalysis. The trisurea H-bond donor (**3-O**) is predicted by DFT calculations to have much longer average H-bond lengths versus **3-S**, 2.92 ± 0.81 Å.

The application of the trisU (**3-O**) catalyst in combination with organic bases effects the fastest organocatalytic ROP of lactones that has been reported, yet the reaction remains highly controlled.^{3,17-21} The **3-O**/MTBD (1.67 mol % each) catalyzed ROP of VL (2 M, 100 mg) from benzyl alcohol (2 mol %) proceeds to full conversion in 3 min, Table 2.2. The comparable reactions with **2-S**/MTBD (2.5 mol % each) or **1-S**/MTBD (5 mol % each) achieve full conversion in 102 min or 2 h, respectively. The rate

acceleration for the ROP of CL with **3-O**/MTBD is even more remarkable; this reaction achieves full conversion in 26 min. This constitutes a marked rate acceleration versus **2-S** or **1-S** with MTBD, which achieves full conversion in 10 or 45 h, respectively, and the polydispersities for the **3-O**/MTBD catalyzed ROP of VL or CL remain less than $M_w/M_n = 1.07$, Table 2.2. The **3-O** mediated ROPs of both monomers are highly controlled, exhibiting the characteristics of “living” polymerizations, (see Figures 2.10 and 2.11). Initiation of a CL ROP from 1-pyrenebutanol produces PCL with overlapping refractive index and UV traces in the GPC, suggesting end-group fidelity; the “living” alcohol chain end is susceptible to chain extension by repeated additions of monomer, (see Figure 2.13). The **3-O**/MTBD cocatalysts remain active at low concentration; full conversion for the ROP of VL (2 M, C_6D_6) from benzyl alcohol ($[M]_0/[I]_0 = 50$) was achieved in 5 h at 0.25 mol % **3-O**/MTBD loading, (see Table 2.4).

The efficacy of **3-O**/base cocatalysts for the ROP of other ester and carbonate monomers was evaluated. The **3-O**/MTBD (1.67 mol %) cocatalysts are effective for the ROP of trimethylene carbonate (TMC). This reaction (100 mg TMC, 1 M in CH_2Cl_2) reaches 97% conversion in 1 min ($M_n = 9,000$; $M_w/M_n = 1.05$; $[M]_0/[I]_0 = 50$), which is more active than the **1-S**/DBU catalyzed ROP of TMC.⁵ For the ROP of LA, **3-O** (with tris[2-(dimethylamino)ethyl]amine) exhibits a solvent incompatibility with LA and PLA, resulting in the precipitation of polymer or catalyst prior to full conversion (see Figure 2.17). The best conversion was achieved in o-dichlorobenzene, 55% in 30 min ($M_n = 2,700$; $M_w/M_n = 1.11$; $[M]_0/[I]_0 = 25$; 52% yield). This is less active than our previously reported catalyst, **2-S**, which reaches full conversion in minutes.²² MALDI analysis of the PLA resulting from the ROP of LA shows only minor transesterification ($m/z = \pm 72n$; see

Figure 2.17). A copolymerization of VL and CL was conducted with **3-O**/MTBD. As determined by ^1H NMR, the consumption of VL is almost complete prior to the incorporation of CL units, suggesting the formation of a gradient-copolymer (see Figure 2.12 and Experimental Section; $M_n = 21,400$; $M_w/M_n = 1.29$; 91% yield). The H-bond donor **3-O** with MTBD is not active for the ROP of β -butyrolactone, which is consistent with other H-bonding ROP catalysts.⁸

It is proposed here that **3-O**/MTBD cocatalyzed ROP occurs via an activated-urea mechanism, whereby a single **3-O** activates a lactone and MTBD activates an alcohol chain end through H-bonding, Scheme 2.2. A plot of observed rate constant (k_{obs}) versus [**3-O**] for the ROP of VL from benzyl alcohol suggests that the ideal stoichiometry of the **3-O**/MTBD catalyzed reaction is 1:1 (see Figure 2.14). Further, the **3-O**/MTBD cocatalyzed ROP of VL is first order in monomer (see Figure 2.9), which suggests that a single **3-O** molecule acting at one monomer is present in the transition state. This is consistent with previous reports that suggest that H-bond donors featuring multiple (thio)urea moieties activate one reagent prior to the TU-reagent complex undergoing further chemistry,^{22,32} and it is also consistent with a report of a urea-thiourea H-bond donating catalyst, which was proposed to be operative via an activated-(thio)urea mechanism.²⁸ Indeed, ^1H NMR spectra (in acetone) of **1-O**, **2-O**, and **3-O** show a progressive downfield shift of the N–H protons, which can be interpreted to arise from stronger intramolecular H-bonding in **3-O** and **2-O** versus **1-O**. A multiurea activated mechanism (e.g., Eq. 2.1), which is reminiscent of a solvophobic pocket, cannot be ruled out. However, the marked inefficacy toward ROP of **3-S**, which is geometrically able to

adopt a conformation featuring strong intramolecular H-bonds (see Figure 2.15 and 2.16), suggests that the activated-urea mechanism is the more robust proposal.

Among catalysts for the ROP of lactones, the **3-O**/base cocatalysts stand out due to the extremely rapid rate that they exhibit at room temperature. For comparison, we conducted the ROP of CL (2 M) from benzyl alcohol (1 mol %) with the bifunctional catalyst TBD, Table 2.2. The guanidine base, TBD (Figure 2.1), has been regarded as one of the most active organocatalysts available for the ROP of lactones.¹⁶ The TBD catalyzed ROP of CL from benzyl alcohol (Table 2.2, entry 12) proceeds to 93% conversion in 140 min ($M_w/M_n = 1.37$), whereas the same ROP with **3-O**/MTBD (Table 2.2, entry 8) achieves 97% conversion in 26 min ($M_w/M_n = 1.05$).

In small molecule transformations, urea H-bond donating catalysts have been observed to possess similar activity to their heavy chalcogen counterparts.³³ The development of urea and thiourea H-bond donating catalysts continued apace until the turn of the millennium when several reports emerged that extolled the operational (e.g., increased solubility)^{34,35} and synthetic (e.g., higher yields and enantioselectivities)³⁵⁻³⁷ benefits of thioureas over ureas. In our estimation, the ubiquity of the thiourea motif in H-bond mediated transformations may be more due to the coincidental timing of these reports than any general superiority of thioureas over urea H-bonding catalysts. Indeed, ureas are more polar than thioureas and should be expected to be better H-bond activators,³³ and in some catalysis applications, urea catalysts are clearly superior.^{38,39} The late Margaret Etter may have presaged our observation of **3-O** as an effective H-bond donating catalyst in her characterization of aryl ureas featuring meta-electron withdrawing groups by noting that urea carbonyls are good H-bond acceptors.³⁸

The urea versions of **2** and **1** were synthesized and evaluated for their efficacy in the ROP of VL (2 M, 100 mg, 1 equiv.) from benzyl alcohol (2 mol %) in C₆D₆. In general, all n-O (n = 1, 2, or 3) catalysts were more active than the corresponding n-S H-bond donors, Tables 2.1 and 2.2. For the 2-X (X = O, S, or OS) H-bond donors, the rate of ROP increases with the progressive substitution of O (versus S) and M_w/M_n remains low. These results suggest the increased utility of ureas versus thioureas for H-bond-mediated ROP. All reported urea catalysts are soluble under the desired reaction conditions with the exception of **2-O**, which requires an extra equivalent of MTBD to become homogeneous in C₆D₆.⁴⁰ A plot of the observed rate constant (k_{obs}) versus [MTBD] for the ROP of CL from benzyl alcohol increases linearly under conditions [MTBD] ≤ [**2-S**], but becomes zero order in [MTBD] when [MTBD] > [**2-S**], (see Figure 2.7). This suggests that the proper stoichiometry of the **2-S**/MTBD catalyzed reaction is 1:1. The catalysts (1–3 with MTBD) are all operative in CH₂Cl₂, CHCl₃, and THF albeit with slightly reduced reaction rates or M_w/M_n (see Table 2.5).

Preliminary studies suggest that these catalysts exhibit the same reactivity trends in small molecule transesterification and, hence, may have general applicability beyond ROP. The transesterification of ethyl acetate (1.6 M) with benzyl alcohol (1.6 M) was conducted in C₆D₆. Observed rate constants (k_{obs}) at early reaction time were measured for each H-bond donor/MTBD cocatalyzed transesterification. These rate constants show the same trends in catalyst activity that were observed for the ROP reactions: **3-O** is the most rapid catalyst and it is 1–2 orders of magnitude more rapid than **1-S**, (see Table 2.3). This suggests a general role for the increased activation of esters by urea H-bond donors (versus thioureas), yet the slower rates for the transesterification of s-trans (versus

s-cis) esters accounts for the low rate of transesterification post polymerization, (see Table 2.6).

CONCLUSION

Urea H-bond donors in combination with base cocatalysts have been shown to be highly effective for the ROP of lactones. Despite being among the most rapid organocatalysts for ROP, the **3-O**/MTBD cocatalyzed ROPs of VL and CL are among the most controlled polymerizations, exhibiting the characteristics of “living” polymerizations and producing polymers with narrow M_w/M_n . The source of the rate acceleration versus mono- and bisurea H-bond donors is proposed to arise from successively increased intramolecular H-bond activation with each additional urea moiety. The reintroduction of the urea motif of H-bond donors to the lexicon of organocatalytic (ROP) chemistry provides a rich diversity of catalyst scaffolds to explore in mono-, bis-, tris-, and poly-H-bond donors. Previous to the discovery of trisurea cocatalyzed ROP, one was forced to choose between a highly active or highly selective organocatalyst; this age is over.

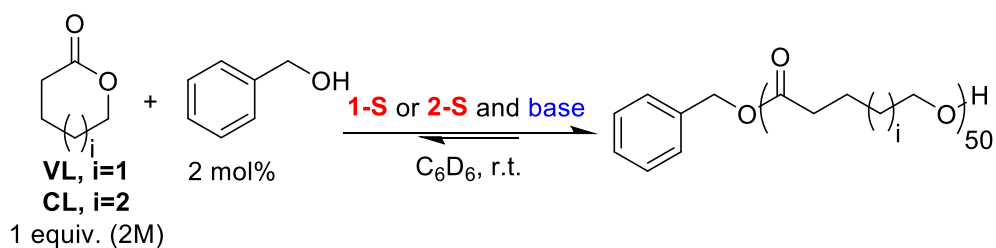
LIST OF REFERENCES

- (1) Dove, A. P.; Pratt, R. C.; Lohmeijer, B. G. G.; Waymouth, R. M.; Hedrick, J. L. *J. Am. Chem. Soc.* **2005**, *127* (40), 13798–13799.
- (2) Kamber, N. E.; Jeong, W.; Waymouth, R. M.; Pratt, R. C.; Lohmeijer, B. G. G.; Hedrick, J. L. *Chem. Rev.* **2007**, *107* (12).
- (3) Kiesewetter, M. K.; Shin, E. J.; Hedrick, J. L.; Waymouth, R. M. *Macromolecules* **2010**, *43* (5), 2093–2107.
- (4) McKinlay, C. J.; Waymouth, R. M.; Wender, P. A. *J. Am. Chem. Soc.* **2016**, *138* (10), 3510–3517.
- (5) Pratt, R. C.; Nederberg, F.; Waymouth, R. M.; Hedrick, J. L. *Chem. Commun.* **2008**, No. 1, 114–116.
- (6) Sanders, D. P.; Fukushima, K.; Coady, D. J.; Nelson, A.; Fujiwara, M.; Yasumoto, M.; Hedrick, J. L. *J. Am. Chem. Soc.* **2010**, *132* (42), 14724–14726.
- (7) Blake, T. R.; Waymouth, R. M. *J. Am. Chem. Soc.* **2014**, *136* (26), 9252–9255.
- (8) Bas G. G. Lohmeijer Frank Leibfarth, John W. Logan, R. C. P.; David A. Long Fredrik Nederberg, Jeongsoo Choi, A. P. D.; Charles Wade and James L. Hedrick, R. M. W.; Lohmeijer, B. G. G.; Pratt, R. C.; Leibfarth, F.; Logan, J. W.; Long, D. A.; Dove, A. P.; Nederberg, F.; Choi, J.; Wade, C.; Waymouth, R. M.; Hedrick, J. L. *Macromolecules* **2006**, *39* (25), 8574–8583.
- (9) Pratt, R. C.; Lohmeijer, B. G. G.; Long, D. A.; Lundberg, P. N. P.; Dove, A. P.; Li, H.; Wade, C. G.; Waymouth, R. M.; Hedrick, J. L. *Macromolecules* **2006**, *39* (23), 7863–7871.
- (10) Kiesewetter, E. T.; Randoll, S.; Radlauer, M.; Waymouth, R. M. *J. Am. Chem.*

- Soc.* **2010**, *132* (16), 5566–5567.
- (11) Cohen, A.; Kopilov, J.; Lamberti, M.; Venditto, V.; Kol, M. *Macromolecules* **2010**, *43* (4), 1689–1691.
- (12) Miyake, G. M.; Chen, E. Y. X. *Macromolecules* **2011**, *44* (11), 4116–4124.
- (13) Zhu, J.-B.; Chen, E. Y.-X. *J. Am. Chem. Soc.* **2015**, *137* (39), 12506–12509.
- (14) Delcroix, D.; Martín-Vaca, B.; Bourissou, D.; Navarro, C. *Macromolecules* **2010**, *43* (21), 8828–8835.
- (15) Makiguchi, K.; Kikuchi, S.; Satoh, T.; Kakuchi, T. *J. Polym. Sci. Part A Polym. Chem.* **2013**, *51* (11), 2455–2463.
- (16) Pratt, R. C.; Lohmeijer, B. G. G.; Long, D. A.; Waymouth, R. M.; Hedrick, J. L. *J. Am. Chem. Soc.* **2006**, *128* (14), 4556–4557.
- (17) Jeong, W.; Shin, E. J.; Culkin, D. A.; Hedrick, J. L.; Waymouth, R. M. *J. Am. Chem. Soc.* **2009**, *131* (13), 4884–4891.
- (18) Naumann, S.; Scholten, P. B. V.; Wilson, J. A.; Dove, A. P. *J. Am. Chem. Soc.* **2015**, *137* (45), 14439–14445.
- (19) Li, X.; Zhang, Q.; Li, Z.; Xu, S.; Zhao, C.; Chen, C.; Zhi, X.; Wang, H.; Zhu, N.; Guo, K. *Polym. Chem.* **2016**, *7* (7), 1368–1374.
- (20) Guillaume, S. M.; Kirillov, E.; Sarazin, Y.; Carpentier, J.-F. *Chem. – A Eur. J.* **2015**, *21* (22), 7988–8003.
- (21) Du, G.; Wei, Y.; Zhang, W.; Dong, Y.; Lin, Z.; He, H.; Zhang, S.; Li, X. *Dalt. Trans.* **2013**, *42* (4), 1278–1286.
- (22) Spink, S. S.; Kazakov, O. I.; Kiesewetter, E. T.; Kiesewetter, M. K. *Macromolecules* **2015**, *48* (17), 6127–6131.

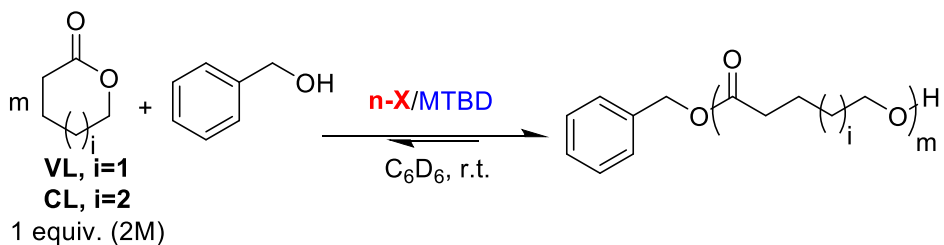
- (23) Bas G. G. Lohmeijer, Frank Leibfarth, John W. Logan, R. C. P.; David A. Long, Fredrik Nederberg, Jeongsoo Choi, A. P. D.; Charles Wade and James L. Hedrick, R. M. W.; Lohmeijer, B. G. G.; Pratt, R. C.; Leibfarth, F.; Logan, J. W.; Long, D. A.; Dove, A. P.; Nederberg, F.; Choi, J.; Wade, C.; Waymouth, R. M.; Hedrick, J. L. *Macromolecules* **2006**, *39* (25), 8574–8583.
- (24) Bertucci, M. A.; Lee, S. J.; Gagne, M. R. *Chem. Commun.* **2013**, *49* (20), 2055–2057.
- (25) Tripathi, C. B.; Mukherjee, S. *J. Org. Chem.* **2012**, *77* (3), 1592–1598.
- (26) Anslyn, E. V.; Dougherty, D. A. In *Modern Physical Organic Chemistry*; University Science, 2006; pp 145–222.
- (27) Kazakov, O. I.; Kieseewetter, M. K. *Macromolecules* **2015**, *48* (17), 6121–6126.
- (28) Jones, C. R.; Dan Pantoş, G.; Morrison, A. J.; Smith, M. D. *Angew. Chemie Int. Ed.* **2009**, *48* (40), 7391–7394.
- (29) Shi, Y.; Lin, A.; Mao, H.; Mao, Z.; Li, W.; Hu, H.; Zhu, C.; Cheng, Y. *Chem. – A Eur. J.* **2013**, *19* (6), 1914–1918.
- (30) Sohtome, Y.; Tanatani, A.; Hashimoto, Y.; Nagasawa, K. *Tetrahedron Lett.* **2004**, *45* (29), 5589–5592.
- (31) Li, X.; Deng, H.; Luo, S.; Cheng, J.-P. *European J. Org. Chem.* **2008**, *2008* (25), 4350–4356.
- (32) Breugst, M.; Houk, K. N. *J. Org. Chem.* **2014**, *79* (13), 6302–6309.
- (33) Doyle, A. G.; Jacobsen, E. N. *Chem. Rev.* **2007**, *107* (12), 5713–5743.
- (34) Curran, D. P.; Kuo, L. H. *Tetrahedron Lett.* **1995**, *36* (37), 6647–6650.
- (35) Wittkopp, A.; Schreiner, P. R. *Chem. - A Eur. J.* **2003**, *9* (2), 407–414.

- (36) Wenzel, A. G.; Jacobsen, E. N. *J. Am. Chem. Soc.* **2002**, *124* (44), 12964–12965.
- (37) Vachal, P.; Jacobsen, E. N. *J. Am. Chem. Soc.* **2002**, *124* (34), 10012–10014.
- (38) Etter, M. C.; Panunto, T. W. *J. Am. Chem. Soc.* **1988**, *110* (17), 5896–5897.
- (39) Berkessel, A.; Cleemann, F.; Mukherjee, S.; Mueller, T. N.; Lex, J. *Angew. Chemie - Int. Ed.* **2005**, *44* (5), 807–811.
- (40) Kazakov, O. I.; Datta, P. P.; Isajani, M.; Kiesewetter, E. T.; Kiesewetter, M. K. *Macromolecules* **2014**, *47*, 7463–7468.



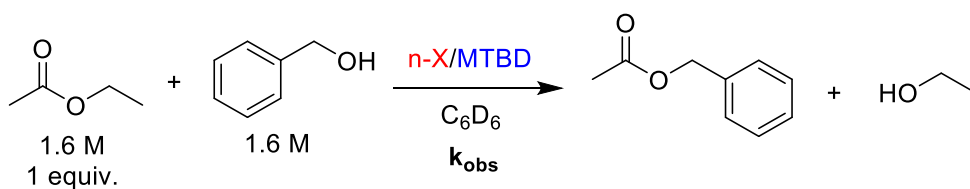
Entry	Monomer	TU (mol%)	Base (mol%)	Time (min)	Conv. ^a (%)	M_n^b (g/mol)	M_w/M_n^b
1	VL	1-S (5%)	MTBD (5%)	110	94	8,300	1.06
2		2-S (2.5%)	MTBD (2.5%)	80	90	6,800	1.07
3		2-S (2.5%)	BEMP (2.5%)	84	91	8,900	1.06
4		2-S (2.5%)	DBU (2.5%)	90	86	8,400	1.05
5		3-S (1.67%)	MTBD (1.67%)	230	90	7 600	1.06
6	CL	1-S (5%)	MTBD (5%)	45 h	90	7,200	1.09
7		2-S (2.5%)	MTBD (2.5%)	10 h	89	7,200	1.11
8		3-S (1.67%)	MTBD (1.67%)	42 h	55	6,100	1.07

Table 2.1. MTBD and **1-S**, **2-S** or **3-S** catalyzed ROP of VL and CL. Reaction conditions: VL or CL (1.0 mmol, 1 equiv., 2M), benzyl alcohol (2 mol%), C_6D_6 . a) monomer conversion was determined via 1H NMR. b) M_n and M_w/M_n were determined by GPC (CH_2Cl_2) versus polystyrene standards.



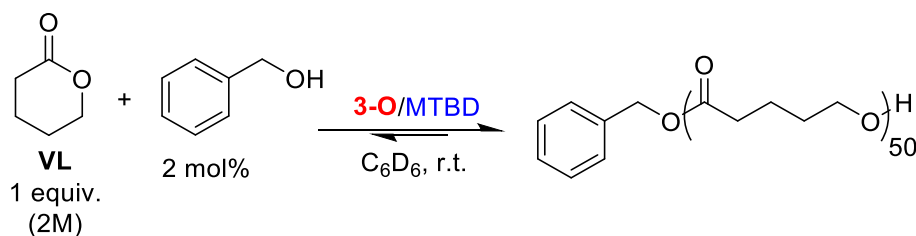
Entry	Monomer	TU or U (mol%)	$[\text{M}]_0/[\text{I}]_0$	Time (min)	Conv. ^a (%)	M_n^b (g/mol)	M_w/M_n^b
1	VL	1-O (5%)	50	70	90	6,100	1.08
2		2-OS (2.5%)	50	88	90	8,100	1.07
3		2-O (2.5%) ^d	50	34	90	8,000	1.07
4		3-O (1.67%)	50	3	89	7,500	1.07
5			100	6	90	15,000	1.04
6			200	10	92	28,600	1.02
7			500	16	92	41,500	1.02
8	CL	3-O (1.67%)	50	26	97	7,900	1.05
9			100	57	94	18,500	1.02
10			200	116	94	30,700	1.03
11			500	166	93	58,600	1.03
12 ^d		TBD (1.67%)	50	140	93	10,400	1.37

Table 2.2. **1-O**, **2-O** or **3-O** and MTBD cocatalyzed ROP of lactones. Reaction conditions: VL or CL (1.0 mmol, 1 equiv., 2M), urea or thiourea (given mol%), MTBD (mol% matched to H-bond donor). a) Monomer conversion monitored via ¹H NMR. b) M_n and M_w/M_n were determined by GPC (CH₂Cl₂) versus polystyrene standards. c) **2-O** (2.5 mol%) and MTBD (5 mol%) cocatalysts. d) no (thio)urea or MTBD cocatalysts were used in this run.



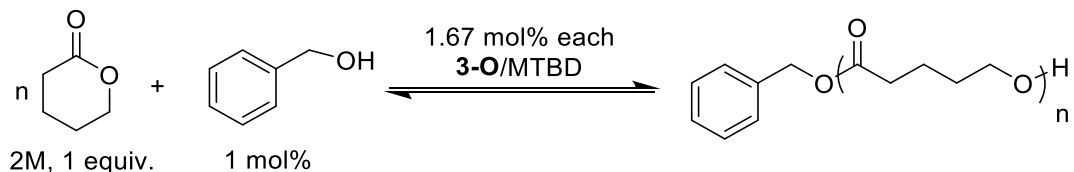
Entry	TU or U (mol%)	k_{obs} (1/min) ^a	[EA] _{eq} (M) ^b
1	1-S (5%)	0.000 80	1.08
2	1-O (5%)	0.003 57	0.88
3	2-S (2.5%)	0.000 55	0.99
4	2-O (2.5%)	0.004 10	0.99
5	3-S (1.67%)	0.000 61	1.19
6	3-O (1.67%)	0.002 11	0.89

Table 2.3. Transesterification of ethyl acetate. a) Observed rate constant for the first order disappearance of [EA] versus time. Rate constant was extracted from the linear portion of the data, up to ~20% conversion. b) Concentration of ethyl acetate remaining at equilibrium.



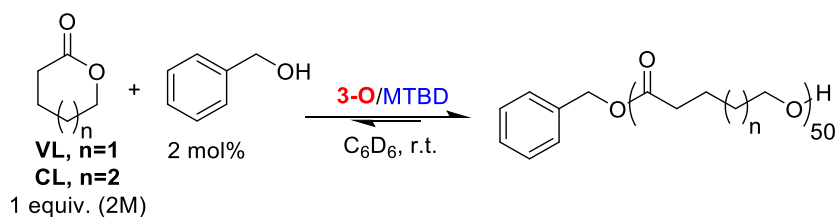
Entry	mol% cats. (each)	Time (min)	Conv. ^a	M_n^b	M_w/M_n^b
1	1.67	3	89	7,500	1.07
2	1	10	91	7,100	1.07
3	0.5	40	93	7,700	1.07
4	0.25	300	93	7,200	1.07
5	0.1	24hr	0	NA	NA

Table 2.4. Low **3-O/MTBD** Cocatalyst Loadings in the ROP of VL. Reaction conditions: VL(0.998 mmol, 1 equiv., 2M), C_6D_6 and benzyl alcohol (2 mol%). a) Monomer conversion was monitored via ^1H NMR. b) M_n and M_w/M_n were determined by GPC (CH_2Cl_2) versus polystyrene standards.



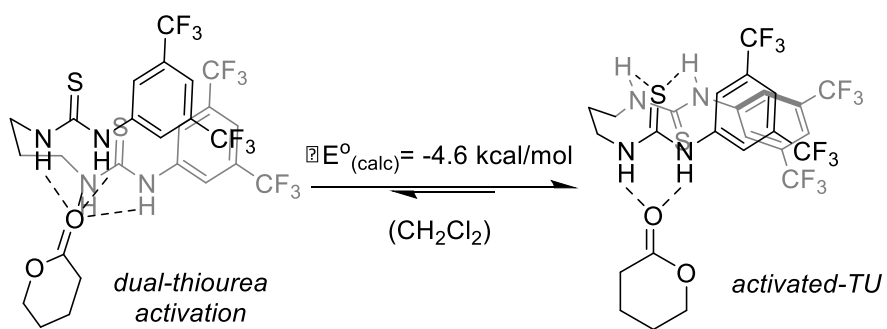
Entry	Solvent	Time (min)	Conv ^a	M_n^b	M_w/M_n^b
1	C ₆ D ₆	4	91	12,200	1.04
2	CH ₂ Cl ₂	5	90	14,800	1.05
3	CHCl ₃	5	90	7,000	1.07
4	Cl-C ₆ H ₅	4	93	10,000	1.08
5	THF	5	89	13,600	1.05

Table 2.5. Solvent Screen in the **3-O**/MTBD Cocatalyzed ROP of VL. Reaction conditions: VL (0.998 mmol, 1 equiv., 2M), 1 mol% benzyl alcohol, a) monomer conversion was monitored via ¹H NMR. b) M_n and M_w/M_n were determined by GPC.

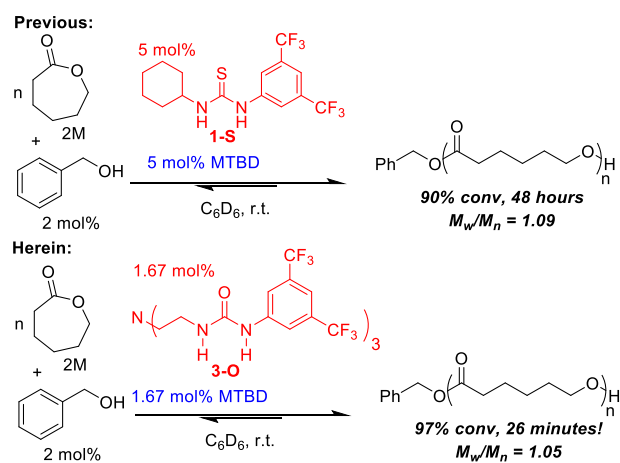


Entry	Monomer	Time (min)	Conv ^a	M_n^b	M_w/M_n^b
1	VL	3	93	6,200	1.10
2	VL	6	93	6,300	1.12
3	VL	60	94	6,600	1.21
4	CL	25	91	9,000	1.04
5	CL	60	98	10,000	1.05
6	CL	120	99	10,000	1.09

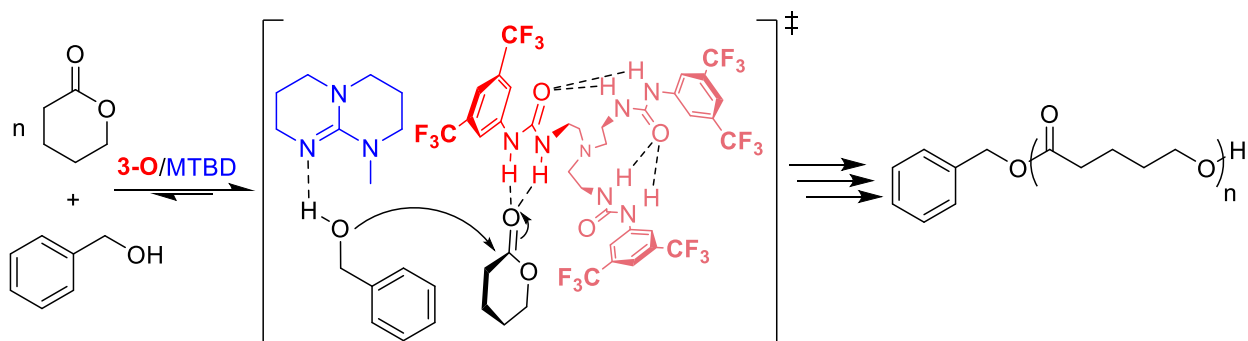
Table 2.6. Post-polymerization Transesterification in **3-O**/MTBD Cocatalyzed ROP. Reaction conditions: VL (0.998 mmol, 1 equiv., 2M), 2 mol% benzyl alcohol, a) monomer conversion was monitored via ¹H NMR. b) M_n and M_w/M_n were determined by GPC.



Eq. 2.1. Intramolecular conformational arrangement of **2-S** done computationally.



Scheme 2.1. Highly active and highly selective H-bond donor **3-O**.



Scheme 2.2. Proposed mechanism for **3-O**/MTBD catalyzed ROP.

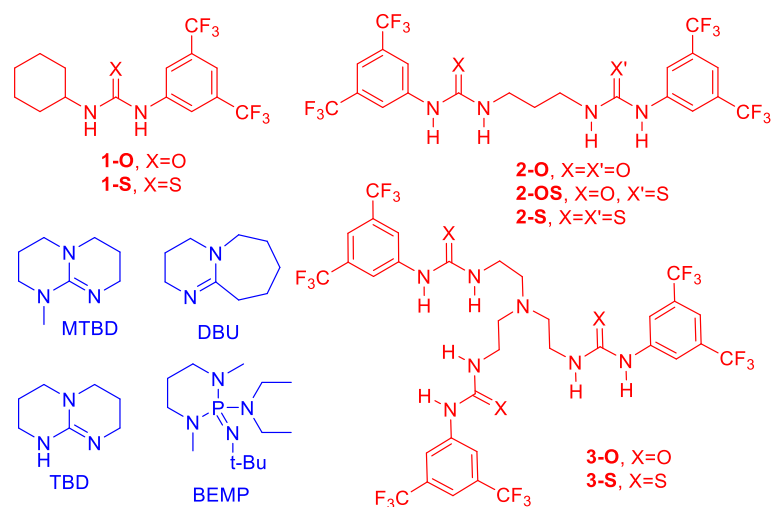


Figure 2.1. Base and (thio)urea cocatalysts evaluated for ROP.

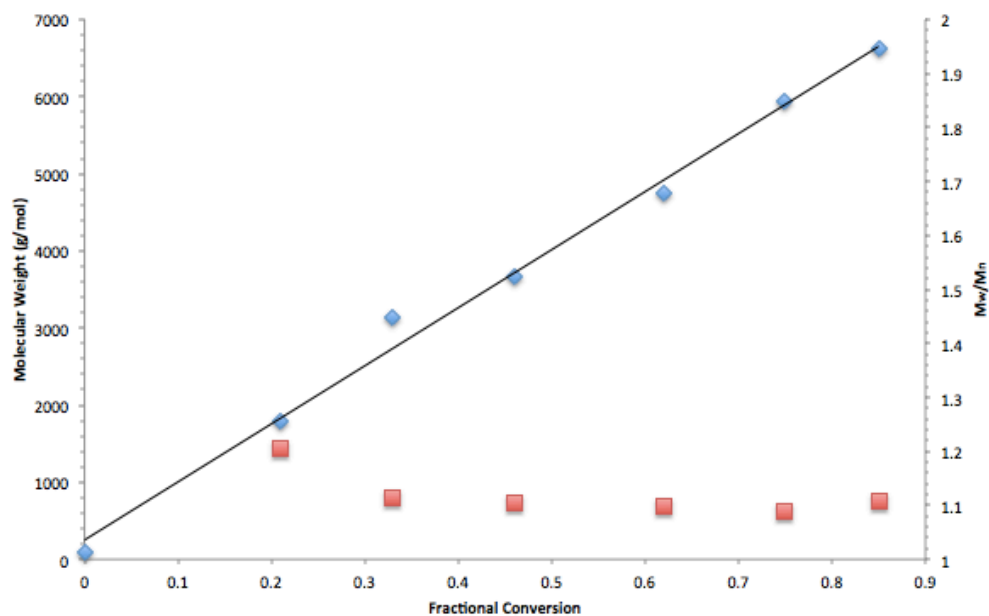


Figure 2.2. M_n versus conversion for the **2-S**/MTBD catalyzed ROP of VL. Conditions: VL (2.994 mmol, 1 equiv., 1M in C_6D_6), benzyl alcohol (2 mol%, 0.0598 mmol), MTBD (5 mol%, 0.1497 mmol) and **2-S** (5 mol%, 0.1496 mmol). (blue is M_n , red is M_w/M_n).

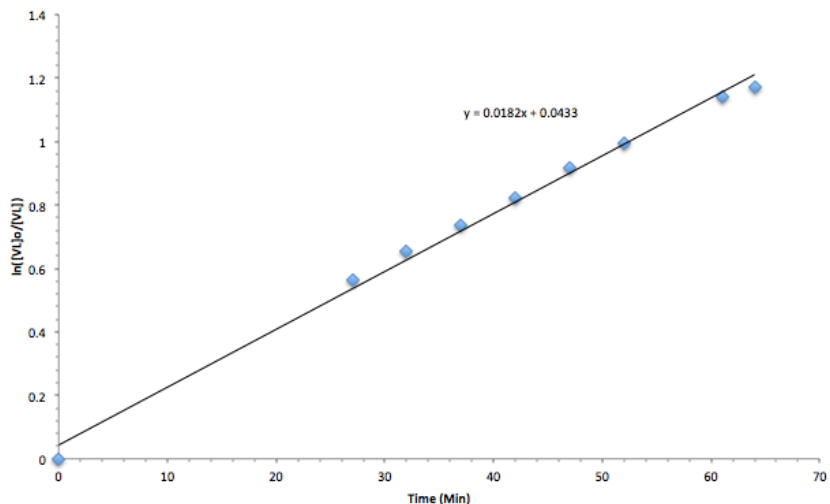


Figure 2.3. First order evolution of [VL] versus time for the **2-S**/MTBD catalyzed ROP of VL. Conditions: VL (0.999 mmol, 1 equiv., 2M in C₆D₆), benzyl alcohol (2.0 mol%, 0.0199 mmol), MTBD (5.0 mol%, 0.0499 mmol) and **2-S** (5.0 mol%, 0.0499 mmol).

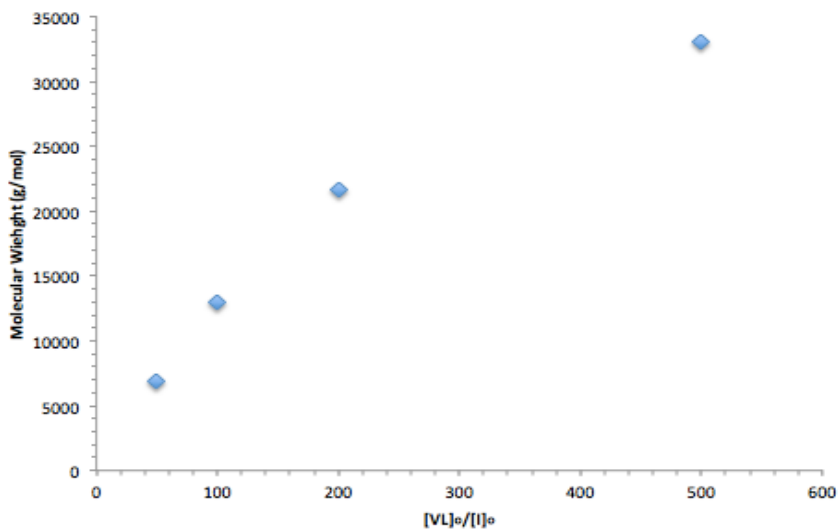


Figure 2.4. M_n versus $[VL]_0/[I]_0$ for the **2-S**/MTBD catalyzed ROP of VL. Conditions: VL (0.999 mmol, 1 equiv., 1M in C₆D₆), benzyl alcohol (2 mol%, 0.0199 mmol), MTBD (5.0 mol%, 0.0499 mmol) and **2-S** (5.0 mol%, 0.0499 mmol).

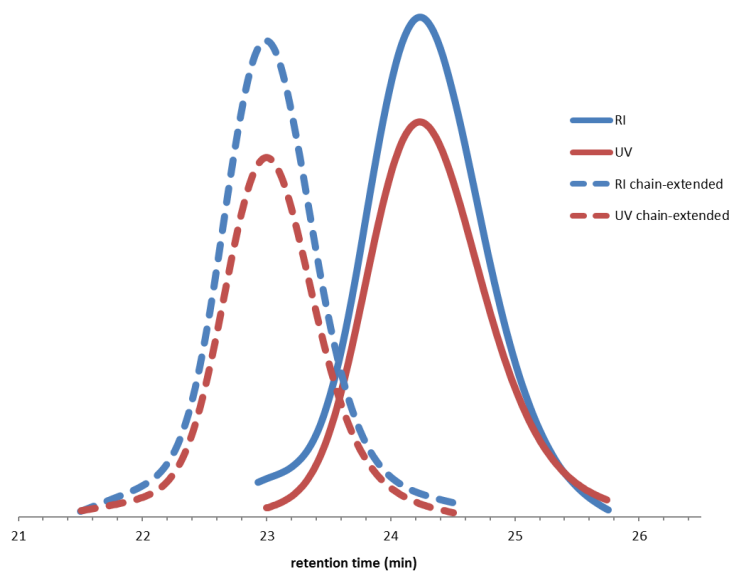


Figure 2.5. GPC traces of the polymer resulting from the **2-S**/MTBD (5 mol% each, 0.0499 mmol) cocatalyzed ROP and subsequent chain extension of VL (0.999 mmol, then 0.999 mmol more) from 1-pyrenebutanol (0.0199 mmol) in C₆D₆ (999 μL).

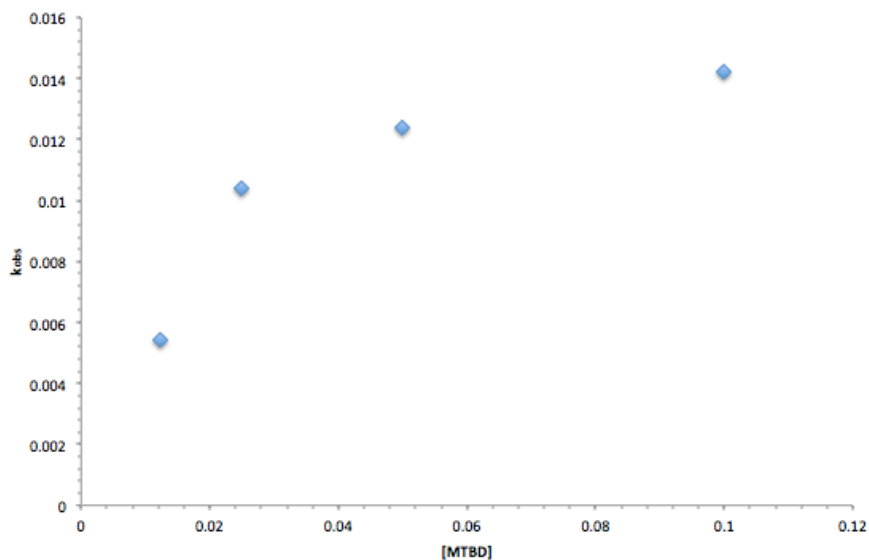


Figure 2.6. Observed rate constant (k_{obs} , min^{-1}) versus [MTBD] in the **2-S**/MTBD catalyzed ROP of VL. Conditions: VL (0.999 mmol, 1 equiv, 1M in C₆D₆), benzyl alcohol (2 mol%, 0.0199 mmol), MTBD (2.5 mol%, 0.025M).

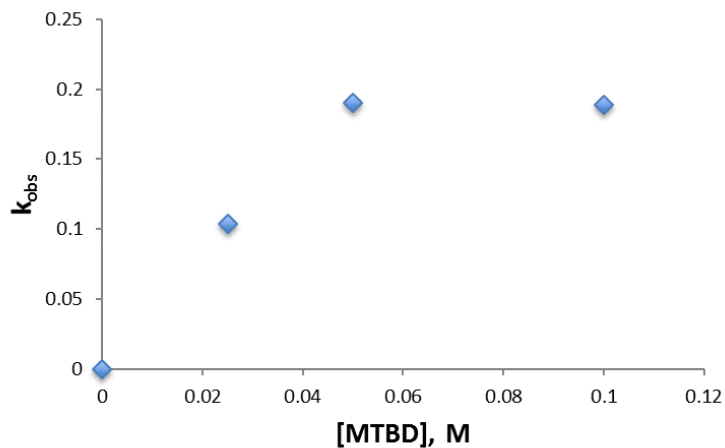


Figure 2.7. Observed rate constant (k_{obs} , h^{-1}) versus [2-S] in the 2-S/MTBD catalyzed ROP of CL. Conditions: CL (0.999 mmol, 1 equiv., 2M in C_6D_6), benzyl alcohol (2 mol%, 0.0199 mmol), 2-S (0.05M).

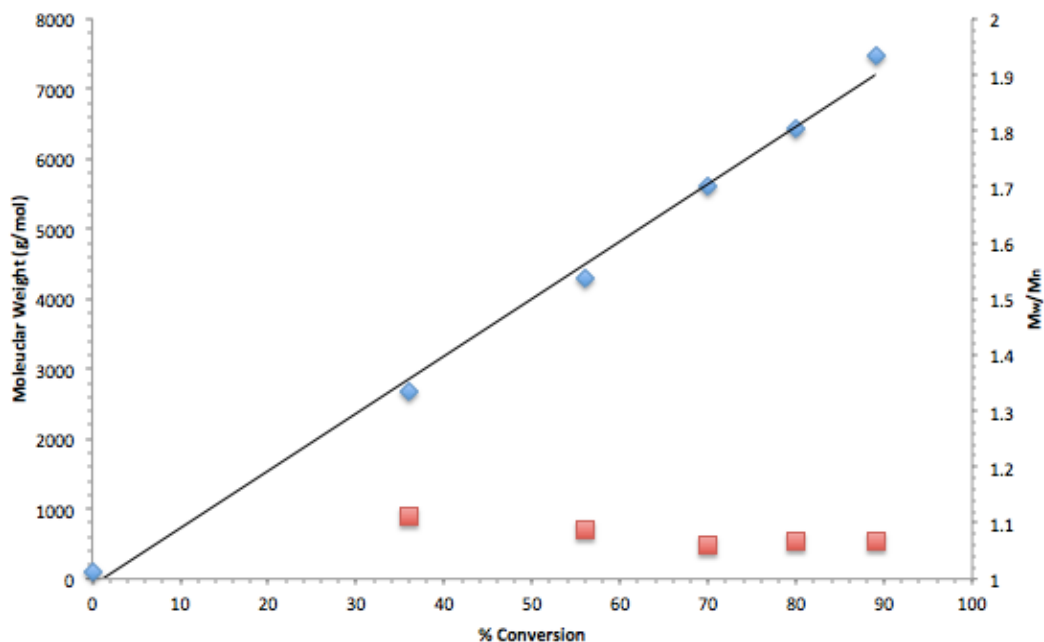


Figure 2.8. M_n vs conversion of VL for the 3-O/MTBD catalyzed ROP of VL. Conditions: VL (0.999 mmol, 1 equiv., 2M in C_6D_6), benzyl alcohol (1mol%, 0.0199 mmol), MTBD (1.67 mol%, 0.0166 mmol) and 3-O (1.67 mol%, 0.0166 mmol). (blue is M_n , red is M_w/M_n).

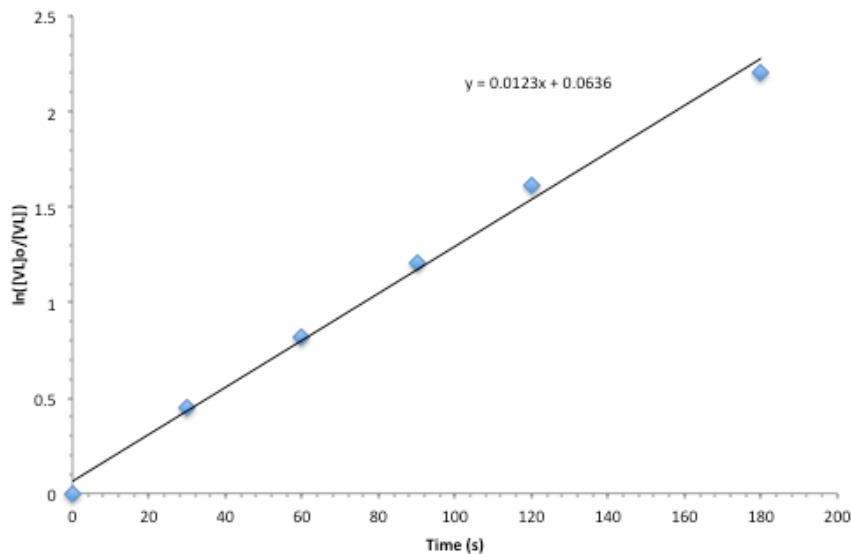


Figure 2.9. First order evolution of [VL] vs time for the **3-O**/MTBD catalyzed ROP of VL. Conditions: VL (0.999 mmol, 1 equiv., 2M in C₆D₆), benzyl alcohol (2 mol%, 0.0199 mmol), MTBD (1.67 mol%, 0.0166 mmol) and **3-O** (1.67 mol%, 0.0166 mmol).

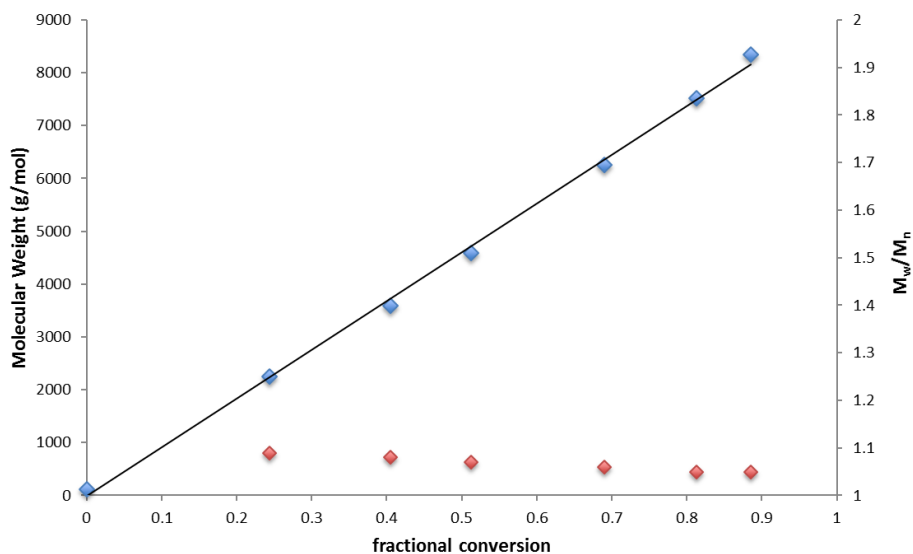


Figure 2.10. M_n vs conversion for the **3-O**/MTBD catalyzed ROP of CL. Conditions: CL (1.752 mmol, 1 equiv, 2M in C₆D₆), benzyl alcohol (2 mol%, 0.035 mmol), MTBD (1.67 mol%, 0.029 mmol) and **3-O** (1.67 mol%, 0.029 mmol). (blue is M_n , red is M_w/M_n).

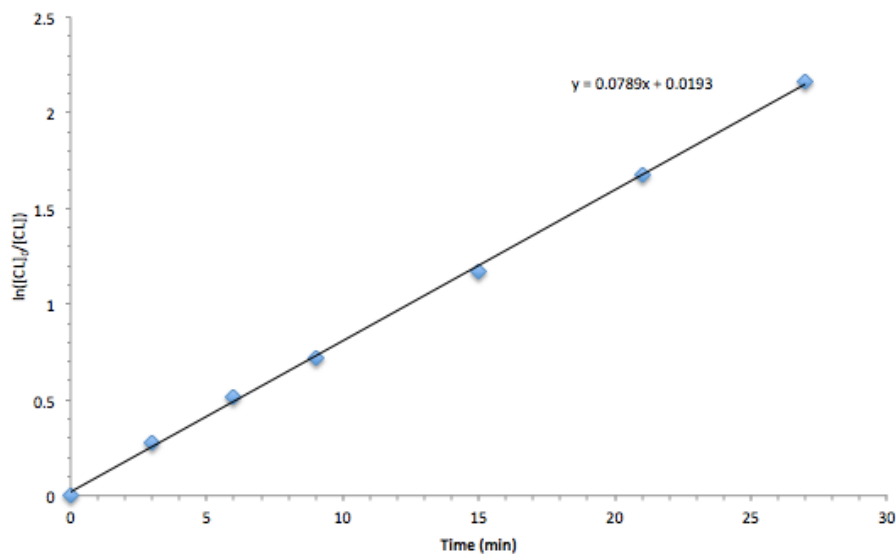


Figure 2.11. First order evolution of [CL] vs time for the **3-O**/MTBD catalyzed ROP of CL. Conditions: CL (1.752 mmol, 1 equiv., 2M in C₆D₆), benzyl alcohol (2 mol%, 0.035 mmol), MTBD (1.67 mol%, 0.029 mmol) and **3-O** (1.67 mol%, 0.029 mmol).

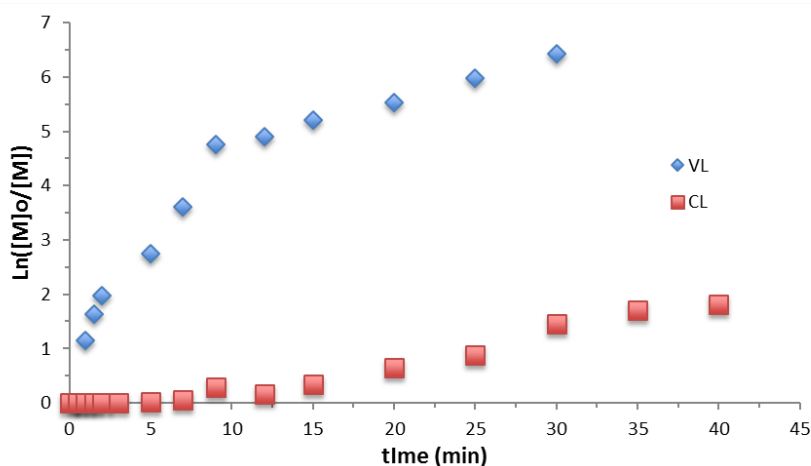


Figure 2.12. First order evolution of [CL] and [VL] vs time for the **3-O**/MTBD catalyzed copolymerization of CL. Conditions: CL (1.752 mmol, 1 equiv., 2M in C₆D₆), benzyl alcohol (2 mol%, 0.035 mmol), MTBD (1.67 mol%, 0.029 mmol) and **3-O** (1.67 mol%, 0.029 mmol).

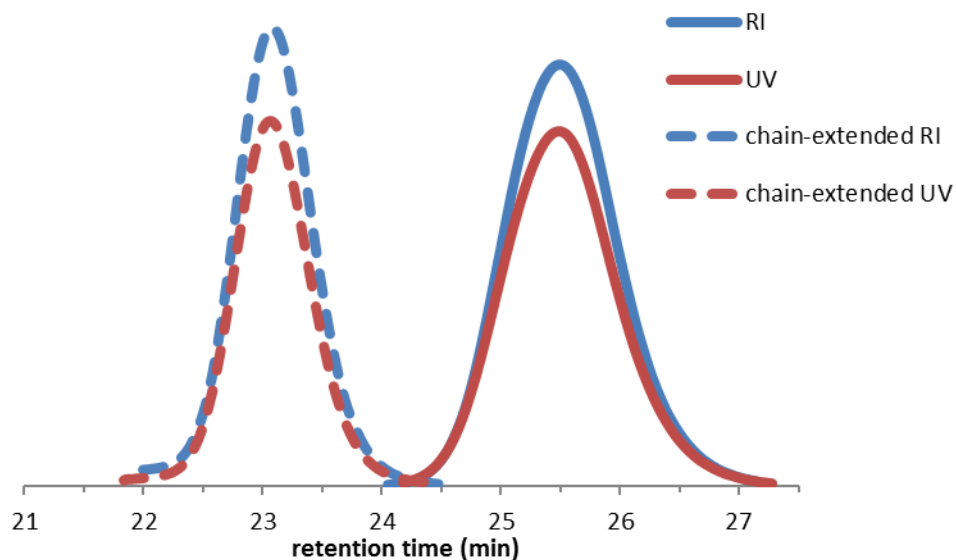


Figure 2.13. GPC traces of the polymer resulting from the **3-O**/MTBD (1.67 mol% each, 0.015 mmol) cocatalyzed ROP and subsequent chain extension of CL (0.876 mmol, then 1.1723 mmol more) from 1-pyrenebutanol (0.035 mmol) in C_6D_6 (219 μ L).

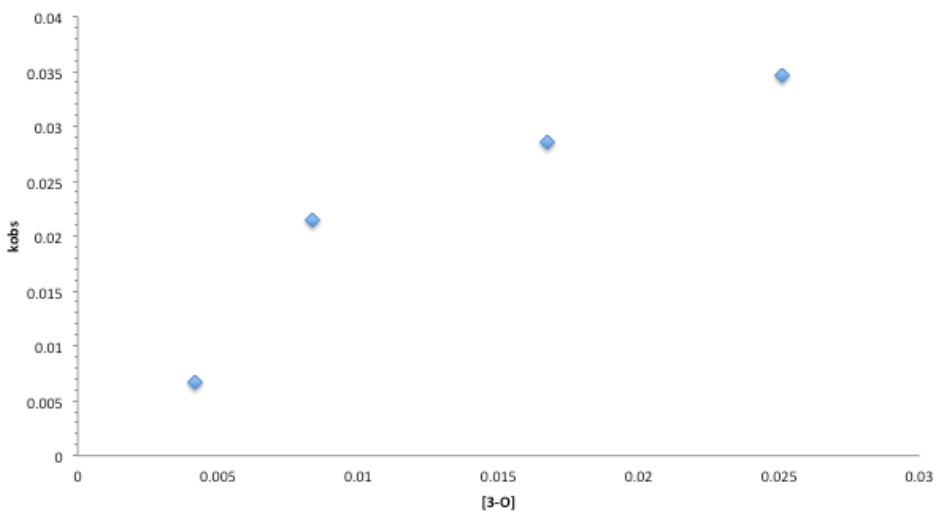


Figure 2.14. Observed rate constant (k_{obs} , min^{-1}) vs **[3-O]** in the **3-O**/MTBD catalyzed ROP of VL. Conditions: VL (0.999 mmol, 1 equiv., 0.5M in C_6D_6), benzyl alcohol (2 mol%, 0.0199 mmol), MTBD (1.67 mol%, 0.0166 mmol, 0.008 M).

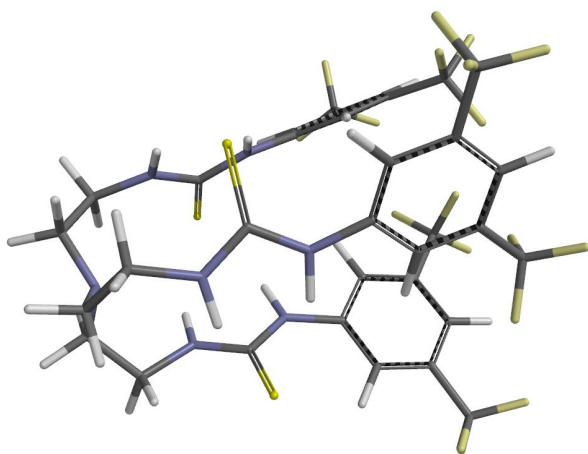


Figure 2.15. DFT B3LYP//6-31G** geometry optimized structures of **3-S**.

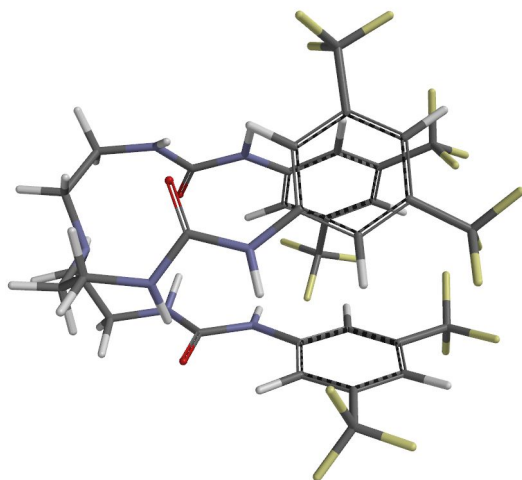


Figure 2.16. DFT B3LYP//6-31G** geometry optimized structures of **3-O**.

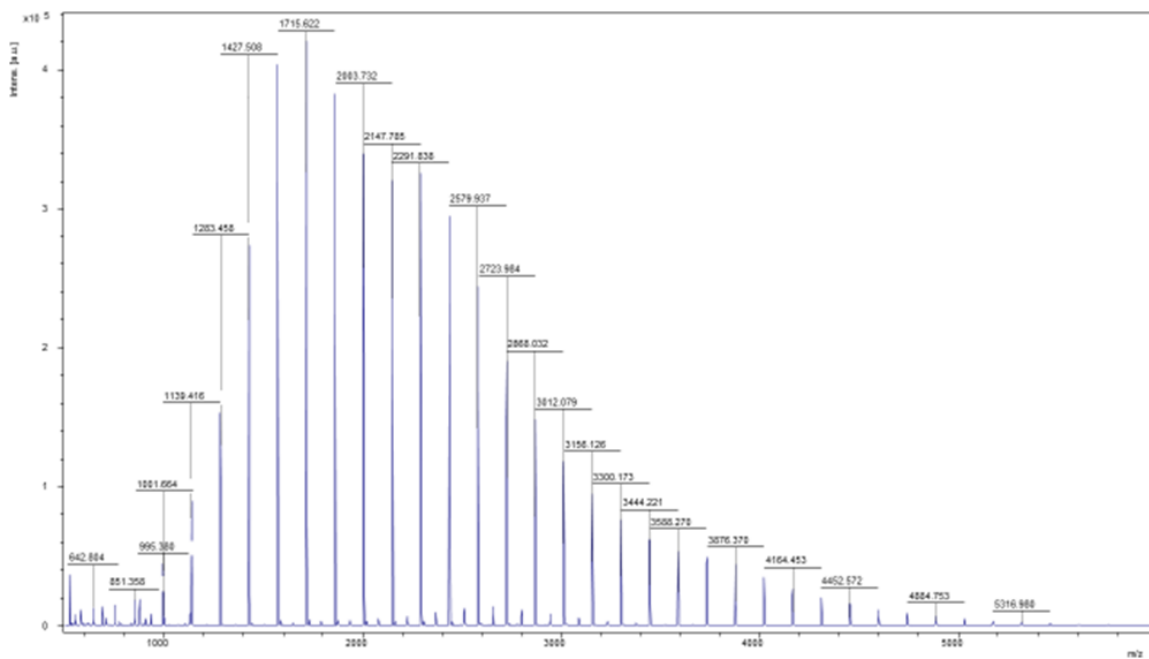


Figure 2.17. MALDI-TOF of the PLA resulting from the **3-O**/(tris[2-(dimethylamino)ethyl]amine) catalyzed ROP of L-LA.

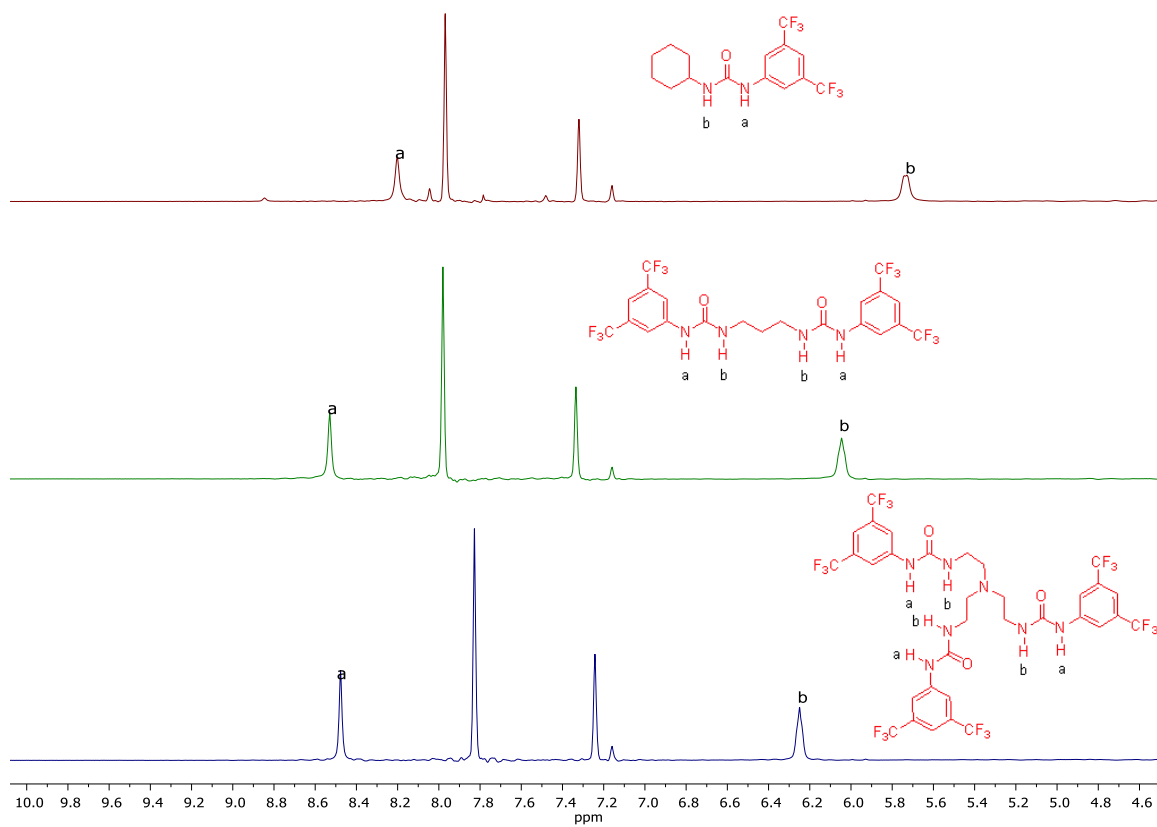


Figure 2.18. Downfield half of the ¹H NMR spectra (acetone + trace benzene-*d*₆ (lock), 400 MHz) of (upper) **1-O**, (middle) **2-O**, and (lower) **3-O**. The progressive downfield shift of the NH protons is indicative of increased (**2-O** versus **3-O**) intramolecular H-bonding.

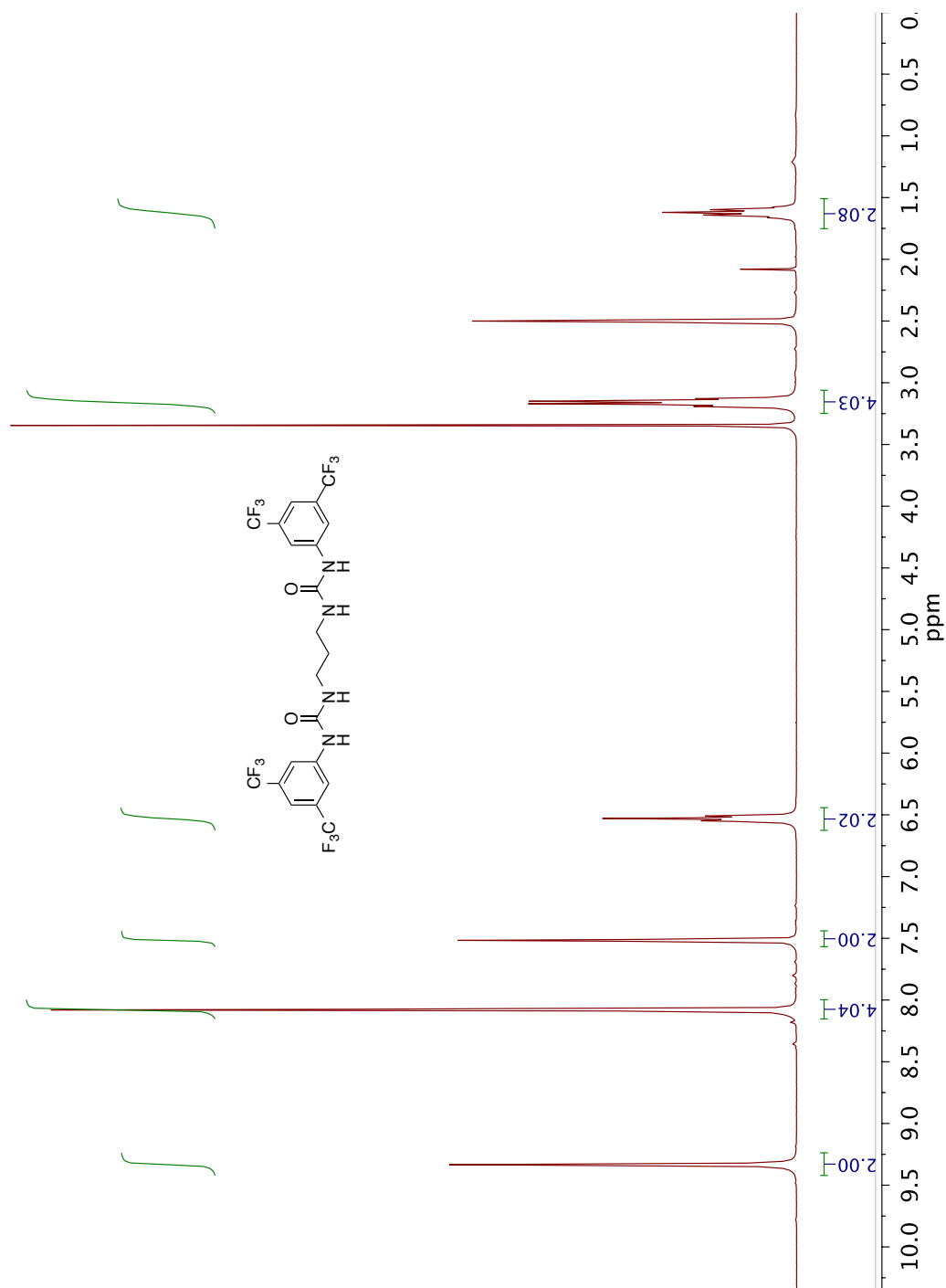


Figure 2.19. ^1H NMR (300 MHz, $\text{DMSO-}d_6$) of **2-O**.

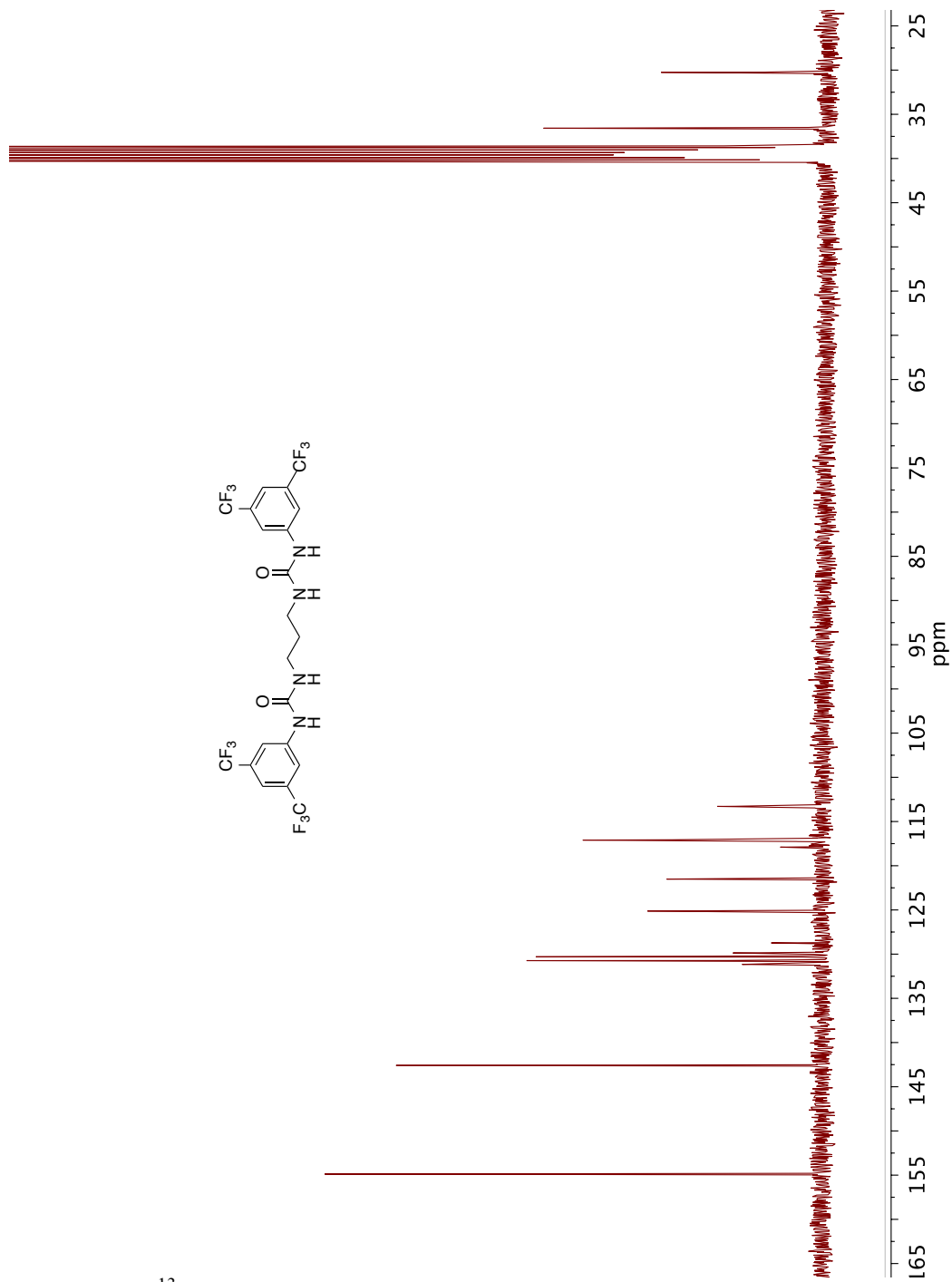


Figure 2.20. ^{13}C NMR (75 MHz, $\text{DMSO-}d_6$) of **2-O**.

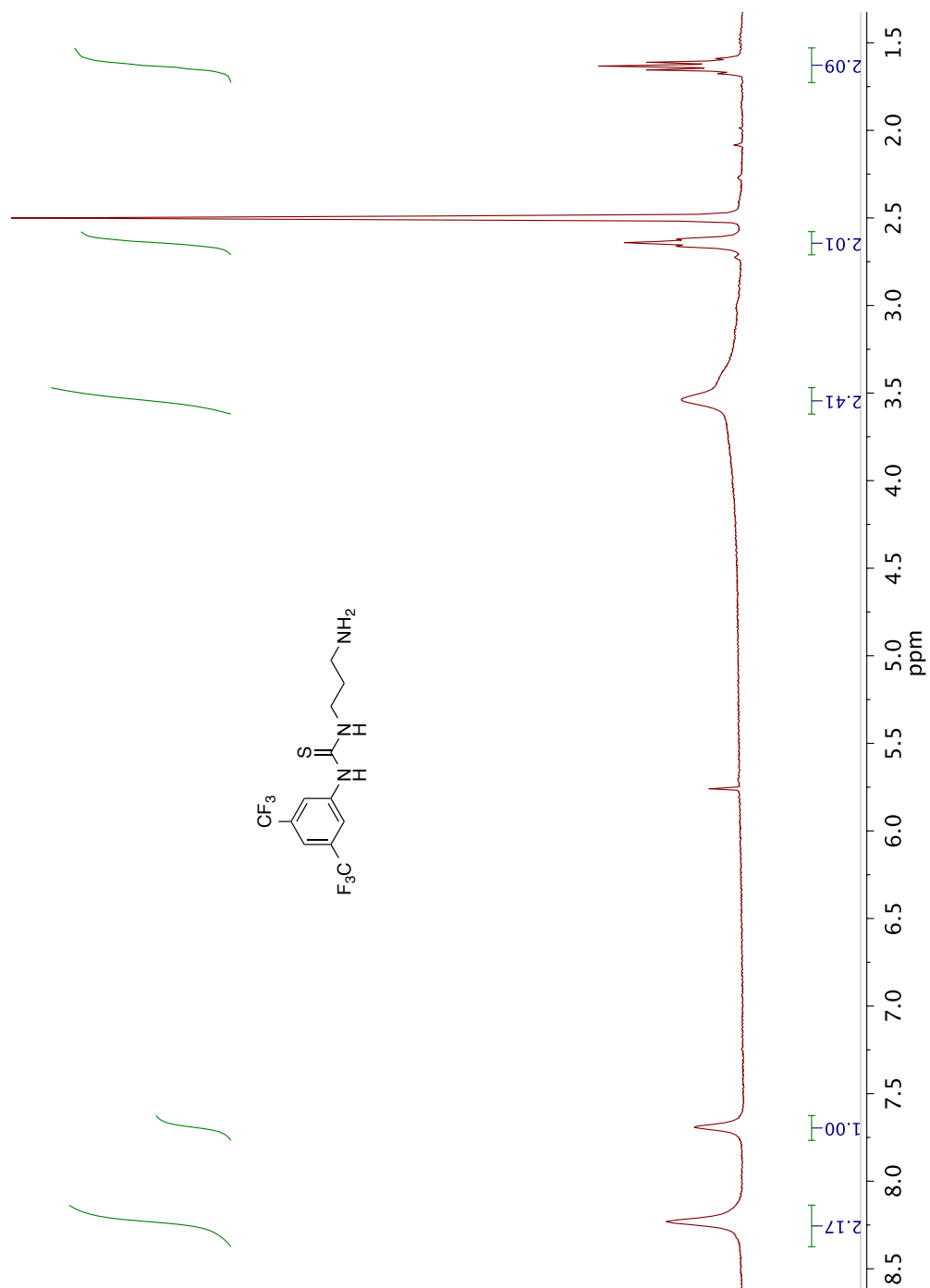


Figure 2.21. ^1H NMR (300 MHz, $\text{DMSO}-d_6$) of 1-[3,5-bis(trifluoromethyl)phenyl thiourea]-3-aminopropane.

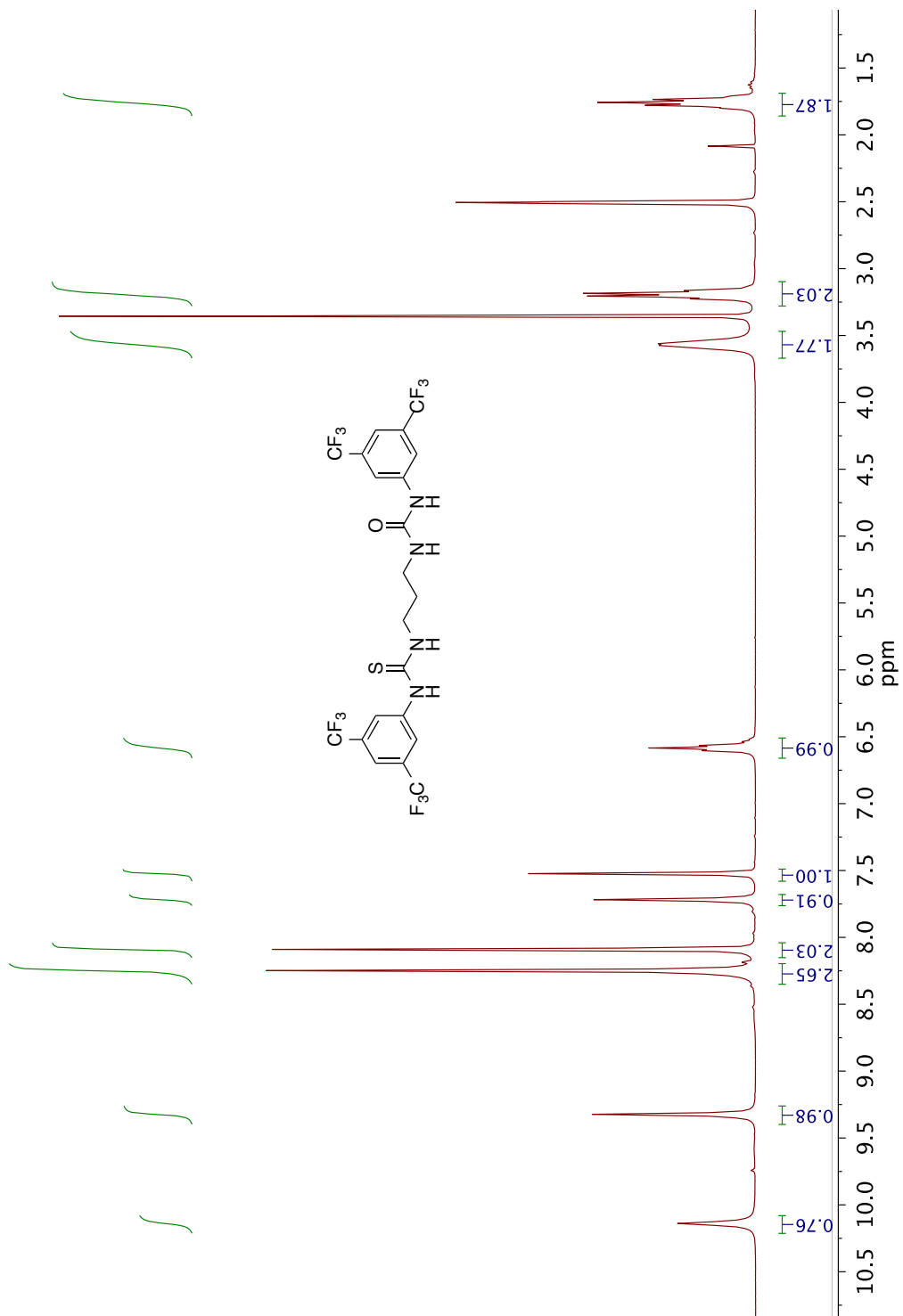


Figure 2.22. ^1H NMR (300 MHz, $\text{DMSO-}d_6$) of **2-OS**.

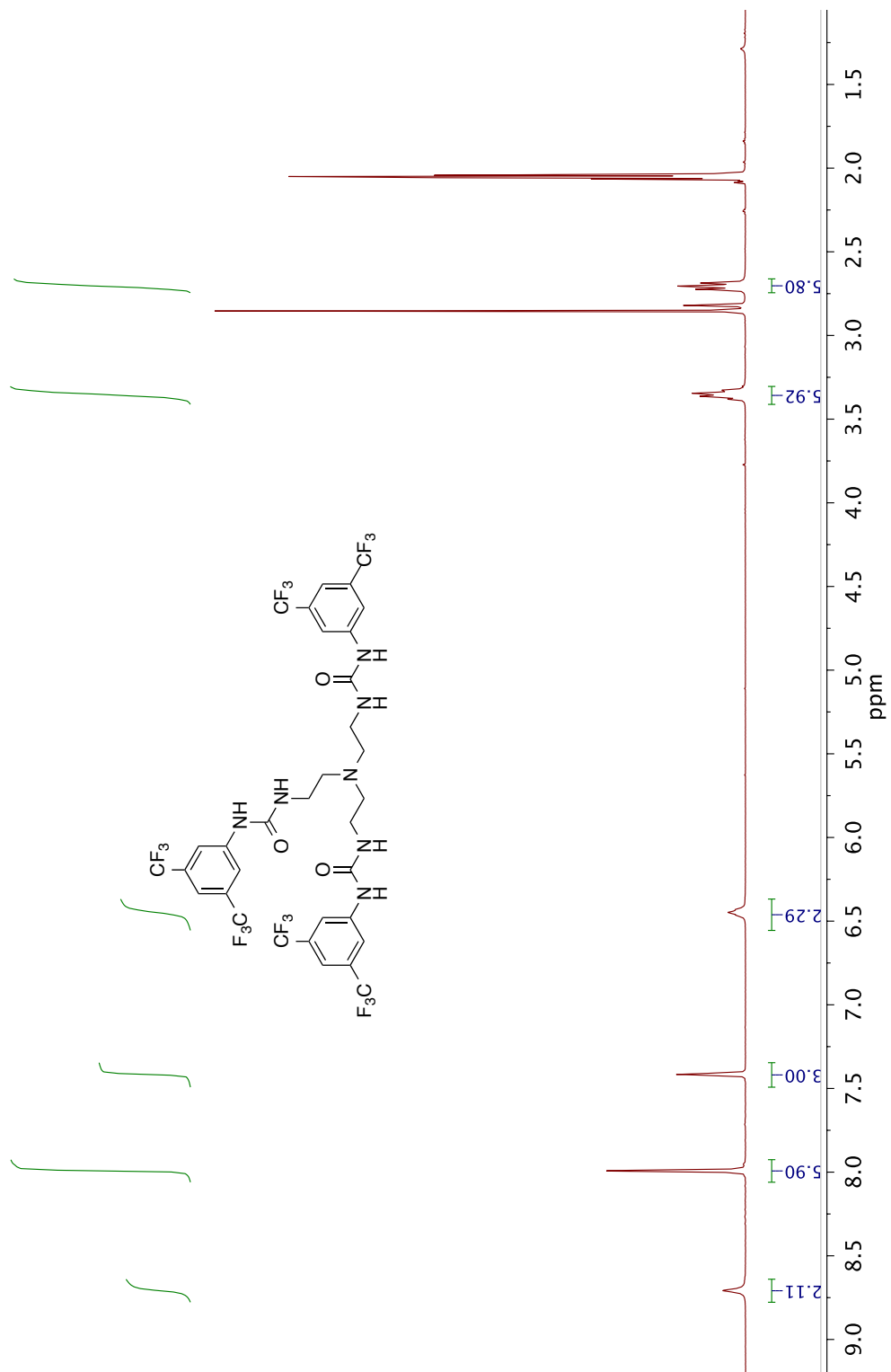


Figure 2.24. ^1H NMR (300 MHz, $\text{acetone-}d_6$) of **3-O**.

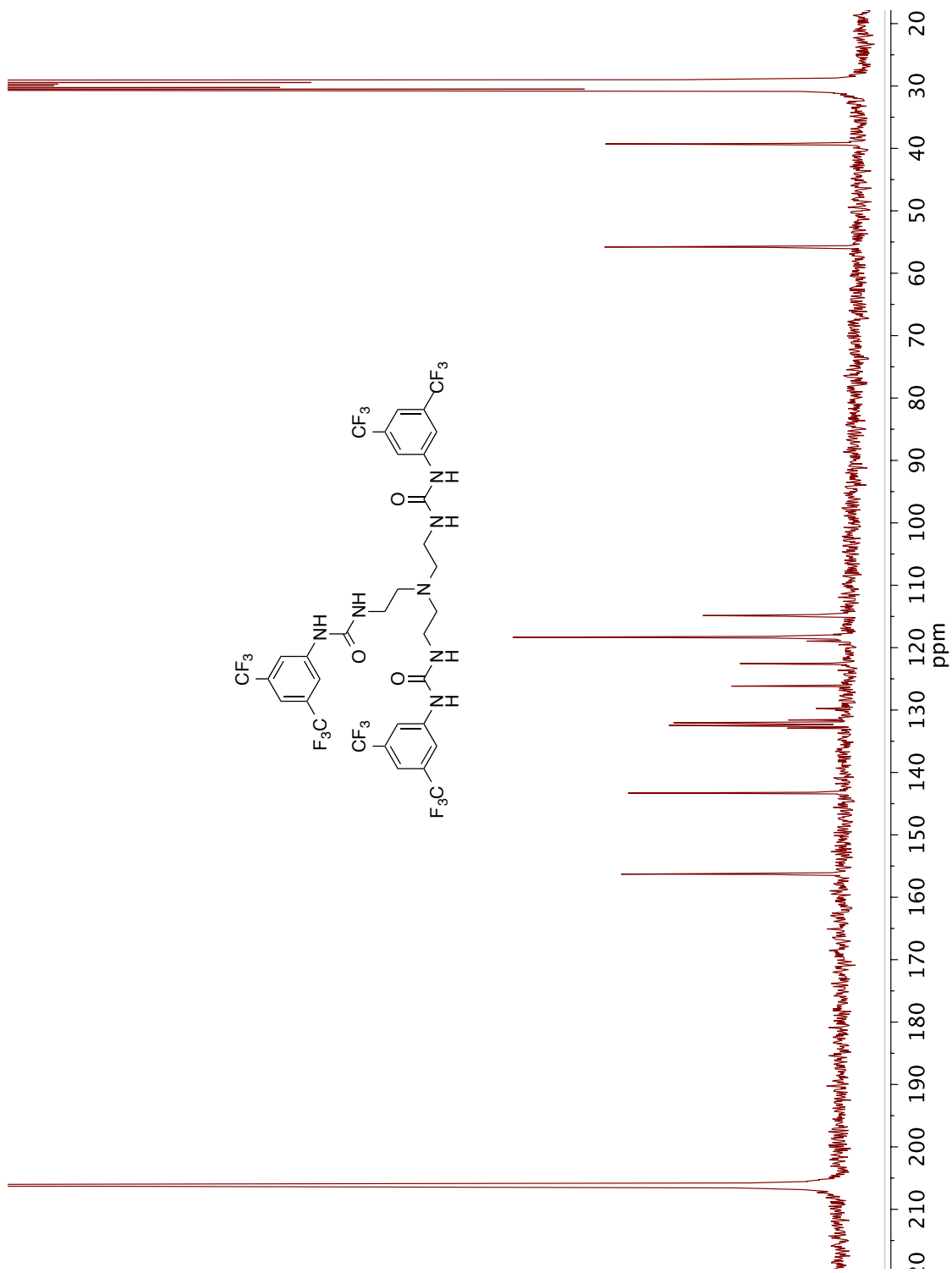


Figure 2.25. ^{13}C NMR (75 MHz, acetone- d_6) of **3-O**.

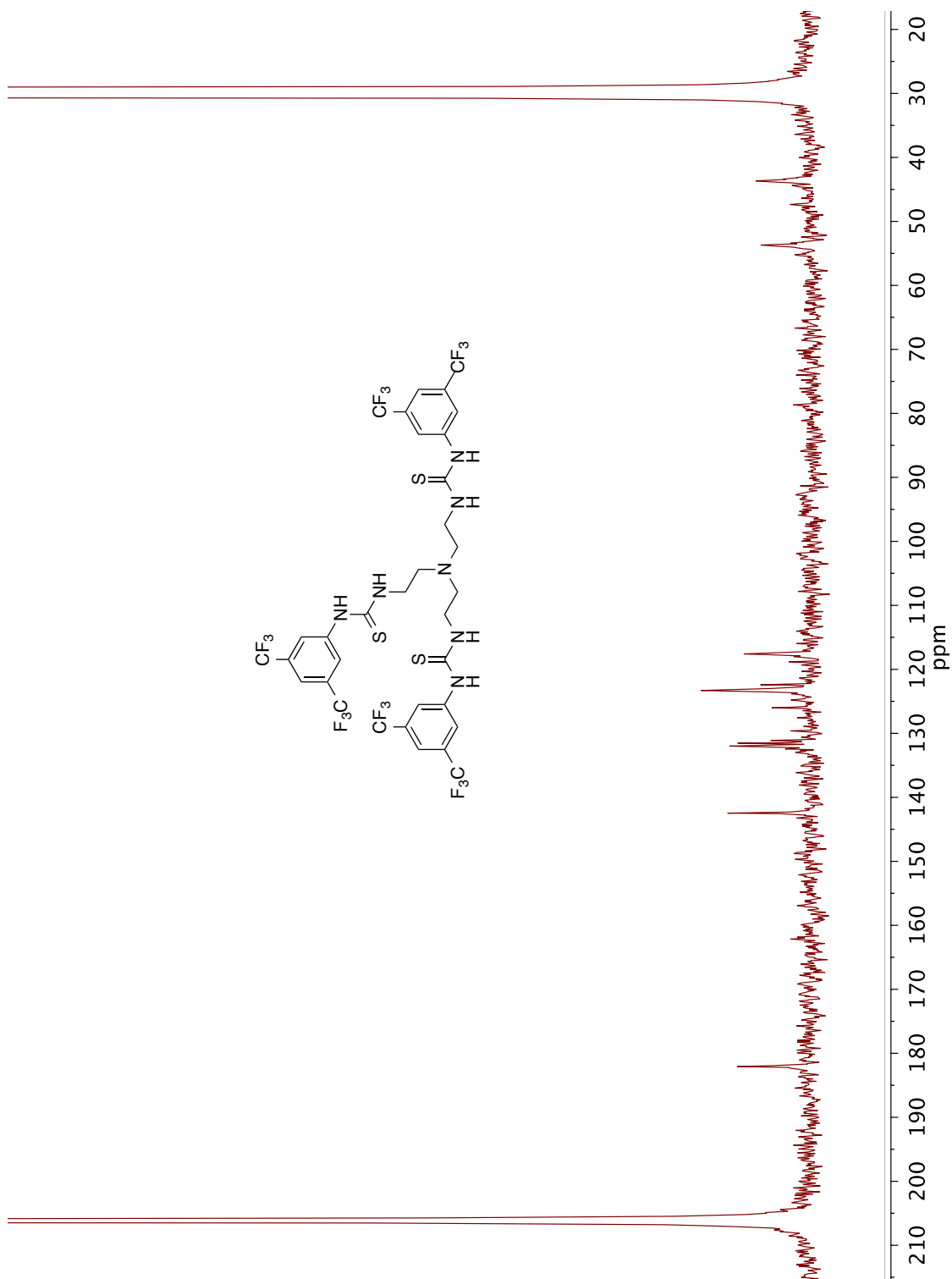
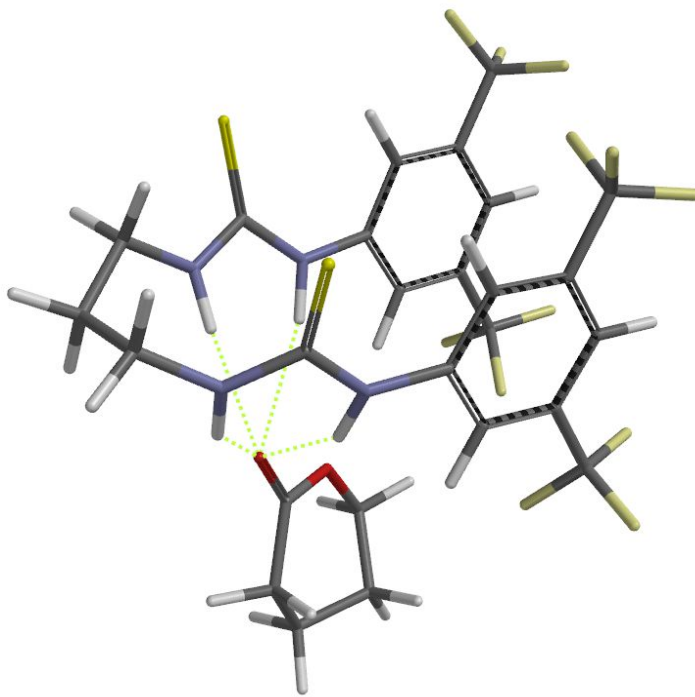


Figure 2.27. ^{13}C NMR (75 MHz, acetone- d_6) of **3-S**.

Computational Data
Dual-thiourea activation in DCM



Job type: Single point.
Method: RB3LYP
Basis set: 6-31G**
Number of shells: 258
Number of basis functions: 818
Multiplicity: 1

Solvation: dichloromethane [SM8]
Free Energy of Solvation : -111.5381226 kJ/mol
SCF total energy: -3369.3171898 hartrees

SPARTAN '14 Properties Program: (Win/64b)
Use of molecular symmetry disabled

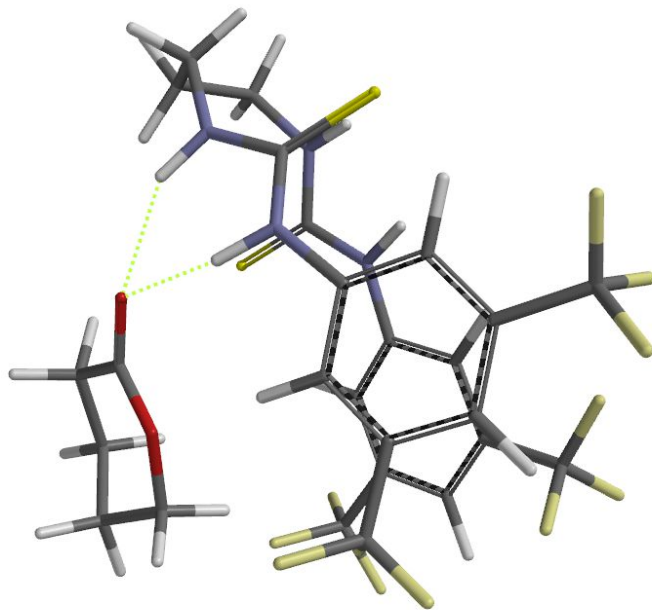
Release 1.1.8

Cartesian Coordinates (Angstroms)			
Atom	X	Y	Z
1 C C1	3.0236320	1.8782697	-1.5793812
2 S S1	2.4865855	3.2691914	-2.3431680
3 N N1	4.1615953	1.8195168	-0.8199347
4 H H4	4.3807088	0.9334757	-0.3754557
5 N N2	2.4147858	0.6395117	-1.6440053
6 H H3	2.8892309	-0.0770555	-1.1048418
7 C C2	1.1325107	0.2212543	-2.0380878
8 C C4	-1.4114202	-0.8709745	-2.5894579
9 C C3	0.9092347	-1.1643141	-1.9771559

10 C C6	0.0704432	1.0587976	-2.4057200
11 C C5	-1.1820850	0.5015117	-2.6687443
12 C C7	-0.3459752	-1.7004420	-2.2407846
13 H H6	1.7244618	-1.8277314	-1.7058464
14 H H7	0.2227144	2.1268062	-2.4722793
15 H H10	-2.3930742	-1.2817497	-2.7895526
16 C C10	4.9143846	2.9692703	-0.3332953
17 H H11	4.5344106	3.8436800	-0.8652759
18 H H14	5.9699149	2.8446241	-0.6074915
19 C C12	3.4027906	3.4954232	1.7271696
20 H H15	2.9363627	4.2861218	1.1280701
21 H H18	3.4772296	3.8782160	2.7517105
22 N N3	2.5369424	2.3192087	1.7215030
23 H H20	2.9203006	1.4691364	1.3284096
24 C C13	1.2067155	2.3544009	1.9901580
25 N N4	0.6109505	1.1232290	1.7699492
26 H H22	1.2548396	0.3613405	1.5797141
27 C C14	-0.7331750	0.7225280	1.7506543
28 C C15	-3.3546714	-0.3089651	1.5817556
29 C C16	-1.8288593	1.5927093	1.6175975
30 C C17	-0.9686276	-0.6575333	1.7958613
31 C C18	-2.2638136	-1.1643464	1.7001179
32 C C19	-3.1155194	1.0670046	1.5420799
33 H H21	-1.6699138	2.6600289	1.5790835
34 H H23	-0.1285243	-1.3372930	1.8897131
35 H H26	-4.3634555	-0.6988767	1.5185011
36 S S2	0.4404338	3.7350223	2.5568843
37 C C9	4.8032256	3.1640599	1.1907223
38 H H5	5.2007974	2.2820671	1.7151565
39 H H66	5.4672919	3.9953370	1.4584577
40 C C8	-2.3348816	1.4323499	-2.9566642
41 C C11	-0.5287562	-3.1927444	-2.1923754
42 C C20	-2.4486148	-2.6540574	1.7596442
43 C C21	-4.2949114	1.9896479	1.3633098
44 F F1	-1.5855148	-3.2933792	0.9172092
45 F F2	-3.6909519	-3.0390037	1.4192127
46 F F3	-2.1937480	-3.1488662	2.9941791
47 F F4	-5.2867990	1.6844871	2.2341956
48 F F5	-4.8239995	1.8788063	0.1239271
49 F F6	-3.9711423	3.2821442	1.5505404
50 F F7	-1.9478724	2.4963754	-3.6880106
51 F F8	-2.8730393	1.9085369	-1.8120448
52 F F9	-3.3238961	0.8070089	-3.6323087
53 F F10	-1.7988703	-3.5416596	-1.9232477
54 F F11	-0.1879272	-3.7820470	-3.3600940
55 F F12	0.2611471	-3.7628518	-1.2373203
56 O O1	3.4367224	-0.7462457	0.7948371
57 C C22	3.2789749	-1.9494030	0.9874045
58 O O2	2.0981603	-2.3565783	1.4442692
59 C C23	4.3678470	-2.9558988	0.6627870
60 H H1	5.3107962	-2.5327712	1.0237134
61 C C25	1.7615096	-3.7600728	1.7091266
62 H H2	1.8528809	-3.8888231	2.7924874
63 C C24	4.1149410	-4.3742363	1.1861986
64 C C26	2.6466391	-4.7344629	0.9547784

65 H H9	4.4431817	-2.9637701	-0.4338844
66 H H12	0.7120346	-3.8367938	1.4267382
67 H H16	4.7842542	-5.0791288	0.6833204
68 H H17	4.3433540	-4.4264428	2.2584168
69 H H19	2.4193356	-5.7464532	1.3082089
70 H H24	2.4038772	-4.7036553	-0.1143083

Activated-TU plus VL in DCM



Job type: Single point.
 Method: RB3LYP
 Basis set: 6-31G**
 Number of shells: 258
 Number of basis functions: 818
 Multiplicity: 1

Solvation: dichloromethane [SM8]
 Free Energy of Solvation : -77.8518861 kJ/mol
 SCF total energy: -3369.3245007 hartrees

SPARTAN '14 Properties Program: (Win/64b)
 Use of molecular symmetry disabled

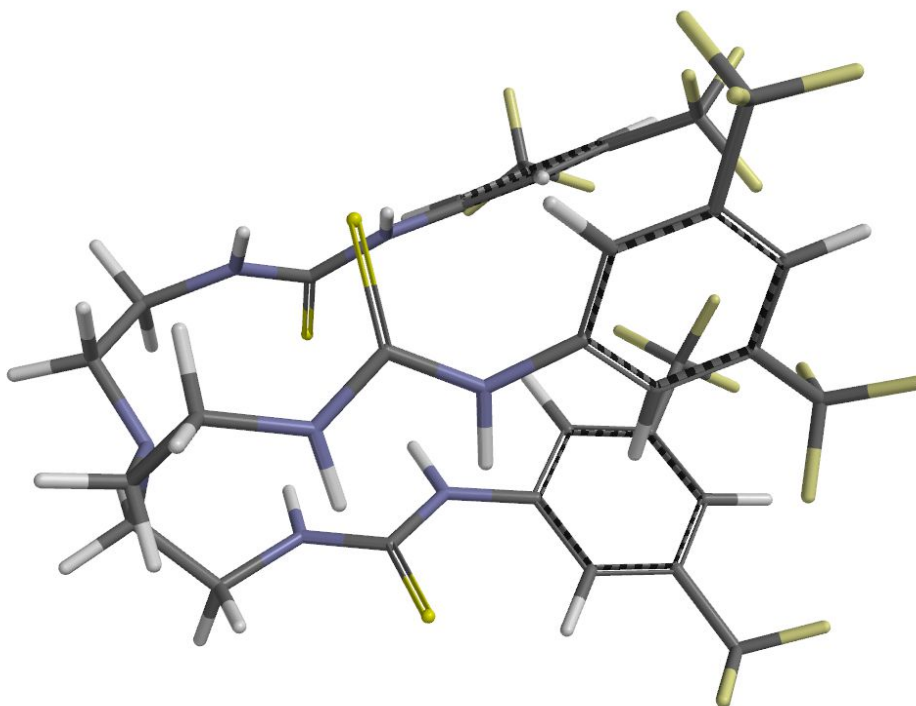
Release 1.1.8

		Cartesian Coordinates (Angstroms)		
Atom		X	Y	Z
1 C	C1	0.6186602	3.4506147	-0.4942311
2 S	S1	-0.1839783	4.1767400	0.8241190
3 N	N1	1.9063132	3.7081440	-0.8145935
4 H	H4	2.3364448	3.0985513	-1.5079477
5 N	N2	0.0531547	2.5251892	-1.3346437
6 H	H3	0.7188179	2.0849533	-1.9741357
7 C	C2	-1.1547538	1.8052874	-1.2340656
8 C	C4	-3.4580090	0.1851075	-1.1642309

9 C C3	-1.1316466	0.5028274	-1.7487208
10 C C6	-2.3542935	2.3143430	-0.7172609
11 C C5	-3.4821723	1.4924413	-0.6759791
12 C C7	-2.2707223	-0.2955969	-1.7112994
13 H H6	-0.2138590	0.1114105	-2.1743285
14 H H7	-2.4085778	3.3304717	-0.3544325
15 H H10	-4.3392201	-0.4410508	-1.1138825
16 C C10	2.8027843	4.6914441	-0.2147555
17 H H11	2.2071707	5.3416025	0.4302030
18 H H14	3.1967392	5.3095899	-1.0312663
19 C C12	3.6869285	3.6006471	1.9812784
20 H H15	3.4926792	4.4774002	2.6093305
21 H H18	4.5555740	3.0769033	2.3864867
22 N N3	2.5249512	2.7335360	2.1290191
23 H H20	1.6271786	3.2234830	2.1204578
24 C C13	2.5094968	1.3974966	1.9057752
25 N N4	1.2256902	0.8893739	1.9753434
26 H H22	0.5039979	1.5998622	2.0720812
27 C C14	0.6984366	-0.4058478	1.8631176
28 C C15	-0.5781053	-2.9147839	1.6314277
29 C C16	1.4548726	-1.5782301	1.7537946
30 C C17	-0.7080836	-0.5063312	1.8791934
31 C C18	-1.3281747	-1.7434602	1.7746406
32 C C19	0.8068657	-2.8102748	1.6216030
33 H H21	2.5337814	-1.5241645	1.7735517
34 H H23	-1.3157391	0.3883894	1.9709278
35 H H26	-1.0674423	-3.8761542	1.5331906
36 S S2	3.9137885	0.5130018	1.5863986
37 C C9	3.9823780	4.0499365	0.5409167
38 H H5	4.3622406	3.1976526	-0.0342216
39 H H66	4.7977458	4.7836087	0.5904183
40 C C8	-4.7350832	2.0133800	-0.0202682
41 C C11	-2.1500066	-1.7036538	-2.2285185
42 C C20	-2.8297569	-1.8589628	1.8102446
43 C C21	1.6636565	-4.0277290	1.4065496
44 F F1	-3.4379221	-0.6675959	1.9789275
45 F F2	-3.2341444	-2.6701329	2.8116355
46 F F3	-3.3103570	-2.3975544	0.6612719
47 F F4	2.2021271	-4.0279014	0.1506788
48 F F5	0.9720086	-5.1765982	1.5310462
49 F F6	2.7028943	-4.0758489	2.2624221
50 F F7	-4.7381778	1.7499162	1.3069433
51 F F8	-5.8465881	1.4468122	-0.5385132
52 F F9	-4.8560965	3.3509353	-0.1561754
53 F F10	-3.3293734	-2.3455705	-2.2770265
54 F F11	-1.6167016	-1.7291299	-3.4757367
55 F F12	-1.3143128	-2.4466695	-1.4544742
56 C C27	3.2831624	-2.6893528	-2.7877261
57 C C26	4.2042838	-1.8989580	-1.8562757
58 C C23	1.8607816	-2.1796104	-2.6467576
59 H H1	1.4433504	-2.4372747	-1.6707839
60 O O3	1.7549042	-0.7255085	-2.7677807
61 C C24	4.1439872	-0.4106729	-2.2166165
62 H H2	4.5853662	0.2219220	-1.4415431
63 C C25	2.7476791	0.1196308	-2.4682591

64 O O4	2.4921707	1.3173809	-2.4670203
65 H H19	4.7032344	-0.2167170	-3.1438153
66 H H24	1.1890437	-2.5577159	-3.4195913
67 H H25	3.8858802	-2.0439632	-0.8171413
68 H H27	5.2374791	-2.2545185	-1.9257839
69 H H29	3.6188117	-2.5973989	-3.8292343
70 H H30	3.2857759	-3.7555044	-2.5347410

3-S vacuum



Job type: Single point.

Method: RB3LYP

Basis set: 6-31G**

Number of shells: 328

Number of basis functions: 1062

Multiplicity: 1

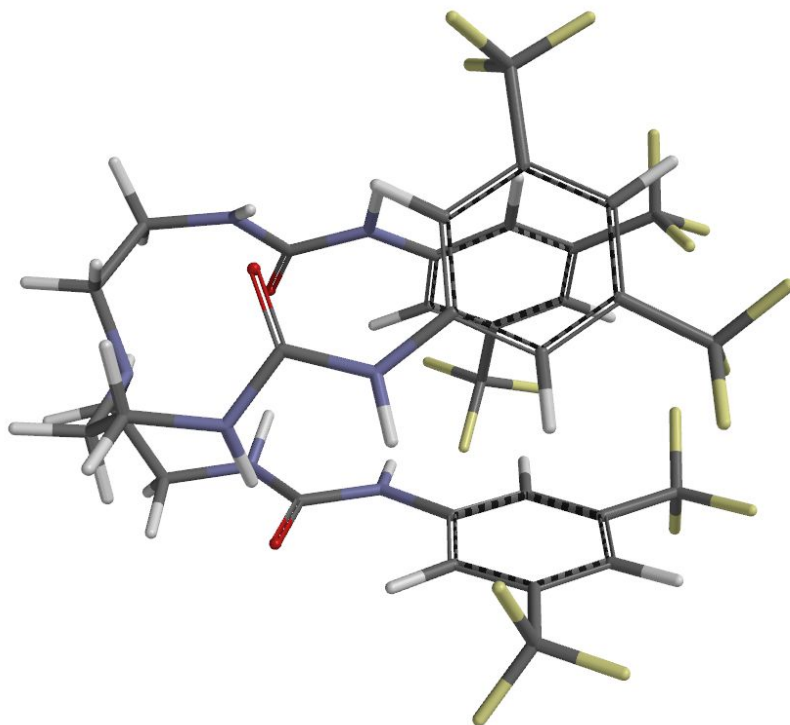
SCF total energy: -4648.8994977 hartrees

Atom	Cartesian Coordinates (Angstroms)		
	X	Y	Z
1 C C2	2.7640909	1.5991396	-1.8183489
2 S S1	2.7485580	3.1262167	-1.0447103
3 N N1	3.9056042	0.9614619	-2.1515710
4 H H5	3.8171067	0.0156768	-2.5219318
5 N N2	1.6401143	0.8812915	-2.1324001
6 H H6	1.7976801	-0.1118807	-2.3241979
7 C C3	0.3013170	1.2854719	-2.3201684
8 C C4	-2.3985949	1.8898648	-2.8274305

9 C C5	-0.6568049	0.2633989	-2.3905650
10 C C6	-0.0979427	2.6145578	-2.5214042
11 C C7	-1.4411826	2.8999161	-2.7585829
12 C C8	-1.9912618	0.5700573	-2.6483517
13 H H7	-0.3550712	-0.7708386	-2.2578626
14 H H8	0.6245689	3.4167849	-2.4885809
15 H H10	-3.4400894	2.1260593	-3.0079652
16 C C10	5.2607492	1.4663694	-1.9949113
17 H H11	5.2004357	2.3893175	-1.4161725
18 H H14	5.6613762	1.7333310	-2.9831061
19 C C12	5.2614840	1.0846459	2.2224675
20 H H15	5.6552614	1.8030174	2.9553352
21 H H18	5.2238331	0.1128850	2.7169096
22 N N3	3.8972486	1.4512082	1.8763081
23 H H20	3.7898009	2.2354648	1.2335711
24 C C13	2.7688079	0.8382435	2.2910562
25 N N4	1.6323822	1.4610792	1.8454412
26 H H22	1.7761138	2.1258750	1.0805754
27 C C14	0.2952149	1.3955875	2.2898815
28 C C15	-2.4076716	1.4772893	3.0662460
29 C C16	-0.1001634	0.8644173	3.5247431
30 C C17	-0.6697046	1.9795466	1.4542447
31 C C18	-2.0048731	2.0203529	1.8476473
32 C C19	-1.4452920	0.9000425	3.8901120
33 H H21	0.6266397	0.4189908	4.1874706
34 H H23	-0.3707644	2.4090036	0.5031227
35 H H26	-3.4498786	1.4932500	3.3590253
36 S S2	2.7872540	-0.5873993	3.2373224
37 C C9	6.1953142	0.4363981	-1.3527427
38 H H66	6.1888855	-0.4701462	-1.9683179
39 C C11	-1.8674470	4.3253073	-3.0057754
40 C C20	-3.0179504	-0.5330077	-2.6738316
41 C C21	-3.0397027	2.5973303	0.9165316
42 C C22	-1.8526707	0.3468162	5.2322748
43 F F1	-3.5124705	1.6644908	0.0579004
44 F F2	-2.5334476	3.6035368	0.1693208
45 F F3	-4.1002269	3.0852263	1.5924522
46 F F4	-1.7965399	1.2987129	6.1932143
47 F F5	-1.0460150	-0.6600559	5.6273026
48 F F6	-3.1163949	-0.1241728	5.2138338
49 F F7	-3.0493461	4.5979143	-2.4148542
50 F F8	-2.0241180	4.5658245	-4.3285172
51 F F9	-0.9633317	5.2130042	-2.5444791
52 F F10	-4.0540158	-0.2298086	-3.4835079
53 F F11	-2.4869431	-1.6987577	-3.1065017
54 F F12	-3.5312931	-0.7659805	-1.4445504
55 H H2	7.2278878	0.8305944	-1.4034350
56 N N5	5.8050047	0.0710587	0.0077225
57 C C1	5.3031898	-2.3644845	-0.2073505
58 H H12	5.7187878	-3.3500893	0.0462233
59 N N6	3.9444816	-2.2719799	0.3039059
60 H H13	3.8481195	-2.1103761	1.3062523
61 C C23	2.8079859	-2.3397588	-0.4200681

62 N N7	1.6771503	-2.2902165	0.3516485
63 H H16	1.8200060	-1.9728928	1.3139804
64 C C24	0.3476586	-2.6736662	0.0707355
65 C C25	-2.3355466	-3.4584339	-0.2512243
66 C C26	-0.0128164	-3.5441791	-0.9645950
67 C C27	-0.6411242	-2.2147546	0.9557636
68 C C28	-1.9660771	-2.6107041	0.7933034
69 C C29	-1.3494205	-3.9144412	-1.1196988
70 H H17	0.7365180	-3.9304652	-1.6412965
71 H H19	-0.3679088	-1.5593844	1.7769814
72 H H24	-3.3673969	-3.7561716	-0.3826470
73 S S3	2.8039171	-2.4388198	-2.1286046
74 C C30	-3.0225496	-2.0715427	1.7241143
75 C C31	-1.6964523	-4.8350935	-2.2620423
76 F F13	-3.4712995	-0.8605647	1.3225534
77 F F14	-2.5472708	-1.9197359	2.9816806
78 F F15	-4.0938615	-2.8882522	1.7904528
79 F F16	-3.0010486	-5.1748762	-2.2628214
80 F F17	-0.9777024	-5.9799826	-2.2020364
81 F F18	-1.4211603	-4.2665814	-3.4560206
82 H H25	5.2463778	-2.3130804	-1.2958413
83 C C32	6.2160596	-1.2822943	0.3756853
84 H H9	7.2550846	-1.5046887	0.0680968
85 H H27	6.2005151	-1.3631277	1.4678909
86 C C33	6.1849094	1.0733869	1.0009875
87 H H1	6.1513581	2.0605765	0.5272716
88 H H33	7.2243617	0.9408821	1.3561298

3-O in vacuum



Job type: Single point.
Method: RB3LYP
Basis set: 6-31G**
Number of shells: 325
Number of basis functions: 1050
Multiplicity: 1

SCF total energy: -3680.0562311 hartrees

Cartesian Coordinates (Angstroms)			
Atom	X	Y	Z
1 C C2	-2.8191769	-1.4459723	1.9139004
2 N N1	-3.6837952	-2.1887576	1.1546312
3 H H5	-3.3678728	-2.4709288	0.2289292
4 N N2	-1.4891232	-1.8088459	1.7201386
5 H H6	-1.3189721	-2.6347168	1.1595125
6 C C3	-0.3503171	-1.2225691	2.2807562
7 C C4	2.0493416	-0.0862620	3.2500984
8 C C5	0.8981553	-1.7653417	1.9324703
9 C C6	-0.3880865	-0.1375919	3.1660749
10 C C7	0.8077738	0.4196093	3.6248772
11 C C8	2.0751581	-1.2017548	2.4093743
12 H H7	0.9430649	-2.6421333	1.2986243
13 H H8	-1.3417631	0.2382549	3.5069152
14 H H10	2.9675834	0.3607257	3.6085817
15 C C10	-5.1238809	-2.0446915	1.3102056
16 H H11	-5.2929735	-1.5776720	2.2812241
17 H H14	-5.5727231	-3.0456003	1.3512156
18 C C12	-5.0034839	2.3026999	1.1529605
19 H H15	-5.4141876	2.8510338	2.0107121
20 H H18	-5.1638710	2.9229996	0.2706689
21 N N3	-3.5626078	2.1839246	1.3289192
22 H H20	-3.2552643	1.5176639	2.0341170
23 C C13	-2.7075480	2.4561068	0.2947921
24 N N4	-1.3695918	2.4426817	0.6796475
25 H H22	-1.1808298	2.3856234	1.6730415
26 C C14	-0.2468647	2.6493585	-0.1300865
27 C C15	2.1192833	2.9594669	-1.6481134
28 C C16	-0.3128602	2.8382121	-1.5177245
29 C C17	1.0130801	2.6622575	0.4901460
30 C C18	2.1732307	2.8145091	-0.2614320
31 C C19	0.8652741	2.9766362	-2.2530596
32 H H21	-1.2765799	2.9083830	-1.9996946
33 H H23	1.0841378	2.5679058	1.5672095
34 H H26	3.0246836	3.0602805	-2.2319525
35 C C9	-5.8077784	-1.2796189	0.1690927
36 H H66	-5.6264522	-1.8391170	-0.7522703
37 C C11	0.7017128	1.6374689	4.4992039
38 C C20	3.3929018	-1.7795935	1.9584829
39 C C21	3.4964690	2.7661755	0.4591288
40 C C22	0.7286742	3.0647507	-3.7472031

41 F F1	3.7883104	1.5106720	0.8698746
42 F F2	3.4783570	3.5405298	1.5685110
43 F F3	4.5149046	3.1852040	-0.3163414
44 F F4	-0.1933562	3.9728184	-4.1229471
45 F F5	0.3041618	1.8626279	-4.2545865
46 F F6	1.8827161	3.3625955	-4.3652558
47 F F7	1.8768286	2.0056603	5.0334528
48 F F8	-0.1816778	1.4698727	5.5017425
49 F F9	0.2438951	2.7088936	3.7708375
50 F F10	4.3632951	-1.5832125	2.8730045
51 F F11	3.3009087	-3.1113309	1.7348205
52 F F12	3.8139235	-1.2205603	0.8016466
53 H H2	-6.9020118	-1.3084428	0.3481495
54 N N5	-5.3242305	0.0878459	-0.0254913
55 C C1	-4.9805141	-0.0027500	-2.5265910
56 H H12	-5.3647749	0.4806546	-3.4344254
57 N N6	-3.5335039	0.1592466	-2.4979075
58 H H13	-3.2003848	1.0939897	-2.2725799
59 C C23	-2.7136441	-0.8963614	-2.2004932
60 N N7	-1.3641707	-0.5966324	-2.3694008
61 H H16	-1.1452379	0.2902806	-2.8060456
62 C C24	-0.2640861	-1.4257205	-2.1210107
63 C C25	2.0520690	-2.9541406	-1.5814598
64 C C26	-0.3764353	-2.7544235	-1.6878494
65 C C27	1.0182818	-0.8888841	-2.3224627
66 C C28	2.1546345	-1.6471006	-2.0585374
67 C C29	0.7775112	-3.4885720	-1.4103902
68 H H17	-1.3550647	-3.2014190	-1.5908365
69 H H19	1.1224511	0.1238865	-2.6959210
70 H H24	2.9366803	-3.5290567	-1.3426359
71 C C30	3.5015073	-1.0197297	-2.3155295
72 C C31	0.5869700	-4.8638394	-0.8351782
73 F F13	3.6211695	0.1677586	-1.6766378
74 F F14	3.6770187	-0.7671852	-3.6332394
75 F F15	4.5179740	-1.8043213	-1.9139979
76 F F16	1.7373992	-5.5432264	-0.7016732
77 F F17	-0.2571635	-5.6138996	-1.5707294
78 F F18	0.0265986	-4.7772247	0.4138683
79 H H25	-5.1789666	-1.0708885	-2.6262966
80 C C32	-5.7176408	0.6174481	-1.3316820
81 H H9	-6.8064816	0.5068331	-1.5117772
82 H H27	-5.5059394	1.6890298	-1.3407401
83 C C33	-5.7494111	0.9645796	1.0671436
84 H H1	-5.5772680	0.4377785	2.0084475
85 H H33	-6.8350147	1.1876081	1.0191279
86 O O1	-3.1162551	-2.0179532	-1.8707390
87 O O2	-3.1675940	-0.5810756	2.7256196
88 O O3	-3.0718983	2.7369773	-0.8530852

INTENTIONALLY BLANK PAGE

MANUSCRIPT – III

Unpublished Results

Chiral H-Bond Donors for the Kinetic Resolution of Racemic Lactide by Ring-Opening Polymerization

Kurt V. Fastnacht and Matthew K. Kiesewetter

Chemistry, University of Rhode Island, Kingston, RI, USA

Corresponding Author: Matthew Kiesewetter, Ph.D.
Chemistry
University of Rhode Island
140 Flagg Road
Kingston, RI, 02881, USA
Email address: mkiesewetter@chm.uri.edu

ABSTRACT

Chiral, multi-H-bonding (thio)urea catalysts have been employed for the kinetic resolution ring-opening polymerization (ROP) of racemic lactide (*rac*-LA). The chiral catalysts dictate the enchainment of monomer to the propagating chain. The obtained polymers were evaluated for tacticity through selectively decoupled ^1H NMR, allowing for the determination of probability of enchainment with retention of stereochemistry (P_m). Multi-H-bonding (thio)ureas saw increases in reaction rate versus previous chiral mono-H-bonding species. An increase in P_m value was also observed for all catalysts examined. Lowering of the reaction temperature to -10°C resulted in an increase in P_m value relative to room temperature.

INTRODUCTION

Poly lactide (PLA) is one of the most important polymeric materials because it is a bio-renewable feedstock, biodegradable and biocompatible. For these reasons, it is highly sought after for applications in biomedical and electronic fields.¹⁻³ PLA's properties are tied directly to the microstructure of the polymer chain, and consequently, the applications in which the polymers will be used for. For example, atactic (random sequence of stereocenters) poly lactide (PLA) has a melting point of 40°C, while isotactic (propagation of repeating stereocenter) PLA has a melting point of 180°C. The change in melting point exemplifies the drastic differences in properties that can be seen when control of the polymer microstructure is achievable. Through the kinetic resolution of lactide, these highly controlled microstructures are achievable. Metal catalysts, typically early transition metals, have dominated the kinetic resolution of *rac*-LA to produce isotactic enriched materials with fast rates and good selectivity.⁴⁻⁸ Metal catalysts follow a coordination insertion mechanism, which covalently bind to the propagating chain end, significantly enhancing stereoselective potential. Alternatively, there are fewer examples of organic catalyst species able to produce isotactic enriched polymers, and they are typically less active and selective,⁹⁻¹² with a select few producing highly isotactic PLA.¹³⁻

15

Through organic catalysis there are three possible routes envisaged for the kinetic resolution of *rac*-LA: 1) chain end control, 2) enantiosite control and 3) a combination of both 1 and 2. In chain end control, the chirality of the propagating chain end dictates the addition of subsequent monomers. Typically, chain end control is done with bulky catalysts which reside in close proximity with the chain end, resulting in kinetic

resolution.^{13,14,16} Enantiosite control uses chiral catalysts which favor the activation of either D or L-LA.^{9,10,17}

(Thio)ureas have made great advances in the ROP community, rivaling some of the fastest known metal catalysts available.¹⁸⁻²¹ Although they have been shown to be fast and selective, little work has been done to illustrate their ability towards stereoselective polymerizations.²² Due to their non-covalent, H-bonding interactions, stereospecific reactions could be perceived as too difficult. However, many small molecule transformations have been performed using chiral thioureas and with great success.²³⁻²⁵ The functional group tolerance of (thio)urea H-bonding catalysts signifies a great opportunity for catalyst optimization for stereocontrolled ROP of *rac*-LA.^{18,26,27}

EXPERIMENTAL SECTION

General Considerations. All manipulations were performed in an MBRAUN stainless steel glovebox equipped with a gas purification system or using Schlenk technique under a nitrogen atmosphere. All chemicals were purchased from Fisher Scientific and used as received unless stated otherwise. Tetrahydrofuran and dichloromethane were dried on an Innovative Technologies solvent purification system with alumina columns and nitrogen working gas. Benzene- d_6 and chloroform- d were purchased from Cambridge Isotope Laboratories and distilled from CaH_2 under a nitrogen atmosphere. Benzyl alcohol was distilled from CaH_2 under reduced pressure. 3,5-bis(trifluoromethyl)phenyl isocyanate was purchased from Acros Organics. 3,5-bis(trifluoromethyl)phenyl isothiocyanate and PyBOP was purchased from Oakwood Products. Naproxen was purchased from MP Biomedicals. N-Boc-L-tert-leucine was purchased from Accela Chembio. Methyl isobutyl ketone was purchased from Alpha Aesar. NMR experiments were performed on Bruker Avance III 300 or 400 MHz spectrometers. Selectively decoupled ^1H NMR experiments were performed on a Varian 500 MHz spectrometer.

Synthesis of tert-butyl-bis(2-aminoethyl)carbamate: A 50 mL round bottom was charged with diethylene triamine (2.54 g, 25 mmol), methyl isobutyl ketone (MIBK, 10.02 g, 100 mmol) and a stir bar. The round bottom was equipped with a dean stark trap filled with methyl isobutyl ketone. The dean stark trap was equipped with a reflux condenser and a needle with active nitrogen pressure. The round bottom was placed in an aluminum bead bath and set to 165°C. The solution was refluxed until the collection of

900 μ L of water (50 mmol) in the dean stark trap (*ca.* 5 hours). The solution was then cooled to 0°C. To the cool flask, a solution of di-*tert*-butyl-dicarbonate (5.9 g, 27 mmol) in 5 ml of methyl isobutyl ketone was added dropwise over a 5 minute period and then let stir overnight. The next morning, 20 mL of a 1:1 mixture of water and isopropanol was added to the reaction and heated to 50°C for 2 hrs. The solution was then let cool to room temp, and the water/alcohol layer was separated. Distillation of MIBK afforded pure product. Yield 3.45 g, 69%. ¹H NMR (300 MHz, CDCl₃) δ 1.46 (s, 9H), 2.96 (t, 4H), 3.08 (b, 4H), 3.35 (b, 4H).

Synthesis of 1,1'-(azanediylbis(ethane-2,1-diyl))bis(3-(3,5-bis(trifluoromethyl)phenyl)thiourea): To a dry Schlenk flask equipped with N₂ purge, *tert*-butyl-bis(2-aminoethyl)carbamate (500 mg, 2.45 mmol), dry THF (25 mL) and a stir bar were charged. 3,5-bis(trifluoromethyl)phenyl isothiocyanate (890 μ L, 4.9 mmol) was added drop wise over a period of 5 minutes. The reaction was stirred overnight. Solvent was removed under reduced pressure, and the product was crystallized with the addition of DCM and isolated by gravity filtration. The product was deprotected by dissolving it in 15 mL of a 4M HCl solution in dioxane. The solution was let stir for 2 hours. Distillation of HCl solution afforded product. Yield 1.03 g, 95%. ¹H NMR (300 MHz NMR, DMSO-*d*₆) δ 3.23 (b, 2H), 3.46 (s, 4H), 3.86 (b, 2H), 7.77 (s, 1H), 8.30 (s, 2H), 8.59 (s, 1H), 8.93 (b, 1H), 10.8 (b, 1H)

Synthesis of 1,1'-(azanediylbis(ethane-2,1-diyl))bis(3-(3,5-bis(trifluoromethyl)phenyl)urea): To a dry Schlenk flask equipped with N₂ purge, *tert*-butyl-bis(2-aminoethyl)carbamate (750 mg, 3.68 mmol), dry DCM (25 mL) and a stirbar were charged. 3,5-bis(trifluoromethyl)phenyl isocyanate (1.8 mL, 7.4 mmol) was added

dropwise over a period of 5 minutes. Product crashed out of solution, separated by gravity filtration and washed with cold DCM. Product was deprotected by dissolving it in 15 mL of a 4M HCl solution in dioxane. The solution was let stir for 2 hours. Distillation of HCl solution afforded product. Yield 1.55 g, 60%. ¹H NMR (300 MHz NMR, DMSO-*d*₆) δ 3.1 (b, 4H), 3.43 (b, 4H), 6.86 (m, 2H), 7.52 (s, 2H), 8.09 (s, 4H), 8.7 (b, 1H), 9.87 (s, 2H).

Synthesis of 4: 1,1'-(azanediylbis(ethane-2,1-diyl))bis(3-(3,5-bis(trifluoromethyl)phenyl)thiourea) (200 mg, 0.31 mmol), naproxen 78.5 mg, 0.34 mmol), PyBOP (177.5 mg, 0.34 mmol), THF (15 mL) and a stir bar were charged to a dry Schlenk flask. Diisopropylethylamine was added dropwise to the flask and let stir for 3 days. The solvent was removed under reduced pressure. The product was extracted using ethyl acetate, washed with 1M HCl and saturated sodium bicarbonate solution and dried with MgSO₄. Solvent was removed under reduced pressure, and the resulting yellow oil was purified by column chromatography 1:4 ethyl acetate to hexanes. Yield 193 mg, 73%. ¹H NMR (300 MHz NMR, C₆D₆) δ 0.29 (s, 3H), 0.69 (s, 3H), 3.11 (b, 4H), 3.53 (b, 4H), 6.85 – 7.72 (m, 12H), 7.88 (s, 2H), 8.65 (s, 2H).

Synthesis of 5: 1,1'-(azanediylbis(ethane-2,1-diyl))bis(3-(3,5-bis(trifluoromethyl)phenyl)urea) (250 mg, 0.38 mmol), N-Boc-L-tert-leucine (98.2 mg, 0.42 mmol), PyBOP (220.5 mg, 0.42 mmol), THF (15 mL) and a stir bar were charged to a dry Schlenk flask. Diisopropylethylamine (425 μL, 3.3 mmol) was added dropwise. The reaction was stirred for 3 days. Solvent was removed under reduced pressure. The product was extracted using ethyl acetate, washed with 1M HCl and saturated bicarb solution and dried using MgSO₄. Solvent was removed under reduced pressure, and the

resulting yellow oil was purified by column chromatography, 3% MeOH in DCM. Purified material was then dissolved in a 4M HCl in dioxane solution. Solvent was removed by distillation. The product was then extracted using ethyl acetate, washed with a saturated sodium bicarbonate solution and dried using MgSO₄. 120 mg of obtained yellow oil was then added to a dry Schlenck flask with dry DCM. 3,5-bis(trifluoromethyl)phenyl isocyanate (28.5 μ L, 0.165 mmol) was added drop wise to the solution. A white solid crashed out of solution and was separated by gravity filtered. Yield 111 mg, 69%. ¹H NMR (300 MHz NMR, DMSO-*d*₆) δ 0.95 (s, 9H), 3.17 (m, 2H), 3.34 (m, 2H), 3.45 (b, 2H), 3.84 (b, 2H), 4.74 (s, 1H), 6.61 (b, 3H), 7.40 (s, 1H), 7.45 (s, 1H), 7.50 (s, 1H), 7.88 (d, 4H), 8.06 (s, 2H), 9.14 (b, 1H), 9.4 (b, 2H).

Example ROP of Lactide. *Rac*-lactide (68.5 mg, 0.475 mmol) and acetone-*d*₆ (0.475 mL) were added into a 7 mL vial and stirred until a homogenous solution was obtained. To a second 7 mL vial, benzyl alcohol (.51 mg, 0.00475 mmol), Me₆TREN (2.74 mg, 0.0119 mmol) and **5** (11.7 mg, 0.0119 mmol) were added. Contents from the first vial were transferred into vial 2 via Pasteur pipette. The contents were mixed and transferred to an NMR tube. Reaction progression was monitored by ¹H NMR until reaction reached 50% conversion. Sample was quenched using benzoic acid (2.9 mg, 0.0238 mmol) and purified via dialysis. Yield: 33.4 mg, 48%.

RESULTS AND DISCUSSION

The ability to perform stereoselective polymerizations would mean little if the ability to analyze the polymers was not adequate. Determination of stereo sequences has been described previously and is used widely for the analysis of these polymers.^{28,29} Through the selective ¹H decoupled NMR, stereo sequences can be analyzed (Figure 3.1). From analysis of these NMRs, a P_m value can be obtained, which denotes the probability to propagate a meso stereocenter. A value equal to one indicates isotactic polymer.

Initial studies into the kinetic resolution of *rac*-lactide by thioureas have been done previously within our research group with promising results.³⁰ This study looked at various H-bond donors for the kinetic resolution of *rac*-LA and the resulting P_m values. The catalysts shown in Figure 3.2, contain the same thiourea backbone, with changes only of a single substituent resulting in altered P_m values.²⁴ The polymerization of *rac*-LA by **1**, **2** and **3** gave P_m values of 0.61, 0.72 and 0.81 (Table 3.1). The change from a dimethyl cyclohexyl amine (**1**), to a cyclohexyl piperidine (**2**), to a cinchona alkaloid (**3**) gave drastic increases in P_m value. This suggests great sensitivity of kinetic resolution to the steric bulk around the H-bond donors. The rates obtained for these catalysts are moderately slow with times to completion of >72hrs for all H-bond donors. H-bond donating (thio)ureas have shown in the past to favor rate acceleration with the incorporation of additional of H-bonding groups within the catalyst scaffold.¹⁸

In an effort to increase both selectivity and kinetics of these transformations, chiral multi-H-bonding catalysts were investigated. The first organocatalyst in this study developed for the polymerization of *rac*-LA was **4** (Figure 3.2). This multi-H-bond donating catalyst species contains two exterior thioureas with a chiral group, naproxen,

bound in the middle via an amide functionality. The ROP of *rac*-LA (0.5M) in CDCl₃ with **4**/Me₆TREN (2.5 mol% each) from benzyl alcohol (1 mol%) gave a P_m value of 0.60 (Table 3.2). The reaction was monitored until it reached 50% conversion and subsequently quenched. Time to 50% completion was 8 hours. While this reaction is not fast relative to other multi-H-bond donating (thio)ureas,¹⁸ a rate acceleration relative to the chiral mono-H-bond donors is observed. The isotacticity, however, is inferior to those obtained by the mono-thioureas but a small enhancement of P_m versus achiral PLA (P_m ≈ 0.5)²⁸ is produced. The H-bond donors are likely within close proximity to each other but without any interactions between the H-bond donors and naproxen, it could be envisaged that the two thioureas in **4** act independently of the chiral architecture. Which would result in less selectivity for one hand over the other.

To force the chiral species into the H-bonding architecture, a third H-bonding arm located on the peripheral of the chiral fragment was envisaged. The addition of this third H-bonding group has the potential to induce intramolecular interactions, forcibly engaging the chiral component in catalysis. Using the same dual H-bonding arm scaffold as used in **4**, chiral catalyst **5** was synthesized (Figure 3.2). Polymerization of *rac*-LA using **5** was done in acetone-*d*₆ due to poor solubility of **5** within CDCl₃. *Rac*-LA (0.5M, 0.475 mmol) cocatalyzed by **5** (11.6mg, 0.012 mmol) and Me₆TREN (2.74 mg, 0.012 mmol) from benzyl alcohol (0.51 mg, 0.005 mmol) in acetone-*d*₆. Reaction progression was monitored to approximately 50% conversion and quenched using benzoic acid. Catalyst **5** gave a P_m value of 0.72. This significant increase in P_m value indicates greater selectivity for one monomer hand over the other.

The polymerization can follow one of three pathways: 1) chain end control, 2) enantiosite control or 3) a combination of the first two. A Curtin-Hammett relationship exists in this transformation. As indicated by the elevated P_m value while using chiral catalyst **5**. In either of the mechanistic scenarios, a lowering of temperature could result in an increase in selectivity for the transformation, increasing the P_m value. This same technique has been employed before and has shown drastic increases in P_m values, producing isotactic enriched PLA.^{13,14,31,32} The ROP of *rac*-LA by **5** was done at -10°C . The decrease in temperature produced an increase in P_m value to 0.82. The reaction temperature was dropped even lower to -78°C . However, due to solubility issues, no conversion of monomer was seen after 20 hours of monitoring (Table 3.2).

CONCLUSION

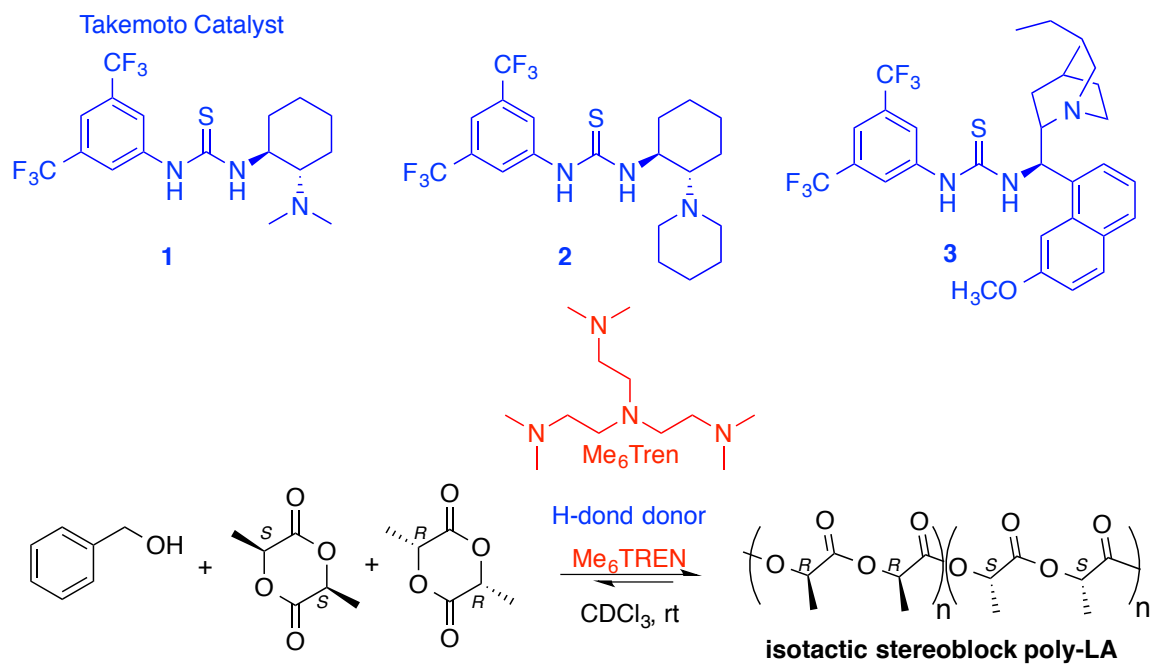
The ROP of *rac*-LA was done using a series of chiral H-bond donors (**4** and **5**) paired with an alkyl amine base (Me₆TREN). To improve both rate and stereoselectivity of the reaction, chiral multi-H-bonding catalysts were synthesized. These catalysts saw great enhancement in reaction rate versus the previous mono-thioureas. H-bonding species **4**, saw only slight enhancement of P_m value versus atactic polymer (P_m ≈ 0.5) and was inferior to all mono-thioureas. The addition of the third peripheral H-bonding group produced increased selectivity versus **4**, but was still inferior vs. the best mono-thiourea **3**. The increased selectivity of **5** versus **4** could either be due to the larger chiral group or a consequence of the third available urea forcibly engaging the chiral arm through intramolecular H-bonding. Lowering the reaction temperature to -10°C produced P_m values competitive with those obtained from the mono-thiourea **3**.

LIST OF REFERENCES

- (1) Albertsson, A. C.; Varma, I. K. *Biomacromolecules* **2003**, *4* (6), 1466–1486.
- (2) Feig, V. R.; Tran, H.; Bao, Z. *ACS Cent. Sci.* **2018**, *4* (3), 337–348.
- (3) Riley, T.; Heald, C. R.; Stolnik, S.; Garnett, M. C.; Illum, L.; Davis, S. S.; King, S. M.; Heenan, R. K.; Purkiss, S. C.; Barlow, R. J.; Gellert, P. R.; Washington, C. *Langmuir* **2003**, *19* (20), 8428–8435.
- (4) Spassky, N.; Wisniewski, M.; Pluta, C.; Le, A. *Macromol. Chem. Phys.* **1996**, *197*, 2627–2637.
- (5) Tang, Z.; Chen, X.; Pang, X.; Yang, Y.; Zhang, X.; Jing, X. *Biomacromolecules* **2004**, *5* (3), 965–970.
- (6) Bakewell, C.; Cao, T. P. A.; Long, N.; Le Goff, X. F.; Auffrant, A.; Williams, C. K. *J. Am. Chem. Soc.* **2012**, *134* (51), 20577–20580.
- (7) Stanford, M. J.; Dove, A. P. *Chem. Soc. Rev.* **2010**, *39* (2), 486–494.
- (8) Thomas, C. M. *Chem. Soc. Rev.* **2010**, *39* (1), 165–173.
- (9) Miyake, G. M.; Chen, E. Y. X. *Macromolecules* **2011**, *44* (11), 4116–4124.
- (10) Makiguchi, K.; Yamanaka, T.; Kakuchi, T.; Terada, M.; Satoh, T. *Chem. Commun.* **2014**, *50* (23), 2883–2885.
- (11) Li, H.; Ai, B.; Hong, M. *Chinese J. Polym. Sci.* **2018**, 1–6.
- (12) Dove, A. P.; Li, H.; Pratt, R. C.; Lohmeijer, B. G. G.; Culkin, D. A.; Waymouth, R. M. R. M.; Hedrick, J. L. *Chem. Commun.* **2006**, No. 27, 2881–2883.
- (13) Zhang, L.; Nederberg, F.; Messman, J. M.; Pratt, R. C.; Hedrick, J. L.; Wade, C. G. *J. Am. Chem. Soc.* **2007**, *129* (42), 12610–12611.
- (14) Liu, S.; Li, H.; Zhao, N.; Li, Z. *ACS Macro Lett.* **2018**, *7* (6), 624–628.

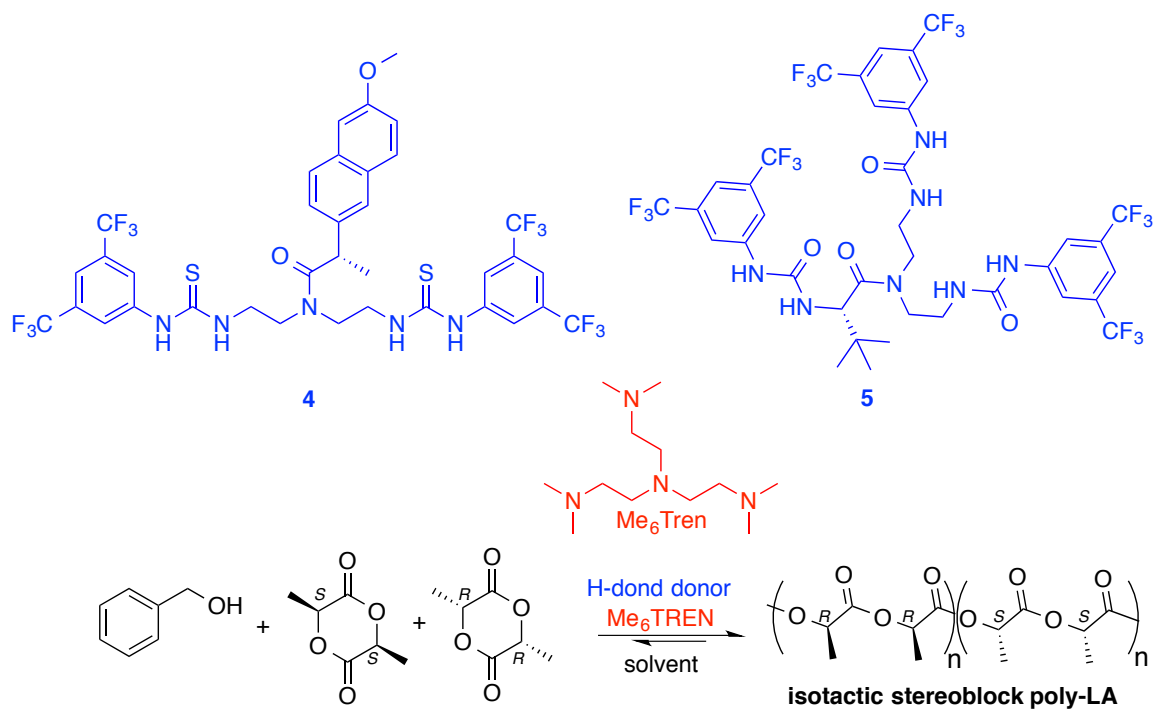
- (15) Sanchez-Sanchez, A.; Rivilla, I.; Agirre, M.; Basterretxea, A.; Etxeberria, A.; Veloso, A.; Sardon, H.; Mecerreyes, D.; Cossío, F. P. *J. Am. Chem. Soc.* **2017**, *139* (13), 4805–4814.
- (16) Jensen, T. R.; Breyfogle, L. E.; Hillmyer, M. A.; Tolman, W. B. *Chem. Commun.* **2004**, *10* (21), 2504–2505.
- (17) Pratt, R. C.; Lohmeijer, B. G. G.; Long, D. a.; Lundberg, P. N. P.; Dove, A. P.; Li, H.; Wade, C. G.; Waymouth, R. M. R. M.; Hedrick, J. L. *Macromolecules* **2006**, *39* (23), 7863–7871.
- (18) Fastnacht, K. V.; Spink, S. S.; Dharmaratne, N. U.; Pothupitiya, J. U.; Datta, P. P.; Kiesewetter, E. T.; Kiesewetter, M. K. *ACS Macro Lett.* **2016**, *5* (8), 982–986.
- (19) Dharmaratne, N. U.; Pothupitiya, J. U.; Bannin, T. J.; Kazakov, O. I.; Kiesewetter, M. K. *ACS Macro Lett.* **2017**, *6* (4), 421–425.
- (20) Lin, B.; Waymouth, R. M. R. M. *J. Am. Chem. Soc.* **2017**, *139* (4), 1645–1652.
- (21) Lin, B.; Waymouth, R. M. R. M. *Macromolecules* **2018**, *51* (8), 2932–2938.
- (22) Zhu, J. B.; Chen, E. Y. X. *J. Am. Chem. Soc.* **2015**, *137* (39), 12506–12509.
- (23) Klausen, R. S.; Jacobsen, E. N. *Org. Lett.* **2009**, *11* (4), 887–890.
- (24) Okino, T.; Hoashi, Y.; Takemoto, Y. *J. Am. Chem. Soc.* **2003**, *125* (42), 12672–12673.
- (25) Breugst, M.; Houk, K. N. *J. Org. Chem.* **2014**, *79* (13), 6302–6309.
- (26) Pothupitiya, J. U.; Hewawasam, R. S.; Kiesewetter, M. K. *Macromolecules* **2018**, No. 51, 3203–3211.
- (27) Lippert, K. M.; Hof, K.; Gerbig, D.; Ley, D.; Hausmann, H.; Guenther, S.; Schreiner, P. R. *European J. Org. Chem.* **2012**, No. 30, 5919–5927.

- (28) Ovitt, T. M.; Coates, G. W. *J. Am. Chem. Soc.* **2002**, *124* (7), 1316–1326.
- (29) Dove, A. P.; Pratt, R. C. R. C.; Lohmeijer, B. G. G.; Waymouth, R. M. R. M.; Hedrick, J. L. *J. Am. Chem. Soc.* **2005**, *127* (40), 13798–13799.
- (30) Oleg, K. Fundamental Investigations In Organocatalytic Ring-Opening Polymerization: A Trek To New Catalysts, University of Rhode Island, 2018.
- (31) Wang, H.; Ma, H. *Chem. Commun.* **2013**, *49* (77), 8686–8688.
- (32) Chen, H. Y.; Tang, H. Y.; Lin, C. C. *Macromolecules* **2006**, *39* (11), 3745–3752.



Catalyst	Time (hrs)	% Conv. ^a	P _m ^b
1	24	58	0.61
2	89	96	0.72
3	120	88	0.81

Table 3.1. Mono-chiral thioureas for the kinetic resolution ROP of *rac*-lactide. a. Conversion determined by ¹H NMR. b. P_m value determined by selectively decoupled ¹H NMR.



Catalyst	Conc. (M)	Solvent	Temp (°C)	Time (hrs)	% Conv.	P _m
4	0.5	CDCl ₃	r.t.	8	50	0.60
5	0.5	acetone- <i>d</i> ₆	r.t.	6	48	0.72
5	0.5	acetone- <i>d</i> ₆	-10	6	50	0.82
5	0.25	acetone- <i>d</i> ₆	-78	20	0	N/A

Table 3.2. Chiral multi-H-bond donor catalysts used for the stereocontrolled ROP of *rac*-lactide. a. Conversion determined by ¹H NMR. b. P_m value determined by selectively decoupled ¹H NMR.

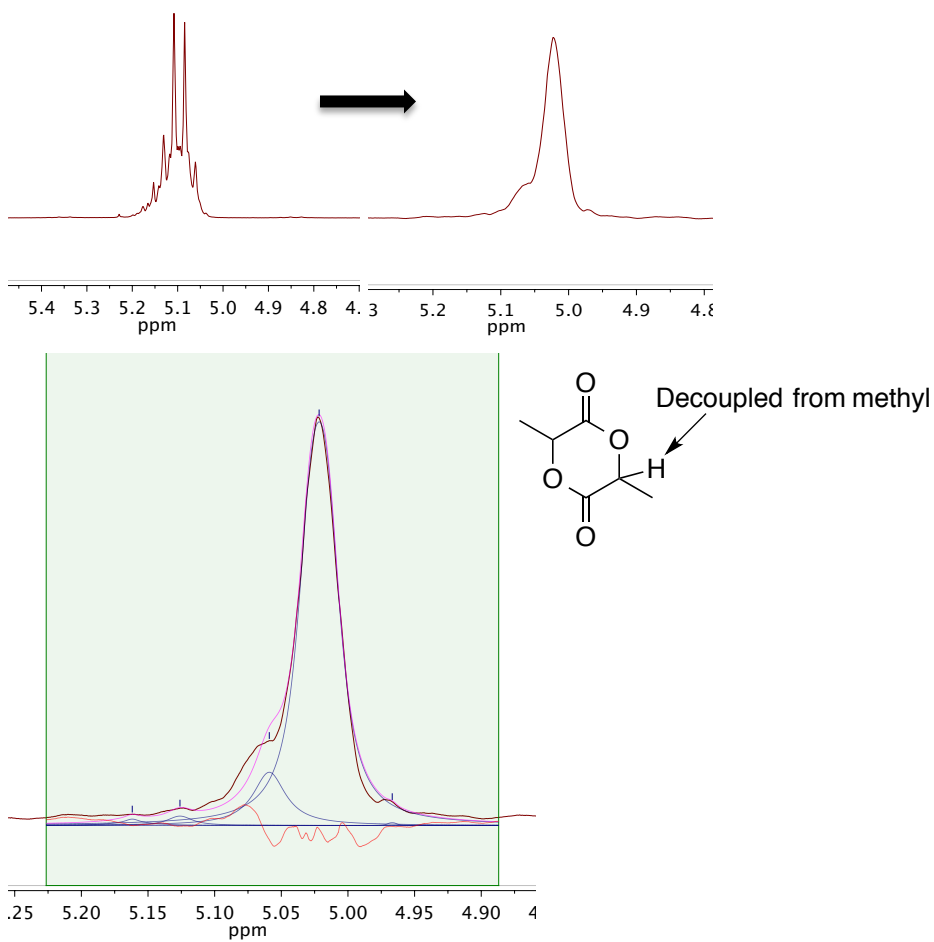
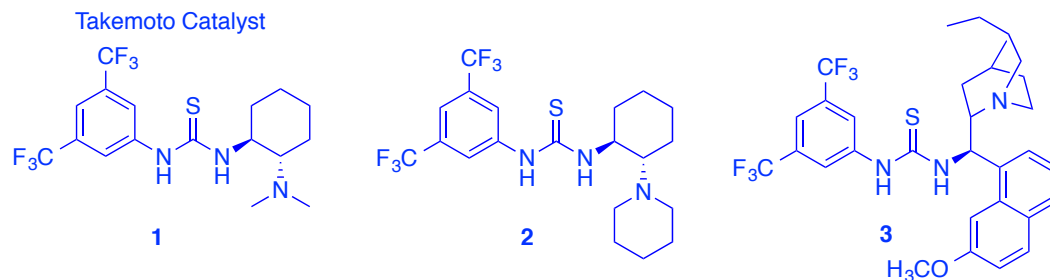


Figure 3.1. Example of selectively decoupled ¹H NMR of methine region of PLA. Left to right shows before and after decoupled ¹H NMR. (top image, 300MHz, CDCl₃). Example curve fitting for stereo sequenced peaks (bottom image, 500MHz, CDCl₃).

Previous Work:



Current Work:

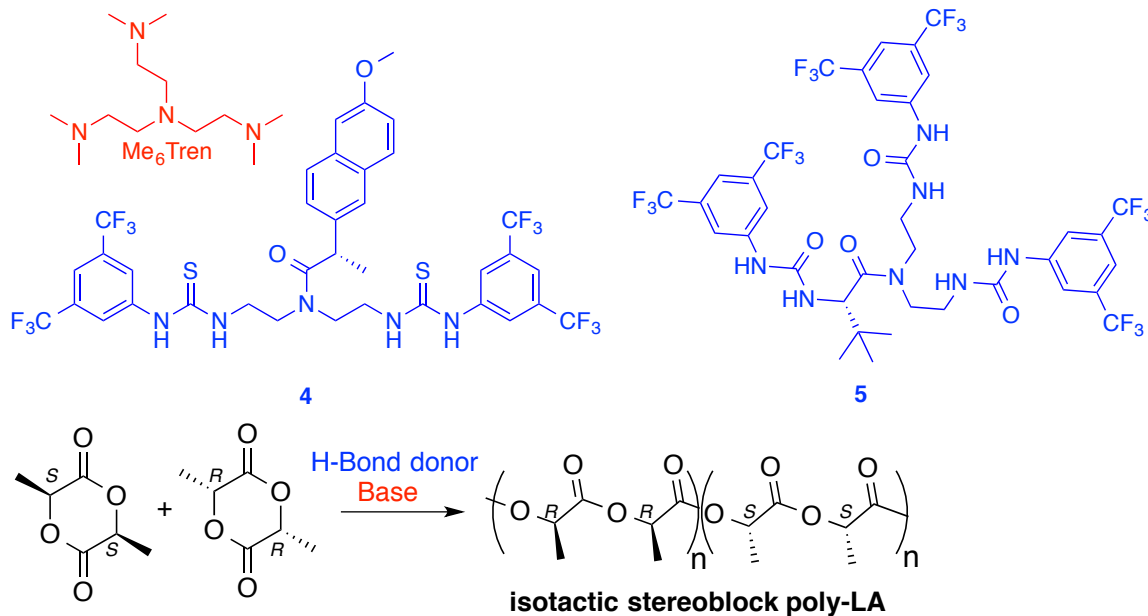


Figure 3.2. Chiral H-bonding catalysts developed for the kinetic resolution of *rac*-LA.

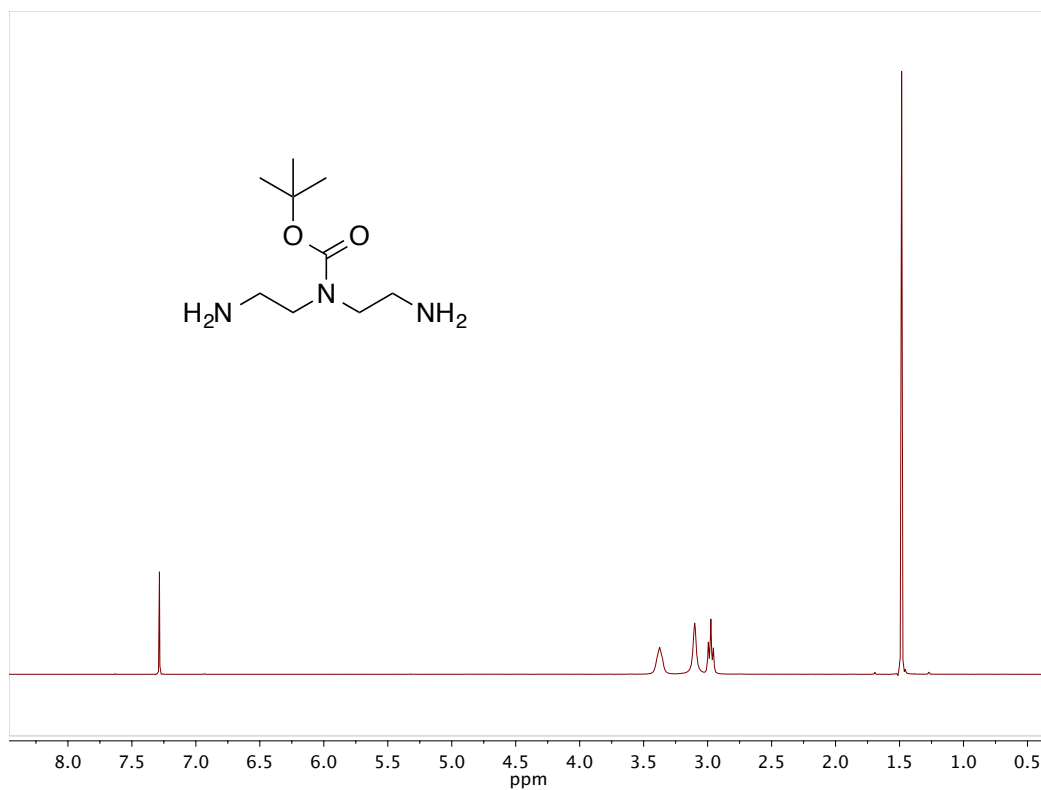


Figure 3.3. ¹H NMR (300 MHz, CDCl₃) of *tert*-butyl-bis(2-aminoethyl)carbamate.

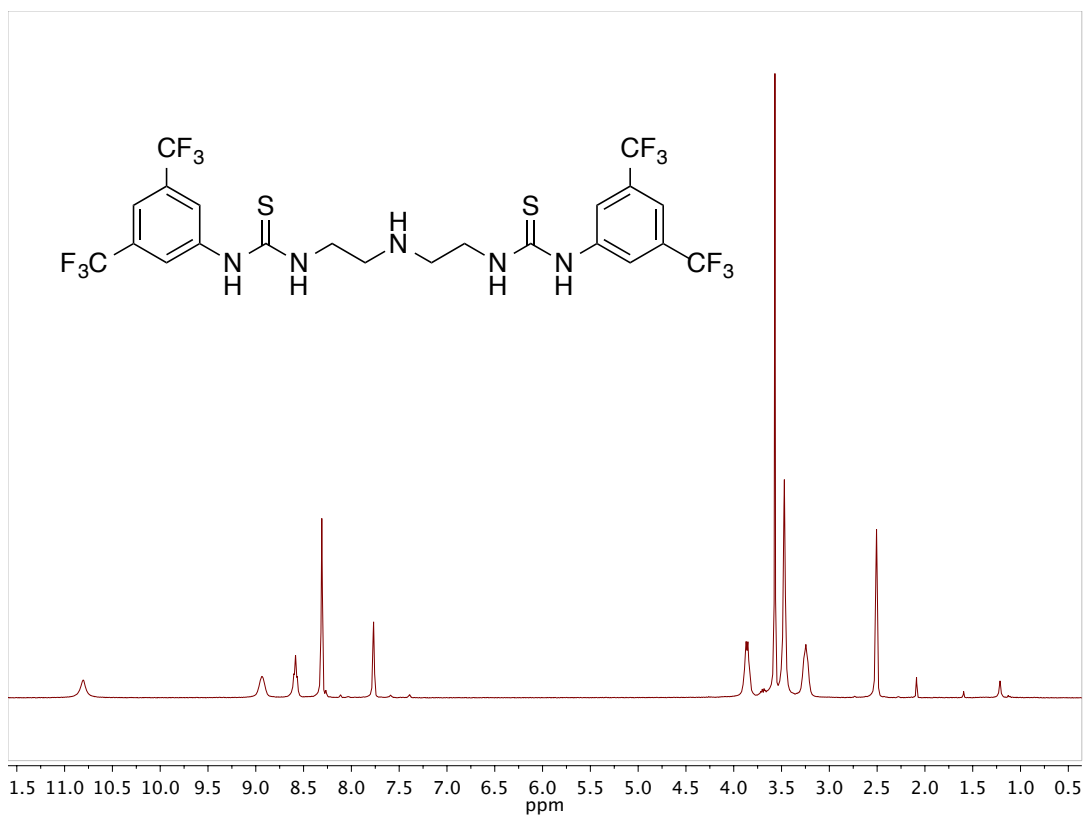


Figure 3.4. ¹H NMR (300 MHz, DMSO-*d*₆) of 1,1'-(azanediylbis(ethane-2,1-diyl))bis(3-(3,5-bis(trifluoromethyl)phenyl)thiourea).

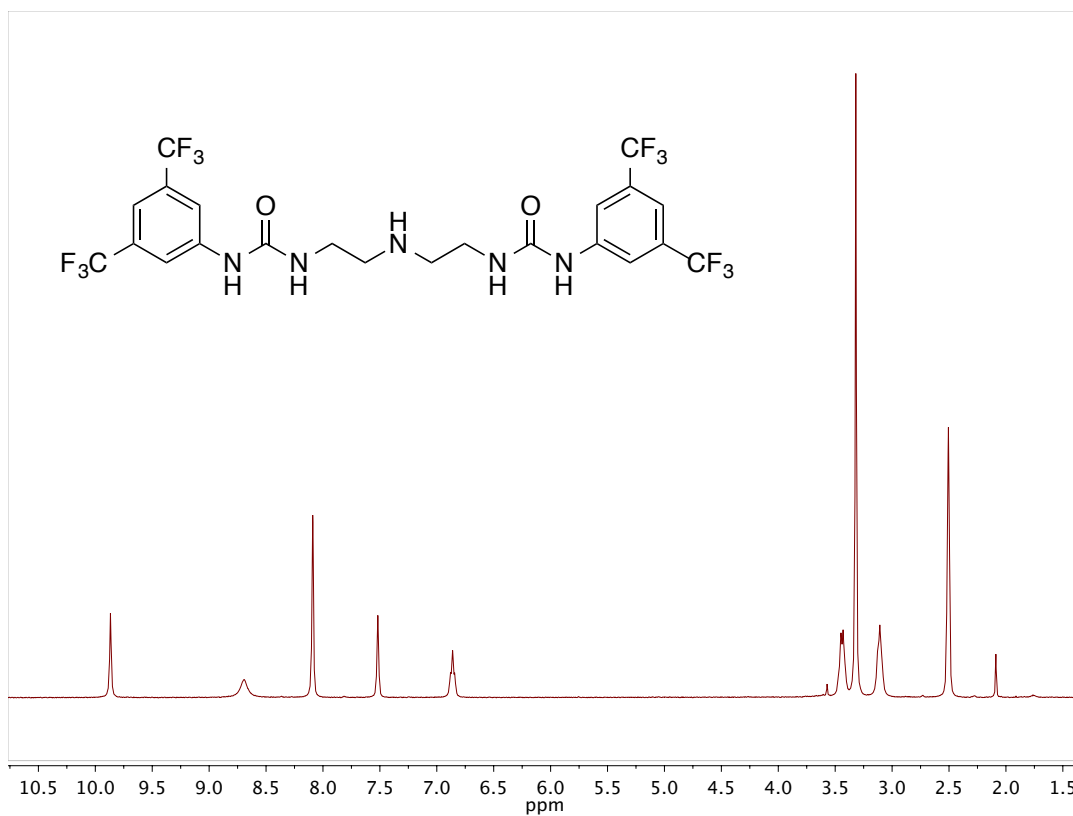


Figure 3.5. ¹H NMR (300 MHz, DMSO-*d*₆) of 1,1'-(azanediylbis(ethane-2,1-diyl))bis(3,5-bis(trifluoromethyl)phenyl)urea).

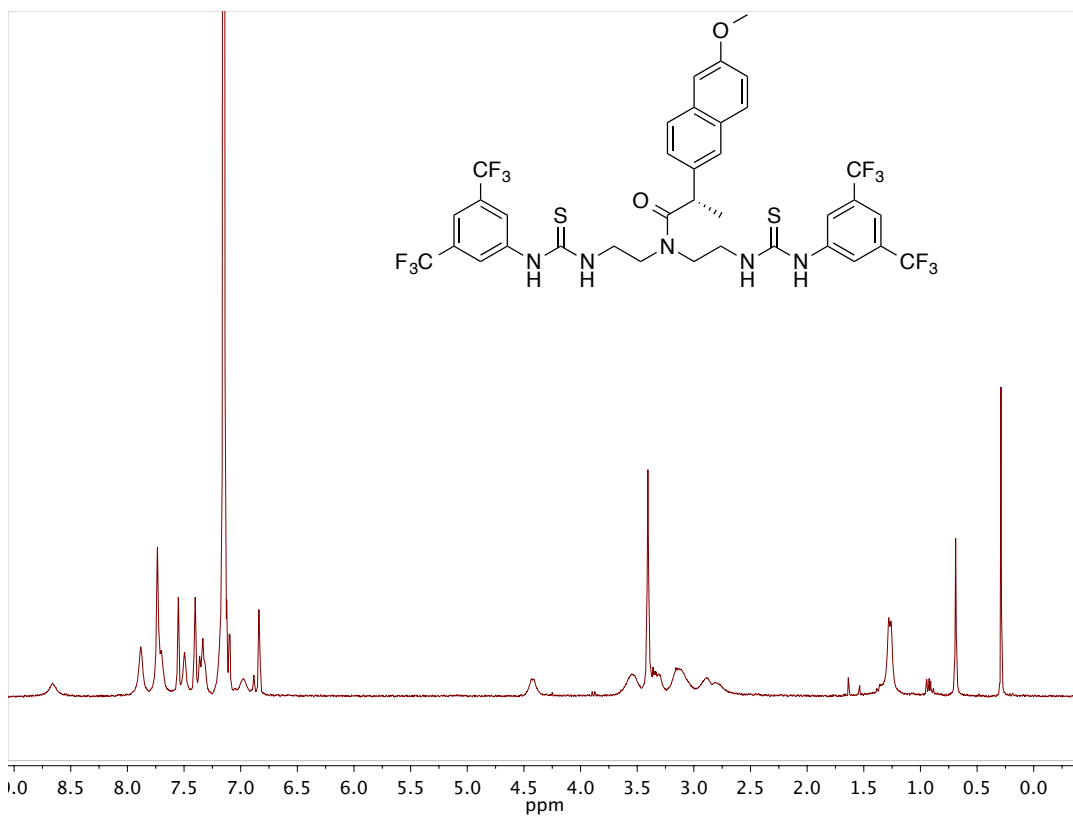


Figure 3.6. ^1H NMR (300 MHz, C_6D_6) of 4.

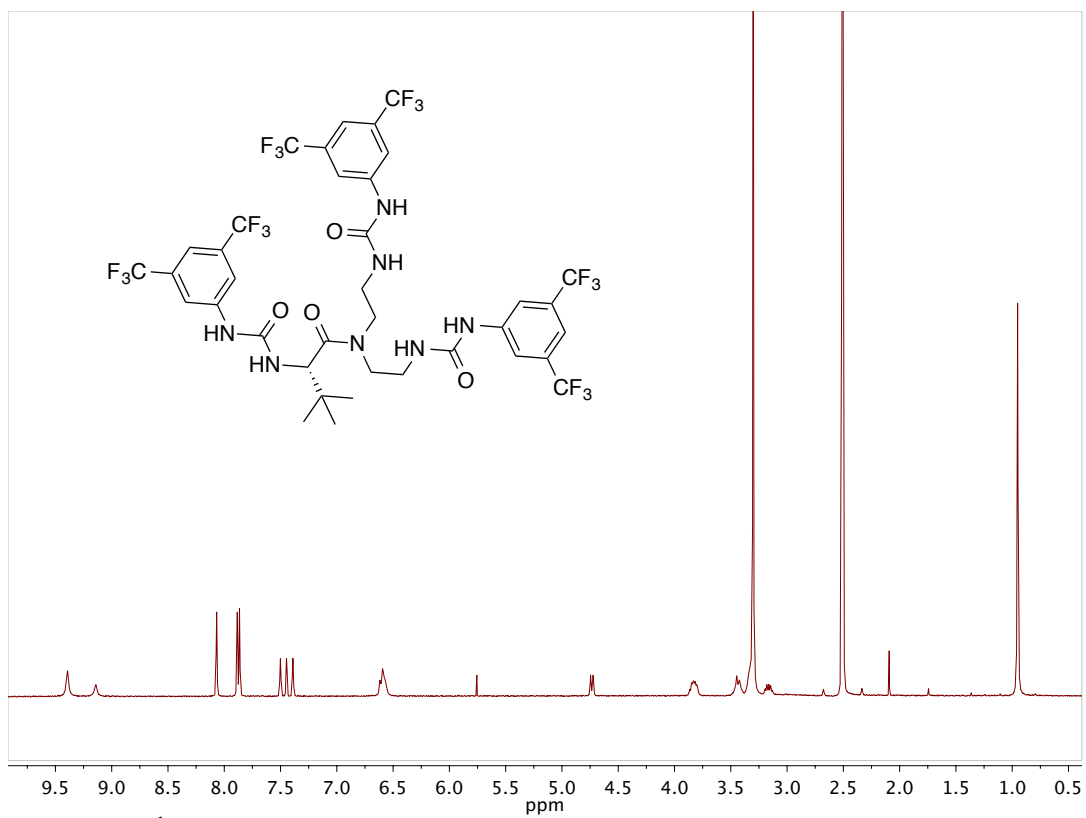


Figure 3.7. ^1H NMR (300 MHz, $\text{DMSO-}d_6$) of **5**.

INTENTIONALLY BLANK PAGE

MANUSCRIPT – IV

Published in Macromolecules

**H-bonding Organocatalysts for the Living, Solvent-free Ring-Opening
Polymerization of Lactones: Towards an All-Lactones, All-Conditions Approach**

Jinal U. Pothupitiya, Nayanthara U. Dharmaratne, Terra Marie M. Jouaneh, Kurt V.
Fastnacht, Danielle N. Coderre and Matthew K. Kiesewetter
Chemistry, University of Rhode Island, Kingston, RI, USA

Corresponding Author: Matthew Kiesewetter, Ph.D.
Chemistry
University of Rhode Island
140 Flagg Road
Kingston, RI, 02881, USA
Email address: mkiesewetter@chm.uri.edu

ABSTRACT

The developing urea class of H-bond donors facilitates the solvent-free ROP of lactones at ambient and elevated temperatures, displaying enhanced rates and control versus other known organocatalysts for ROP under solvent-free conditions. The ROPs retain the characteristics of living polymerizations despite solidifying prior to full conversion, and copolymers can be accessed in a variety of architectures. One-pot block copolymerizations of lactide and valerolactone, which had previously been inaccessible in solution phase organocatalytic ROP, can be achieved under these reaction conditions, and one-pot triblock copolymers are also synthesized. For the ROP of lactide, however, thioureas remain the more effective H-bond donating class. For all (thio)urea catalysts under solvent-free conditions and in solution, the more active catalysts are generally more controlled. A rationale for these observations is proposed. The trichloro-carban (TCC) plus base systems are particularly attractive in the context of solvent-free ROP due to their commercial availability which could facilitate the adoption of these catalysts.

INTRODUCTION

Conducting ring-opening polymerization under solvent-free conditions is an appealing strategy from several perspectives. Such situations include industrial polymerizations,¹ 'green' processes² and other applications where use and disposal of solvent is of concern as well as the ROP of macrolactones and other monomers with high equilibrium monomer concentration $[M]_{eq}$ where neat conditions are suggested by reaction thermodynamics.³⁻⁵ The H-bonding class of organocatalysts – consisting of urea or thiourea plus base – stand out among the controlled methods for ROP in their precise control for polymerization over transesterification,^{6,7} but they have not been widely applied to solvent-free ROP. These catalysts have facilitated the construction of highly tailored polymers including highly functionalized monomer feeds.⁸⁻¹³ Thiourea/base systems are widely viewed as operating through an H-bond mediated pathway whereby thiourea H-bond activates monomer and base cocatalyst activates the initiating/propagating chain end, Scheme 4.1.¹²⁻¹⁴ Nascent urea/base systems are believed to effect their highly active ROP via an imidate mediated mechanism that is more analogous to that of the guanidine organocatalyst 1,5,7-triazabicyclodec-5-ene (TBD) than their heavy chalcogen counterparts, Scheme 4.1.¹⁵⁻¹⁷ Among the larger pantheon of organic catalysts, TBD, which can operate via an H-bond mediated mechanism,¹⁸⁻²⁰ has become popular for solvent-free ROP of strained and macrolactones,²⁰⁻²² and certainly, metal-containing²³ and enzymatic catalysts²⁴⁻²⁶ are often used under solvent free conditions. The amidine organocatalyst, 1,8-diazabicycloundec-7-ene (DBU), has also been applied for the ROP of lactide in eutectic monomer blends.²⁷ Regardless, (thio)urea systems have not been applied in solvent free

conditions because, ironically, highly polar lactone monomers are poor solvents for the H-bond ROP mediated by thioureas.^{13,28} However, several urea/base cocatalysts have been recently shown to be effective in polar solvent,^{16,17} which led us to speculate that these systems may remain active under solvent-free conditions. The trichloro-carban (TCC)^{17,29} plus base systems seemed particularly attractive in this context due to their commercial availability which could facilitate wider adoption by the polymer community.

EXPERIMENTAL SECTION

General Considerations. All chemicals were purchased from Fisher Scientific and used as received unless stated otherwise. Ethylene Brassylate was purchased from Sigma Aldrich. Benzyl alcohol was distilled from calcium hydride under high vacuum. 1-pyrenebutanol was purchased from Sigma Aldrich. δ -valerolactone (VL) and ϵ -caprolactone (CL) were distilled from calcium hydride under high vacuum. L-Lactide (L-LA) was purchased from Acros Organics and recrystallized from dry toluene. 7-Methyl-1,5,7-triazabicyclo[4.4.0]dec-5-ene (MTBD), 1,8-Diazabicyclo(5.4.0)undec-7-ene (DBU) was purchased from Tokyo Chemical Industry Co. LTD. and 2-tert-butylimino-2-diethylamino-1,3-dimethylperhydro-1,3,2-diazaphosphorine (BEMP) from Acros Organics. Benzene- d_6 and chloroform- d were purchased from Cambridge Isotope Laboratories and distilled from calcium hydride. Experiments were conducted using pre-dried glassware in an MBRAUN or INERT stainless steel glovebox under N_2 atmosphere. NMR experiments were conducted on a Bruker Avance III 300 MHz or 400 MHz spectrometer, and 1H decoupled spectra were acquired on a Varian 500 MHz spectrometer. Gel Permeation Chromatography (GPC) was performed at 40 °C using HPLC grade dichloromethane eluent on an Agilent Infinity GPC system equipped with three Agilent PLGel columns 7.5 mm \times 300 mm (5 μ m, pore sizes: 10^3 , 10^4 , 50 Å). M_n and M_w/M_n were determined versus polystyrene standards (500 g/mol-3150 kg/mol, Polymer Laboratories). DSC experiments were conducted using a Shimadzu DSC-60A instrument, calibrated with an indium standard using aluminum pans under inert conditions.

Example solvent-free ROP. A 1 mL vial was charged with TCC (6.3 mg, 0.019 mmol), benzyl alcohol (0.86 mg, 0.008 mmol), VL (200 mg, 1.995 mmol), magnetic stir bar and stirred until homogeneous. A second vial was charged with MTBD (3.06 mg, 0.019 mmol) and VL (200 mg, 1.99 mmol) and agitated to mix. The contents of the second vial were transferred to the first vial using a Pasteur pipette, and the solution was stirred. Reaction progress was monitored by taking aliquots of the reaction mixture – either ~1.5 μ L solution or a small amount of solid extracted via spatula – at different time intervals and quenched in a solution of benzoic acid in chloroform-d. Conversion was determined via ^1H NMR. The polymer was isolated by precipitating with hexanes, and the volatiles were removed under high vacuum before characterization via GPC.

Example solvent-free ROP with TBD. A 1 mL vial was charged with TBD (2.8 mg, 0.019 mmol), benzyl alcohol (0.86 mg, 0.008 mmol), VL (400 mg, 3.99 mmol), magnetic stir bar and stirred vigorously to mix. The TBD does not completely dissolve under these reaction conditions. Reaction progress was monitored by taking aliquots of the reaction mixture – either ~1.5 μ L solution or a small amount of solid extracted via spatula – at different time intervals and quenched in a solution of benzoic acid in chloroform-d. Conversion was determined via ^1H NMR. The polymer was isolated by precipitating with hexanes, and the volatiles were removed under high vacuum before characterization via GPC.

Example solution ROP of LA. A 7 mL vial was charged with **2-S** (10.7 mg, 0.0174 mmol), L-LA (100 mg, 0.694 mmol), benzyl alcohol (0.72 μ L, 0.00694 mmol) and toluene (0.25M, toluene 2.77mL). PMDTA (3.63 μ L, 0.0174 mmol) was loaded into a 2 mL vial equipped with septa cap. The vials were transferred from the glovebox to an oil

bath adjusted to the specific temp. The contents of vial 1 were transferred into vial 2. Aliquots were taken via syringe and quenched using a CH₂Cl₂ solution of benzoic acid and conversion was monitored by ¹H NMR.

Example one-pot copolymerization. A 7 mL vial was charged with TCC (6.3 mg, 0.019 mmol), benzyl alcohol (1.72 mg, 0.016 mmol), VL (400 mg, 3.99 mmol), magnetic stir bar and stirred until homogeneous. A second vial was charged with BEMP (5.48 mg, 0.019 mmol) and CL (455.8 mg, 3.99 mmol) and mixed well. The contents of the second vial was transferred to the first vial using a Pasteur pipette, and the mixture was left to stir. The contents of the second vial were transferred to the first vial using a Pasteur pipette, and the solution was stirred. Reaction progress was monitored by taking aliquots of the reaction mixture – either ~1.5 μL solution or a small amount of solid extracted via spatula – at different time intervals and quenched in a solution of benzoic acid in chloroform-d. Conversion was determined via ¹H NMR. The polymer was isolated by precipitating with hexanes, and the volatiles were removed under high vacuum before characterization via GPC.

Example ROP of L-LA. A 7 mL vial was charged with **2-S** (17.1 mg, 0.028 mmol), benzyl alcohol (3 mg, 0.028 mmol), L-LA (400 mg, 2.77 mmol), stir bar, and the contents were heated to 100°C to melt the sample. A second vial was charged with PMDTA (4.80 mg, 0.028 mmol), and PMDTA was transferred via a 10 μL syringe to the first vial and the mixture was left to stir. The reaction was monitored by taking aliquots of the reaction mixture via spatula and quenching in a solution of benzoic acid in chloroform-d. Reaction progress was monitored via ¹H NMR. The polymer was then

isolated by precipitating with methanol, and the volatiles were removed under high vacuum before characterization via GPC.

Determination of percent isotacticity. The ^{13}C and ^1H decoupled NMR spectra of the isolated polymer were acquired on a Varian 500 MHz at 50°C . The samples for ^{13}C and ^1H NMR were prepared as 10 % w/v and 1% w/v solutions, respectively, in CDCl_3 . The ^1H NMR spectrum of the polymer was obtained by selective decoupling by irradiating the methyl region, and tacticity was determined from the methine region according to published procedures, see manuscript for references.

Direct-from-monomer negative mold. A 7 ml polypropylene vial was charged with TCC (13.7 mg, 0.049 mmol), benzyl alcohol (15.6 mg, 0.049 mmol), VL (1000 mg, 10 mmol) and agitated to mixed. The top inside wall of a clean vial cap was charged with BEMP (13.7 mg, 0.049 mmol), which clings to the surface of the cap. The vial was capped with the BEMP containing cap and shaken vigorously to coat the inner wall of the vial during the course of the ROP (~30 sec). The reaction vessel was removed from the glove box. The PVL vial negative is easily freed from the reaction vial.

RESULTS AND DISCUSSION

ROP of Strained Lactones. The solvent-free TCC/base cocatalyzed ROP of δ -valerolactone (VL) from benzyl alcohol at room temperature exhibits the characteristics of a living polymerization. Initial studies were performed on VL (solvent-free, 3.99 mmol) using benzyl alcohol initiator (0.2 mol %), TCC H-bond donor and one of three base cocatalysts (DBU, MTBD or BEMP in Table 4.1). The TCC/base (0.02 mmol each) catalyst systems displayed the same rate trends in neat VL as in solution¹⁷: BEMP > MTBD > DBU, Table 4.1. Polymerizations were conducted in a glovebox, and aliquots were withdrawn, quenched in a CDCl₃ solution of benzoic acid and conversion monitored by ¹H NMR (see Experimental Section). Despite solidification of the reaction mixture during the ROP (~60% conversion), the TCC/MTBD cocatalyzed ROP of VL from benzyl alcohol displays the characteristics of a living polymerization: linear evolution of M_n vs conversion, narrow M_w/M_n , first order evolution of [monomer] (Figure 4.1) and M_n predictable from $[M]_0/[I]_0$ (Table 4.1). ¹H NMR analysis of the polyvalerolactone (PVL) reaction mixture of each system (at $[M]_0/[I]_0 = 100$) confirms the consumption of benzyl alcohol initiator suggesting good initiator efficiency. When the same polymerization is initiated from pyrenebutanol, the resulting PVL displays overlapping UV/vis and RI traces in the GPC chromatogram (Figure 4.2). The TCC/BEMP system displays the same living behavior, but it was too active to effectively monitor at 0.02 mmol catalysts (4 mmol VL), although reduced catalyst loadings remain active (>0.004 mmol, the lowest evaluated) and controlled, see Table 4.5 and Figures 4.3 and 4.2. The TCC/BEMP and TCC/MTBD systems were also applied for the ROP of ϵ -caprolactone (CL). The reaction rates and molecular weight dispersities are attenuated versus the ROP of VL, but

both reactions remain controlled and display living behavior (Figure 4.4 and Table 4.6). PVL and PCL samples can be freed of catalysts impurities by washing with methanol, but PVL samples containing residual catalysts showed no alteration of their materials properties up to 0.5 mol% catalysts loading (the highest loading tested).

Both cocatalysts are required for efficient ROP. Solutions of TCC plus benzyl alcohol (0.1 mol % each) in VL (1 equiv) were stored at room temperature and periodically monitored for 60 days and showed no conversion. Solutions of BEMP or MTBD (0.5 mol%) in VL (1 equiv) were less stable towards conversion at room temperature, reaching 7% and 17% conversion, respectively, after 21 days. Both VL solutions of base were more stable when stored at -10°C, the BEMP solution showing zero conversion to polymer after 20 days, see Figure 4.5. We presume that the observed conversions are due to initiation from base.³⁰ Despite being inert separately, the combined solutions can yield an ROP so rapid, that the combined solvent-free solutions (10 mmol VL, 0.049 mmol TCC/BEMP each, 0.020 mmol benzyl alcohol) can be used to make a negative mold of the reaction vessel in 30 sec (Figure 4.6) directly from monomer. Potential application can be envisaged.

Among H-bond mediated catalysts for ROP, urea/base cocatalysts stand out for the activity and control they exhibit in solvent-free ROP conditions. Among other organic catalysts that have been applied for neat ROP,³¹⁻³³ TBD is of particular interest in the context of the present studies.^{21,22} Some reports of TBD-mediated solvent-free ROP are conducted in the melt or describe ROP to amorphous polymers,^{21,22} which would be expected to produce the narrow molecular weight distributions typical of solution processes. In our hands, TBD (Table 4.1, entry 7) exhibits similar rates as TCC/MTBD

for solvent-free ROP of VL but with broadened M_w/M_n versus the ROP with the urea/base cocatalysts. However, TCC/BEMP produces the narrowest M_w/M_n and is the most active examined under these conditions. When used alone, strong bases have also been shown to effect the ROP of lactones. For example, BEMP has been applied to the room temperature, solvent-free ROP of VL without an H-bond donating cocatalyst.³¹ The ROP appeared to be living in nature but sluggish, reaching full conversion to poly(valerolactone) (PVL) in days and displaying a broadened M_w/M_n .³¹ We believe the ability to conduct rapid and highly controlled ROP of lactones like VL and CL under solvent-free and non-melt conditions constitutes an advantage of the TCC/base cocatalysts over other (organo)catalyst systems.

The observation of highly active TCC/base cocatalyzed ROP under solvent-free conditions corroborates an imidate mechanism of action, Scheme 4.1. Several H-bond donors were evaluated for the solvent-free ROP of VL (Table 4.2), and these results suggest that urea H-bond donors are more effective than thiourea H-bond donors for the ROP of strained lactones. This observation is consistent with a cocatalyst binding argument for thiourea/base cocatalyzed ROP,^{28,34} as the cocatalyst interactions would be greatly attenuated in polar VL solvent whereas thiourea-VL binding should remain active in neat monomer. For the urea/base cocatalyzed ROP under an imidate mechanism, the efficacy of the catalysts would not be disturbed by the polar reaction environment. This is confirmed by NOESY NMR experiments of acetone- d_6 solutions of TCC/MTBD or TCC/BEMP which show intermolecular contact, indicating the formation of the imidate (Figure 4.7). NOESY experiments on **1-S**/MTBD and **1-S**/BEMP show no intermolecular communication in acetone- d_6 or C_6D_6 , which suggests that thioimide

formation is not a prominent mechanism of action for these catalyst pairs. These experiments are corroborated by previous studies performed by our group that show strong H-bonding (no proton transfer) between cocatalyst pairs of thiourea and base,²⁸ but evidence of proton transfer is observed between urea and base.¹⁷ Previous studies have shown that 1:1 mole ratios of H-bond donor and base are optimal for ROP (in solution) no matter how many H-bond donating moieties are present in the donor molecule.^{28,35,36}

ROP of Macrolactones. The TCC/BEMP cocatalyzed ROP of macrolactones, ethylene brassylate and pentadecalactone, under solvent-free conditions proceeds at 80°C. The TCC/BEMP (0.06 mmol) cocatalyzed ROP of EB (2.95 mmol) at room temperature and solvent-free is exceedingly slow (16 h, 60% conversion), but the same ROP at 80°C proceeds in hours to full conversion, Table 4.3. The ROP reactions in Table 4.3 display moderate control of M_n by $[M]_0/[I]_0$ and broad $M_w/M_n \sim 1.5$; however, the M_n evolves linearly with conversion and M_w/M_n remains narrow early in the ROP (Figure 4.8). These observations are consistent with previous reports of the entropically-controlled ROP of macrolactones, which often require heating to favor the formation of polymer,^{22,24,25,37} although enzymatic catalysts do not require excessive heating.^{3,24,26} The results with TCC/BEMP stand in stark contrast to the ROP of EB (0.4 g, 1.47 mmol) mediated by **1-S**/BEMP (0.03 mmol each) from benzyl alcohol (0.03 mmol) which achieves only 25% conversion to polymer in 10 hours. When combined with the **1-S** vs TCC result for the ROP of VL (see ROP of Strained Lactones), these results suggest that ureas are generally more effective than thiourea H-bond donors for ROP.

H-bonding catalysts are effective and thermally stable at 80°C. The ROP of macrolactones are usually conducted at elevated temperatures so that the entropically

controlled enchainment favors the formation of polymer.^{22,37} Hence, the H-bond mediated, solvent-free ROP of macrolactones presents a distinct challenge over that of VL or CL because the H-bonding interactions of thiourea and urea mediated ROP weaken at high temperature.³⁸ Further, organic catalysts are susceptible to charring/decomposition at high temperature.³⁹ However, neither deactivation nor decomposition appear to be a concern for TCC/base cocatalyzed ROP at 80°C (Table 4.3). TCC/BEMP were also applied for the solvent-free ROP of PDL from benzyl alcohol (Table 4.3). Versus EB, the polymerization times (6-8 h) and M_w/M_n (> 2) are attenuated, which may be due to the elevated viscosity of the PDL and PPDL vs EB and PEB.

ROP of Lactide. Contrary to other lactones, thiourea catalysts are more active than their urea analogues in the solvent-free ROP of L-LA conducted at 100°C. L-LA and isotactic PLA are crystalline which requires elevated temperatures to melt the monomer ($T_m = 97^\circ\text{C}$) and, ostensibly, polymer ($T_m = 180^\circ\text{C}$, PLLA). Several H-bond donors with PMDTA cocatalyst (0.0277 mmol each, see Table 4.4) were evaluated for the solvent-free ROP of L-LA (0.40 g, 2.77 mmol) from benzyl alcohol (0.055 mmol) at 100°C. As opposed to the (thio)urea mediated ROP of VL or CL, weak base cocatalysts are optimal for the ROP of LA.^{13,40} Every thiourea H-bond donor is more active for the ROP of LA than its corresponding urea H-bond donor. Indeed, the only urea that stands out in the series is TCC, which is more active in the ROP than the other urea H-bond donors. A similar trend has been observed in solution where TCC is more active than **1-O**,¹⁷ and ureas with fewer electron withdrawing substituents have been observed to be more active.¹⁶

A screen of base cocatalysts with **2-S** showed PMDTA cocatalyst to exhibit a good combination of high rate and control (Table 4.7). The reaction solution solidifies during the course of the polymerization, ~80% conversion, Figure 4.9, and the first order evolution of concentration of monomer exhibits deviation from linearity that may be associated with limited molecular mobility in the crystalline polymer. However, the other characteristics of a living polymerization persist: M_n predictable from $[M]_0/[I]_0$, linear evolution of M_n vs conversion, and narrow M_w/M_n (Figure 4.9). When initiated from pyrenebutanol, the **2-S**/PMDTA cocatalyzed ROP in solvent-free conditions produces PLA that exhibits overlapping UV and RI traces in the GPC (Figure 4.2), which suggests that the polymer chains are initiated from the fluorescent alcohol. Certainly, the results in Table 4.4 suggest that conducting the H-bond mediated ROP of LA in the polymer melt (i.e. $>180^\circ\text{C}$) is not necessary to retain the high level of control associated with a living organocatalytic ROP.

The solvent-free ROP of LA mediated by **2-S**/PMDTA remains active at elevated temperatures. Solution ROPs of LA (0.694 mmol, 0.25 M) from benzyl alcohol (0.0025 M) using **2-S**/PMDTA (0.0063 M each) were conducted in toluene. At 50°C , the ROP proceeds to 24% conversion in 125 min ($k_{\text{obs}} = 0.0021$, Figure 4.10), but at 80°C and above, the reaction proceeds to polymer very slowly (2% conversion at 60 min). Analogous solvent-free ROP remains active up to 180°C (the highest temperature examined), and the ROPs of macrolactones do not experience deactivation at elevated temperature (see ROP of Macrolactones). The low concentrations required to fully dissolve LA in toluene is not the source of the catalyst deactivation at high temperature. A solvent free ROP of LA (6.244 mmol) catalyzed by **2-S**/PMDTA at reduced catalyst

loadings (0.006 mmol each) from benzyl alcohol (0.125 mmol) at 100°C achieves 90% conversion in 24 h. Further, the solution ROP in CDCl₃ (1 M LA; 0.025 M cats; 0.010 M benzyl alcohol) allows for higher reagent concentrations, but a ROP at 40°C in this solvent is not appreciably faster than the low concentration toluene run discussed above ($k_{\text{CDCl}_3}/k_{\text{toluene}} = 2$). Even these reaction conditions experience reduced activity at elevated temperatures. These observations suggest greater synthetic flexibility in the solvent-free (versus solution) ROP of LA.

For the ROP of lactide, the effects of reaction conditions on polymer tacticity must also be considered. For each polymerization in Table 4.4, the percent isotacticity was determined from the isolated polymer by ¹H decoupled ¹³C NMR using previously established tacticity-dependent chemical shifts (Experimental Section).^{13,41,42} A small temperature screen was conducted, and running the **2-S**/PMDTA (0.028 mmol each) cocatalyzed ROP of L-LA at or below ~97°C (the melting point of LA) results in drastically reduced polymerization rates, and reaction temperatures at or above 140°C erode stereochemistry. In the ROP of L-LA, the retention of stereochemistry is important due to the highly tacticity-dependent material properties of PLA.³⁹ The **2-S**/PMDTA cocatalyst system (Table 4.4, entry 1) is not only the most active catalyst of the systems examined, but it exhibits the highest isotacticity (0.94). This observation suggests that **2-S** is highly selective for chain extension vs non-productive reactions and begs for the further optimization of this platform, which will be the focus of future work. In a recent touchstone on the challenges of solvent-free ROP of LA,³⁹ it was noted that commercial samples of PLA are ideally >0.97 isotacticity. This suggests that **2-S**/PMDTA at 0.94 isotacticity is not a ready-made solution to the problem that is the solvent-free,

organocatalytic ROP of LA; however, our results suggest that these H-bond mediated catalysts may be able to provide the answer upon further optimization. Indeed, in a comparable solution experiment (c.f. Table 4.4, entry 1), the **2-S**/PMDTA (0.05 mmol) cocatalyzed ROP of L-LA (1 mmol, 1 M) from benzyl alcohol (0.01 mmol) in CDCl₃ at room temperature yields highly isotactic polymer (%iso = 0.97; T_m = 169°C). In addition to tacticity, the introduction of color to PLA samples from catalyst (or decomposition) impurities can be a concern.³⁹ The **2-S**/PMDTA cocatalyzed ROP (Table 4.4, entry 1) produces an off-white, yellow color at high conversion, but the discoloration is very minimal if freshly-distilled PMDTA is used. Future catalysts with enhanced thermal stability or augmented activity (i.e. lower catalyst loadings) may prevent discoloration, but the color is easily removed by washing the polymer with methanol. Last, the comparable TBD-catalyzed (0.014 mmol) ROP of L-LA (0.40 g, 2.78 mmol) from benzyl alcohol (0.028 mmol) was conducted under solvent-free conditions (at 100°C) resulting in 90% conversion to polymer in 4 h and yielding PLLA that exhibits lower isotacticity (%iso = 0.78) than the **2-S**/PMDTfA cocatalyzed reaction (TBD polymer: M_n = 19,900; M_w/M_n = 1.30). These results suggest that **2-S**, and indeed most thioureas, plus amine base cocatalysts are more effective than TBD for the solvent-free ROP of LA.

Unlike other monomers examined, thioureas (vs ureas) are superior catalysts – in terms of both activity and control – for the H-bond mediated ROP of lactide. We conducted a rate comparison for the **1-S** vs **1-O** (with PMDTA) mediated ROP of L-LA in acetone-d₆, and the thiourea catalyst is the more active of the two: k_{1-S}/k_{1-O} (acetone-d₆) = 4.4. Contrary to LA, ureas are always more active and controlled than the corresponding thioureas for the ROP of VL and CL regardless of the reaction solvent.^{17,36}

This suggests that the relative activity of urea vs thiourea is not dictated by solvent, and the various monomers seem to exhibit a preference for urea vs thiourea. Our group previously described the activity of thiourea/amine base cocatalysts in the ROP of LA as being related to the nature of cocatalyst binding (i.e. enthalpic vs solvophobic binding),³⁴ and understanding the preference exhibited by LA for thioureas vs ureas may require a full study of the solution interactions at play during an ROP catalyzed by the various catalysts. We are unable to measure a urea/LA binding constant due to poor solubility in non-hydrogen bonding solvents.

Copolymerizations. The generation of copolymers is possible through a one-pot, solvent-free approach. In the one-pot ROP of VL (3.99 mmol) and CL (3.99 mmol) from benzyl alcohol (0.016 mmol) (solvent-free, room temperature), the TCC/MTBD (0.02 mmol) cocatalyst system fully converts VL to polymer in 10 min, but the homopolymer precipitates from CL solution prior to conversion of the slower opening monomer. The TCC/BEMP system, however, allows for the full conversion to PVL-co-PCL ($M_n = 94,000$; $M_w/M_n = 1.41$) in 5 h. The first order evolution of [monomer]s versus time suggests the formation of a gradient-block copolymer (Figure 4.11). The successful formation of block-copolymer with TCC/BEMP versus TCC/MTBD which does not produce copolymer suggests that the former cocatalysts are able to conduct ROP of the slower monomer on a time scale that is competitive with precipitation of the homo-PVL from CL solvent. Copolymerizations were also performed with VL/EB (3.99 mmol/3.99 mmol) and CL/EB (3.5 mmol/3.5 mmol) employing the TCC/BEMP (2 mol%) cocatalysts. In these ROPs, conducted entirely at room temperature and solvent free (see Experimental Section) VL and CL quickly achieve full conversion in 5 min and 6 min,

respectively, and the EB blocks grow slowly over the next ~11 h to give PVL-co-PEB ($M_n = 27,000$; $M_w/M_n = 1.60$) and PCL-co-PEB ($M_n = 28,700$; $M_w/M_n = 1.48$). The relative kinetics (Figure 4.12) suggest the formation of block copolymers. This same approach was used to generate a one-pot triblock copolymer: VL (3.99 mmol), CL (3.99 mmol) and EB (3.99 mmol) were grown from benzyl alcohol (0.1197 mmol) using TCC/BEMP (0.1197 mmol each). The conversion versus time of this ROP suggests a gradient-block polymer (see SI, the previous VL/CL copolymerization produced a gradient-copolymer), and ^1H and ^{13}C NMR of the isolated polymer (see Figure 4.13) indicate that all blocks are present ($M_n = 40,000$, $M_w/M_n = 1.53$).

A solvent-free approach to the copolymerization of LA and VL allows for the one-pot synthesis of block copolymers. In the one-pot synthesis of diblock copolymers of LA and VL in solution, the ROP has been observed to proceed to full conversion of LA when reaction progress halts, resulting in the incorporation of no comonomer.¹¹ To confirm this report, a copolymerization of LA (0.33 mmol, 0.66 M) and VL (0.99 mmol, 2 M) from benzyl alcohol using trimethyl-1,4,7-triazacyclononane (t-TACN, see Table 4.7)/TCC cocatalysts (0.0265 mmol each) was attempted in C_6D_6 .^{34,40} The LA achieved full conversion to polymer in 18 h, but the VL does not convert over the next 24 hours; the expected result. Under solvent-free conditions, however, the copolymerization under otherwise same conditions results in full conversion of both monomer portions in 3.5 h yielding a single peak in the GPC trace ($M_n = 27,600$; $M_w/M_n = 1.57$) and two phase transitions (DSC: $T_m = 52^\circ\text{C}$ and 148°C). First order evolution of [monomer]s vs time suggests the formation of a block copolymer (Figure 4.14). When the one-pot copolymerization of LA and CL is attempted, the LA achieves full conversion in 2 min,

but the CL does not undergo any enchainment over the next 24 h. Typically, alkylamine base cocatalysts are not effective for the ROP of VL or CL, but these results suggest that solvent-free, reaction conditions may provide new opportunities in catalyst development as well as materials synthesis.

CONCLUSION

Thiourea and urea catalysts have been shown to be effective for the solvent-free ROP of lactones at ambient and elevated temperatures. The urea class of H-bond donors facilitates solvent-free ROP for most monomers (VL, CL and EB), the thioureas being exceedingly slow in the ROP of these highly polar lactones. Solvent polarity is not the primary determining factor, however, as thioureas (not ureas) are more effective for the ROP of LA in solvent and the monomer melt. The ROPs retain the characteristics of a living polymerization despite solidifying prior to full conversion, and copolymers can be accessed in a variety of combinations. For those seeking to employ organocatalysts of this class in polymer synthesis, we offer a succinct summation: 1) urea (vs thiourea) H-bond donors plus base are the most active and most controlled organocatalysts for ROP under any reaction conditions (lactide excluded); 2) TCC/BEMP is the most active, most controlled organocatalytic system but TCC/MTBD is almost as active and probably more readily available; 3) for the ROP of lactide, the bithiourea **2-S** plus PMDTA is the most active and controlled organic cocatalyst system that we are aware of. In catalyst development, the community has come a long way in terms of catalytic activity from **1-S** (PLA: 0.7/min; PVL: 0.2/min) to more active H-bond donors (PLA: 18.2/min (**2-S**); PVL: 63/min (TCC)), but catalyst productivity has so far been limited by catalyst deactivation at reduced loadings. Further, there is no ostensible cost – in terms of reaction control – for employing more active (thio)urea H-bond donors. For (thio)urea ROP catalysts under solvent-free conditions and in solution,^{35,36} more active catalysts are generally more controlled.

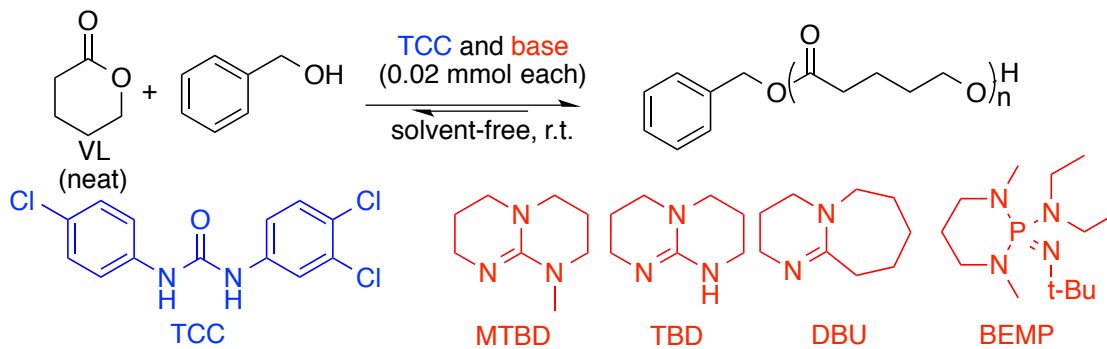
LIST OF REFERENCES

- (1) Lim, L. T.; Auras, R.; Rubino, M. *Prog. Polym. Sci.* **2008**, *33*, 820–852.
- (2) Mathers, R. T.; Meier, M. A. R. In *Green Polymerization Methods: Renewable Starting Materials, Catalysis and Waste Reduction*; Mathers, R. T., Meier, M. a R., Eds.; Wiley-VCH: Federal Republic of Germany, 2011; pp 1–7.
- (3) Albertsson, A.-C.; Varma, I. K.; Srivastava, R. K. In *Handbook of Ring-Opening Polymerization*; Dubois, P., Coulembier, O., Raquez, J.-M., Eds.; Wiley-VCH: Federal Republic of Germany, 2009; pp 287–302.
- (4) Olsén, P.; Odelius, K.; Albertsson, A. C. *Biomacromolecules* **2016**, *17* (3), 699–709.
- (5) James, S. L.; Adams, C. J.; Bolm, C.; Braga, D.; Collier, P.; Friščić, T.; Grepioni, F.; Harris, K. D. M.; Hyett, G.; Jones, W.; Krebs, A.; Mack, J.; Maini, L.; Orpen, a G.; Parkin, I. P.; Shearouse, W. C.; Steed, J. W.; Waddell, D. C. *Chem. Soc. Rev.* **2012**, *41* (1), 413–447.
- (6) Kiesewetter, M. K.; Shin, E. J.; Hedrick, J. L.; Waymouth, R. M. *Macromolecules* **2010**, *43* (5), 2093–2107.
- (7) Kamber, N. E. N. E.; Jeong, W.; Waymouth, R. M. R. M.; Pratt, R. C. R. C.; Lohmeijer, B. G. G.; Hedrick, J. L. *Chem. Rev.* **2007**, *107* (12), 5813–5840.
- (8) Cooley, C. B.; Trantow, B. M.; Nederberg, F.; Kiesewetter, M. K.; Hedrick, J. L.; Waymouth, R. M.; Wender, P. A. *J. Am. Chem. Soc.* **2009**, *131*, 16401–16403.
- (9) Geihe, E. I.; Cooley, C. B.; Simon, J. R.; Kiesewetter, M. K.; Edward, J. a; Hickerson, R. P.; Kaspar, R. L.; Hedrick, J. L.; Waymouth, R. M.; Wender, P. a. *Proc. Natl. Acad. Sci. U. S. A.* **2012**, *109* (33), 13171–13176.

- (10) Pratt, R. C.; Nederberg, F.; Waymouth, R. M.; Hedrick, J. L. *Chem. Commun.* **2008**, 114–116.
- (11) Lohmeijer, B. G. G.; Pratt, R. C.; Leibfarth, F.; Logan, J. W.; Long, D. A.; Dove, A. P.; Nederberg, F.; Choi, J.; Wade, C.; Waymouth, R. M.; Hedrick, J. L. *Macromolecules* **2006**, *39* (25), 8574–8583.
- (12) Dove, A. P.; Pratt, R. C.; Lohmeijer, B. G. G.; Waymouth, R. M.; Hedrick, J. L. *J. Am. Chem. Soc.* **2005**, *127* (40), 13798–13799.
- (13) Pratt, R. C.; Lohmeijer, B. G. G.; Long, D. a.; Lundberg, P. N. P.; Dove, A. P.; Li, H.; Wade, C. G.; Waymouth, R. M.; Hedrick, J. L. *Macromolecules* **2006**, *39* (23), 7863–7871.
- (14) Thomas, C.; Bibal, B. *Green Chem.* **2014**, *16* (4), 1687–1699.
- (15) Zhang, X.; Jones, G. O.; Hedrick, J. L.; Waymouth, R. M. *Nat. Chem.* **2016**, *8* (11), 1047–1053.
- (16) Lin, B.; Waymouth, R. M. *J. Am. Chem. Soc.* **2017**, *139* (4), 1645–1652.
- (17) Dharmaratne, N. U.; Pothupitiya, J. U.; Bannin, T. J.; Kazakov, O. I.; Kiesewetter, M. K. *ACS Macro Lett.* **2017**, *6* (4), 421–425.
- (18) Chuma, A.; Horn, H. W.; Swope, W. C.; Pratt, R. C.; Zhang, L.; Lohmeijer, B. G. G.; Wade, C. G.; Waymouth, R. M.; Hedrick, J. L.; Rice, J. E. *J. Am. Chem. Soc.* **2008**, *130* (21), 6749–6754.
- (19) Simón, L.; Goodman, J. M. *J. Org. Chem.* **2007**, *72* (25), 9656–9662.
- (20) Pratt, R. C.; Lohmeijer, B. G. G.; Long, D. A.; Waymouth, R. M.; Hedrick, J. L. *J. Am. Chem. Soc.* **2006**, *128* (14), 4556–4557.
- (21) Martello, M. T.; Burns, A.; Hillmyer, M. *ACS Macro Lett.* **2012**, *1* (1), 131–135.

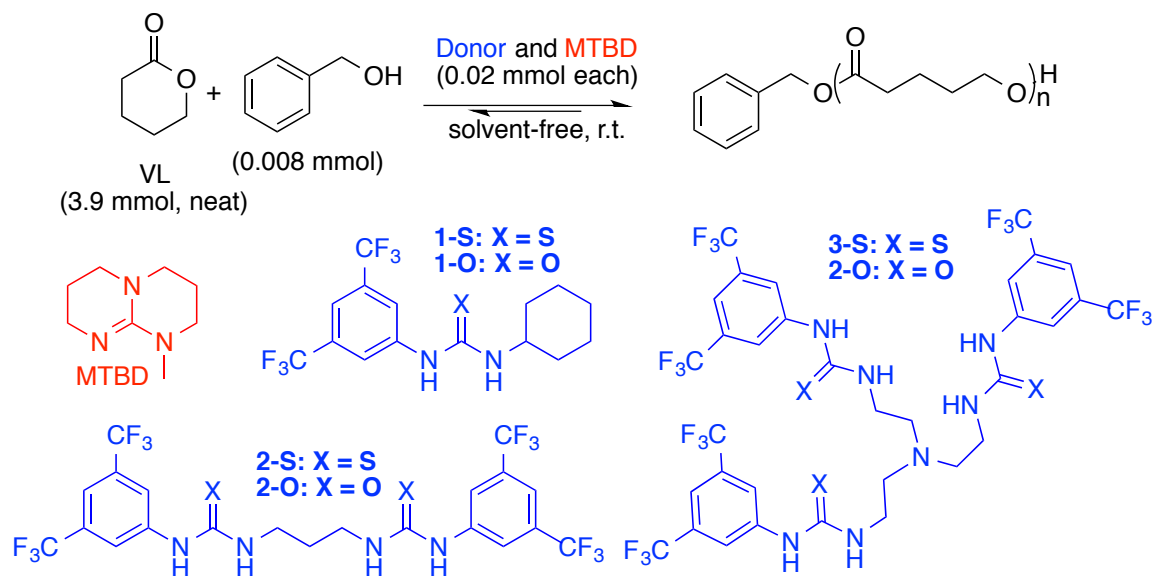
- (22) Pascual, A.; Sardon, H.; Veloso, A.; Ruiperez, F.; Mecerreyes, D. *ACS Macro Lett.* **2014**, *3* (9), 849–853.
- (23) Ding, L.; Jin, W.; Chu, Z.; Chen, L.; Lü, X.; Yuan, G.; Song, J.; Fan, D.; Bao, F. *Inorg. Chem. Commun.* **2011**, *14* (8), 1274–1278.
- (24) Van Der Mee, L.; Helmich, F.; De Bruijn, R.; Vekemans, J. A. J. M.; Palmans, A. R. A.; Meijer, E. W. *Macromolecules* **2006**, *39* (15), 5021–5027.
- (25) Duda, A.; Kowalski, A.; Penczek, S.; Uyama, H.; Kobayashi, S. *Macromolecules* **2002**, *35* (11), 4266–4270.
- (26) Heise, A.; Duxbury, C. J.; Palmans, A. R. A. In *Handbook of Ring-Opening Polymerization*; Dubois, P., Coulembier, O., Raquez, J.-M., Eds.; Wiley-VCH: Federal Republic of Germany, 2009; pp 379–394.
- (27) Coulembier, O.; Lemaur, V.; Josse, T.; Minoia, A.; Cornil, J.; Dubois, P. *Chem. Sci.* **2012**, *3* (3), 723–726.
- (28) Kazakov, O. I.; Datta, P. P.; Isajani, M.; Kiesewetter, E. T.; Kiesewetter, M. K. *Macromolecules* **2014**, *47* (21), 7463–7468.
- (29) Erickson, B. E. *Chem. Eng. News* **2016**, *94* (36), 16.
- (30) Stukenbroeker, T. S.; Bandar, J. S.; Zhang, X.; Lambert, T. H.; Waymouth, R. M. *ACS Macro Lett.* **2015**, *4* (8), 853–856.
- (31) Zhang, L.; Nederberg, F.; Pratt, R. C.; Waymouth, R. M.; Hedrick, J. L.; Wade, C. G.; V, S. U.; February, R. V; Re, V.; Recci, M.; April, V. *Macromolecules* **2007**, *40*, 4154–4158.
- (32) Ladelta, V.; Bilalis, P.; Gnanou, Y.; Hadjichristidis, N. *Polym. Chem.* **2017**, *8* (3), 511–515.

- (33) Kadota, J.; Pavlović, D.; Hirano, H.; Okada, A.; Agari, Y.; Bibal, B.; Deffieux, A.; Peruch, F. *RSC Adv.* **2014**, *4* (28), 14725.
- (34) Kazakov, O. I.; Kieseewetter, M. K. *Macromolecules* **2015**, *48* (17), 6121–6126.
- (35) Spink, S. S.; Kazakov, O. I.; Kieseewetter, E. T.; Kieseewetter, M. K. *Macromolecules* **2015**, *48* (17), 6127–6131.
- (36) Fastnacht, K. V.; Spink, S. S.; Dharmaratne, N. U.; Pothupitiya, J. U.; Datta, P. P.; Kieseewetter, E. T.; Kieseewetter, M. K. *ACS Macro Lett.* **2016**, *5* (8), 982–986.
- (37) Duda, A.; Kowalski, A. In *Handbook of Ring-Opening Polymerization*; Dubois, P., Coulembier, O., Raquez, J.-M., Eds.; Wiley-VCH Verlag GmbH & Co. KGaA, 2009; pp 1–52.
- (38) Anslyn, E. V.; Dougherty, D. A. In *Modern Physical Organic Chemistry*; 2006; pp 162–194.
- (39) Mezzasalma, L.; Dove, A. P.; Coulembier, O. *Eur. Polym. J.* **2017**, No. May, 0–1.
- (40) Coady, D. J.; Engler, A. C.; Horn, H. W.; Bajjuri, K. M.; Fukushima, K.; Jones, G. O.; Nelson, A.; Rice, J. E.; Hedrick, J. L. *ACS Macro Lett.* **2012**, *1* (1), 19–22.
- (41) Ovitt, T. M.; Coates, G. W. *J. Am. Chem. Soc.* **2002**, *124* (7), 1316–1326.
- (42) Thakur, K. a M.; Kean, R. T.; Hall, E. S.; Kolstad, J. J.; Lindgren, T. a; Doscotch, M. a; Siepmann, J. I.; Munson, E. J. *Macromolecules* **1997**, *30* (8), 2422–2428.



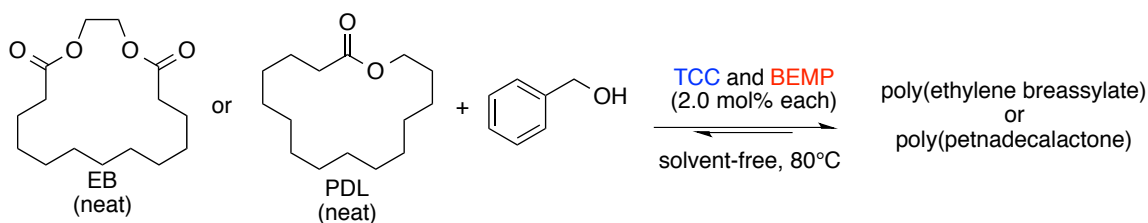
Entry	Base	$[M]_0/[I]_0$	Time (min)	Conv. ^a (%)	M_n^b (g/mol)	M_w/M_n^b
1	DBU	500	65	97	99,500	1.12
2	BEMP	500	3	95	108,000	1.04
3	MTBD	500	31	99	100,500	1.08
4		200	15	96	43,900	1.07
5		100	15	98	22,000	1.16
6		50	10	98	10,300	1.10
7 ^c	TBD	500	27	99	115,500	1.21

Table 4.1. TCC plus base cocatalyzed ROP of VL. Reaction conditions: VL (3.99 mmol, 1 equiv, neat), TCC and base (0.02 mmol, each). a) monomer conversion was monitored via ^1H NMR. b) M_n and M_w/M_n were determined by GPC (CH_2Cl_2) vs polystyrene standards. c) no TCC, only TBD (0.02 mmol).



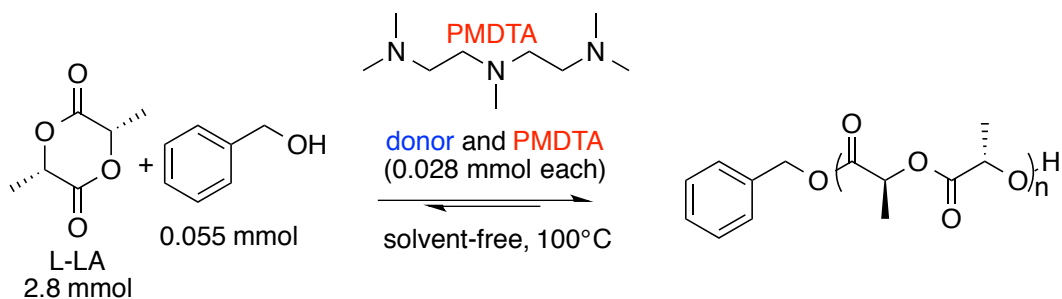
Entry	Donor	Time (min)	Conv. ^a (%)	M_n^b (g/mol)	M_w/M_n^b
1	1-S	1,200	94	71,500	1.29
2	1-O	440	96	97,800	1.17
3	2-S	1,420	96	82,300	1.17
4	2-O	30	97	101,000	1.13
5	3-S	1,900	99	85,700	1.19
6	3-O	6	98	94,500	1.07

Table 4.2. H-bond donor plus base cocatalyzed ROP of VL. Reaction conditions: VL (3.99 mmol, 1 equiv, solvent-free), benzyl alcohol (0.008 mmol) and (thio)urea/MTBD (0.02 mmol each). a) monomer conversion was monitored via ¹H NMR. b) M_n and M_w/M_n were determined by GPC (CH₂Cl₂) vs polystyrene standards.



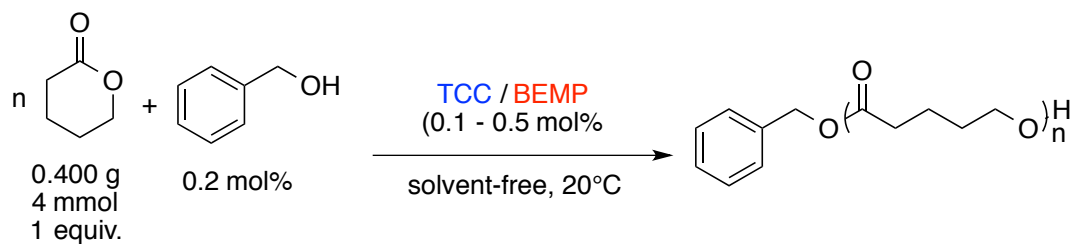
Entry	Mon.	$[\text{M}]_0/[\text{I}]_0$	Time (min)	Conv. ^a (%)	M_n^b (g/mol)	M_w/M_n^b
1	EB	50	90	99	28,200	1.64
2		100	130	97	42,800	1.62
3		200	330	96	51,000	1.60
4	PDL	50	360	96	24,800	2.23
5		100	900	97	33,000	2.46

Table 4.3. TCC plus base cocatalyzed ROP of macrolactones. Reaction conditions: EB and PDL (2.95 and 1.66 mmol respectively, 1 equiv, solvent free), benzyl alcohol, TCC/BEMP (0.06 (for EB) and 0.033 (for PDL) mmol). a) monomer conversion was monitored via ^1H NMR. b) M_n and M_w/M_n were determined by GPC (CH_2Cl_2) vs polystyrene standards.



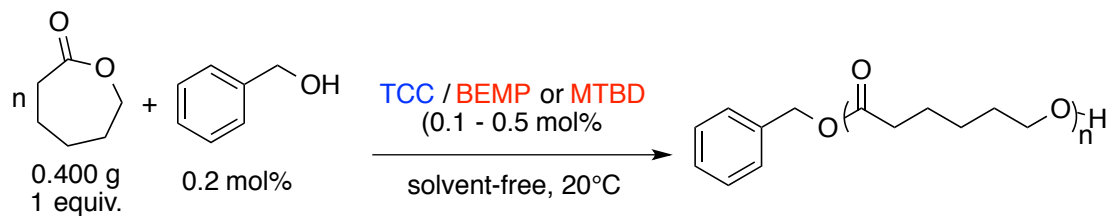
Entry	Donor	Time (min)	Conv. ^a (%)	M_n^b (g/mol)	M_w/M_n^b	%Iso ^c
1	2-S	5	90	10,700	1.06	0.94
2	3-S	20	90	14,600	1.07	0.80
3	TCC	33	90	15,800	1.09	0.82
4	3-O	102	91	11,300	1.16	0.85
5	1-S	130	90	11,300	1.11	0.83
6	2-O	230	90	10,400	1.18	0.83
7	1-O	540	92	12,100	1.11	0.82

Table 4.4. H-bond Mediated Solvent-free ROP of L-LA. Reaction conditions: L-LA (400 mg, 2.77 mmol), benzyl alcohol (2 mol%, 0.055 mmol), donor (1 mol%, 0.028 mmol), PMDTA (1 mol%, 0.028 mmol) in the monomer melt at 100°C. a. Conversion determined by ¹H NMR. b. M_n and M_w/M_n determined by GPC versus PS standards. c. %iso = fractional percent isotactic, see *Experimental section*.



Entry	Base loading (mol%)	Time (min)	Conv. (%) ^a	M_n (g/mol) ^b	M_w/M_n ^b
1	0.1	60	95	100,500	1.21
2	0.2	10	99	103,200	1.12
3	0.4	8	99	114,500	1.06
4	0.5	3	96	108,400	1.04
5	0.6	2	98	113,200	1.23

Table 4.5. Solvent free ROP of VL with TCC/BEMP. a. Conversion determined by ¹H NMR. b. M_n and M_w were obtained by GPC.



Entry	Base	Base loading (mol%)	Time (min)	Conv. (%) ^a	M_n (g/mol) ^b	M_w/M_n ^b
1	BEMP	0.1	47	160	n/a	n/a
2		0.2	95	142	83,000	1.17
3		0.3	98	60	85,000	1.22
4		0.4	98	40	89,100	1.20
5		0.5	97	30	82,500	1.20
6	MTBD	0.1	9	450	n/a	n/a
7		0.3	40	240	n/a	n/a
8		0.5	98	300	92,000	1.28

Table 4.6. TCC plus MTBD or BEMP cocatalyzed ROP of CL. a. Conversion determined by ¹H NMR. b. M_n and M_w/M_n were obtained by GPC.

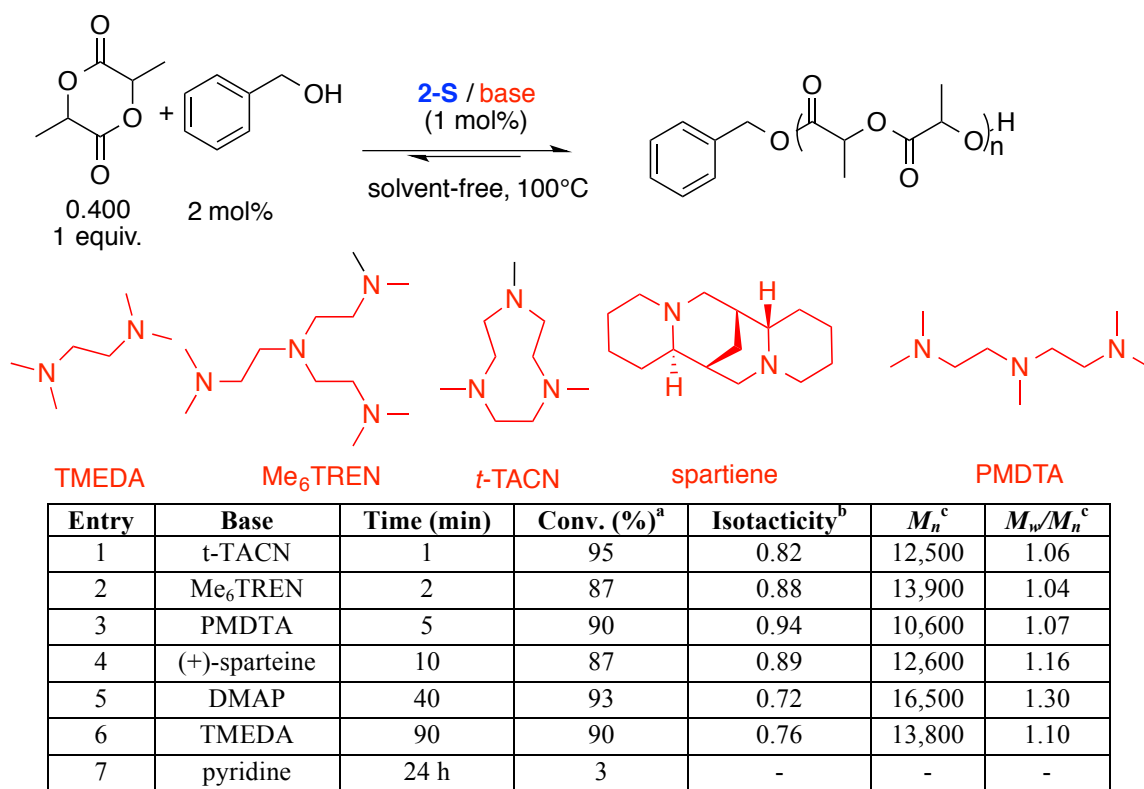
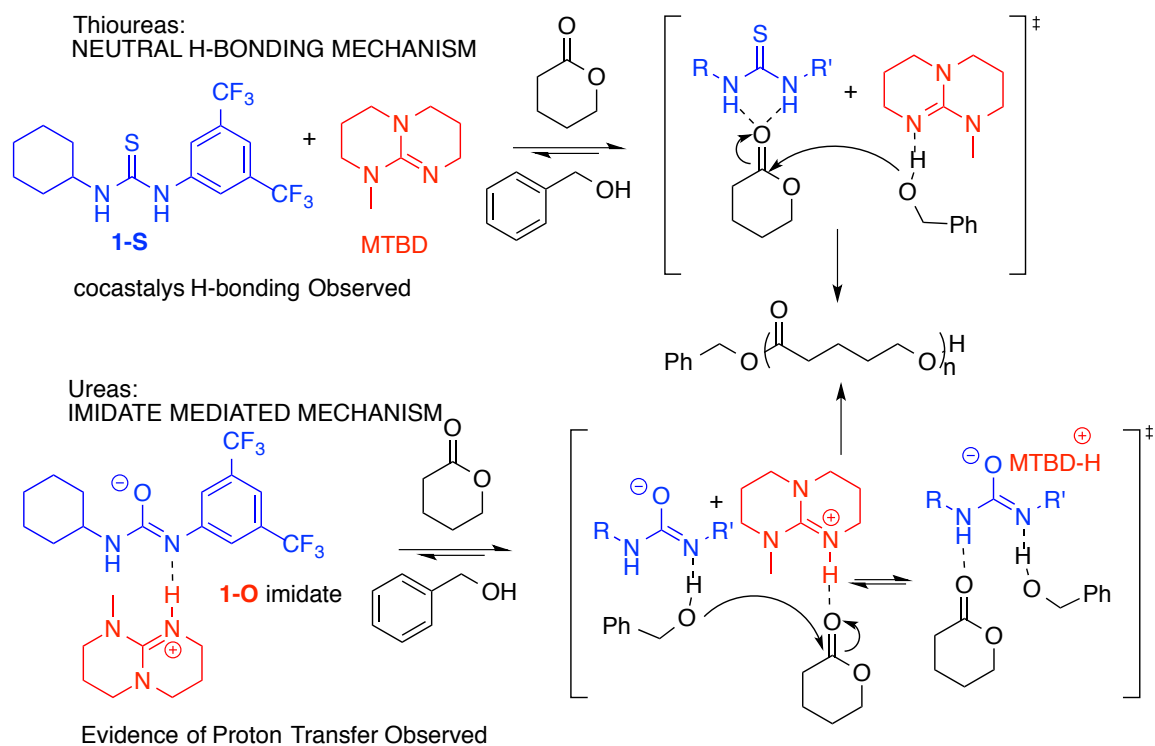


Table 4.7. Base Screen in the **2-S** Mediated ROP of L-LA. a. Conversion determined by ¹H NMR. b. Isotacticity determined by selectively decoupled ¹H NMR at 50 °C. M_n and M_w/M_n were obtained by GPC.



Scheme 4.1. Mechanism for the urea or thiourea plus base cocatalyzed ROP.

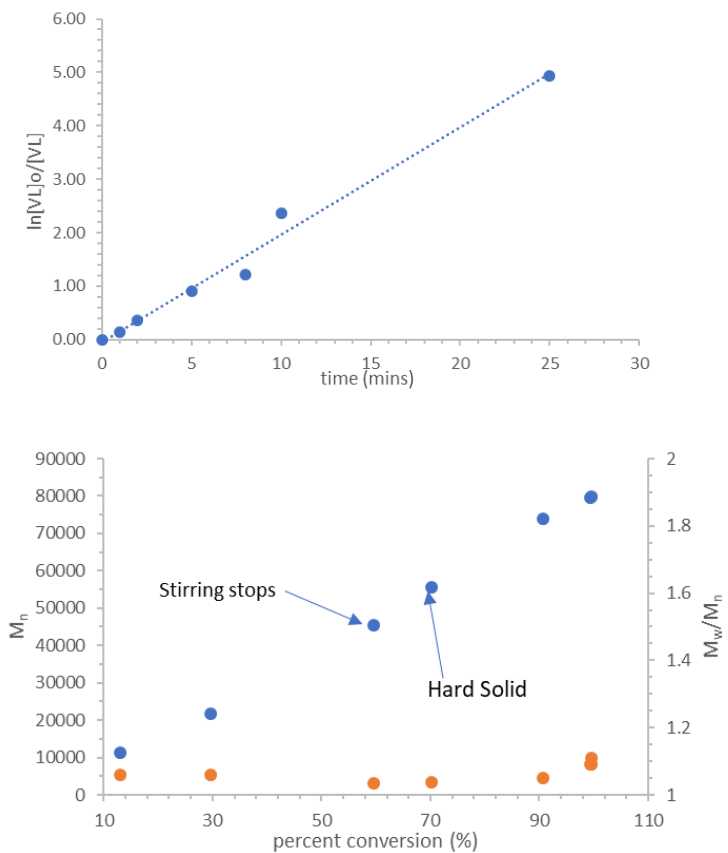


Figure 4.1. (upper) First order evolution of [monomer] versus time and (lower) M_n and M_w/M_n versus conversion for the TCC/MTBD cocatalyzed ROP of VL. Conditions: VL (3.99 mmol), TCC (0.02 mmol), MTBD (0.02 mmol) and benzyl alcohol (0.008 mmol) at room temperature.

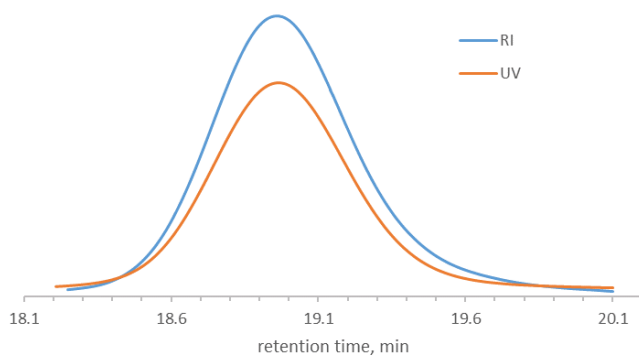
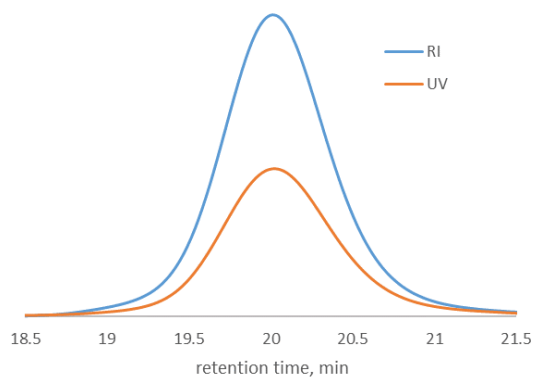


Figure 4.2. RI and UV GPC traces of the ROP initiated from pyrenebutanol for (top) PVL (TCC/BEMP) and (bottom) PLA (2-S/PMDTA).

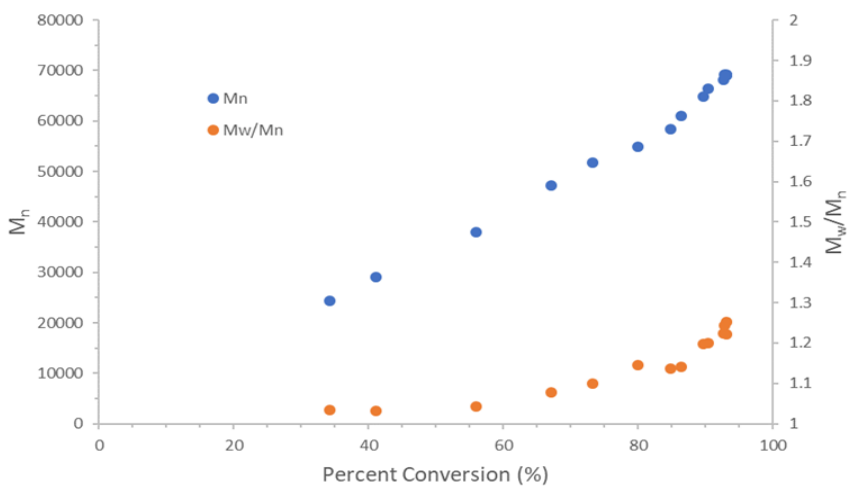
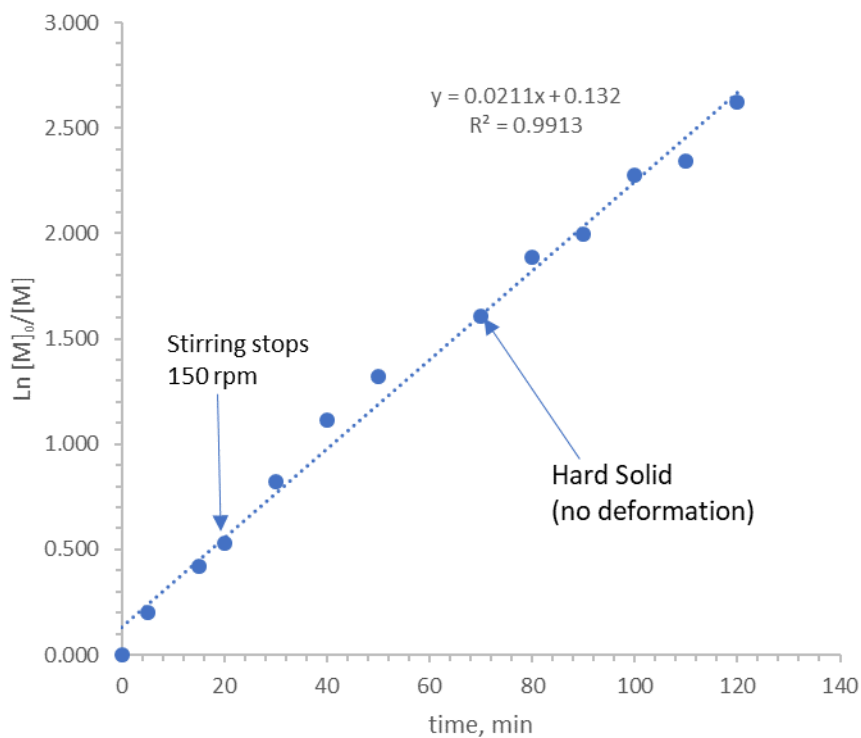


Figure 4.3. (upper) First order evolution of [monomer] versus time; and (lower) M_n and M_w/M_n versus conversion for the TCC/BEMP cocatalyzed ROP of VL. Conditions: VL (3.99 mmol), TCC (0.019 mmol), BEMP (0.019 mmol) and benzyl alcohol (0.008 mmol) at room temperature.

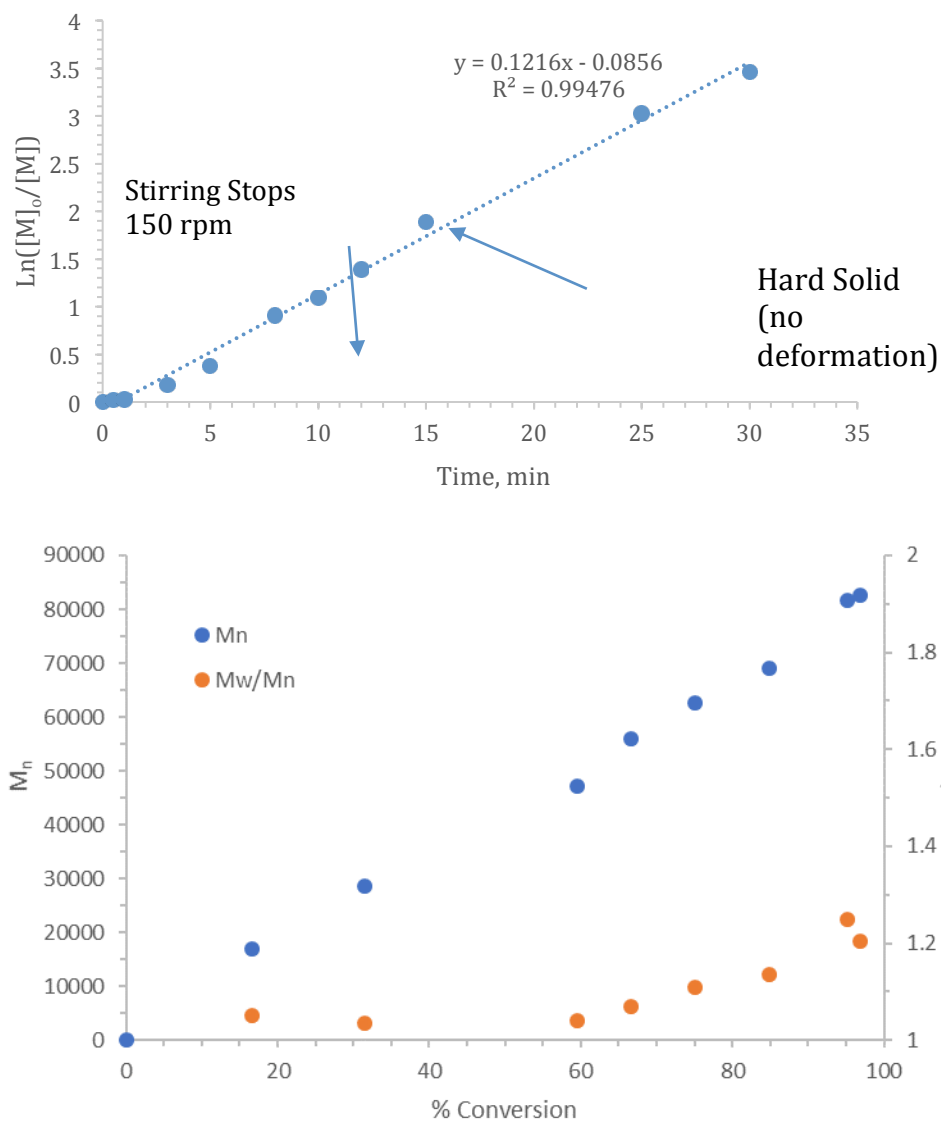


Figure 4.4. (upper) First order evolution of [monomer] versus time and (lower) M_n and M_w/M_n versus conversion for the TCC/BEMP cocatalyzed ROP of CL. Conditions: CL (3.50 mmol), TCC (0.018 mmol), BEMP (0.018 mmol) and benzyl alcohol (0.007 mmol) at room temperature.

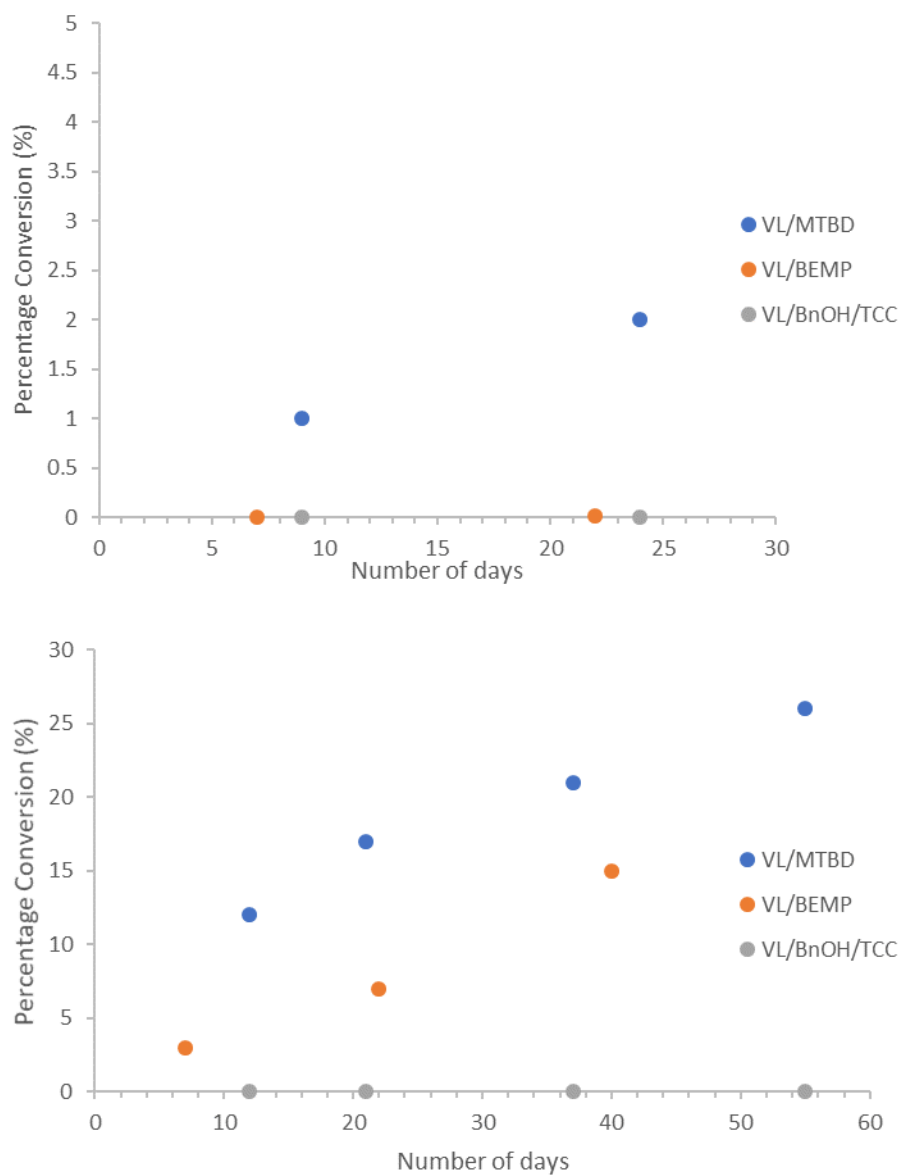


Figure 4.5. Percent conversion to polymer of VL solutions of MTBD, BEMP and TCC plus benzyl alcohol (0.5 mol%, 0.02 mmol for all catalysts) at (upper) -10°C and (lower) room temperature. Conversions were determined via aliquot by ^1H NMR (CDCl_3).



Figure 4.6. Solvent-free ROP allows for the direct-from-monomer creation of a negative mold in seconds. Above, the hollow, PVL negative mold is of a polypropylene reaction vial. Conditions: 10 mmol VL, 0.049 mmol TCC/BEMP (each), 0.020 mmol benzyl alcohol (see Experimental Section).

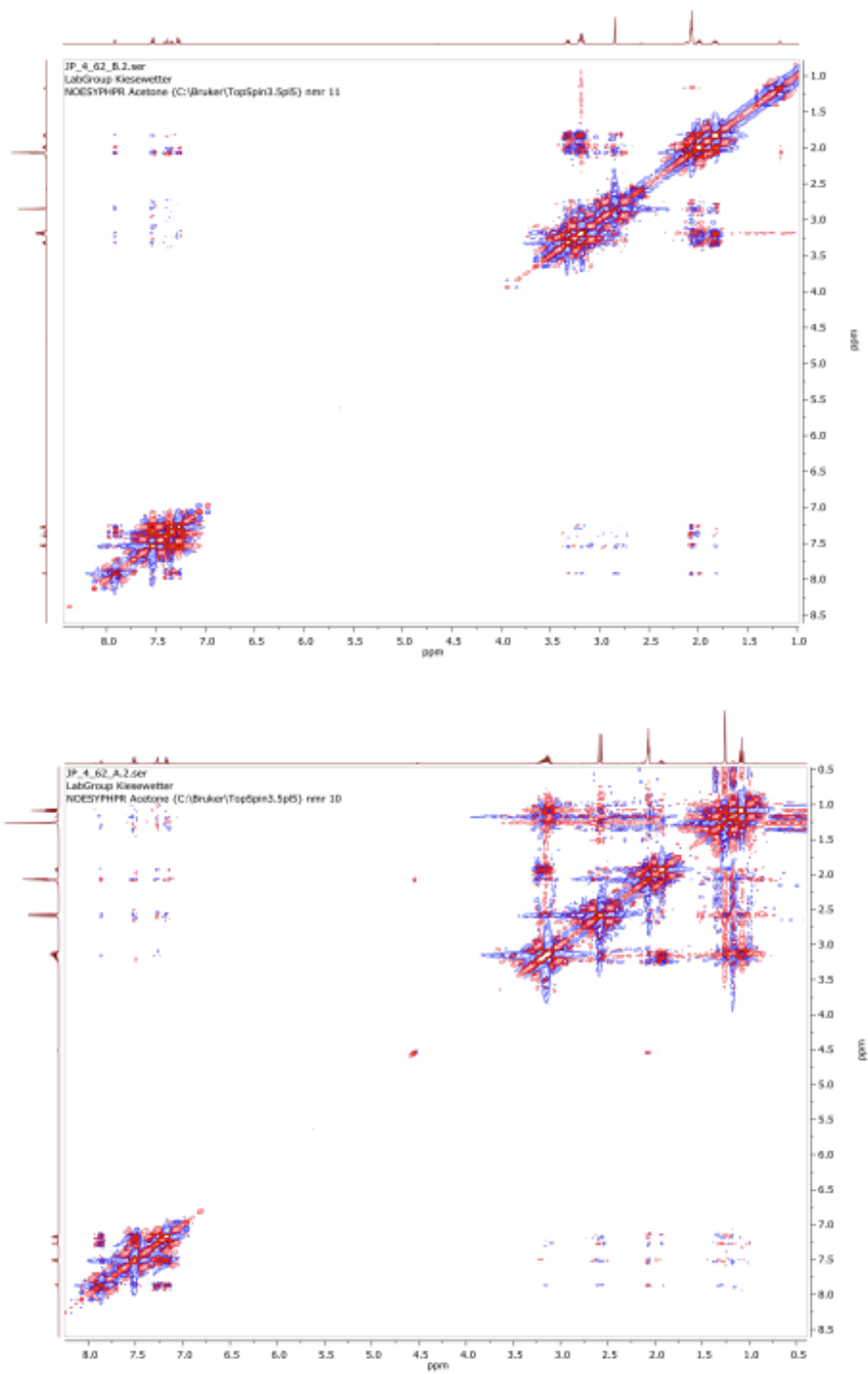


Figure 4.7. 400 MHz ¹H NOESY in acetone-d₆ of (upper) TCC/MTBD (0.05 mmol each), and (lower) TCC/BEMP (0.05 mmol each). **1-S**/MTBD show no cross peaks in acetone-d₆ or C₆D₆ at 0.05 mmol.

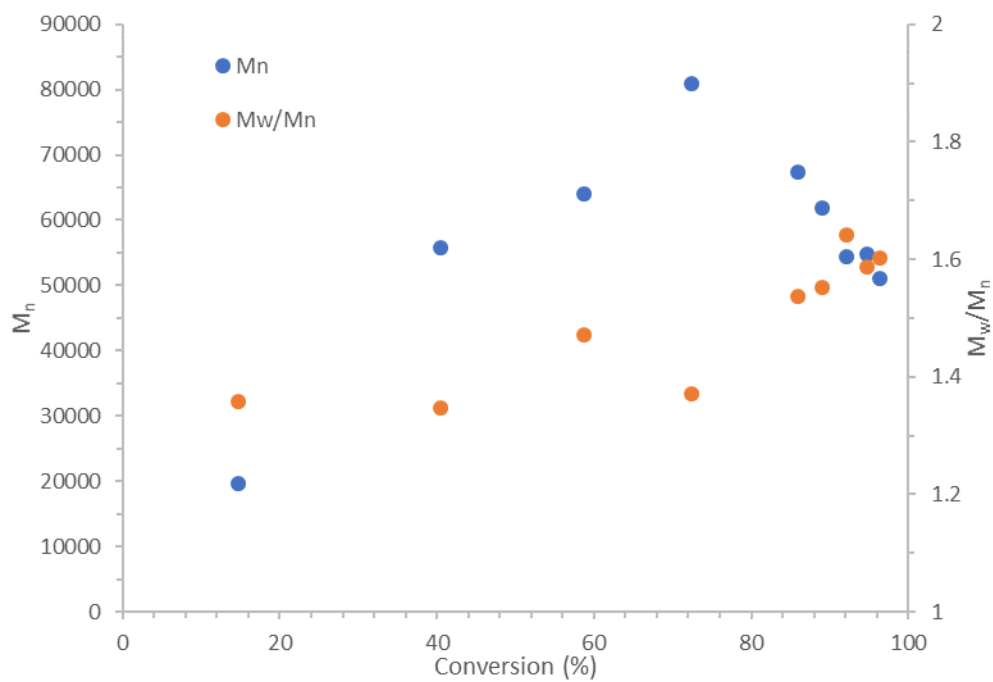


Figure 4.8. M_n and M_w/M_n vs conversion for the TCC/BEMP cocatalyzed ROP of EB. Conditions: EB (2.95 mmol), TCC (0.059 mmol), BEMP (0.059 mmol) and benzyl alcohol (0.015 mmol) at 80°C.

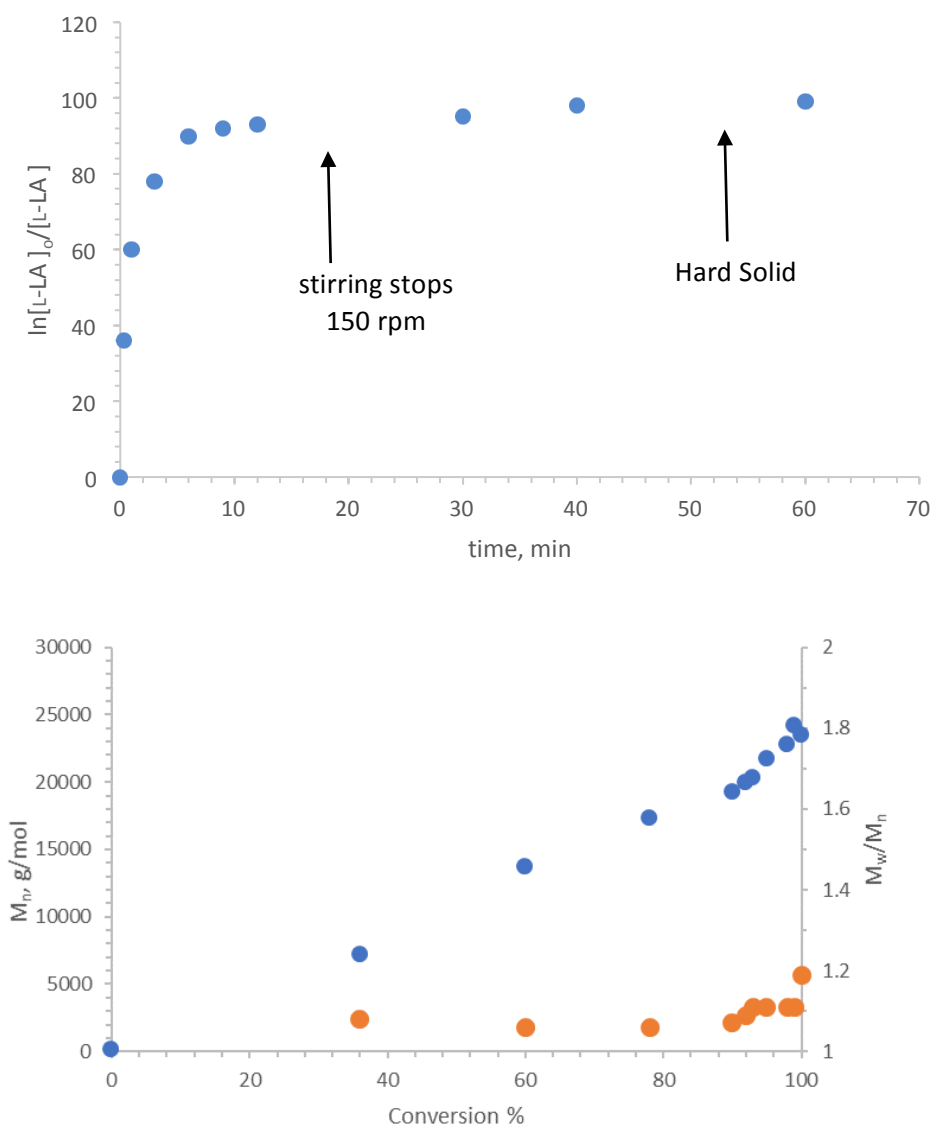


Figure 4.9. (upper) First order evolution of [LA] vs time, and (lower) M_n and M_w/M_n vs conversion. Reaction conditions: L-LA (400 mg, 2.77 mmol), benzyl alcohol (1mol%, 0.028 mmol), **2-S** (1 mol%, 0.028 mmol), PMDTA (1 mol%, 0.028 mmol) at 100°C.

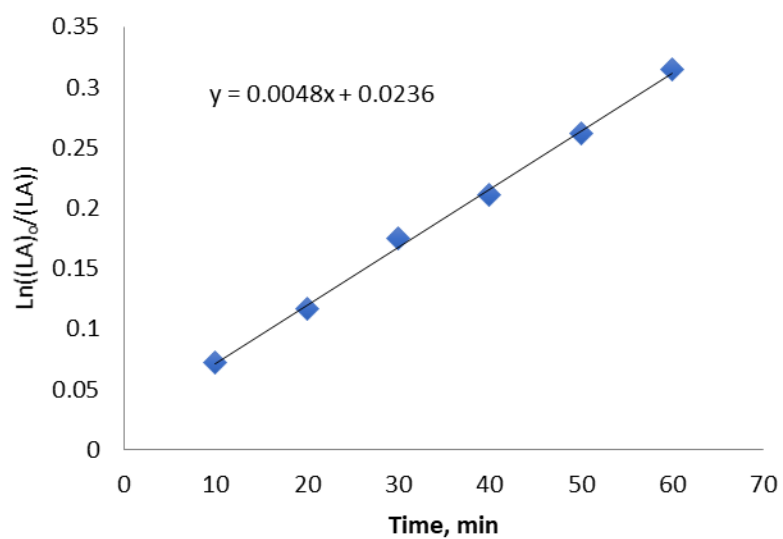
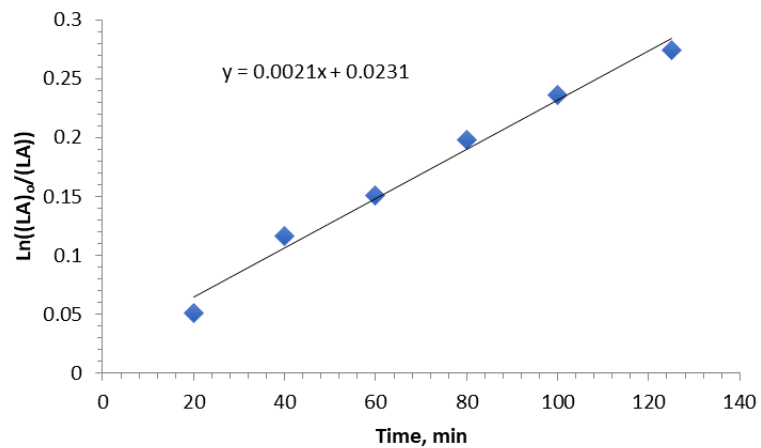


Figure 4.10. First order evolution of $[LA]$ vs time for the 2-S/PMDTA (2.5 mol% each) cocatalyzed ROP from benzyl alcohol (1 mol%) in (upper) toluene at 50°C (0.25 M, 0.694 mmol), and (lower) $CDCl_3$ at 40°C (1 M, 0.694 mmol).

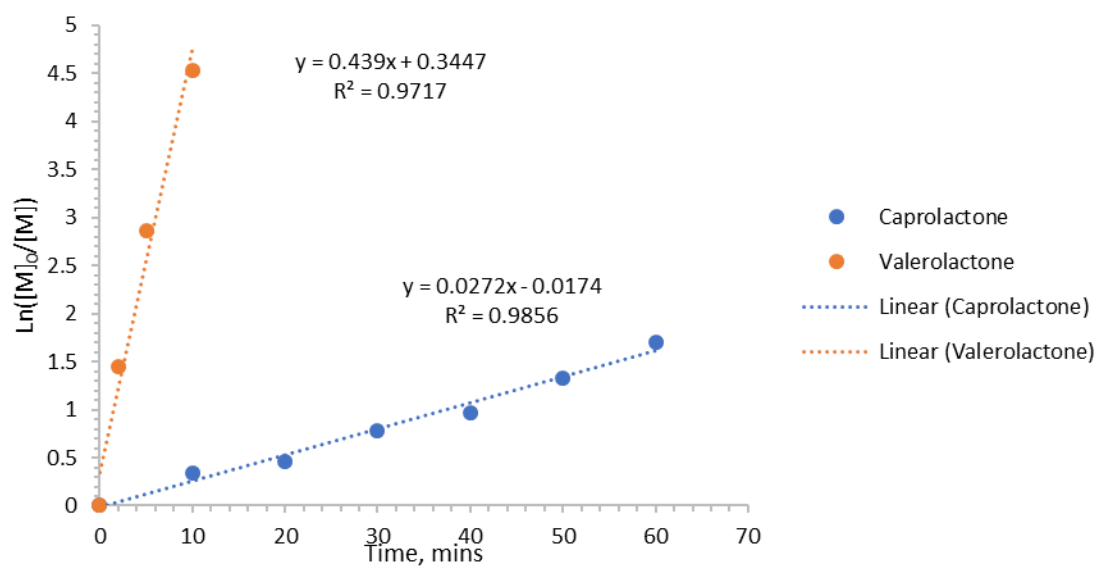


Figure 4.11. First order evolution of [VL] and [CL] vs time for the one-pot copolymerization catalyzed by TCC/BEMP. Conditions: VL (3.99 mmol), CL (3.99 mmol), TCC (0.02 mmol), BEMP (0.02 mmol) and benzyl alcohol (0.016 mmol)

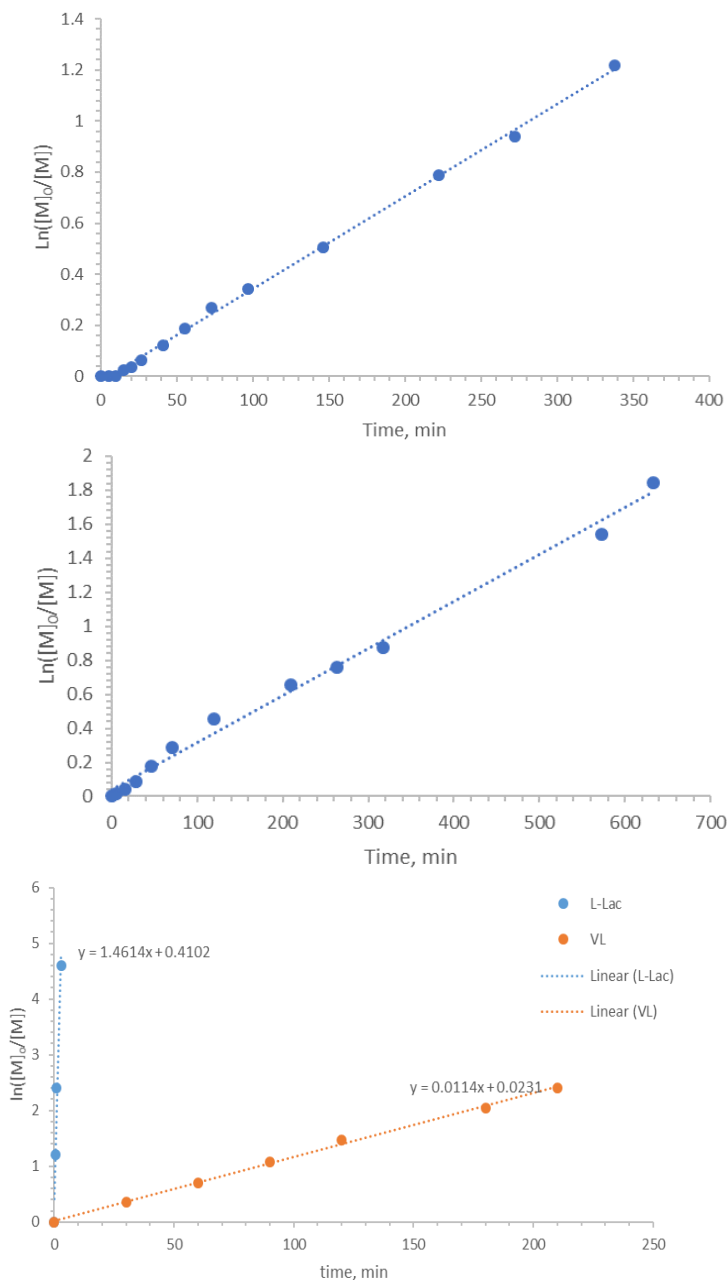


Figure 4.12. First order evolution of [monomer] vs time for the copolymerization of: (upper) VL and EB. Conditions: VL (3.99 mmol), EB (3.99 mmol), TCC (0.079 mmol), BEMP (0.079 mmol) and benzyl alcohol (0.16 mmol). VL had reached full conversion by first interrogation. (middle) CL and EB. Conditions: CL (3.99 mmol), EB (3.99 mmol), TCC (0.070 mmol), BEMP (0.070 mmol) and benzyl alcohol (0.140 mmol). CL had reached full conversion by first interrogation. (lower) VL and LA. Conditions: VL (3.99

mmol), L-LA (1.33 mmol), TCC (0.133 mmol), t-TACN (0.133 mmol) and benzyl alcohol (0.0532mmol).

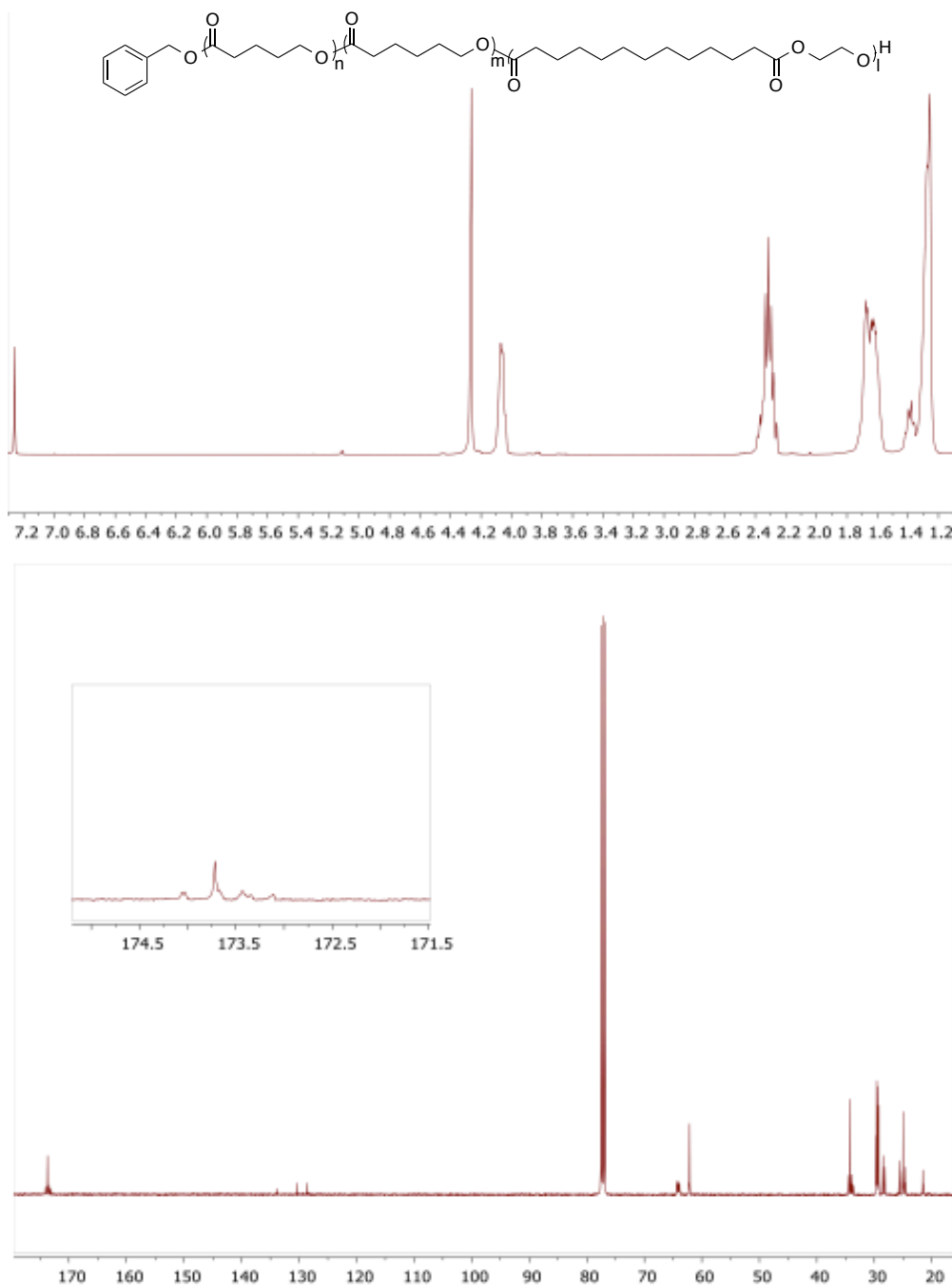


Figure 4.13. ¹H and ¹³C NMR (400 MHz ¹H, CDCl₃) of the poly(VL-co-CL-co-EB). ¹H NMR suggests a mole ratio of the monomers in the polymer to be 1:1 (VL+CL:EB).

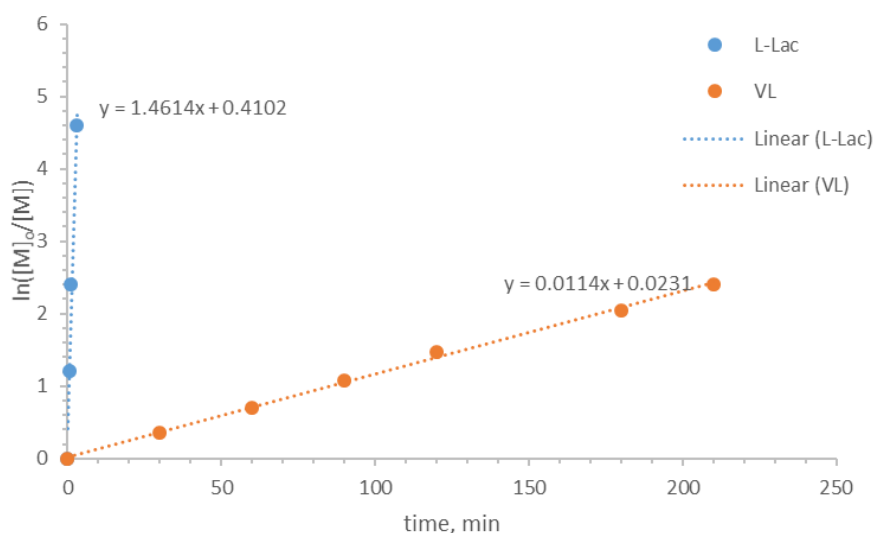


Figure 4.14. First order evolution of $[\text{monomer}]$ vs time for the copolymerization of VL and L-LA. Conditions: VL (3.99 mmol), L-LA (1.33 mmol), TCC (0.133 mmol), t-TACN (0.133 mmol) and benzyl alcohol (0.053mmol).

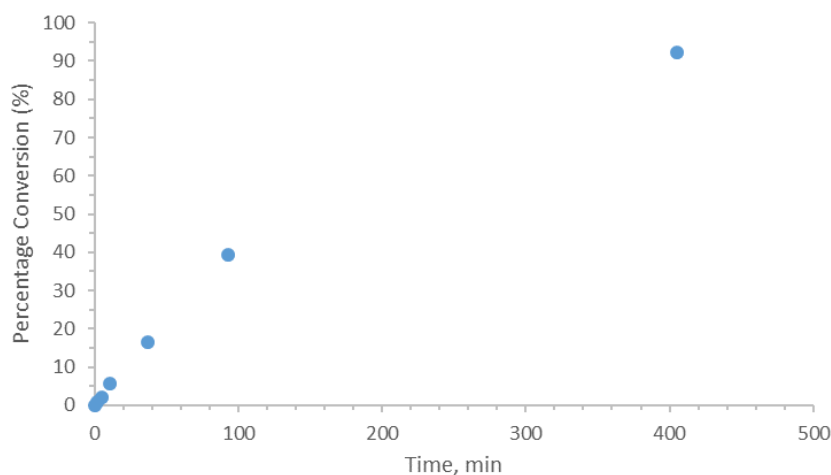


Figure 4.15. Percentage conversion of EB vs time for the copolymerization of: VL, CL and EB. Conditions: VL (3.99 mmol), CL (3.99mmol), EB (3.99 mmol), TCC (1 mol%, 0.119 mmol), BEMP (1 mol%, 0.119 mmol) and benzyl alcohol (1 mol%, 0.119 mmol). VL had reached full conversion by first interrogation (at 2 min) and CL by third interrogation (at 5 min).

INTENTIONALLY BLANK PAGE

MANUSCRIPT – V

Unpublished Results

**H-bonding Organocatalysts for Ring-Opening Polymerization at Elevated
Temperatures – Some Like it Hot**

Kurt V. Fastnacht, Danielle N. Coderre, Nayanthara N. Dharmaratne, Thomas Wright
and Matthew K. Kiesewetter

Chemistry, University of Rhode Island, Kingston, RI, USA

Corresponding Author: Matthew Kiesewetter, Ph.D.
Chemistry
University of Rhode Island
140 Flagg Road
Kingston, RI, 02881, USA
Email address: mkiesewetter@chm.uri.edu

ABSTRACT

Organocatalysts for ring-opening polymerization (ROP) are usually subjected to mild reactions conditions for the benefit of both catalyst life and reaction control. The ROP kinetics of ϵ -caprolactone and lactide with various H-bonding (thio)ureas paired with an amine cocatalyst were evaluated at temperatures ranging from 22 – 110°C. Eyring plots produced from a mono-urea or a bis-urea H-bond donor cocatalyzed ROP display normal linear behavior out to 110°C in non-polar solvent. In non-polar solvent, where an H-bonding mechanism is preferred, the mono-urea H-bond donor, trilocarban, and all thiourea H-bond donors display non-linear Eyring plots due to catalyst decomposition at temperatures exceeding 80°C. The onset temperature of cocatalyst decomposition must be measured under reaction conditions. In polar solvent, when the more active imidate form of the (thio)urea is favored, some catalysts become thermally stable up to 110°C, exhibiting linear Eyring behavior. A mechanistic explanation is suggested.

INTRODUCTION

H-bonding organocatalysts for ring-opening polymerization (ROP) are highly controlled systems for the synthesis of macromolecules.¹⁻³ This class of catalyst is constituted by one of a host of H-bond donating moieties (most commonly a thiourea or urea) and a base cocatalyst, which effect ROP of lactones and carbonates by simultaneous activation of monomer by (thio)urea and of initiating/propagating alcohol by base.^{1,4} A nascent enchainment mechanism whereby base cocatalyst abstracts a proton from (thio)urea, reversibly generating an imidate catalyst, is thought to be favored under certain conditions: acidic H-bond donors (e.g. thioureas), strong base cocatalysts and polar solvent.⁵⁻⁹ Urea H-bond donors have been shown to be more active than the corresponding thioureas.^{5,7,10,11} These trends also hold for the multi-(thio)urea H-bond donors developed by our group for ROP of esters.^{10,12} The internal H-bond stabilization rendered by the extra (thio)urea moieties is thought to be the source of the augmented activity (versus mono-(thio)urea donors).^{10,12} The active catalytic forms – H-bonding and imidate – are in rapid equilibrium unless a strong inorganic base (e.g. alkoxide or hydride) is applied, in which case the imidate is the catalytic species, Figure 5.1.^{7,9,10}

One advantage of the H-bonding class of catalysts is their efficacy for room temperature ROP,¹ but some applications mandate the application of elevated temperatures. For example, the solvent-free ROP of lactide (LA) had been identified as a challenge for organocatalysts.¹³ The high temperature required to melt the polymer (180°C) typically results in charring when organic catalysts are applied.¹³ We recently obviated this problem by conducting the solvent-free ROP of LA in the monomer melt (ROP at 100°C) using a bithiourea H-bond donor (**2-S**, Figure 5.1) and a commercially

available alkylamine base.¹¹ Despite the reaction ‘solution’ solidifying prior to full conversion, the ROP exhibited characteristics of a ‘living’ polymerization – linear evolution of molecular weight versus conversion and M_n predictable by $[M]_0/[I]_0$.¹¹ Similar behavior was observed for the ROPs of d-valerolactone (VL, m.p = -13) and ϵ -caprolactone (CL, m.p. = -1), whose solvent free-ROP can be conducted at room temperature. However, one-pot chain extension under solvent-free conditions proved difficult unless the A block polymer was melted to achieve homogeneity with the B block monomer. Surprisingly, in neither of these high temperature applications did we observe catalyst deactivation, which we had expected to happen.¹¹ H-bonds are known to weaken at elevated temperatures, charring has been observed in the solvent-free ROP of LA, and, certainly, other organocatalytic reactions have been observed to suffer deactivation at elevated temperatures.¹⁴ Contrary to catalyst deactivation, the touchstone study of H-bond mediated ROP showed linear Arrhenius behavior for the **1-S**/MTBD cocatalyzed ROP of VL up to 50°C,¹⁵ but we sought to examine the thermal stability of a host of H-bonding catalysts far above room temperature.

EXPERIMENTAL SECTION

General Considerations: All manipulations were performed in an INERT stainless-steel glovebox equipped with a N₂ gas purification system. All chemicals were purchased from Fisher Scientific and used as received unless stated otherwise. Tetrahydrofuran and dichloromethane were dried on an Innovative Technologies solvent purification system with alumina columns and N₂ working gas. Benzene-*d*₆, chloroform-*d* and toluene-*d*₈ were purchased from Cambridge Isotope Laboratories and distilled from CaH₂. δ -valerolactone (VL; 99%), ϵ -caprolactone (CL; 99%) and benzyl alcohol were distilled from CaH₂ under reduced pressure. L-lactide was purchased from Acros Organics and recrystallized from dry toluene. The H-bond donors **1-S**, **1-O**, **2-S**, **2-O**, **3-S** and **3-O** were prepared according to published procedures. TCC was purchased from Tokyo Chemical Company and used as received. NMR experiments were performed on Bruker Avance III 300 MHz or 400 MHz spectrometer. Size exclusion chromatography (SEC) was performed at 40°C using dichloromethane eluent on an Agilent Infinity GPC system equipped with three Agilent PLGel columns 7.5 mm \times 300 mm (5 μ m, pore sizes: 50, 103, 104 Å). M_n and M_w/M_n were determined versus PS standards (162 g/mol-526 kg/mol, Polymer Laboratories).

Example CL Polymerization Experiment. A 7 mL vial was charged with **1-S** (16.2 mg, 0.0438 mmol), MTBD (6.7mg, 0.0438 mmol), benzyl alcohol (0.95 mg, 0.00876 mmol) and toluene (200 μ L). In a second 7 mL vial, CL (100 mg, 0.876 mmol) was dissolved in toluene (238 μ L). The contents of the second vial were transferred to the first via pipette and stirred until homogenous, approx. 1 min. The vial was capped with a septa cap and placed in an oil bath heated to 80°C. 50 μ L aliquots were taken with a fine-needle

syringe. The aliquots were quenched using benzoic acid (10.7 mg, 0.0874 mmol) and removed of volatiles under vacuum. The contents were dissolved in CDCl₃, transferred to an NMR tube via pipette, and monomer conversion was determined by ¹H NMR. Eyring plots were constructed using the observed first order rate constants (k_{obs}) from the equations below. Yield: 89%, M_n = 7,500, M_w/M_n = 1.07.

$$\text{Rate} = k_{\text{obs}} [\text{CL}] \quad (1)$$

$$k_{\text{obs}} = k_p [\text{benzyl alcohol}]_o [\text{cocatalysts}]_o \quad (2)$$

Example ROP of lactide. L-lactide (126.26 mg, 0.876 mmol) and methyl isobutyl ketone (438 μL) were added into a 7 mL vial and stirred until a homogenous solution was obtained. To a second 7 mL vial, benzyl alcohol (0.95 mg, 0.0876 mmol), PMDETA (3.8 mg, 0.0219 mmol) and **2-S** (13.5 mg, 0.0219 mmol) were added. Contents from the first vial were transferred into vial 2 via Pasteur pipette. The vial was capped with a septa cap and placed in an oil bath heated to 80°C. 50μL aliquots were taken with a fine-needle syringe periodically. The aliquots were quenched using benzoic acid (5.3 mg, 0.0438 mmol) and placed in the vacuum oven to remove solvent. The contents were transferred to an NMR tube via pipette, and monomer conversion was determined by ¹H NMR.

Example ROP of lactide under solvent free conditions. L-lactide (200 mg, 1.38 mmol), **2-S** (4.3 mg, 0.007 mmol) and benzyl alcohol (1.3 mg, 0.014 mmol) were added into a 7 mL vial and the contents were stirred at 110°C. PMDETA (5.0 μL, 0.007 mmol) from a 1.4 M stock solution of PMDETA in toluene was added to the completely melted content in vial 1. Aliquots were taken periodically, quenched using benzoic acid (1.6 mg, 0.013 mmol) and analyzed by ¹H NMR to determine monomer conversion. Yield 90 %, M_n = 18,000 g/mol, M_w/M_n = 1.10.

RESULTS AND DISCUSSION

The thermal stabilities of various H-bond donors plus MTBD were determined under ROP conditions in solution. The observed rate constant (k_{obs}) for the first order evolution of [CL] ($[\text{CL}]_0 = 2\text{M}$, 0.0876 mmol) were measured for the H-bond donor/MTBD cocatalyzed ROP from benzyl alcohol (0.00876 mmol) in toluene at several temperatures from 22°C to 110°C, and an Eyring plot was constructed for each cocatalyst system, Table 5.1. These ROP have previously been shown to be first order in $[\text{cocatalysts}]_0$ and $[\text{initiator}]_0$, resulting in the rate equation: $\text{Rate} = k_{\text{obs}}[\text{CL}]$, $k_{\text{obs}} = k_p[\text{cocatalysts}]_0[\text{initiator}]_0$.^{10,15-17} The activation parameters of enchainment are superimposed with those of catalyst dynamics/reagent binding,^{9,17} and these *observed* activation parameters ($\Delta H_{\text{obs}}^\ddagger$ and $\Delta S_{\text{obs}}^\ddagger$) are also given in Table 5.1.¹⁸ The ROP of CL was chosen because the slower reaction kinetics (versus VL or lactide) facilitate monitoring by aliquot or ¹H NMR, and the ROP of CL features a high ceiling temperature ($T_{\text{ceil}} = 261\text{ }^\circ\text{C}$)¹⁹, which suggests that any temperature dependent observations are not due to substantially diminished enchainment equilibrium constants. For **1-O** and **2-O**, the Eyring plots are linear over the entire temperature window, whereas all thiourea H-bond donors in addition to TCC and **3-O** exhibit curved Eyring plots with a maximum rate achieved at 80°C, Figure 5.2-7. In the case of **2-S**, the reaction progress stops completely after 30 minutes (42 % conversion) at 110°C.

For those H-bond donors that exhibit a non-linear Eyring plot, the reduction in rate at high temperature is due to catalyst decomposition. A temperature-jump experiment was conducted for the **1-S**/MTBD (0.0438 mmol) cocatalyzed ROP of CL (2 M, 0.876 mmol) from benzyl alcohol (0.00876 mmol) in toluene, where after the first part of the reaction

was conducted at 110°C, the temperature was changed to 80°C, Figure 5.8, resulting in a reduced rate for the latter portion of the ROP. The drop in rate suggests that the catalyst deactivation observed above 80°C (Eyring plot) is not reversible and is due to decomposition. Indeed, ¹H-NMR analysis after a **1-S**/MTBD cocatalyzed ROP in C₆D₆ (2 h at 110°C) reveals additional aromatic resonances presumably originating from the decomposition of **1-S**. Decomposition is also observed when **1-S** and MTBD (0.1M each, C₆D₆) are heated in the absence of monomer and initiator, but **1-S** is stable to 110°C when heated alone. A non-linear Eyring plot can be associated with an abrupt change in mechanism.¹⁸ However, for (thio)urea/MTBD mediated ROP, the H-bonding and imidate mechanisms are in equilibrium,^{7,9} which would be expected to yield a linear Eyring plot.¹⁸

Thermogravimetric analysis (TGA, under nitrogen) of H-bond donors in the presence and absence of MTBD cocatalyst show that catalyst stability must be determined under reaction conditions. Decomposition onsets for the H-bond donors in the absence of MTBD ranged from 166 - 256°C (Table 5.2). In the presence of MTBD, a decrease in decomposition onset temperature was only seen for TCC, **1-O** and **2-O** (decreases of 85, 61 and 94°C, respectively). These temperatures do not correlate to the decomposition evidenced in the Eyring plots. Further, diminished thermal stability in the presence of MTBD does not indicate which catalysts are most thermally stable under reaction conditions. For example, the thioureas exhibit curved Eyring plots yet show minimal change in thermal stability with and without MTBD, and **1-O** and **2-O** exhibit decreased onsets in the TGA with MTBD but display linear Eyring behavior.

When the ROP is conducted in polar solvent, Eyring plots for both TCC, **1-S** and **1-O** become linear, suggesting that the catalysts are more thermally stable under reaction conditions *in polar solvent* up to 110°C. The H-bonding catalysts for ROP exhibit a mechanistic duality that is strongly dictated by solvent, where polar solvent favors imidate mediated ROP and non-polar solvent favors H-bond mediated enchainment, suggesting the polar solvent stabilizes the imidate species.^{7,9} In this study, the more acidic H-bond donors exhibit curved Eyring plots in toluene.^{5,20} (footNote. The pK_a of TCC and **3-O** are not known, but we presume higher acidity of TCC versus **1-O** due to Hammett effects. The internal H-bond stabilization is expected to render **3-O** more acidic than the parent mono-urea.) This suggests that catalyst decomposition may be preceded by proton transfer to form, presumably, (thio)imidate, which decomposes in toluene. The extent of imidate formation is also dictated by the pK_a of the base cocatalyst. When the ROP of CL from benzyl alcohol is catalyzed by TCC/DBU, an attenuation of catalyst decomposition is observed (Figure 5.9) versus the TCC/MTBD ROP (Figure 5.2). This suggests that the augmented pK_a of MTBD (MTBD-H⁺ pK_a^{MeCN} = 25.4)²¹ versus that of DBU (DBU-H⁺ pK_a^{MeCN} = 24.3)²¹ favors the formation of imidate, as previously observed,⁷ which becomes unstable at elevated temperatures.

Conducting the ROPs in polar solvent enhances the thermal stability of some catalysts. We employed methyl isobutyl ketone (MIBK) as the solvent for our temperature dependent studies; acetone and THF have previously been used for (thio)imidate-mediated ROP but are not high boiling.^{5,7} In MIBK, TCC, **1-S**, and **1-O**/MTBD cocatalyzed ROPs examined exhibit linear Eyring plots up to 110°C, Figure 5.10-12, suggesting enhanced catalyst stability in polar solvent. However, the first order

consumption of monomer plot for the **1-S, 2-S and 3-O**/MTBD cocatalyzed ROP of CL (0.876 mmol) from benzyl alcohol (0.00876 mmol) at 110°C showed deviation from linearity after 50% conversion, which suggests some catalyst decomposition. Except for the **1-S, 2-S and 3-O** /MTBD cocatalyzed ROP of CL at 110°C, the ROP display linear first order consumption of monomer to >75% conversion. The **2-S, 2-O and 3-O**/MTBD cocatalyzed ROP of CL in MIBK do not show linear Eyring behavior(Figures 5.13-15), suggesting decomposition is still prevalent despite the stabilization provided by polar solvent on the imidate mechanism.

Temperature dependent ¹H NMR studies corroborate an H-bonding mechanism for H-bond donors in non-polar solvent and an imidate mechanism for H-bond donors in polar solvent. ¹H NMR spectra of a **1-S**/MTBD (0.1 M) solution in C₆D₆ shows that the **1-S** resonances are shifted downfield in the presence of MTBD, which suggests H-bonding.¹⁷ With increasing temperature, the **1-S** ¹H NMR resonances (when mixed with MTBD) shift upfield, indicating an exothermic binding ($\Delta H^{\circ} = -10.7 \pm 2.0$ kcal/mol)¹⁷ and weaker H-bonding at higher temperatures.¹⁷ Binding to monomer is also exothermic.^{15,17} These observations suggest that Arrhenius reaction acceleration outpaces the weakening of H-bonding resulting in faster ROP until catalyst decomposition >80°C. The higher $\Delta H^{\ddagger}_{\text{obs}}$ in non-polar solvent (vs polar) corroborates the suggestion that Arrhenius behavior is resisted by catalyst dynamics – that is, thermal rate effects are partially offset by weakened H-bonding.¹⁸ The upfield shift of **1-S** resonances upon heating could indicate the assumption of imidate character, but at 110°C (the highest temperature recorded), the **1-S** resonances (with MTBD) remain downfield of the **1-S** resonances in the absence of MTBD. The same trend is observed for **1-O** plus MTBD in C₆D₆ upon

heating. This suggests that H-bonding remains the dominate mechanistic form for (thio)urea H-bond donors with MTBD in C₆D₆ at all temperatures. In contrast, **1-O** plus MTBD in acetone-d₆ show **1-O** resonances with an upfield chemical shift (versus **1-O** in the absence of MTBD) that is not a function of temperature (25-60°C, Δppm < 0.1). The relatively static chemical shift suggests that the extent of imidate formation is not highly sensitive to temperature and that higher rates of ROP are thermal in nature (i.e. high rates are not due to higher [imidate]).

Despite the high activity of imidate mediated ROP, the reactions remain highly controlled at room temperature, and the extent of imidate formation appears to be highly sensitive to solvent polarity including the polarity of the evolving reaction solution. We have previously shown that the highly active imidate forms of H-bond donors are in equilibrium with the less active neutral species,⁷ and a larger upfield shift (more imidate character) can be observed with stronger organic bases upon a single H-bond donor or with a more acidic H-bond donor with a single base.^{7,9} A similar effect has been reported where polar solvent favors an imidate mechanism and non-polar solvent favors an H-bonding mechanism.⁹ The polarity of the bulk solution is expected to drop during the course of the polymerization as closed, *s-cis* lactone is converted to open, *s-trans* lactone; indeed, the higher polarity of lactones versus *s-trans* esters has been used to justify the selectivity exhibited by thioureas (and presumably ureas) for the activation of monomer versus polymer.¹⁵ The ¹H NMR spectra of TCC plus MTBD (0.0438 mmol each) in CDCl₃ were recorded at room temperature in the presence of varying amounts of CL (2 M – 0.25 M) in the absence of initiator, conditions under which no ROP is observed, Figure 5.16. The resonances of TCC move upfield in the presence of MTBD but move

back downfield with reduced monomer concentration, indicating less imidate character with reduced monomer concentrations. These observations may explain why urea imidate mediated ROP can be highly active – more active than the structurally similar TBD – but be more controlled. We proposed that the catalyst system deactivates during the course of the ROP by forming less imidate character. This hypothesis will have to be borne out by future studies.

ROP of Lactide. Temperature dependent kinetics suggest that **2-S**/PMDETA cocatalyzed ROP of L-lactide (LA) experiences enhanced thermal stability when solvent-free (deactivation > 110°C) versus in polar solvent (deactivation > 80°C). For the (thio)urea/base mediated ROP of LA, weak base cocatalysts are optimal for ROP. Under these weakly basic conditions, only an H-bond mediated enchainment pathway is thought to occur.^{11,16} Our group recently disclosed that **2-S**/PMDETA was optimal – in terms of rate and isotacticity – for the solvent-free ROP of LA,¹¹ and this was the only catalyst system whose temperature dependent kinetics were examined herein. We have previously shown that the (thio)urea/base cocatalyzed solvent-free ROP of LA can be conducted in the monomer melt and exhibits the characteristics of a ‘living’ ROP despite solidifying prior to full conversion.¹¹ Consistent with previous solution studies, the Eyring analysis of the **2-S**/PMDETA (0.0219 mmol each) cocatalyzed ROP of LA (2M, 0.876 mmol) from benzyl alcohol (0.00876 mmol) showed non-linear behavior above 80°C in MIBK, Figure 5.17, suggesting catalyst deactivation arising from decomposition. Previous studies showed deactivation at high temperature of the same polymerization in CHCl₃, toluene and acetone.¹¹ Under solvent-free conditions, the Eyring plot for the **2-S**/PMDETA cocatalyzed ROP of LA from benzyl alcohol indicates deactivation at

elevated temperature, with a maximum observed rate at 110°C. This coincidental elevation in decomposition onset facilitates the solvent-free ROP of LA just above the monomer melting point ($T_m = 97^\circ\text{C}$)¹³. The solvent-free ROP of LA at 110°C remains highly controlled, $[M]_0/[I]_0 = 100$ yields $M_n = 18,000$ g/mol, $M_w/M_n = 1.10$.

Polymer Molecular Weight and Dispersity. The extent of reaction control is reduced at elevated temperatures, but **3-O**/MTBD remains among the most active and controlled organocatalysts for ROP even at high temperature. The ‘living’ character of the H-bond donor/MTBD cocatalyzed ROP at room temperature in non-polar and polar solvent as well as solvent-free has been described previously.^{5-7,10} For the **1-S**/MTBD (0.0438 mmol each) cocatalyzed ROP of CL (0.876 mmol) from benzyl alcohol in toluene, the M_w/M_n increases with temperature (at 80°C, $[M]_0/[I]_0 = 100$, $M_n = 20,000$, $M_w/M_n = 1.10$; at 110°C, $[M]_0/[I]_0 = 50$, $M_n = 9,900$, $M_w/M_n = 1.17$), but both of these ROP are more controlled than the comparable ROP in MIBK (MIBK at 110°C: $[M]_0/[I]_0 = 50$, $M_n = 6,200$, $M_w/M_n = 1.28$). This trend is also observed for **2-O**/MTBD mediated ROP of CL, which produces a linear Eyring plot in toluene. This suggests that the extent of reaction control is not related to the thermal stability of a cocatalyst system. For the catalyst systems examined, the ROP retain the characteristics of a ‘living’ polymerization, except for **2-O**/MTBD at 110°C, whose M_n versus conversion becomes non-linear late in the reaction (Figure 5.18). In contrast, the **3-O**/MTBD cocatalyzed ROP of CL – which is one of the most active organocatalytic systems for ROP – exhibits a curved Eyring plot in toluene but shows excellent reaction control even at 110°C, Figure 5.19 (95% conversion, 60 min, $M_n = 18,900$ g/mol, $M_w/M_n = 1.05$). At a lower temperature, the reaction is more active and more controlled (80°C, 99% conversion, 60

min, $M_n = 21,900$ g/mol, $M_w/M_n = 1.03$). These observations suggest that to some extent, the level of reaction control (narrow M_w/M_n and predictable M_n) can be maximized if the ROP reaches full conversion before catalyst decomposition or other side reactions become prominent.

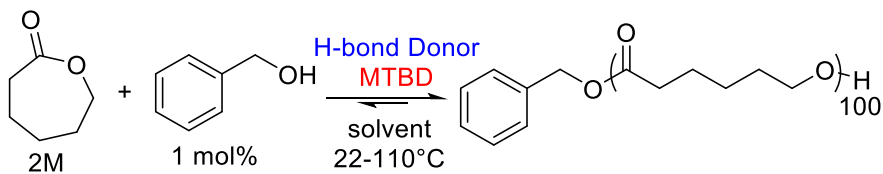
CONCLUSION

The thermal stability of organic catalyst systems for ROP must be determined under reaction conditions. All of cocatalysts examined are thermally stable $\leq 80^\circ\text{C}$ in polar and non-polar solvent, but conducting ROP in polar solvent can extend thermal stability to 110°C for most systems. However, reaction control – as measured by M_w/M_n – deteriorates at elevated temperatures, especially in polar solvent. The one exception appears to be **3-O**/MTBD, which produces a highly controlled and rapid ROP at all temperatures in non-polar solvents and solvent-free. The diversity of conditions under which the H-bonding catalysts for ROP are operable is attributable to their mechanistic duality where non-polar solvent and weakly acidic H-bond donors favor an H-bonding mechanism and polar solvent and more acidic H-bond donors favor an imidate mechanism. In toluene (H-bonding favored), high temperatures ($\geq 80^\circ\text{C}$) may facilitate proton transfer to form the (thio)imidate species, which is unstable and results in catalyst decomposition. In polar solvent, some [imidate] are insensitive to reaction temperature. The H-bonding class of organocatalysts for ROP constitute a platform for macromolecule synthesis that is operable under diverse experimental conditions. Indeed, the very progress of the ROP changes the effective [imidate] by modulating the polarity of the reaction solution. The robustness of these catalysts belies the complicated nature of their discharge, our understanding of which and our concomitant synthetic abilities continue to evolve through targeted study.

LIST OF REFERENCES

- (1) Kamber, N. E. N. E.; Jeong, W.; Waymouth, R. M. R. M.; Pratt, R. C. R. C.; Lohmeijer, B. G. G.; Hedrick, J. L. *Chem. Rev.* **2007**, *107* (12), 5813–5840.
- (2) Kiesewetter, M. K.; Shin, E. J.; Hedrick, J. L.; Waymouth, R. M. R. M. *Macromolecules* **2010**, *43* (5), 2093–2107.
- (3) Dove, A. P. In *Handbook of Ring-Opening Polymerization*²; Dubois, P., Coulembier, O., Raquez, J.-M., Eds.; Wiley-VCH: Federal Republic of Germany, 2009; pp 357–378.
- (4) Thomas, C.; Bibal, B. *Green Chem.* **2014**, *16* (4), 1687–1699.
- (5) Lin, B.; Waymouth, R. M. R. M. *Macromolecules* **2018**, *51* (8), 2932–2938.
- (6) Lin, B.; Waymouth, R. M. R. M. *J. Am. Chem. Soc.* **2017**, *139* (4), 1645–1652.
- (7) Dharmaratne, N. U.; Pothupitiya, J. U.; Bannin, T. J.; Kazakov, O. I.; Kiesewetter, M. K. *ACS Macro Lett.* **2017**, *6* (4), 421–425.
- (8) Zhang, X.; Jones, G. O.; Hedrick, J. L.; Waymouth, R. M. R. M. *Nat. Chem.* **2016**, *8* (11), 1047–1053.
- (9) Pothupitiya, J. U.; Hewawasam, R. S.; Kiesewetter, M. K. *Macromolecules* **2018**, No. 51, 3203–3211.
- (10) Fastnacht, K. V.; Spink, S. S.; Dharmaratne, N. U.; Pothupitiya, J. U.; Datta, P. P.; Kiesewetter, E. T.; Kiesewetter, M. K. *ACS Macro Lett.* **2016**, *5* (8), 982–986.
- (11) Pothupitiya, J. U.; Dharmaratne, N. U.; Jouaneh, T. M. M.; Fastnacht, K. V.; Coderre, D. N.; Kiesewetter, M. K. *Macromolecules* **2017**, *50*, 8948–8954.
- (12) Spink, S. S.; Kazakov, O. I.; Kiesewetter, E. T.; Kiesewetter, M. K. *Macromolecules* **2015**, *48* (17), 6127–6131.

- (13) Mezzasalma, L.; Dove, A. P.; Coulembier, O. *Eur. Polym. J.* **2017**, *95* (May), 628–634.
- (14) Dudziński, K.; Pakulska, A. M.; Kwiatkowski, P. *Org. Lett.* **2012**, *14* (16), 4222–4225.
- (15) Lohmeijer, B. G. G.; Pratt, R. C. R. C.; Leibfarth, F.; Logan, J. W.; Long, D. A.; Dove, A. P.; Nederberg, F.; Choi, J.; Wade, C. G.; Waymouth, R. M. R. M.; Hedrick, J. L. *Macromolecules* **2006**, *39* (25), 8574–8583.
- (16) Kazakov, O. I.; Kieseletter, M. K. *Macromolecules* **2015**, *48* (17), 6121–6126.
- (17) Kazakov, O. I.; Datta, P. P.; Isajani, M.; Kieseletter, E. T.; Kieseletter, M. K. *Macromolecules* **2014**, *47* (21), 7463–7468.
- (18) Espenson, J. H. *Chemical Kinetics and Reaction Mechanism*, 2nd ed.; McGraw-Hill Book Co: New York, 2002.
- (19) Duda, A.; Kowalski, A. In *Handbook of Ring-Opening Polymerization*; Dubois, P., Coulembier, O., Raquez, J.-M., Eds.; Wiley-VCH Verlag GmbH & Co. KGaA, 2009; pp 1–52.
- (20) Bordwell, F. G.; Ji, G. Z. *J. Am. Chem. Soc.* **1991**, *113* (22), 8398–8401.
- (21) Kaljurand, I.; Kütt, A.; Sooväli, L.; Rodima, T.; Mäemets, V.; Leito, I.; Koppel, I. a. *J. Org. Chem.* **2005**, *70* (3), 1019–1028.



Donor	toluene			methyl isobutyl ketone		
	$\Delta H^{\ddagger}_{\text{obs}}$ (kcal/mol)	$\Delta S^{\ddagger}_{\text{obs}}$ (cal/mol K)	k_{obs} (1/min) ^a	$\Delta H^{\ddagger}_{\text{obs}}$ (kcal/mol)	$\Delta S^{\ddagger}_{\text{obs}}$ (cal/mol K)	k_{obs} (1/min) ^a
1-S ^b	6.13 ± 0.40	-52 ± 46	0.0018	5.22 ± 0.77	-56 ± 45	0.0008
2-S ^b	6.21 ± 0.66	-46 ± 45	0.0065	4.24 ± 0.74	-57 ± 45	0.0027
3-S ^b	8.59 ± 0.53	-46 ± 46	0.0006	--	--	--
1-O	5.66 ± 0.54	-42 ± 46	0.0015	3.53 ± 0.26	-59 ± 46	0.0023
2-O	4.00 ± 0.59	-55 ± 45	0.0074	3.3 ± 0.26	-58 ± 46	0.0076
3-O ^b	2.17 ± 0.18	-58 ± 47	0.0323	--	--	0.1134
TCC ^b	5.32 ± 0.95	-50 ± 44	0.0121	5.37 ± 0.49	-50 ± 46	0.0115

Table 5.1. Activation Parameters for H-bond Donor/MTBD Cocatalyzed ROP of CL. Reaction conditions: CL (2M, 0.876 mmol), benzyl alcohol (0.00876 mmol), 1-X, 2-X, 3X and TCC (0.0438 mmol, 0.0219 mmol, 0.0146 mmol and 0.0438 mmol) MTBD (matched to H-bond donor mmol). a) 40°C. b) For curved Eyring plots; activation parameters extracted from the linear portion.

Catalyst	Decomposition Temperature (°C)	Decomposition Temperature w/ MTBD (°C)
1-S	166	168
1-O	212	151
TCC	247	162
2-S	172	NA
2-O	256	162
3-S	187	196

Table 5.2. Thermal decomposition of H-bond donors with and without MTBD. TGA conditions: Sample size ~7 mg were placed in aluminum pans. Start at 25°C, ramp to 500°C at 10°C/min, held for 5 minutes. N₂ gas flow rate of 10 mL/min. Catalyst samples were weighed from bulk samples. H-bond donor/base 1:1 mixtures were first dissolved in dichloromethane and solvent removed under vacuum. Remaining thick oil was used for samples.

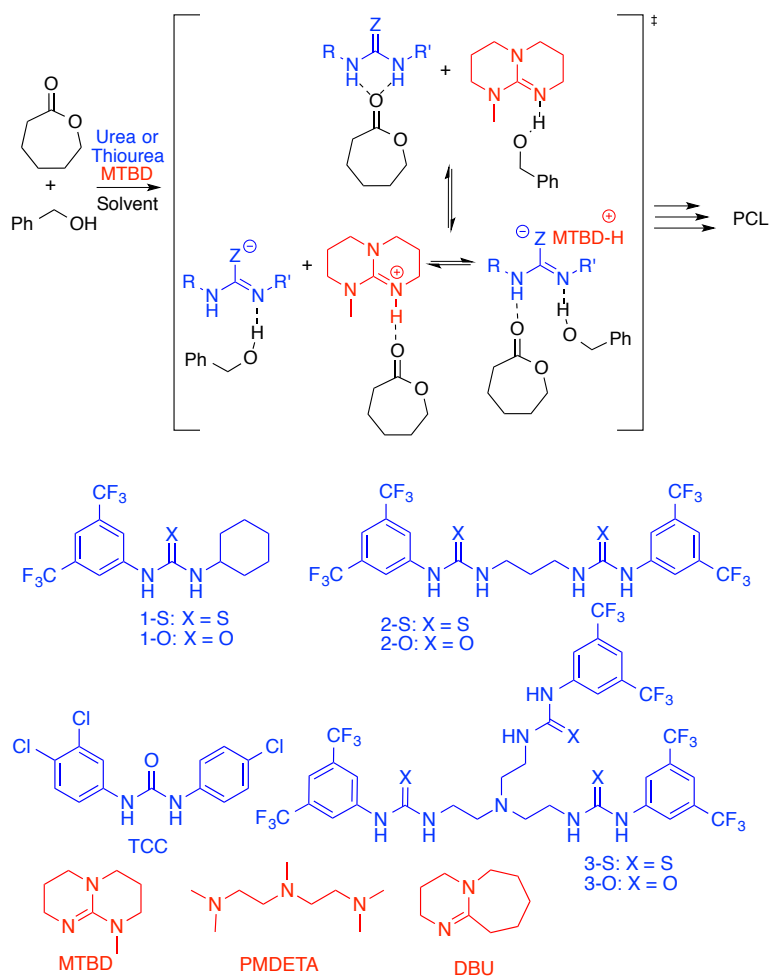


Figure 5.1. H-bonding and imidate mediated ROP of CL.

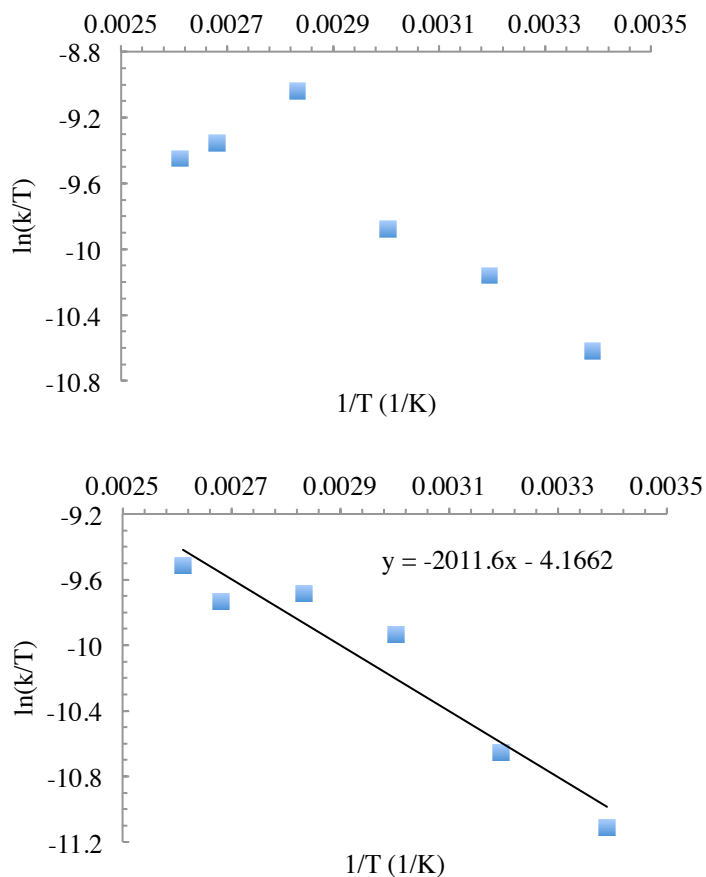


Figure 5.2. Example Eyring plots for the ROP of CL from benzyl alcohol in toluene catalyzed by (upper) **TCC**/MTBD, and (lower) **2-O**/MTBD. Reaction Conditions: CL (2M, 0.876 mmol) cocatalyzed by H-bond donor/MTBD (TCC 0.0438 mmol, **2-O** 0.0219 mmol, MTBD matched to H-bond donor) from benzyl alcohol (0.00876 mmol) in toluene.

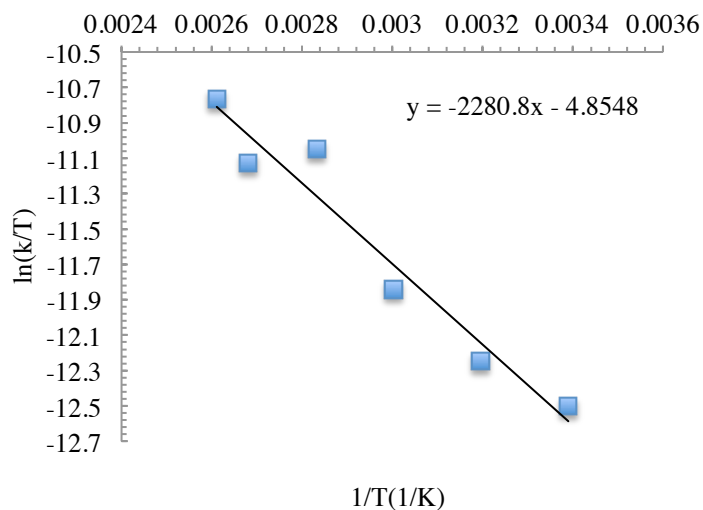


Figure 5.3. Eyring plot constructed from the observed first order rate constants for the **1-O**/MTBD (0.0438 mmol each) cocatalyzed ROP of CL (0.876 mmol, 2M) from benzyl alcohol (0.00876 mmol) in toluene.

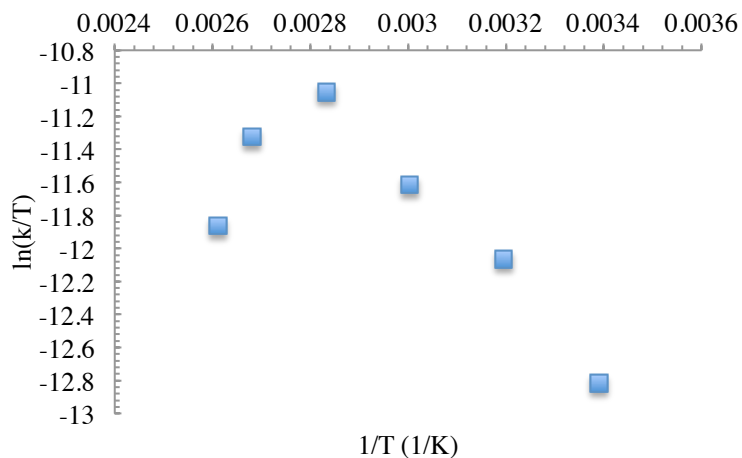


Figure 5.4. Eyring plot constructed from the observed first order rate constants for the **1-S**/MTBD (0.0438 mmol each) cocatalyzed ROP of CL (0.876 mmol, 2M) from benzyl alcohol (0.00876 mmol) in toluene.

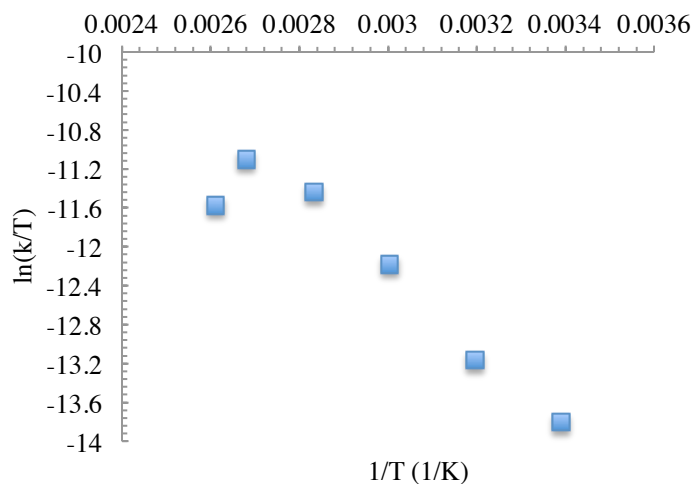


Figure 5.5. Eyring plot constructed from the observed first order rate constants for the **3-S**/MTBD (0.0146 mmol each) cocatalyzed ROP of CL (0.876 mmol, 2M) from benzyl alcohol (0.00876 mmol) in toluene.

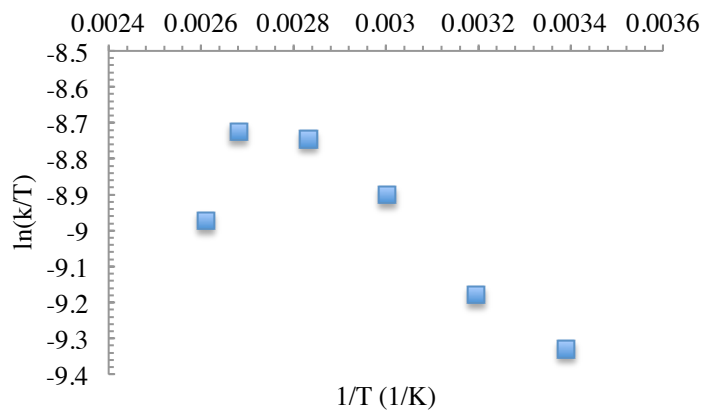


Figure 5.6. Eyring plot constructed from the observed first order rate constants for the **3-O**/MTBD (0.0146 mmol each) cocatalyzed ROP of CL (0.876 mmol, 2M) from benzyl alcohol (0.00876 mmol) in toluene.

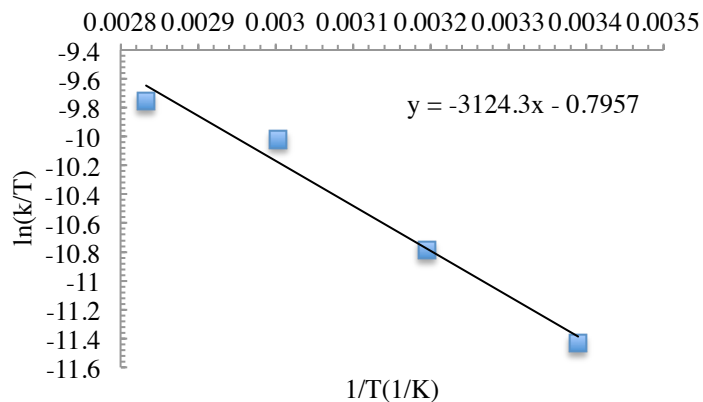


Figure 5.7. Eyring plot constructed from the linear portion of the observed first order rate constants for the **2-S**/MTBD (0.0219 mmol each) cocatalyzed ROP of CL (0.876 mmol, 2M) from benzyl alcohol (0.00876 mmol) in toluene.

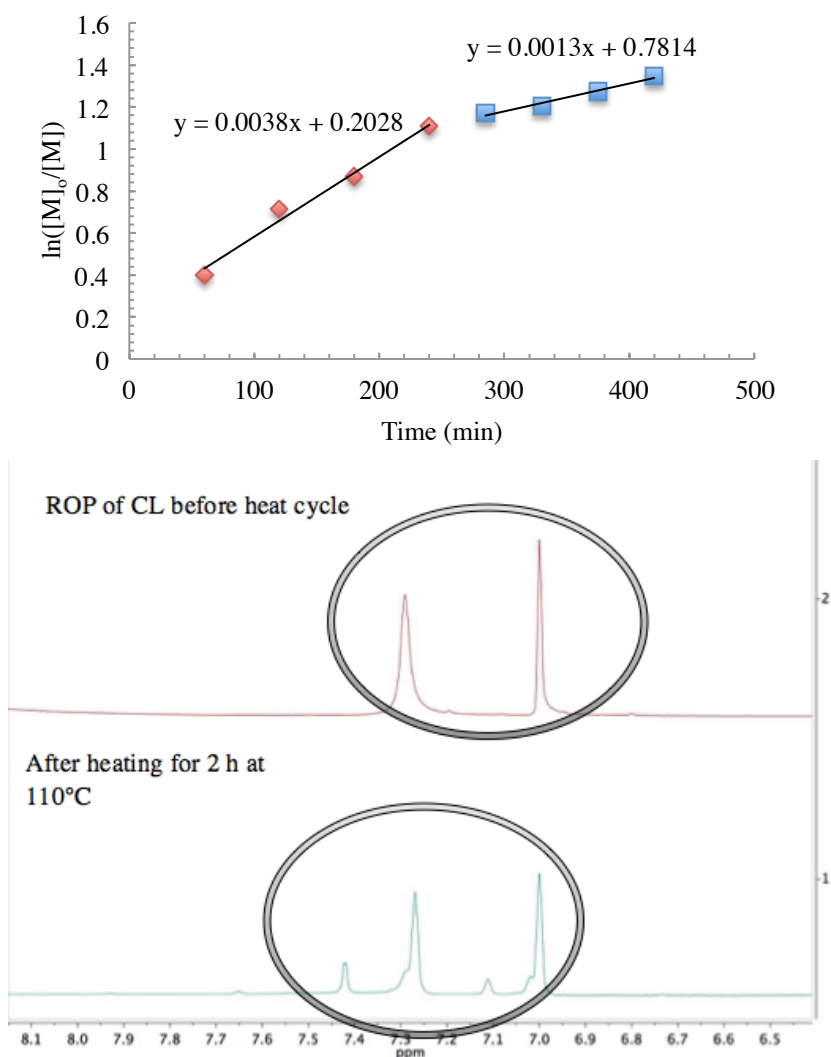


Figure 5.8. (upper) Temperature drop ROP of CL (2M, 0.876 mmol) in toluene, **1-S**/MTBD (0.0438 mmol each) cocatalyzed from benzyl alcohol (0.00876 mmol). A decrease in k_{obs} from 0.0038 min^{-1} to 0.0013 min^{-1} is observed after the temperature change from 110(red) to 80(blue) $^{\circ}\text{C}$. Reaction progression tracked by aliquot, and conversion was determined by ^1H NMR. (lower) ^1H NMR (400 MHz, benzene- d_6) of the ROP of CL (0.876 mmol, 2M), benzyl alcohol (0.00876 mmol), **1-S**/MTBD (0.0438 mmol each). Top image shows the aromatic region of the ^1H NMR of **1-S**. Bottom image shows a second set of aromatic resonances after 2 h of heating at 110 $^{\circ}\text{C}$.

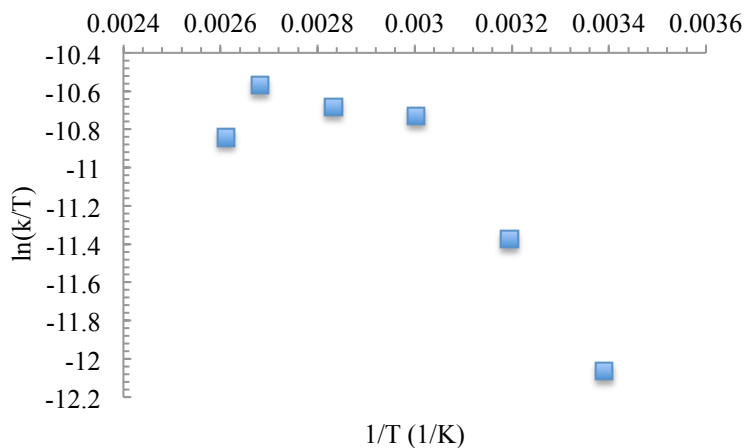


Figure 5.9. Eyring plot constructed from the observed first order rate constants for the TCC/DBU (0.0438 mmol each) cocatalyzed ROP of CL (0.876 mmol, 2M) from benzyl alcohol (0.00876 mmol) in toluene.

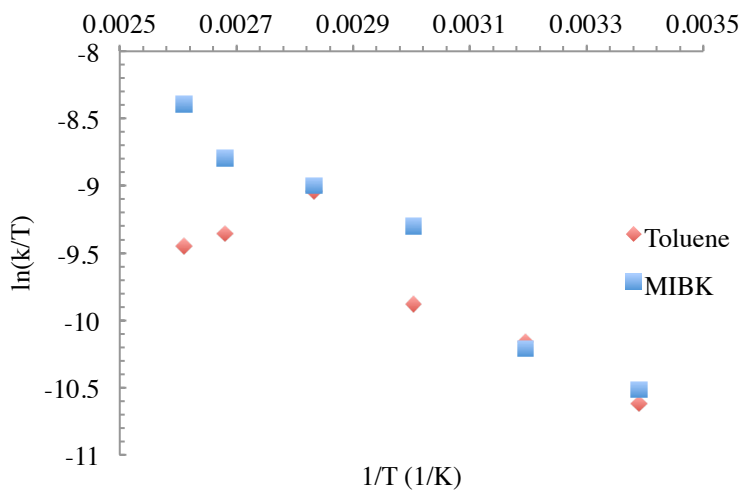


Figure 5.10. Eyring plot for the TCC/MTBD (0.0438 mmol) cocatalyzed ROP of CL (2M, 0.876 mmol) from benzyl alcohol (0.00876 mmol) in toluene and MIBK solvent.

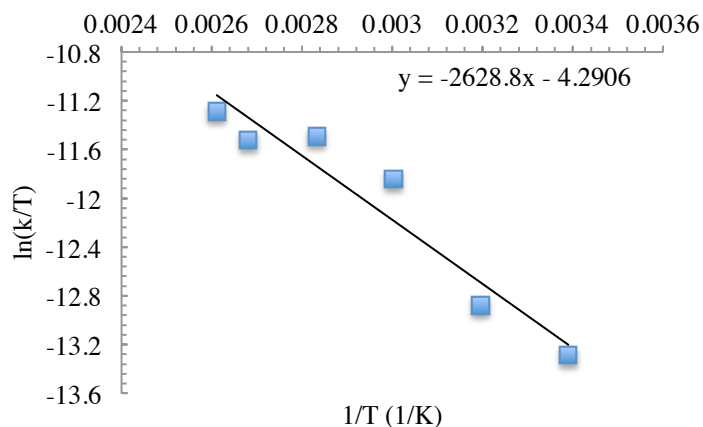


Figure 5.11. Eyring plot constructed from the observed first order rate constants for the **1-S**/MTBD (0.0438 mmol each) cocatalyzed ROP of CL (0.876 mmol) from benzyl alcohol (0.00876 mmol) in methyl isobutyl ketone.

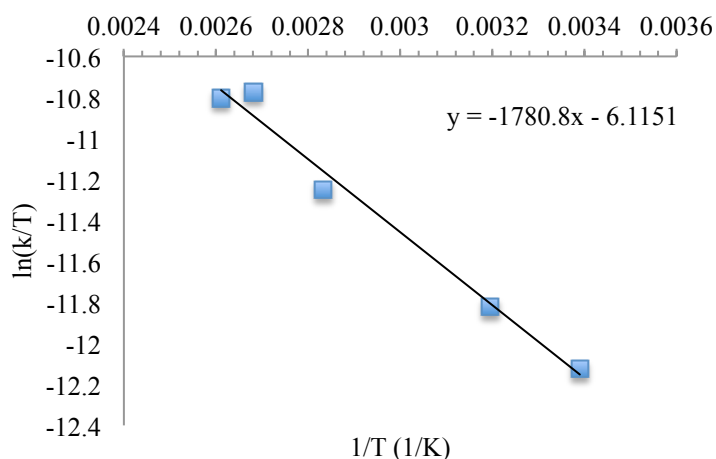


Figure 5.12. Eyring plot constructed from the observed first order rate constants for the **1-O**/MTBD (0.0438 mmol each) cocatalyzed ROP of CL (0.876 mmol) from benzyl alcohol (0.00876 mmol) in methyl isobutyl ketone.

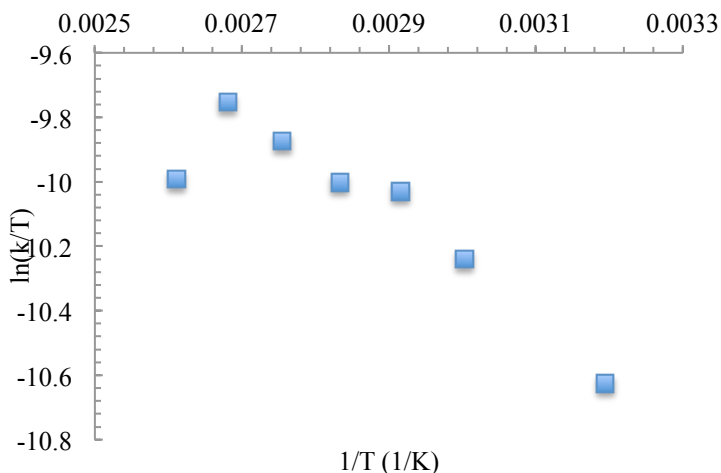


Figure 5.13. Eyring plot constructed from the observed first order rate constants for the **2-O/MTBD** (0.0219 mmol each) cocatalyzed ROP of CL (0.876 mmol) from benzyl alcohol (0.00876 mmol) in methyl isobutyl ketone.

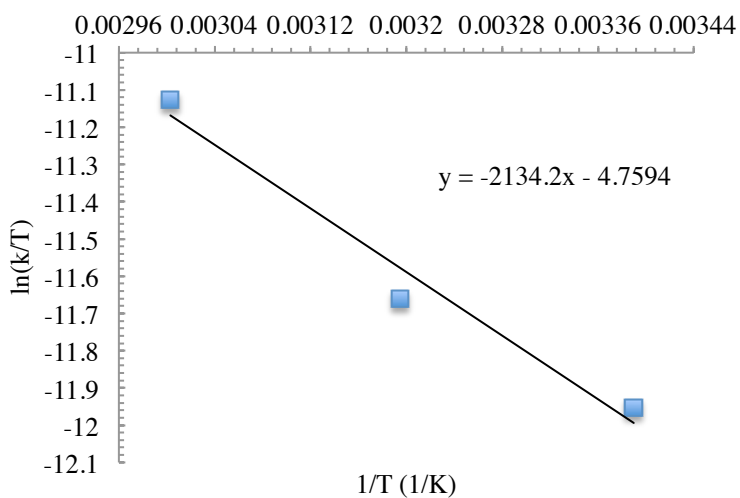


Figure 5.14. Eyring plot constructed from the observed first order rate constants for the **2-S/MTBD** (0.0219 mmol each) cocatalyzed ROP of CL (0.876 mmol) from benzyl alcohol (0.00876 mmol) in methyl isobutyl ketone.

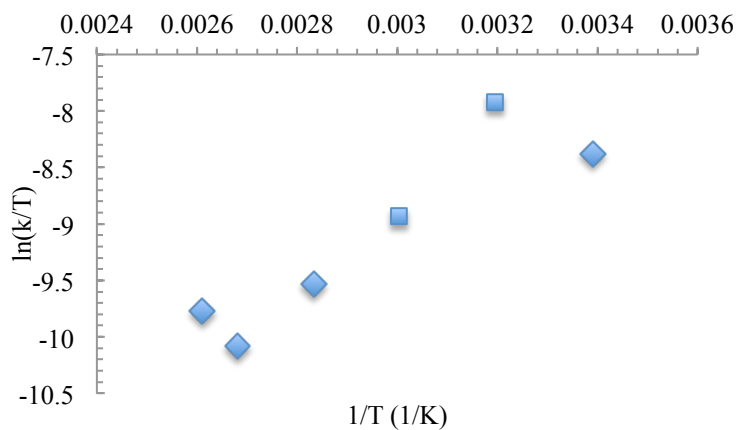


Figure 5.15. Eyring plot constructed from the observed first order rate constants for the **3-O**/MTBD (0.0146 mmol each) cocatalyzed ROP of CL (0.876 mmol) from benzyl alcohol (0.00876 mmol) in methyl isobutyl ketone.

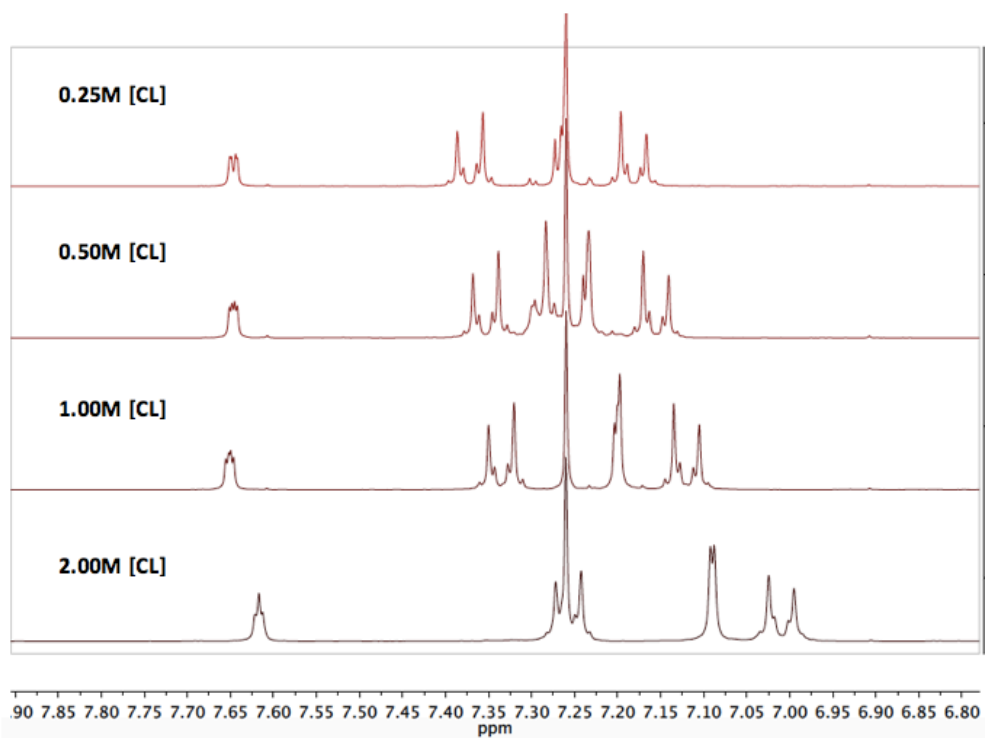


Figure 5.16. ^1H NMR spectra of TCC/MTBD (0.00438 mmol each) cocatalyst in the presence of varying [CL] (0.25-2M) in CDCl_3 .

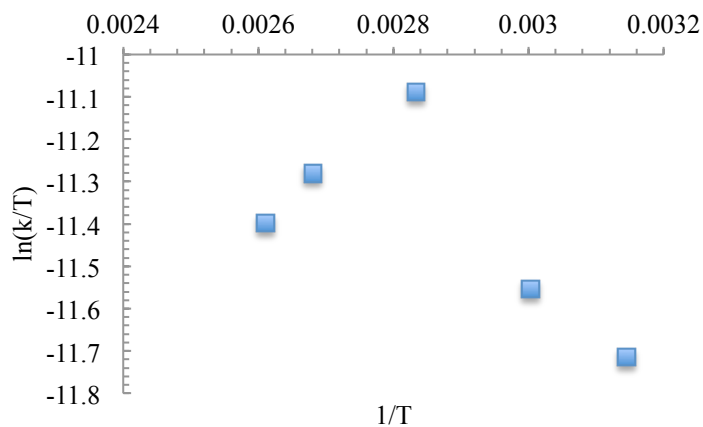


Figure 5.17. Eyring plot constructed from the observed first order rate constants for the **2-S**/PMDETA (0.0219 mmol each) cocatalyzed ROP of L-LA (0.876 mmol) from benzyl alcohol (0.00876 mmol) in methyl isobutyl ketone.

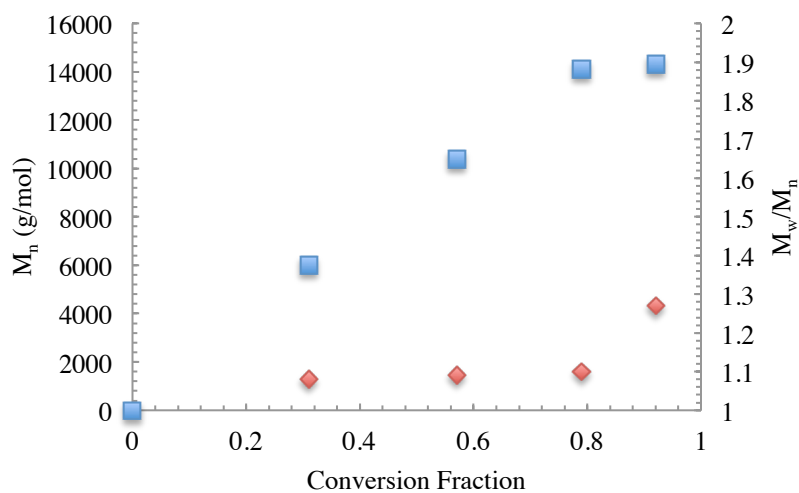


Figure 5.18. M_n and M_w/M_n Versus Conversion plot for **2-O** at 110°C. Reaction conditions: CL (0.876 mmol, 2M) in toluene, **2-O**/MTBD (0.0219 mmol each), benzyl alcohol (0.00876 mmol).

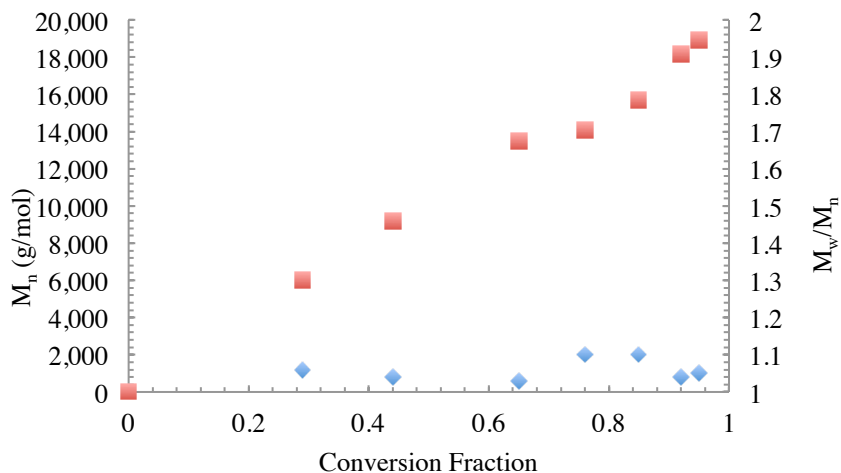


Figure 5.19. M_n and M_w/M_n versus conversion plot for the **3-O**/MTBD cocatalyzed ROP of CL from benzyl alcohol in toluene at 110°C.

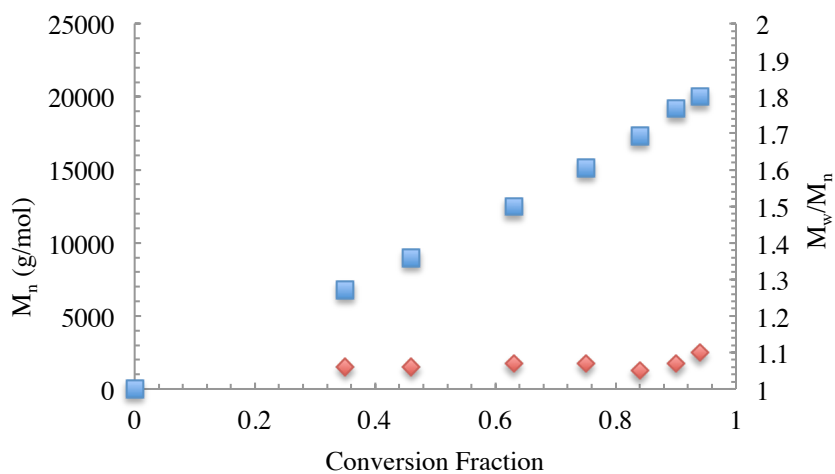


Figure 5.20. M_n and M_w/M_n versus conversion plot for **1-S** at 80°C. Reaction conditions: CL (0.876 mmol, 2M) in toluene, **1-S**/MTBD (0.0438 mmol each) cocatalyzed, from benzyl alcohol (0.00876 mmol).

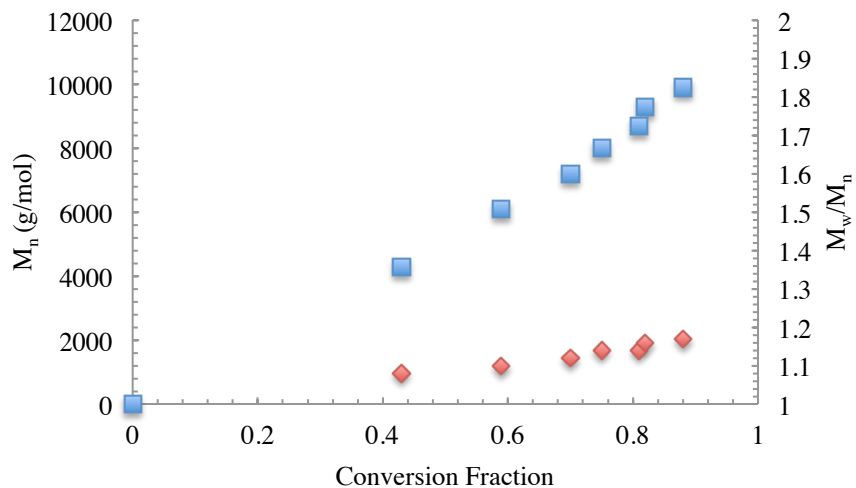


Figure 5.21. M_n and M_w/M_n versus conversion plot for **1-S** at 110°C. Reaction conditions: CL (0.876 mmol, 2M) in toluene, **1-S**/MTBD (0.0438 mmol each) cocatalyzed, from benzyl alcohol (0.0175 mmol).

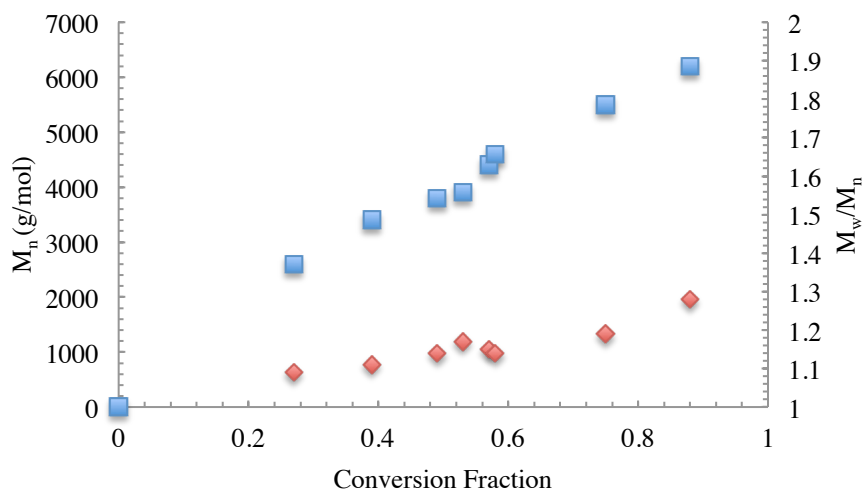


Figure 5.22. M_n and M_w/M_n versus conversion plot for **1-S** at 110°C. Reaction conditions: CL (0.876 mmol, 2M) in methyl isobutyl ketone, **1-S**/MTBD (0.0438 mmol each) cocatalyzed, from benzyl alcohol (0.0175 mmol).

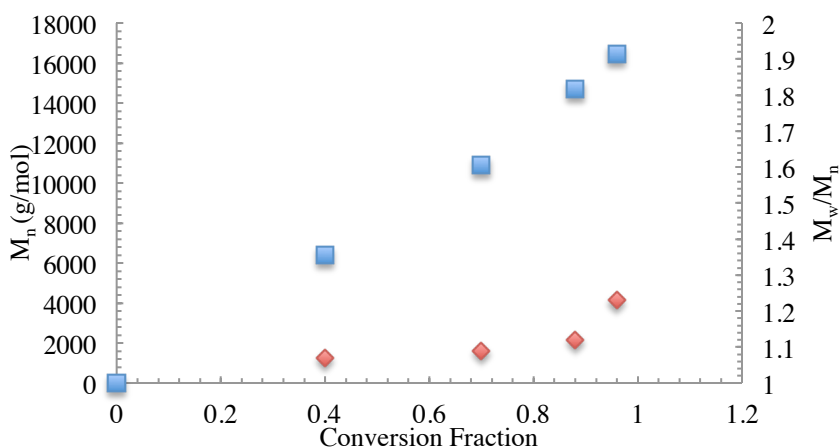


Figure 5.23. M_n and M_w/M_n Versus Conversion plot for **2-O** at 90°C. Reaction conditions: CL (0.876 mmol, 2M) in toluene, **2-O**/MTBD (0.0219 mmol each) cocatalyzed, from benzyl alcohol (0.00876 mmol).

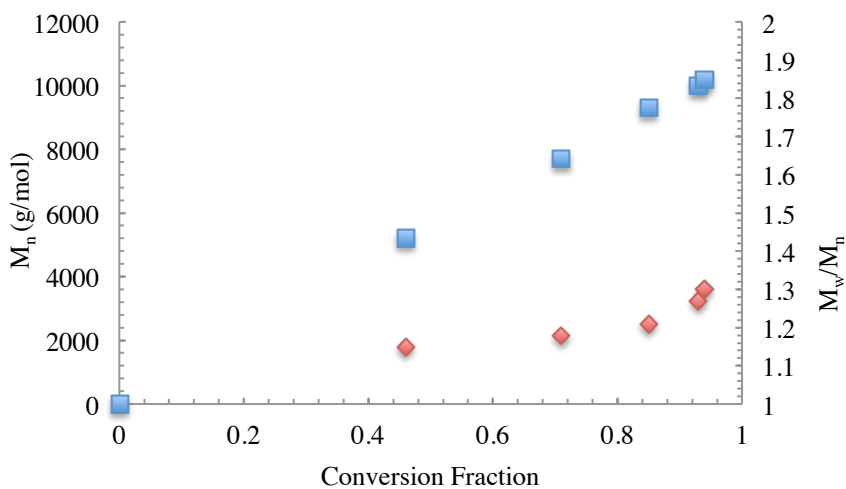


Figure 5.24. M_n and M_w/M_n versus conversion plot for **2-O** at 90°C. Reaction conditions: CL (0.876 mmol, 2M) in methyl isobutyl ketone, **2-O**/MTBD (0.0219 mmol each) cocatalyzed, from benzyl alcohol (0.0175 mmol).

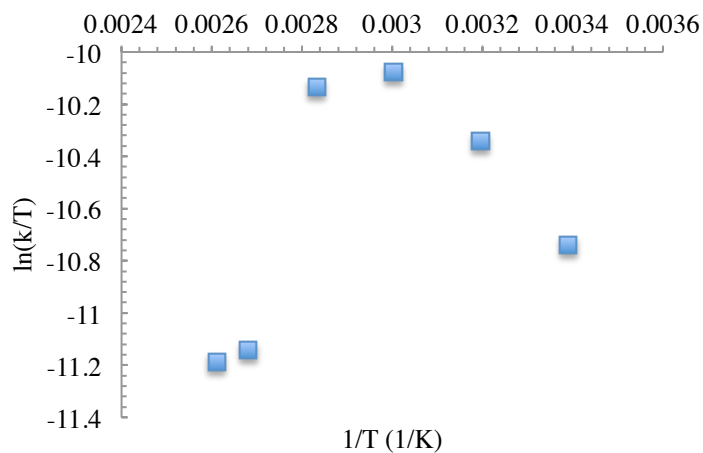


Figure 5.25. Eyring plot constructed from the observed first order rate constants for the TCC/MTBD (0.0438 mmol each) cocatalyzed ROP of CL (0.876 mmol, 1M) from benzyl alcohol (0.00876 mmol) in toluene.

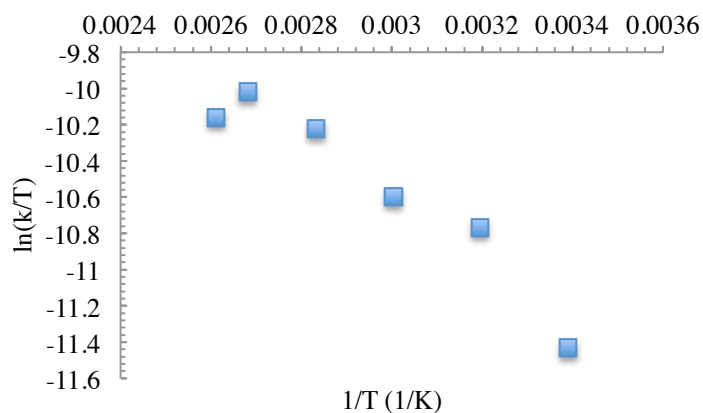


Figure 5.26. Eyring plot constructed from the observed first order rate constants for the 2-O/MTBD (0.0219 mmol each) cocatalyzed ROP of CL (0.876 mmol, 1M) from benzyl alcohol (0.00876 mmol) in toluene.

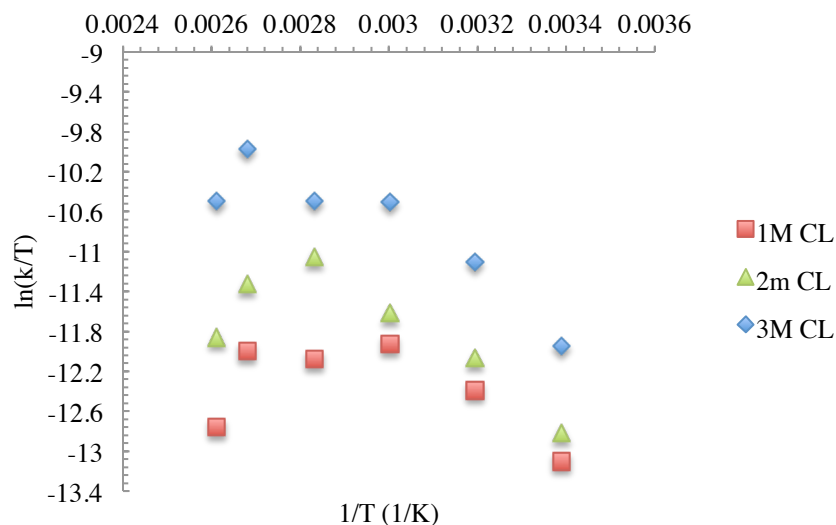


Figure 5.27. Eyring plot constructed from the observed first order rate constants for the **1-S**/MTBD (0.0438 mmol each) cocatalyzed ROP of CL (0.876 mmol) from benzyl alcohol (0.00876 mmol) at 1M, 2M and 3M concentrations in toluene.

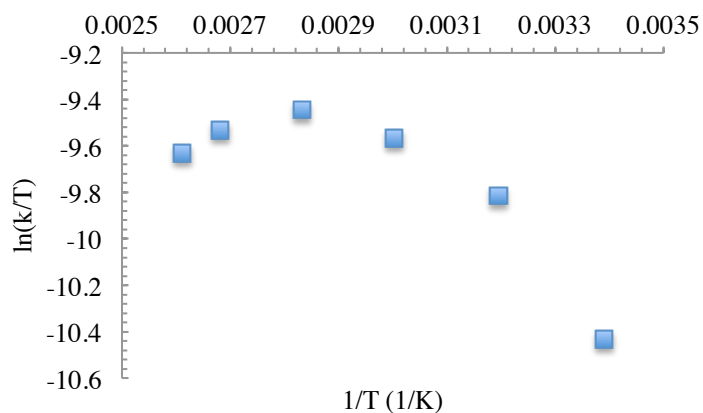


Figure 5.28. Eyring plot constructed from the observed first order rate constants for the TCC/MTBD (0.0438 mmol each) cocatalyzed ROP of CL (0.876 mmol) from benzyl alcohol (0.00876 mmol) in benzene.

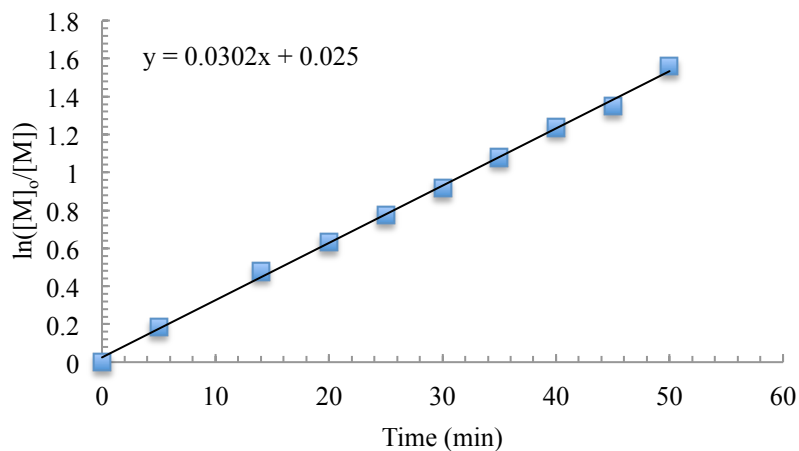


Figure 5.29. First order evolution of [CL] versus time for the TCC/MTBD (0.0438 mmol each) cocatalyzed ROP of CL (2M, 0.876 mmol) from benzyl alcohol (0.00876 mmol) in toluene.

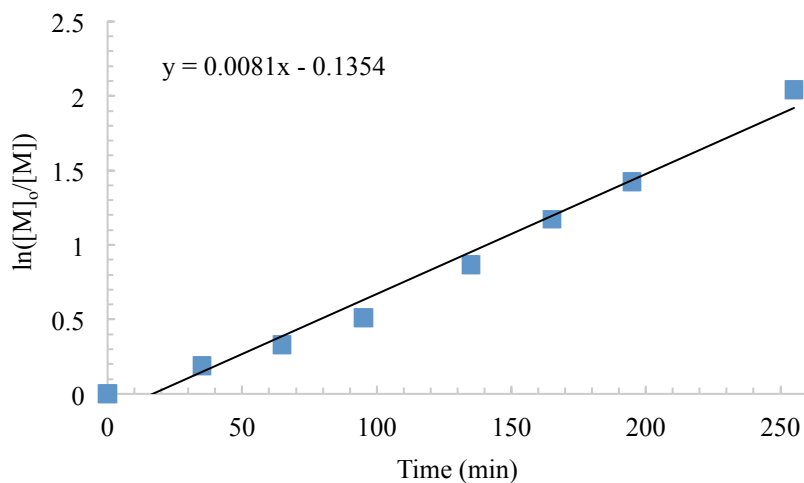


Figure 5.30. First order evolution of [CL] versus time for the **1-O**/MTBD (0.0438 mmol each) cocatalyzed ROP of CL (2M, 0.876 mmol) from benzyl alcohol (0.00876 mmol) in toluene.

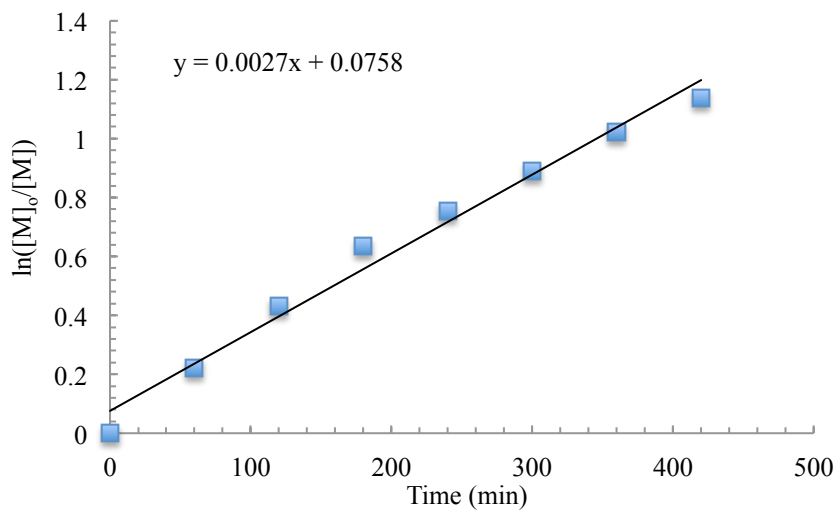


Figure 5.31. First order evolution of [CL] versus time for the **1-S**/MTBD (0.0438 mmol each) cocatalyzed ROP of CL (2M, 0.876 mmol) from benzyl alcohol (0.00876 mmol) in toluene.

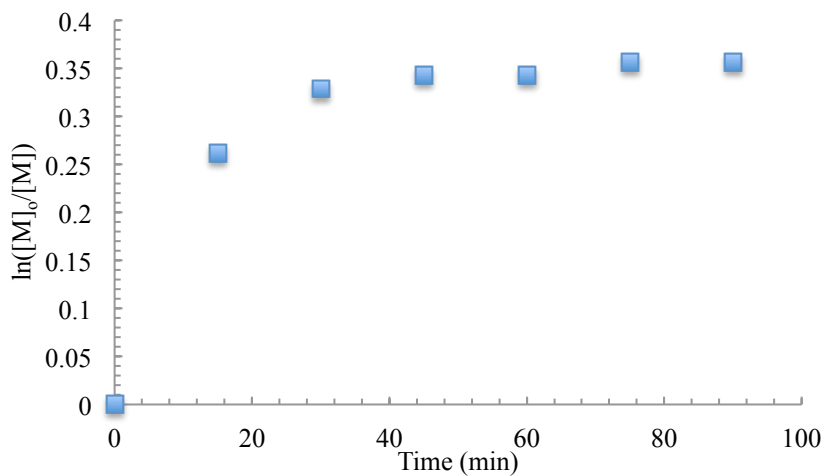


Figure 5.32. First order evolution of [CL] versus time for the **2-S**/MTBD (0.0219 mmol each) cocatalyzed ROP of CL (2M, 0.876 mmol) from benzyl alcohol (0.00876 mmol) in toluene.

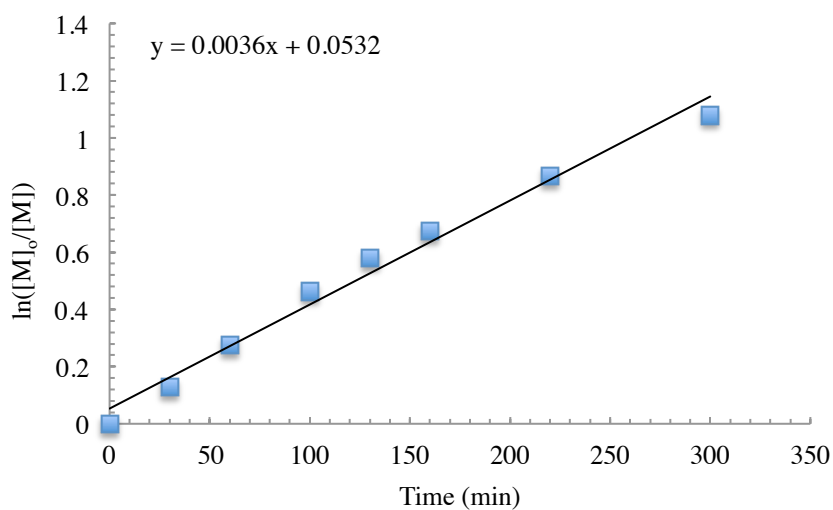


Figure 5.33. First order evolution of [CL] versus time for the **3-S**/MTBD (0.0146 mmol each) cocatalyzed ROP of CL (2M, 0.876 mmol) from benzyl alcohol (0.00876 mmol) in toluene.

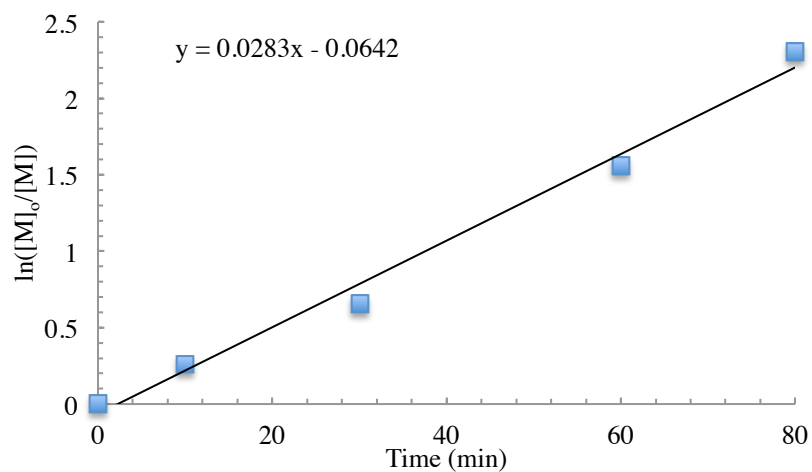


Figure 5.34. First order evolution of [CL] versus time for the **2-O**/MTBD (0.0219 mmol each) cocatalyzed ROP of CL (2M, 0.876 mmol) from benzyl alcohol (0.00876 mmol) in toluene.

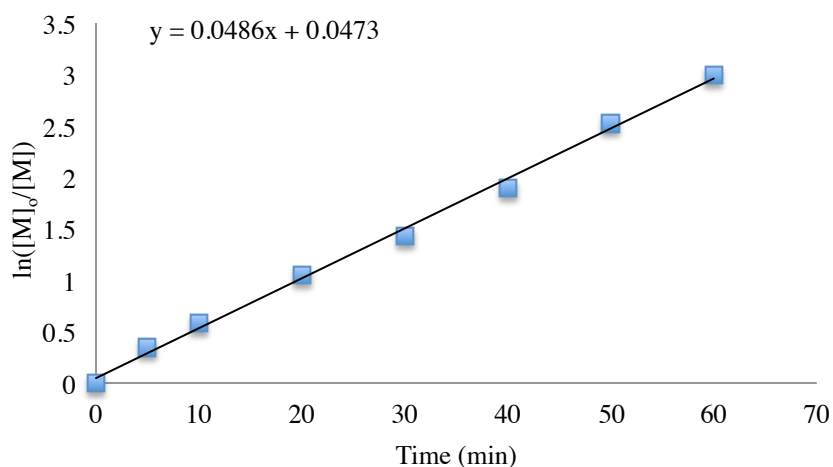


Figure 5.35. First order evolution of [CL] versus time for the **3-O**/MTBD (0.0146 mmol each) cocatalyzed ROP of CL (2M, 0.876 mmol) from benzyl alcohol (0.00876 mmol) in toluene.

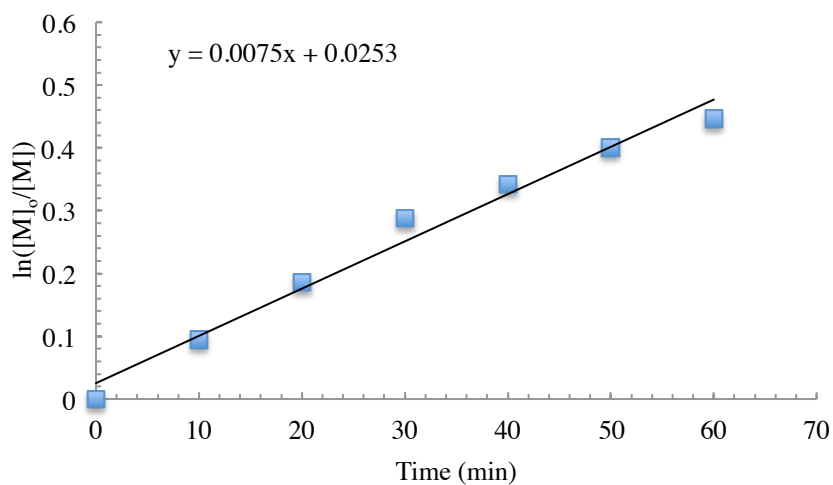


Figure 5.36. First order evolution of [CL] versus time for the TCC/DBU (0.0438 mmol each) cocatalyzed ROP of CL (2M, 0.876 mmol) from benzyl alcohol (0.00876 mmol) in toluene.

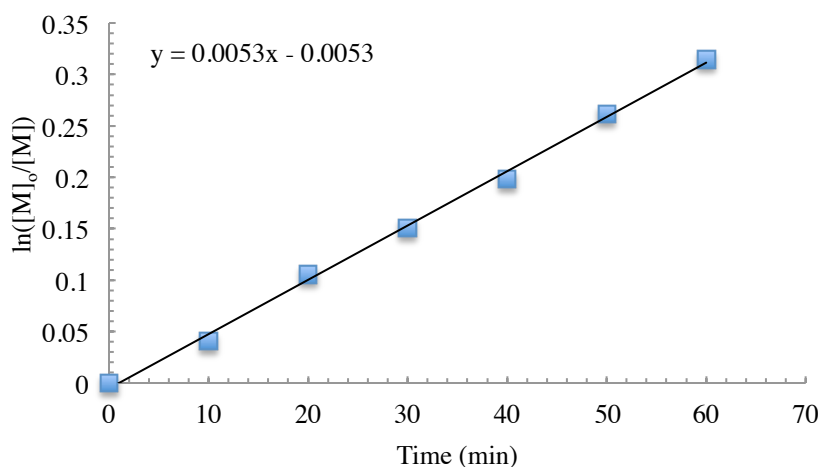


Figure 5.37. First order evolution of [CL] versus time for the TCC/MTBD (0.0438 mmol each) cocatalyzed ROP of CL (1M, 0.876 mmol) from benzyl alcohol (0.00876 mmol) in toluene.

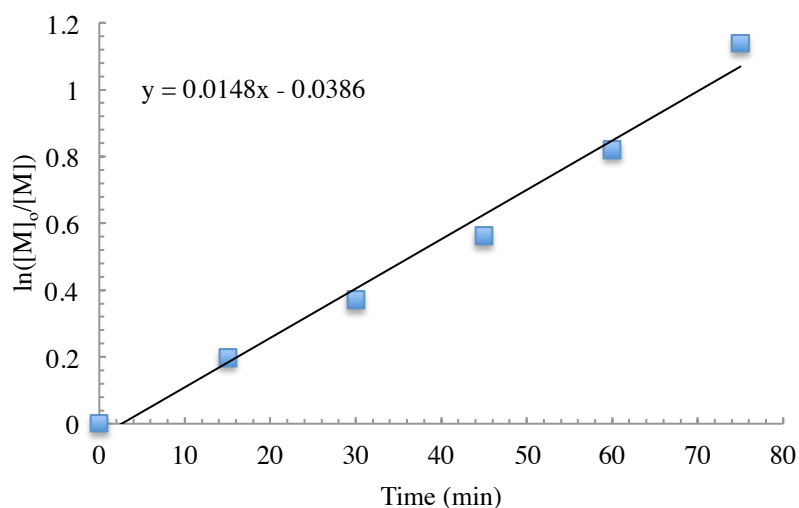


Figure 5.38. First order evolution of [CL] versus time for the **2-O**/MTBD (0.0219 mmol each) cocatalyzed ROP of CL (1M, 0.876 mmol) from benzyl alcohol (0.00876 mmol) in toluene.

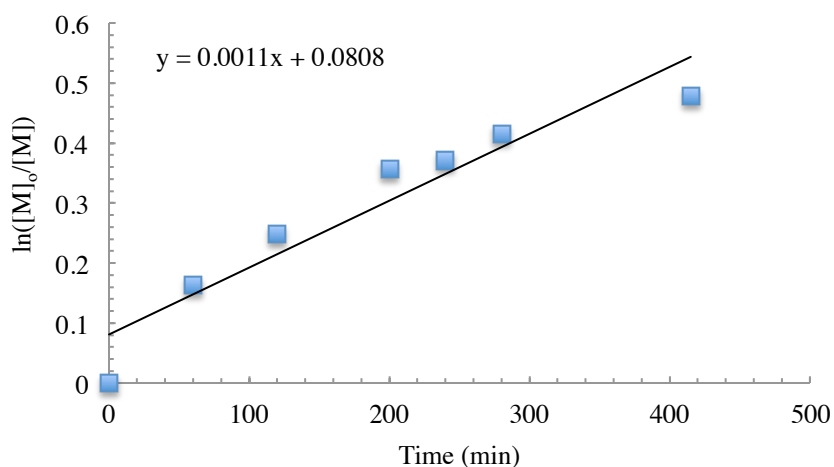


Figure 5.39. First order evolution of [CL] versus time for the **1-S**/MTBD (0.0438 mmol each) cocatalyzed ROP of CL (1M, 0.876 mmol) from benzyl alcohol (0.00876 mmol) in toluene.

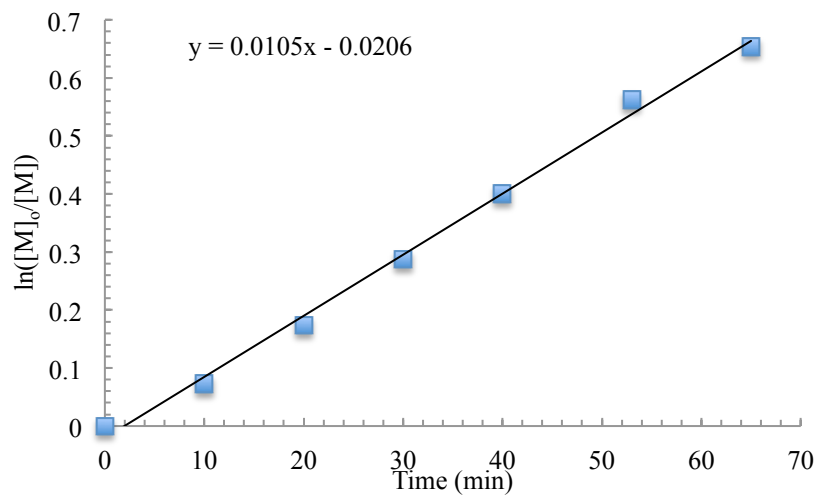


Figure 5.40. First order evolution of [CL] versus time for the **1-S**/MTBD (0.0438 mmol each) cocatalyzed ROP of CL (3M, 0.876 mmol) from benzyl alcohol (0.00876 mmol) in toluene.

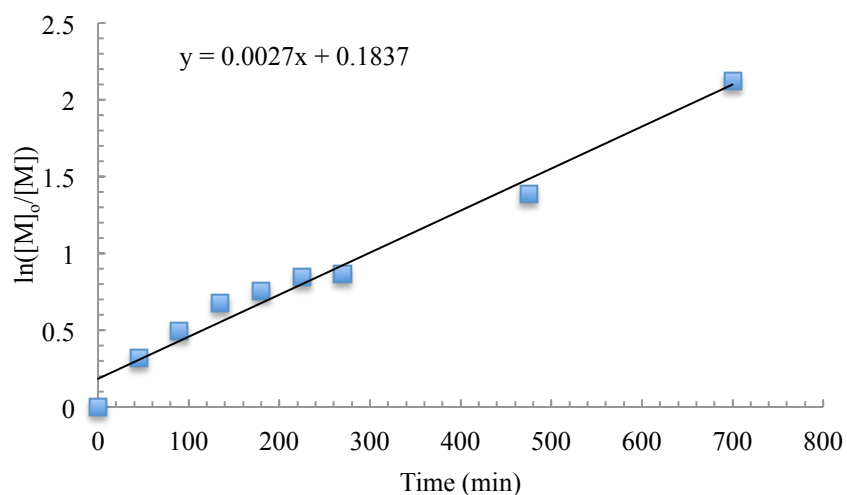


Figure 5.41. First order evolution of [CL] versus time for the **1-S**/MTBD (0.0438 mmol each) cocatalyzed ROP of CL (2M, 0.876 mmol) from benzyl alcohol (0.00876 mmol) in methyl isobutyl ketone.

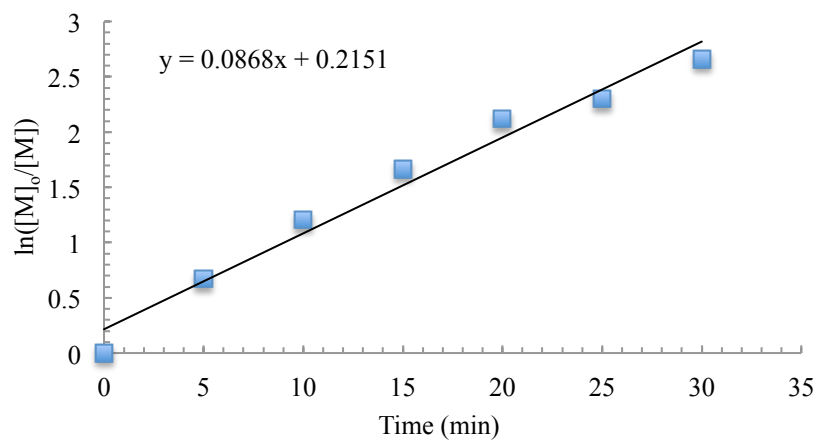


Figure 5.42. First order evolution of [CL] versus time for the **TCC**/MTBD (0.0438 mmol each) cocatalyzed ROP of CL (2M, 0.876 mmol) from benzyl alcohol (0.00876 mmol) in methyl isobutyl ketone.

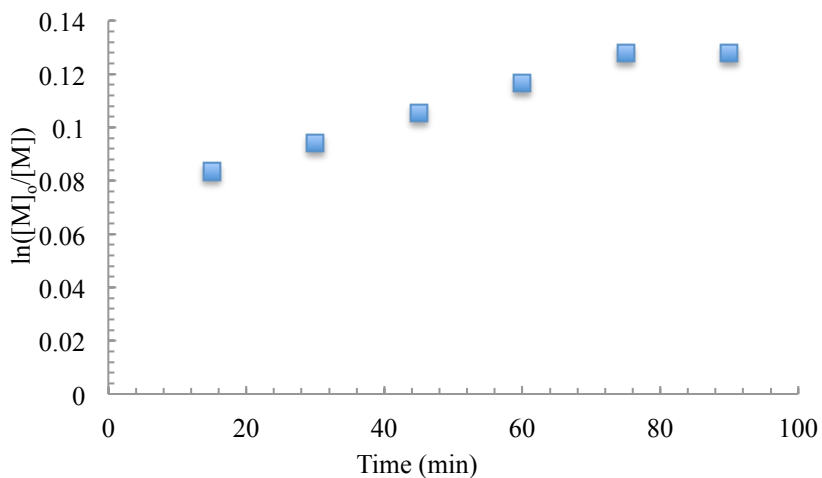


Figure 5.43. First order evolution of [CL] versus time for the **2-S**/MTBD (0.0219 mmol each) cocatalyzed ROP of CL (2M, 0.876 mmol) from benzyl alcohol (0.00876 mmol) in methyl isobutyl ketone.

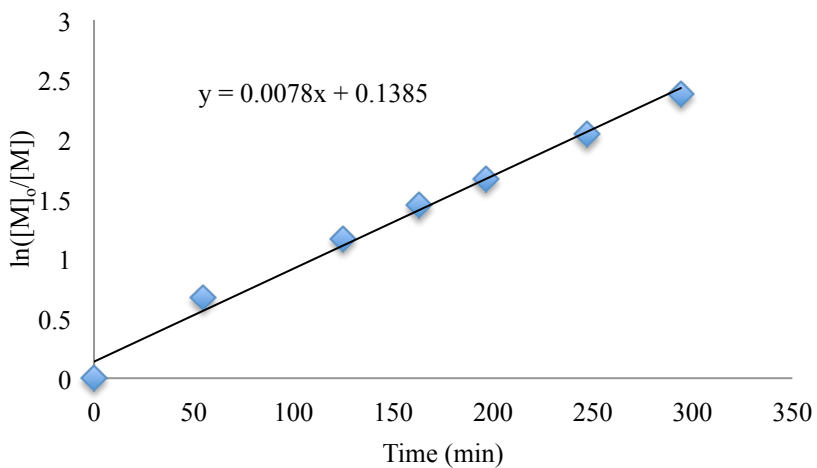


Figure 5.44. First order evolution of [CL] versus time for the **1-O**/MTBD (0.0438 mmol each) cocatalyzed ROP of CL (2M, 0.876 mmol) from benzyl alcohol (0.00876 mmol) in methyl isobutyl ketone.

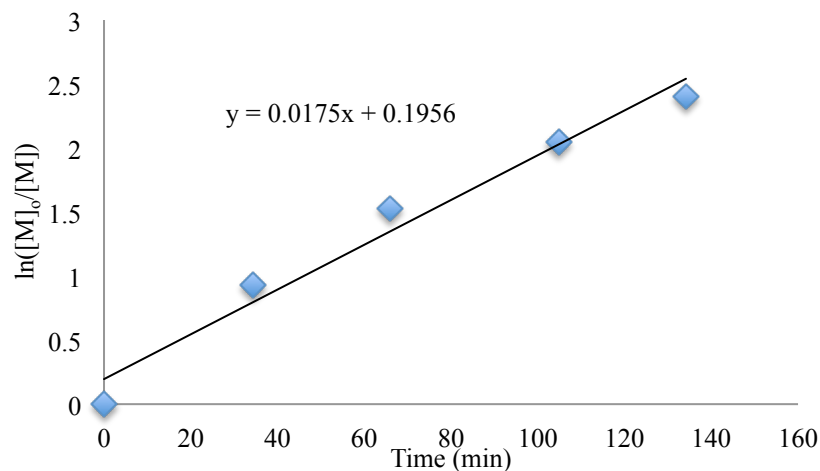


Figure 5.45. First order evolution of [CL] versus time for the **2-O**/MTBD (0.0219 mmol each) cocatalyzed ROP of CL (2M, 0.876 mmol) from benzyl alcohol (0.00876 mmol) in methyl isobutyl ketone.

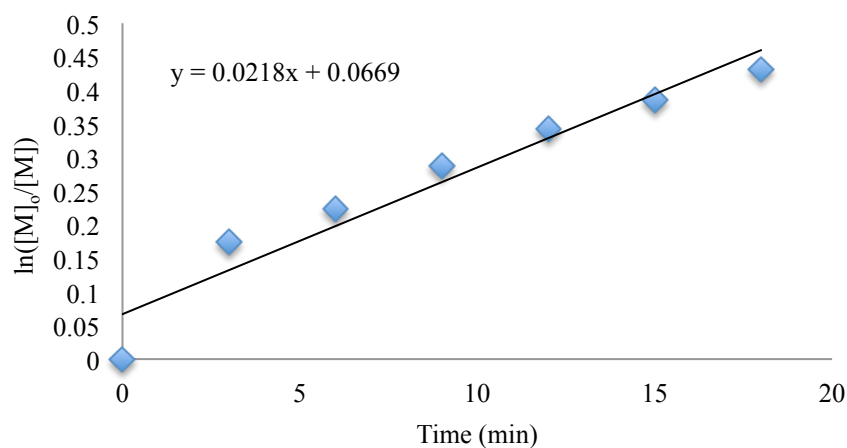


Figure 5.46. First order evolution of [CL] versus time for the **3-O**/MTBD (0.0146 mmol each) cocatalyzed ROP of CL (2M, 0.876 mmol) from benzyl alcohol (0.00876 mmol) in methyl isobutyl ketone.

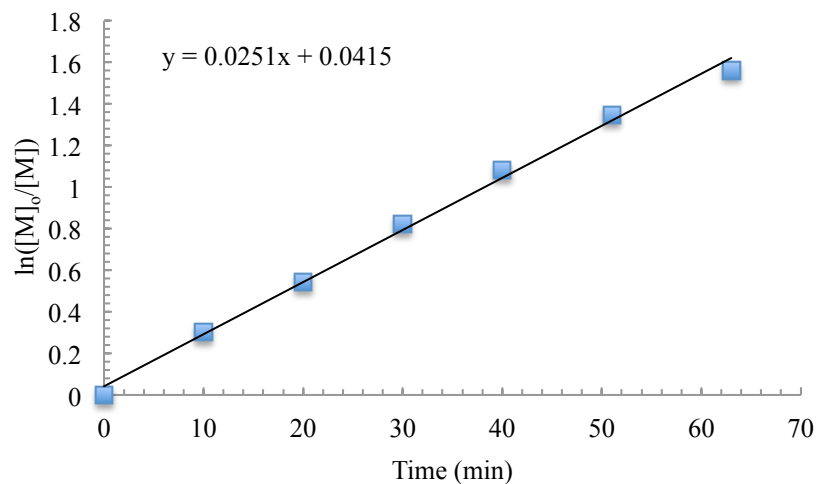


Figure 5.47. First order evolution of $[\text{CL}]$ versus time for the TCC/MTBD (0.0438 mmol each) cocatalyzed ROP of CL (2M, 0.876 mmol) from benzyl alcohol (0.00876 mmol) in benzene.

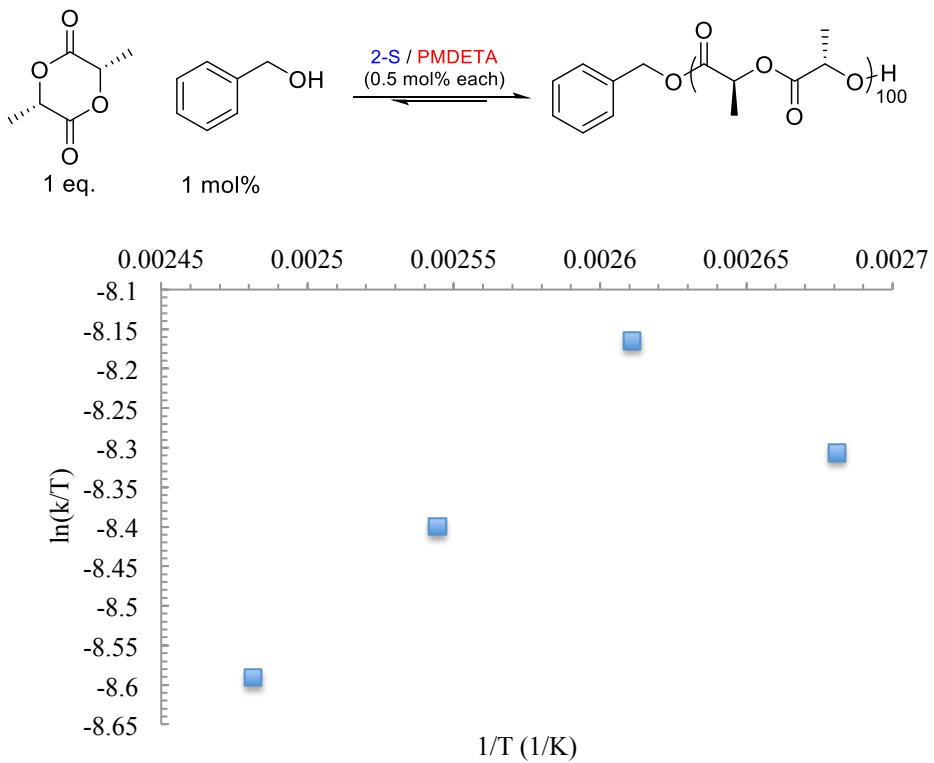


Figure 5.48. Eyring plot for the solvent-free ROP of LA (1.380 mmol) from benzyl alcohol (0.014 mmol) catalyzed by **2-S**/PMDETA (0.007 mmol each).

INTENTIONALLY BLANK PAGE

MANUSCRIPT – VI

Unpublished Results

**Quinoidal Bifunctional Catalyst For The Ring Opening Polymerization of Cyclic
Esters**

Kurt V. Fastnacht and Matthew K. Kiesewetter

Chemistry, University of Rhode Island, Kingston, RI, USA

Corresponding Author: Matthew Kiesewetter, Ph.D.
Chemistry
University of Rhode Island
140 Flagg Road
Kingston, RI, 02881, USA
Email address: mkiesewetter@uri.edu

ABSTRACT

A new class of bifunctional catalysts was developed for the ring-opening polymerization (ROP) of lactone monomers. The bifunctionality is derived from the oxidation of a (thio)urea quinone group allowing for both a lewis acidic and lewis basic site for activation of monomer and alcohol/chain end respectively. Through multiple iterations of the catalyst, an air insensitive catalyst was produced and used for ROP. Unfortunately, attempts at ROP of both δ -valerolactone and L-lactide were unsuccessful. A mechanistic explanation is discussed.

INTRODUCTION

The structural motifs for H-bonding organic catalysts for ring-opening polymerization (ROP) have been developed and optimized for both catalyst activity and reaction control. Reaction rates and control are highly dependent on the H-bond donors selectivity for binding monomer versus polymer.¹ (Thio)ureas have been shown to be superior in both rate and selectivity over other organocatalytic species for ROP.^{2,3} These species by themselves do not possess the ability to effect polymer transformations and must be paired with a base cocatalyst for alcohol/chain end activation.⁴ Due to the highly tunable nature of having separate and active catalyst species, the vast majority of organic catalysts used are dual catalyst systems. However, due to the opportunity for scaffold optimization of the (thio)urea H-bonding species, the ability to build these scaffolds with the needed H-bond accepting component within a single catalyst species capable of doing both types of activation is possible.⁴ Besides (thio)ureas there are many examples of other bifunctional species that perform ROP.⁵⁻⁷ The most popular of these bifunctional catalyst species is the guanidine base, TBD (Figure 6.1.a).^{1,8} Due to its relatively fast reaction rates, moderate control and commercial availability, many default to the use of it over other bifunctional or dual catalyst species, regardless of the better activity and reaction control found in the other catalysts.

Recently, the deprotonation of (thio)ureas to produce (thio)imidate species (Figure 6.1.b) have been shown to be very active for the ROP of cyclic esters.^{2,9-11} Reminiscent of TBD, the (thio)imidate can activate monomer and alcohol/chain end through a bifunctional process. However, with the negative charge on the (thio)imidate, it is possible for the species produce undesired side reactions, potentially decreasing the

overall control of the reaction. As an alternative, we proposed that a quinoidal catalyst (Figure 6.1.c), which is structurally similar to the (thio)imide character but remains chemically neutral, might be the best of both worlds with the rate of the imide catalyst and the control of a neutral (thio)urea species in an easily accessible bifunctional scaffold.

EXPERIMENTAL SECTION

General Considerations: All manipulations were performed in an MBRAUN stainless steel glovebox equipped with a gas purification system or using Schlenk technique under a nitrogen atmosphere. All chemicals were purchased from Fisher Scientific and used as received unless stated otherwise. Tetrahydrofuran and dichloromethane were dried on an Innovative Technologies solvent purification system with alumina columns and nitrogen working gas. Benzene-*d*₆, chloroform-*d* and acetone-*d*₆ were purchased from Cambridge Isotope Laboratories and distilled from CaH₂ under a nitrogen atmosphere. δ -valerolactone (VL; 99%) and benzyl alcohol were distilled from CaH₂ under reduced pressure. L-LA was purchased from Sigma Aldrich and recrystallized from toluene. 4-aminophenol, phenyl isocyanate and 3,5-bis(trifluoromethyl)phenyl isocyanate were purchased from Acros Organics. 3,5-bis(trifluoromethyl)phenyl isothiocyanate was purchased from Oakwood Products. Cyclohexyl isocyanate and 3,5-(dimethoxy)phenyl isocyanate were purchased from Sigma Aldrich. NMR experiments were performed on Bruker Avance III 300 MHz or 400 MHz spectrometer.

Synthesis of 1-(4-hydroxyphenyl)-3-phenylurea (4). A dried 50 mL Schlenk flask was charged with a stir bar, tetrahydrofuran (15.0 mL) and 4-aminophenol (478.0 mg, 4.38 mmol). Phenyl isothiocyanate (0.478 mL, 4.38 mmol) was added drop wise to the flask. The solution was stirred for 12 hours. The product crashed out of solution, was filtered and washed with cold tetrahydrofuran. Yield: 92%. ¹H NMR (300 MHz, C₂D₆OS) δ 6.69 (d, *J* = 2, 2H) 6.94 (t, *J* = 3, 1H) 7.24 (m, 4H) 7.43 (d, *J* = 2, 2H) 8.33 (s, 1H), 8.54 (s, 1H), 9.0.5 (s, 1H).

Synthesis of 1-cyclohexyl-3-(4-hydroxyphenyl)urea (5). A dried 50 mL Schlenk flask was charged with a stir bar, tetrahydrofuran (15.0 mL) and 4-aminophenol (218.26 mg, 2.00 mmol). Cyclohexyl isocyanate (0.255 mL, 2.00mmol) was added drop wise to the flask. The solution was stirred for 12 hours. The product crashed out of solution, was filtered and washed with cold tetrahydrofuran. Yield: 87%. ¹H NMR (300 MHz, C₂D₆OS) δ 1.23 (m, 5H), 1.69 (m, 5H), 3.43 (m, 1H), 5.86 (d, *J* = 3, 1H), 6.62 (d, *J* = 3, 2H), 7.13 (d, *J* = 3, 2H), 7.92 (s, 1H), 8.90 (s, 1H).

1-(3,5-dimethoxyphenyl)-3-(4-hydroxyphenyl)urea (3). A dried 50 mL Schlenk flask was charged with a stir bar, tetrahydrofuran (15.0 mL) and 4-aminophenol (218.26 mg, 2.00 mmol). 3,5-dimethoxyphenyl isocyanate (358.3 mg, 2.00mmol) was then added to the solution. The solution was stirred for 12 hours. The product crashed out of solution, was filtered and washed with cold tetrahydrofuran. Yield: 93%. ¹H NMR (300 MHz, C₂D₆OS) δ 3.70 (s, 6H), 6.12 (m, 1H), 6.68 (m, 4H), 7.21 (d, 2H), 8.32 (s, 1H), 8.52 (s, 1H), 9.06 (s, 1H).

1-(3,5-bis(trifluoromethyl)phenyl)-3-(4-hydroxyphenyl)urea (2). A dried 50 mL Schlenk flask was charged with a stir bar, tetrahydrofuran (15.0 mL) and 4-aminophenol (150 mg, 1.38 mmol). 3,5-bis(trifluoromethyl)phenyl isocyanate (0.239 mL, 1.38 mmol) was then added drop wise to the solution. The solution was stirred for 12 hours. Solvent was removed using reduced pressure. White solid was taken up in DCM and filtered and washed with cold DCM. Yield: 82%. ¹H NMR (300 MHz, C₂D₆OS) δ 6.72 (d, *J* = 3, 2H), 7.22 (d, *J* = 3, 2H), 7.60 (s, 1H), 8.16 (s, 2H), 8.65 (s, 2H), 8.65 (s, 1H), 9.23 (s, 1H), 9.30 (s, 1H).

1-(3,5-bis(trifluoromethyl)phenyl)-3-(4-hydroxyphenyl)thiourea (1). A dried 50 mL Schlenk flask was charged with a stir bar, tetrahydrofuran (15.0 mL) and 4-aminophenol (149.5 mg, 1.387 mmol). 3,5-bis(trifluoromethyl)phenyl isothiocyanate (0.250 mL, 1.37 mmol) was then added drop wise to the solution. The solution was stirred for 12 hours. Solvent was removed using reduced pressure. White solid was taken up in DCM and filtered and washed with cold DCM. Yield: 97%. ¹H NMR (300 MHz, C₂D₆OS) δ 6.77 (d, *J* = 3, 2H), 7.18 (d, *J* = 3, 2H), 7.76 (s, 1H), 8.25 (s, 2H), 9.49 (b, 1H), 9.95 (b, 1H), 10.06 (b, 1H).

1-(4-oxocyclohexa-2,5-dien-1-ylidene)-3-phenylurea (5b). To a 10ml round bottom flask 1-(4-hydroxyphenyl)-3-phenylurea (100 mg, 0.427 mmol), a stir bar and 1mL of acetic acid were charged. The flask was brought to 0°C using an ice bath. To the solution Pb(AcO)₄ (189.32 mg, 0.427 mmol) were added. The solution turns a bright red color. Reaction was let stir and warm up for 10 minutes. Remaining Pb(AcO)₄ was quenched using 5 drops of ethylene glycol. Product was extracted using DCM. Layers were washed with H₂O, bicarb and then brine. DCM was removed under reduced pressure. Yield 85%. ¹H NMR (300 MHz, CDCl₃) δ 1.17 (m, 4H), 1.32 (m, 2H), 1.64 (m, 4H), 1.95 (m, 2H), 3.73 (m, 1H), 5.09 (b, 1H), 6.50 (d-d, *J* = 4, 1H), 6.6 (d-d, *J* = 4, 1H), 7.0 (d-d, *J* = 4, 1H), 7.19 (d-d, *J* = 4, 1H).

Example VL Polymerization Experiment. A 7 mL vial was charged with **5b** (11.6 mg, 0.0499 mmol), benzyl alcohol (2.08 μL, 0.01999 mmol) and acetone-*d*₆ (250 μL). In a second 7 mL vial, VL (0.100 g, 0.999 mmol) was dissolved in acetone-*d*₆ (249 μL). The contents of the second vial were transferred to the first via pipette and stirred until

homogenous. The contents were transferred to an NMR tube via pipette, and the reaction was monitored by ^1H NMR. Reaction progression was monitored for two hours. 0% yield

Example ROP of Lactide. L-lactide (100 mg, 0.69 mmol) and acetone- d_6 (0.345 mL) were added into a 7 mL vial and stirred until a homogenous solution was obtained. To a second 7 mL vial, benzyl alcohol (1.43 μl , 0.014 mmol), **5b** (8.01 mg, 0.035 mmol) and acetone- d_6 (0.345 mL) were added. Contents from the first vial were transferred into vial 2 via Pasteur pipette. The contents were mixed and transferred to an NMR tube. Reaction progression was monitored by ^1H NMR for 2.5 hours. 0% yield

RESULTS AND DISCUSSION

Synthesis of the hydroquinone derivatives were done using 4-aminophenol and an iso(thio)cyanate (Figure 6.2.1-5). 4-aminophenol has two nucleophilic centers, N-H and O-H, but according to Beaver,¹² aryl isocyanates only produce the analogous urea with no formation of the alternative carbamate. All hydroquinone (thio)ureas were synthesized easily and at high yields. The first catalysts synthesized and subjected to subsequent oxidation were urea and thiourea **1** and **2**, to create the bifunctional catalysts **1b** and **2b** (Figure 6.3). Oxidation of these compounds was done using Pb(OAc)₄, and both were fully oxidized within minutes. Isolation of the oxidized species was done with a DCM/H₂O extraction. However, upon isolation of the species by the removal of solvent, both decomposed under atmospheric and inert conditions. ¹H NMR analysis of **2b** under N₂ decomposition of product within 24hrs (Figure 6.4). A switch in color for both **1b** and **2b** from the initial bright red crystals to brown and black crystals also suggests decomposition. This is not surprising given previous reports of acyl substituted quinoidal species described as very reactive and susceptible to nucleophilic attack.^{13,14} Decomposition of the oxidized products, **1b** and **2b**, could be due to similar reactions arising from the highly electron withdrawing character of the trifluoromethyl substituted aryl ring. In response to this hypothesis, two new urea-based catalysts with less electron withdrawing character were synthesized (Figure 6.3.3b and 4b). **3b** containing a 3,5-(dimethoxy)phenyl and **4b** with an un-substituted phenyl. Oxidation and workup for these ureas was performed in the same manner as previously described. Upon isolation of the two oxidized catalysts, both decomposed again. Again, this is apparent in the ¹H NMR of **4b** (Figure 6.5), and a change in crystal color was obtained for both **3b** and **4b**. Due to the

decomposition present in all catalyst species bearing an aryl ring regardless of substitution, a catalyst bearing a cyclohexyl ring was synthesized (Figure 6.2.5). After oxidation and workup, this catalyst species (Figure 6.3.5b) did not decompose under inert conditions and was subsequently used for polymerization reactions.

The ROP of L-LA (100 mg, 0.69 mmol) was conducted at 1M (acetone- d_6 or $CDCl_3$) catalyzed by **5b** (8.01 mg, 0.0345 mmol) and with benzyl alcohol (1.43 μ L, 0.0138 mmol) initiator. The reactions were monitored using 1H NMR. After several hours, both reactions did not produce any conversion to polymer (Table 6.1). Due to the sensitivity of the other catalyst species resulting in decomposition, it could be assumed that polymerization conditions could induce decomposition of the catalyst species rendering the catalyst inactive. However, upon analysis of the polymerization 1H spectra, no evidence of catalyst decomposition was present (Figure 6.6).

The ROP of δ -valerolactone was conducted at 2M (C_6D_6 , $CDCl_3$, acetone- d_6) catalyzed by **5b** (11.6 mg, 0.0499 mmol) and initiated from benzyl alcohol (2.07 μ L, 0.0199 mmol). After several hours of monitoring the reaction using 1H NMR, again no conversion of monomer was observed (Table. 6.1).

The conversion of monomer to polymer in organocatalytic polymerization is due to the activation of both the monomer and initiator/chain end using a catalyst (dual or bifunctional), without these species, conversion does not happen.⁴ The lack of turnover of either δ -VL or L-LA found for **5b**, suggests such weaknesses could be present. A series of 1H binding experiments were conducted to evaluate the extent of interaction between **5b** and both δ -VL (Figure 6.7) and benzyl alcohol (Figure 6.8). To evaluate activation of monomer, **5b** and VL (both 50mM in C_6D_6) were compared to a reference 1H NMR only

containing **5b** at 50mM. A 0.1ppm shift downfield in the N-H resonance of **5b** with the addition of VL indicates only slight interaction between the two components. An even smaller upfield shift of 0.3 ppm was observed for the aromatic protons of **5b** with the addition of benzyl alcohol. In addition, the O-H resonance had 0.04 ppm shift downfield with the addition of **5b** relative to the reference. These small changes in the ¹H NMR resonances suggests minimal binding between **5b** and both monomer and alcohol/chain end, which is likely the reason for the inactivity of the catalytic species. In contrast, the treatment of **1-S** with an equivalent of VL produces 1.5 and 2.0 ppm downfield shifts of the two N-H resonances.¹

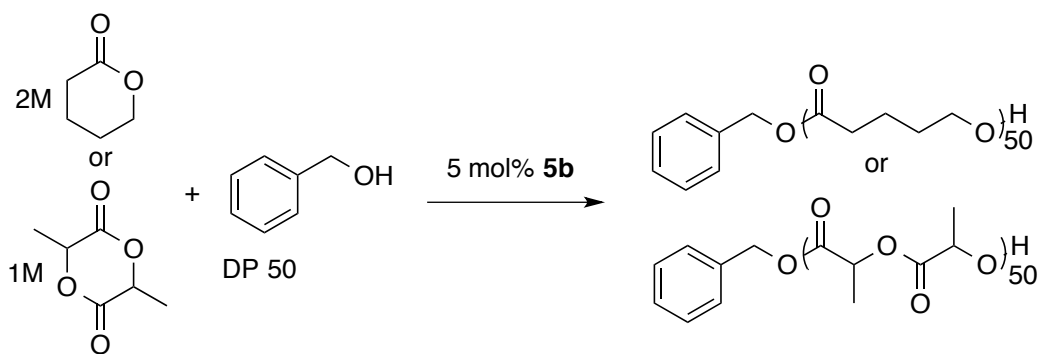
CONCLUSION

The quinoidal bifunctional catalyst species, **5b**, was inactive for the ROP of both L-LA and δ -valerolactone. This is likely a result of minimal binding interaction between the catalyst and both monomer and alcohol/chain end, which was shown through multiple binding experiments between the species. The lack of activity when compared to the highly active imidate or guanidine base TBD represents the importance of binding interactions for ROP. The absence of binding interactions for **5b** are likely due to the substituents on either side of the urea moiety. Without the strong electron withdrawing group found in the **1b** or **2b** substituted structure, the ability of H-bonding for **5b** to a monomer is hindered. Attempts at synthesizing a more active quinoidal catalyst remains difficult given the decomposition observed with those bearing aromatic groups. However, an electron deficient alkyl chain could be created potentially circumventing this problem. The quinoidal substituted side also lacks the ability to accept an H-bond, which could be due to the electron density of the quinone group moving away from the nitrogen, rendering the basic nitrogen weaker. TBD on the other hand has a much more basic nitrogen with perhaps just enough H-bonding characteristic to be capable of ROP which is likely the reason for its high activity and its low controllability. The imidate catalyst, **b** (Figure 6.1), formed from a proton transfer is active to H-bonding due to the electron withdrawing aryl ring and strong basic character to accept an H-bond due to the negative charge of the imidate itself. While it is possible the quinone derived catalyst species could be active for ROP, the current scaffolds lack the capabilities. Further work within this avenue could produce active catalysts that are highly active and controlled.

LIST OF REFERENCES

- (1) Lohmeijer, B. G. G.; Pratt, R. C.; Leibfarth, F.; Logan, J. W.; Long, D. A.; Dove, A. P.; Nederberg, F.; Choi, J.; Wade, C.; Waymouth, R. M.; Hedrick, J. L. *Macromolecules* **2006**, *39* (25), 8574–8583.
- (2) Dharmaratne, N. U.; Pothupitiya, J. U.; Bannin, T. J.; Kazakov, O. I.; Kiesewetter, M. K. *ACS Macro Lett.* **2017**, *6* (4), 421–425.
- (3) Fastnacht, K. V.; Spink, S. S.; Dharmaratne, N. U.; Pothupitiya, J. U.; Datta, P. P.; Kiesewetter, E. T.; Kiesewetter, M. K. *ACS Macro Lett.* **2016**, *5* (8), 982–986.
- (4) Dove, A. P.; Pratt, R. C.; Lohmeijer, B. G. G.; Waymouth, R. M.; Hedrick, J. L. *J. Am. Chem. Soc.* **2005**, *127* (40), 13798–13799.
- (5) He, X.; Ji, Y.; Jin, Y.; Kan, S.; Xia, H.; Chen, J.; Liang, B.; Wu, H.; Guo, K.; Li, Z. *J. Polym. Sci. Part A Polym. Chem.* **2014**, *52* (7), 1009–1019.
- (6) Delcroix, D.; Couffin, A.; Susperregui, N.; Navarro, C.; Maron, L.; Martin-Vaca, B.; Bourissou, D. *Polym. Chem.* **2011**, *2* (10), 2249–2256.
- (7) Rostami, A.; Sadeh, E.; Ahmadi, S. *J. Polym. Sci. Part A Polym. Chem.* **2017**, 1–11.
- (8) Pratt, R. C.; Lohmeijer, B. G. G.; Long, D. A.; Waymouth, R. M.; Hedrick, J. L. *J. Am. Chem. Soc.* **2006**, *128* (14), 4556–4557.
- (9) Lin, B.; Waymouth, R. M. *J. Am. Chem. Soc.* **2017**, *139* (4), 1645–1652.
- (10) Lin, B.; Waymouth, R. M. *Macromolecules* **2018**, *51* (8), 2932–2938.
- (11) Pothupitiya, J. U.; Hewawasam, R. S.; Kiesewetter, M. K. *Macromolecules* **2018**, No. 51, 3203–3211.
- (12) Beaver, D. J.; Roman, D. P.; Stoffel, P. J. *J. Med. Chem.* **1963**, *6* (5), 501–506.

- (13) Trettin, A.; Batkai, S.; Thum, T.; Jordan, J.; Tsikas, D. *J. Chromatogr. B Anal. Technol. Biomed. Life Sci.* **2014**, *963*, 99–105.
- (14) Avdeenko, A. P.; Konovalova, S. A.; Sergeeva, A. G.; Zubatyuk, R. I.; Palamarchuk, G. V.; Shishkin, O. V. *Russ. J. Org. Chem.* **2008**, *44* (12), 1765–1772.



Monomer	Solvent	Time (hrs)	Conversion ^a
δ -VL	C_6D_6	24	None
δ -VL	CDCl_3	2	None
δ -VL	Acetone- d_6	2	None
LA	CDCl_3	5	None
LA	Acetone- d_6	2.5	None

Table 6.1. Table shows the results of various polymerization attempts using **5b** for δ -VL and L-LA. a. Determined with ^1H NMR.

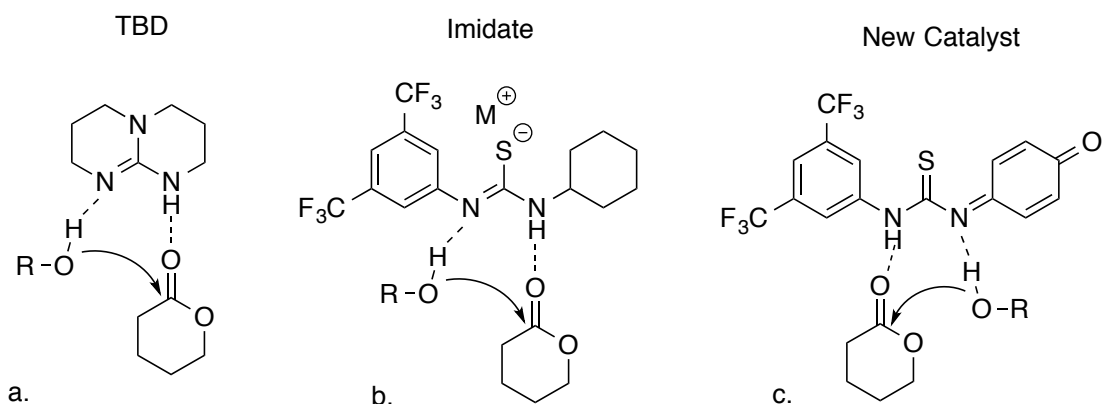


Figure 6.1. Bifunctional catalysts a and b have both been employed for the ROP of cyclic esters. Catalyst c is proposed to be active for the ROP of cyclic esters.

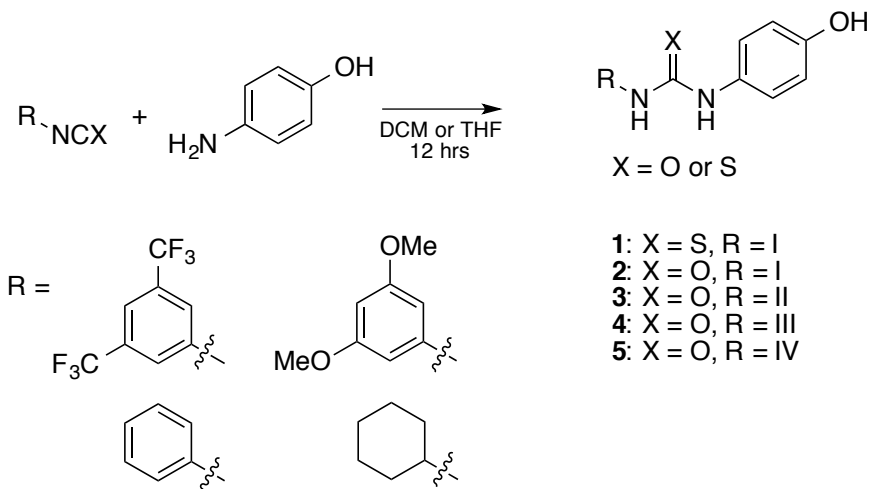


Figure 6.2. Synthesis of hydroquinone derived compounds through click style reaction between 4-aminophenol and the corresponding iso(thio)cyanate.

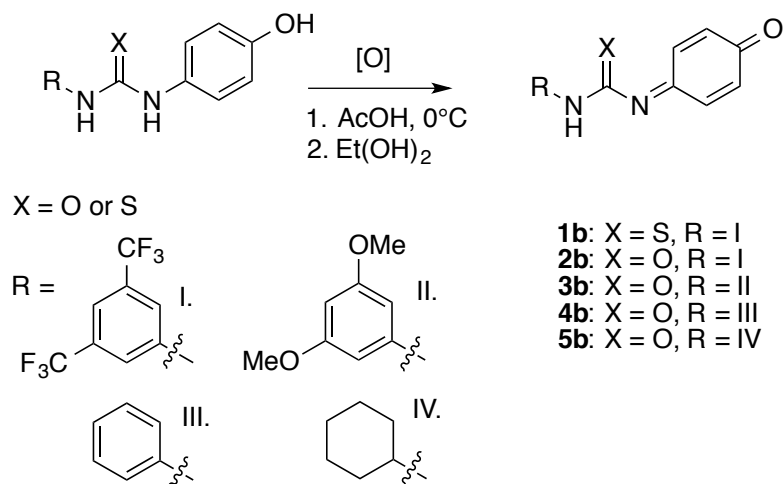


Figure 6.3. Oxidation of hydroquinone species was done in acetic acid as solvent at 0°C and quenched using Et(OH)₂.

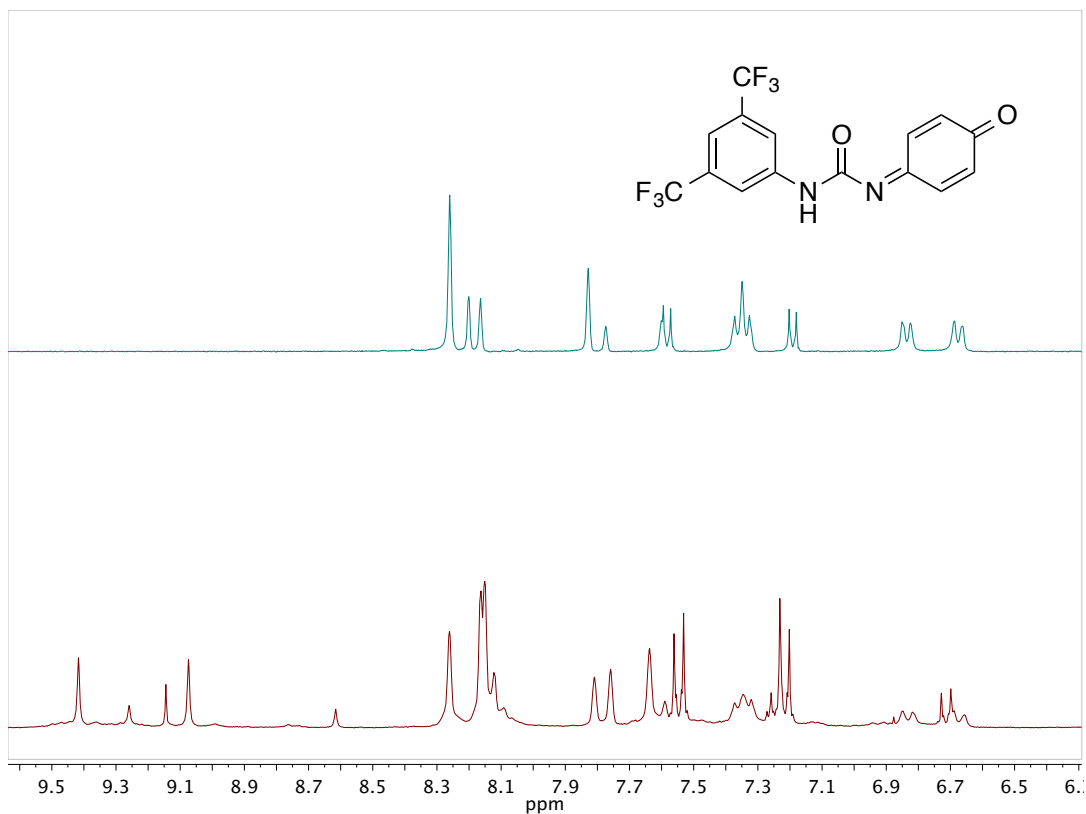


Figure 6.4. Decomposition of **2b**. Top spectra shows the ¹H NMR of the isolated product and the bottom spectra is the same product after 24 hrs.

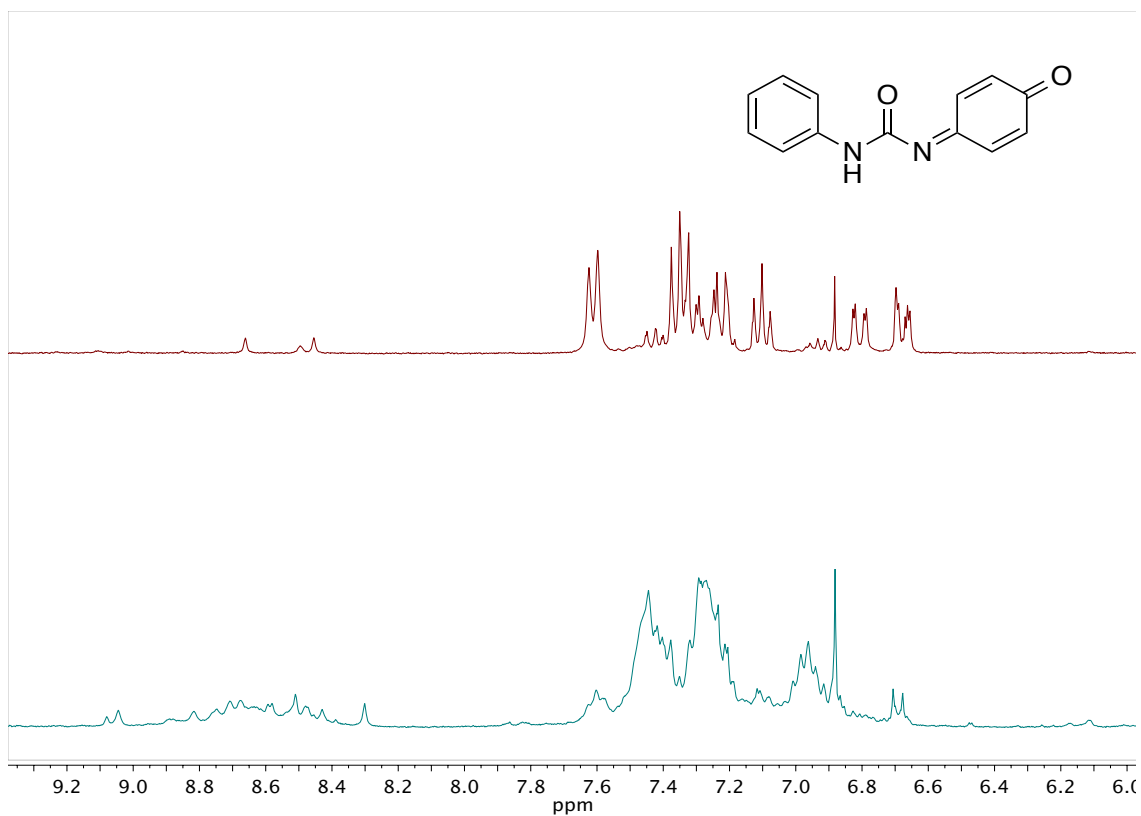


Figure 6.5. Decomposition of **4b**. Top spectra shows isolated product, bottom spectra shows the same product after 24 hrs.

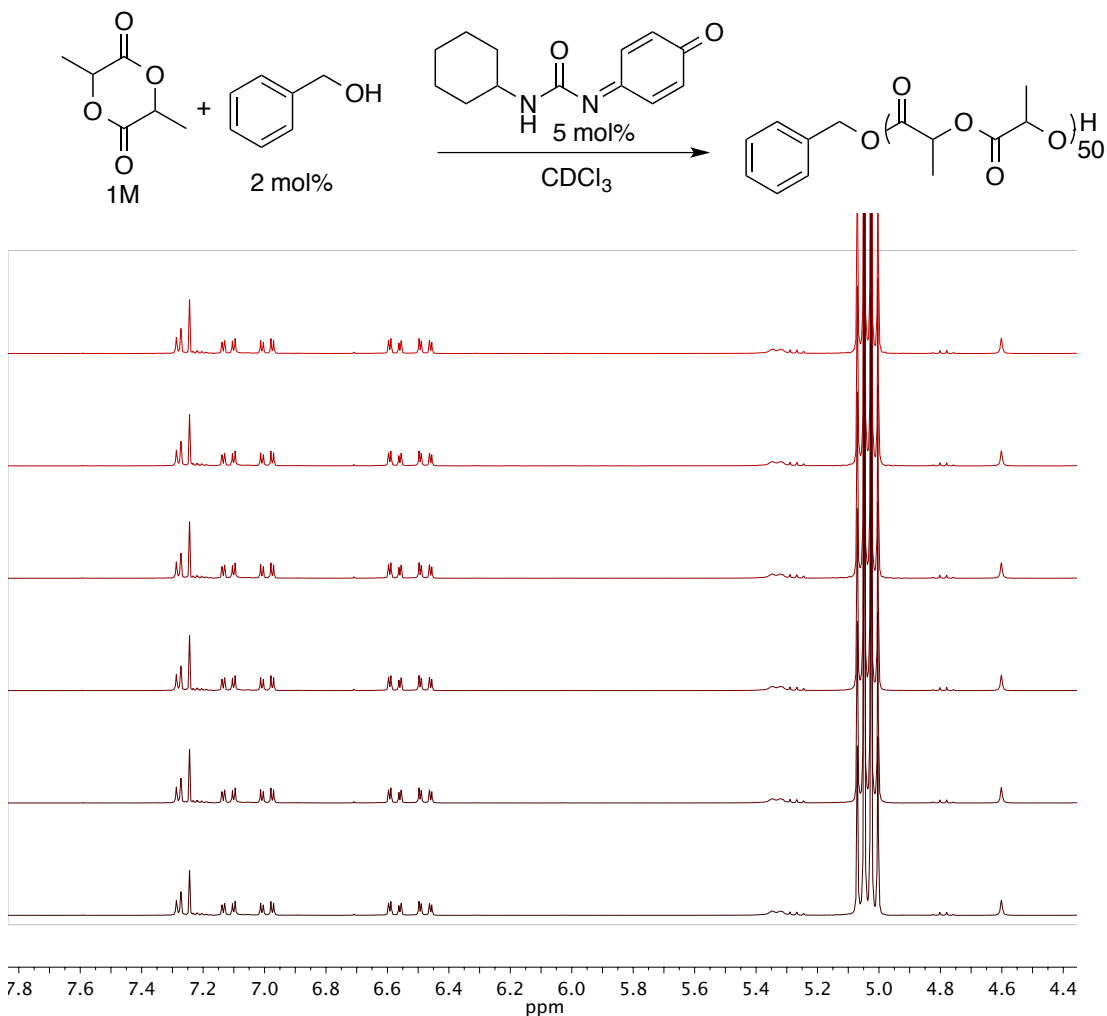


Figure 6.6. ¹H NMR spectra taken for the polymerization of L-LA by **5b**. Chronological order from bottom to top. Last spectra taken at 5 hours of reaction time. The triplet resonance at 5.1ppm represents the methine proton of the monomer. Aromatic quinone remain sharp and no indication of decomposition.

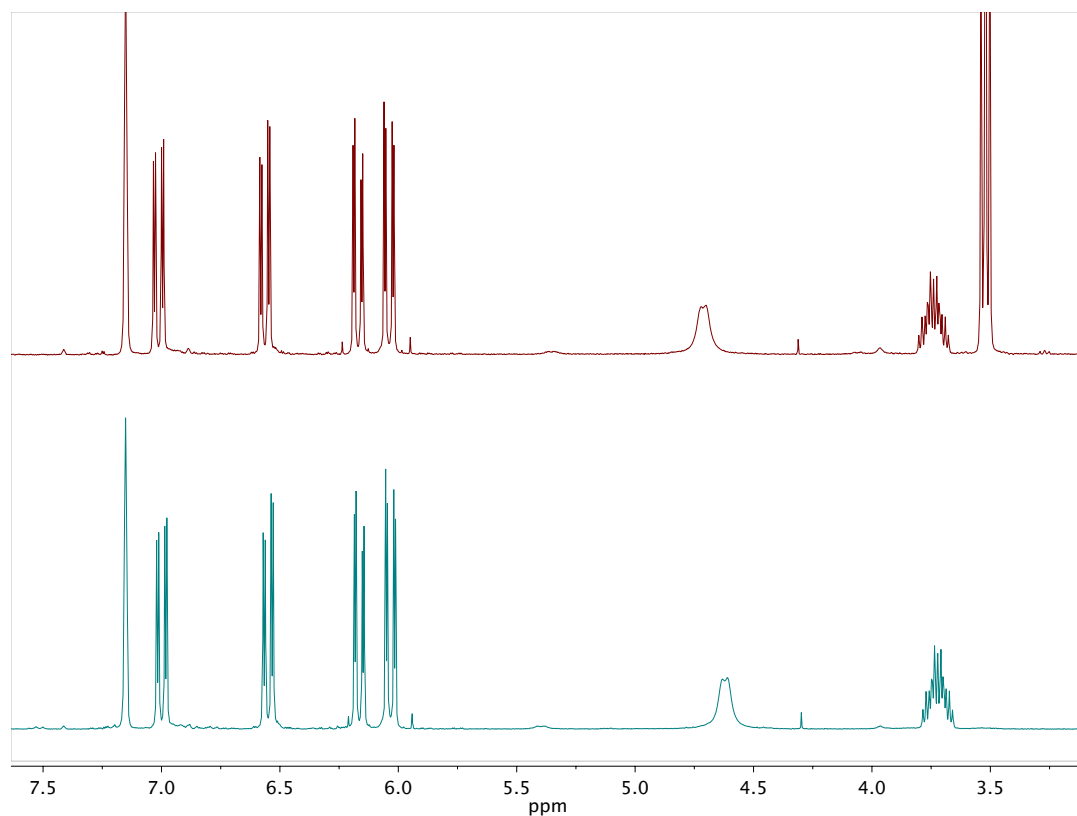
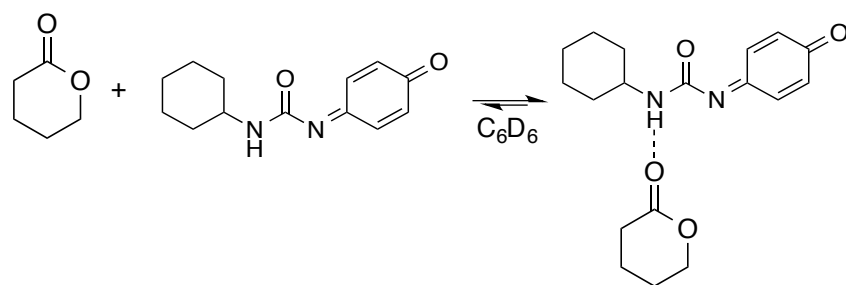


Figure 6.7. 1H NMR (400 MHz, C_6D_6) analysis of binding interaction between **5b** and VL. Top spectra contains both **5b** and VL (50mM each), bottom image is **5b** alone (50mM). A 0.1 ppm shift downfield of the N-H resonance of **5b** with the introduction of VL from 4.62 to 4.72 ppm.

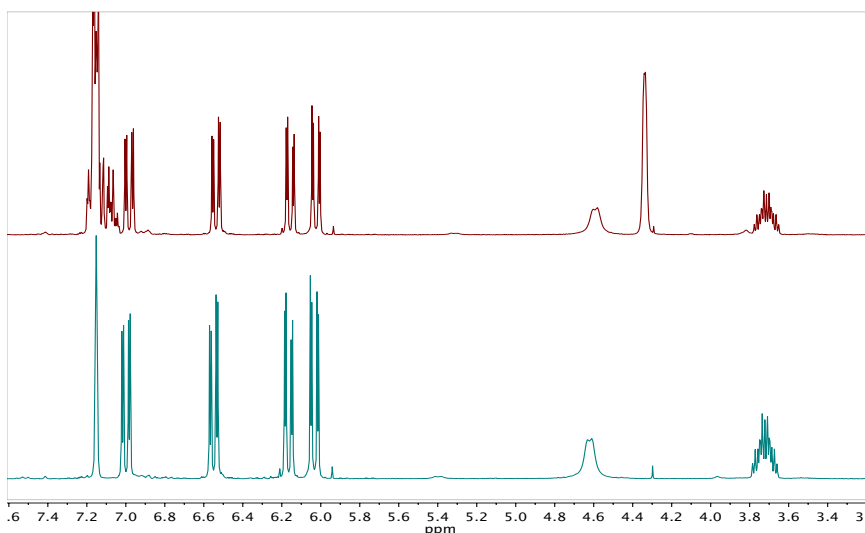
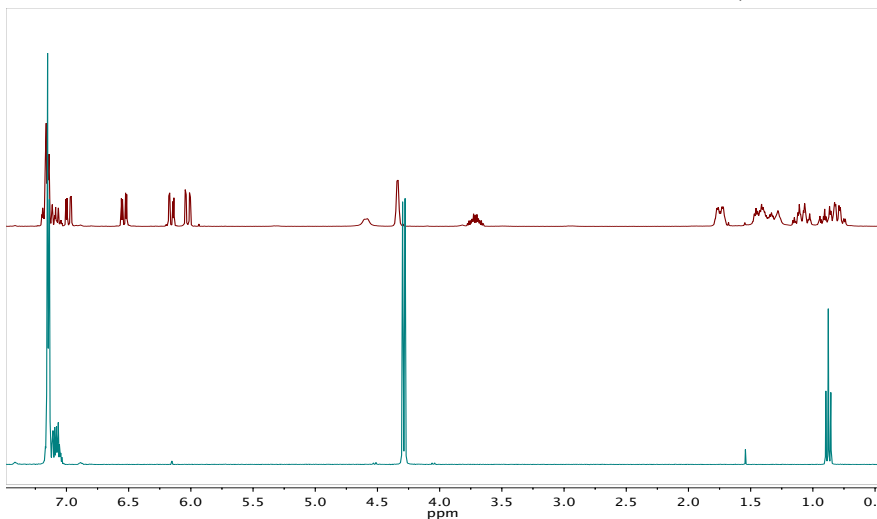
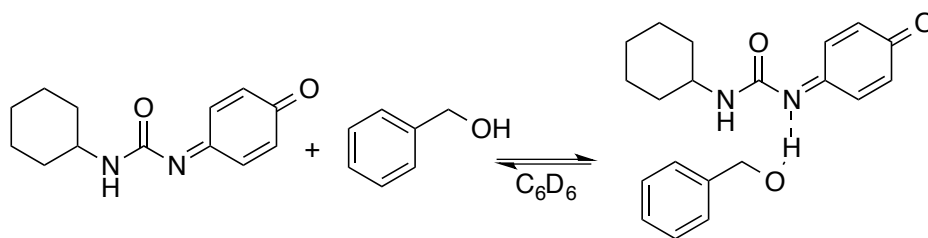


Figure 6.8. Both images show 1H NMR (400 MHz, C_6D_6) analysis of binding interaction between **5b** and BnOH (**5b** and benzyl alcohol at 50 mM each). Top stacked image shows **5b** and benzyl alcohol (top spectra) with a benzyl alcohol reference beneath. A 0.04 ppm shift downfield of the O-H resonance with the addition of **5b** is seen. Bottom image contains both **5b** and BnOH (top spectra), with a **5b** reference underneath. A 0.03 ppm shift downfield of the aromatic resonances of **5b** with the introduction of BnOH is seen.

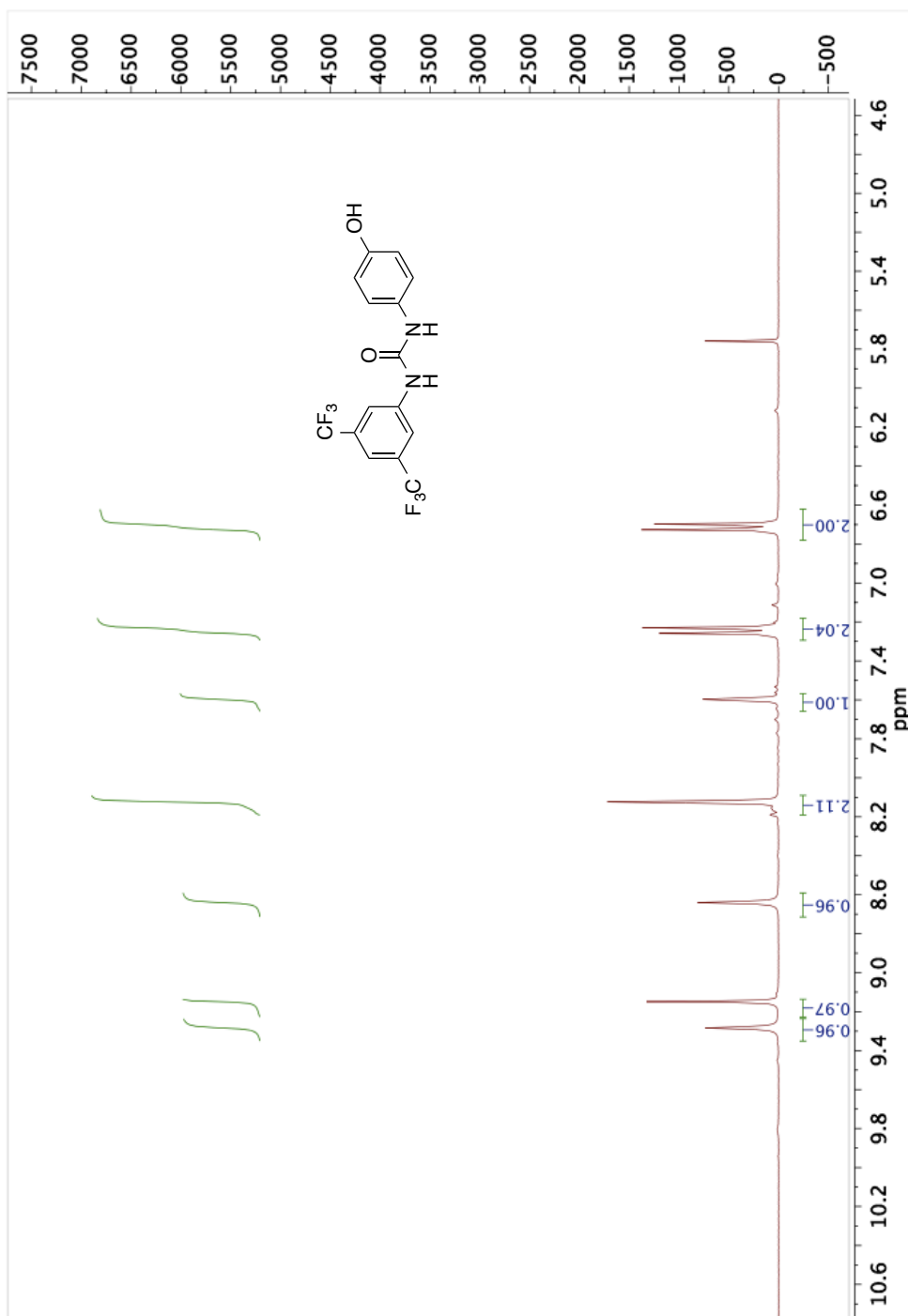


Figure 6.9. ^1H NMR (300 MHz, $\text{DMSO-}d_6$) of **2**.

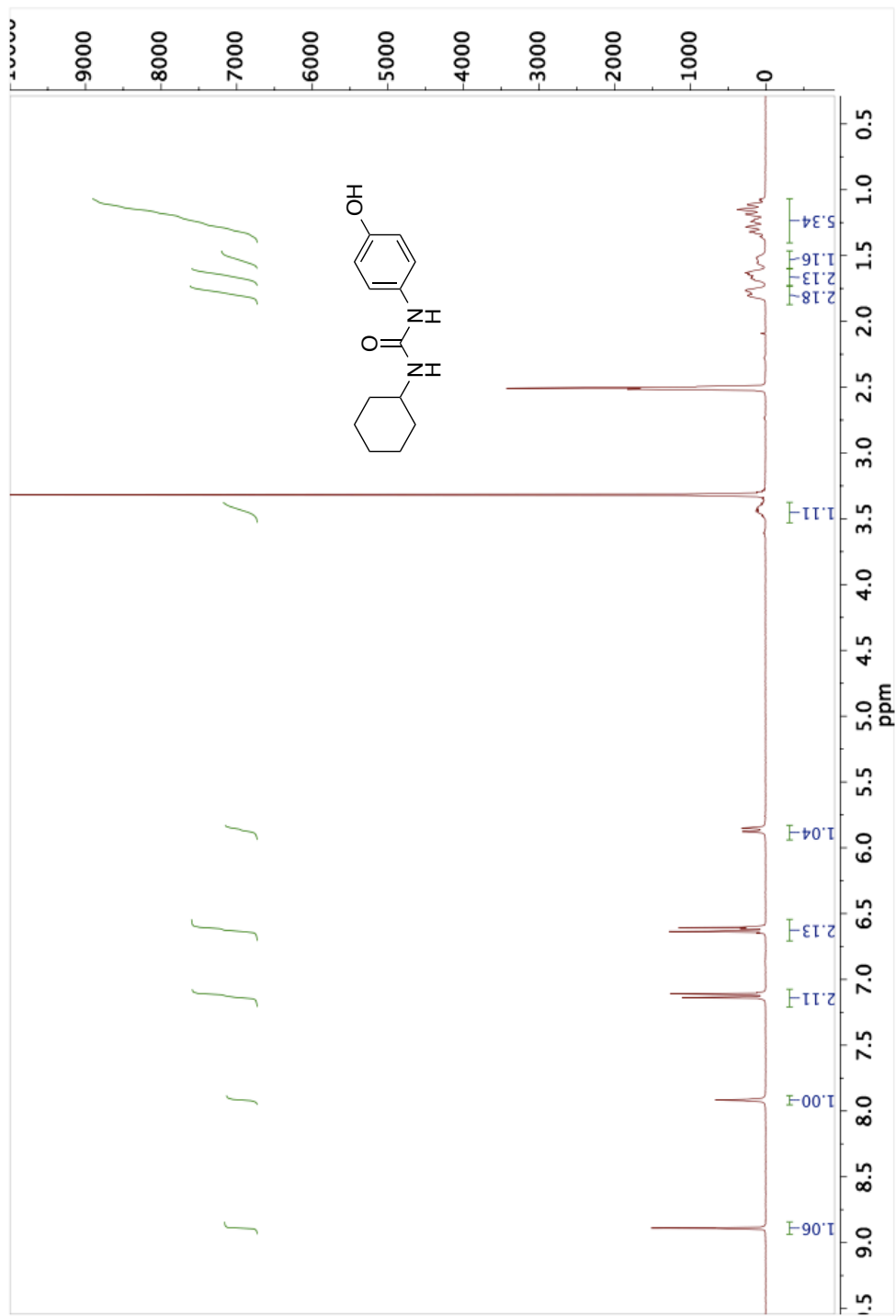


Figure 6.10. ^1H NMR (300 MHz, DMSO-d_6) of **5**.

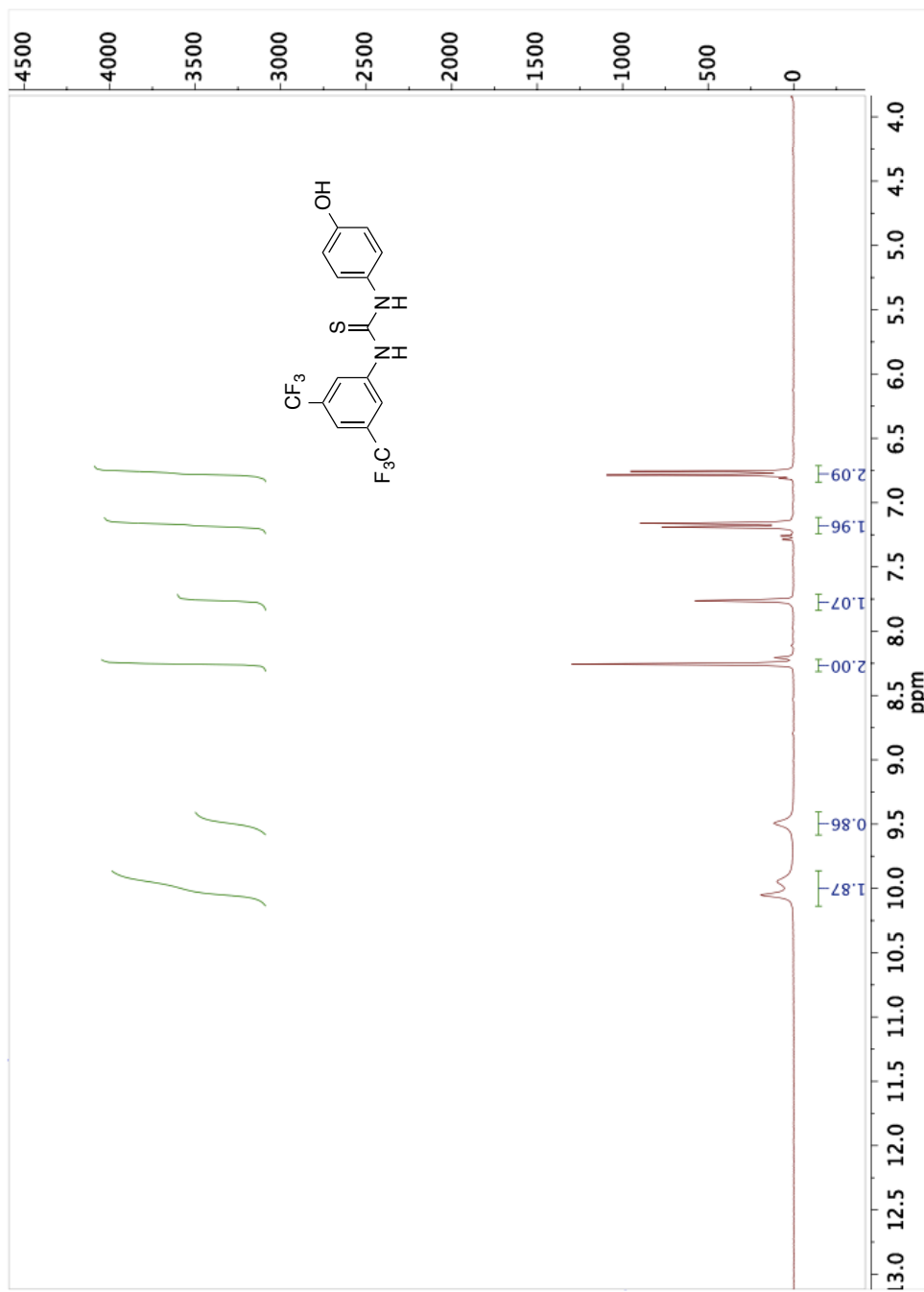


Figure 6.11. ^1H NMR (300 MHz, DMSO-d_6) of **1**.

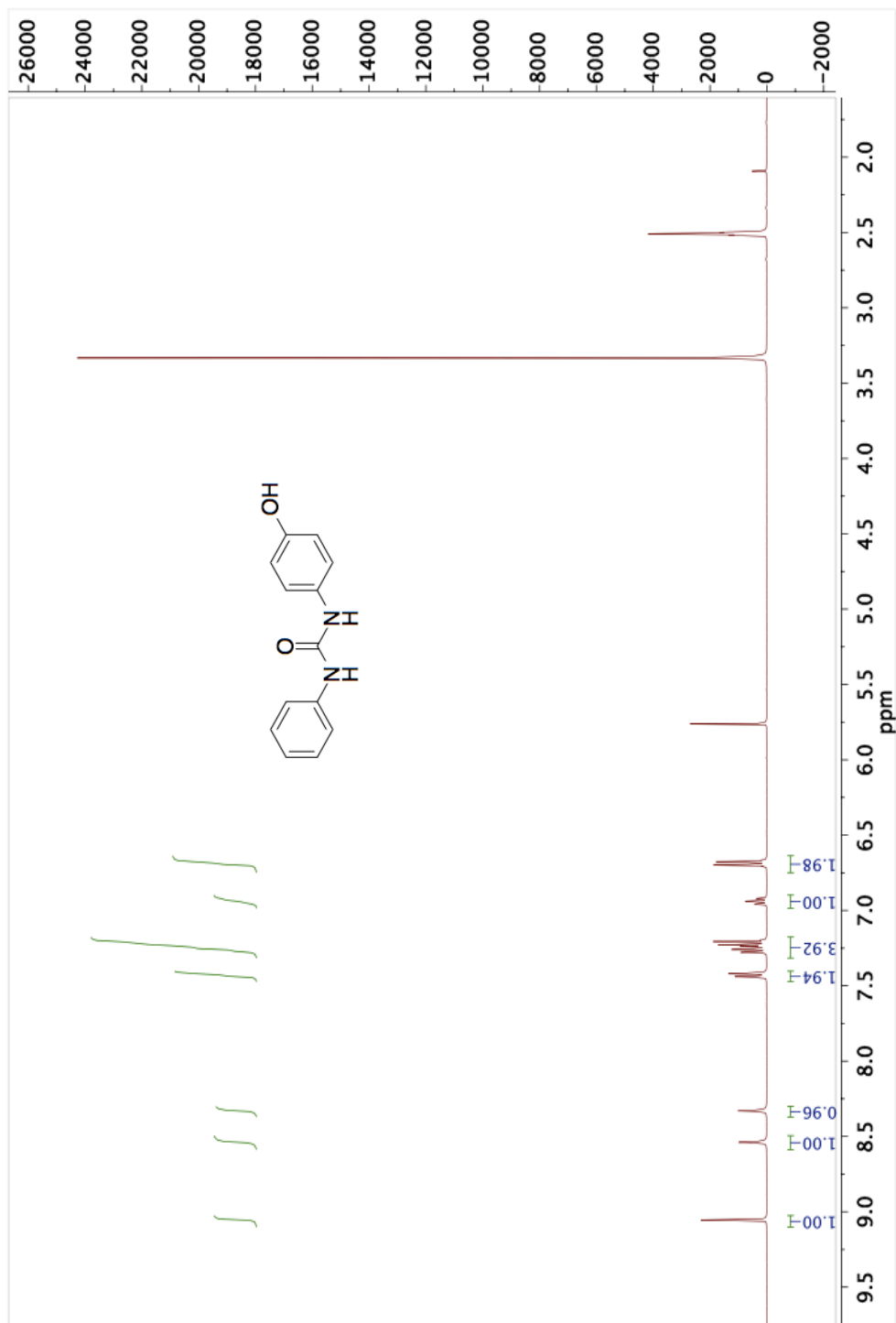


Figure 6.12. ^1H NMR (300 MHz, DMSO-d_6) of **4**.

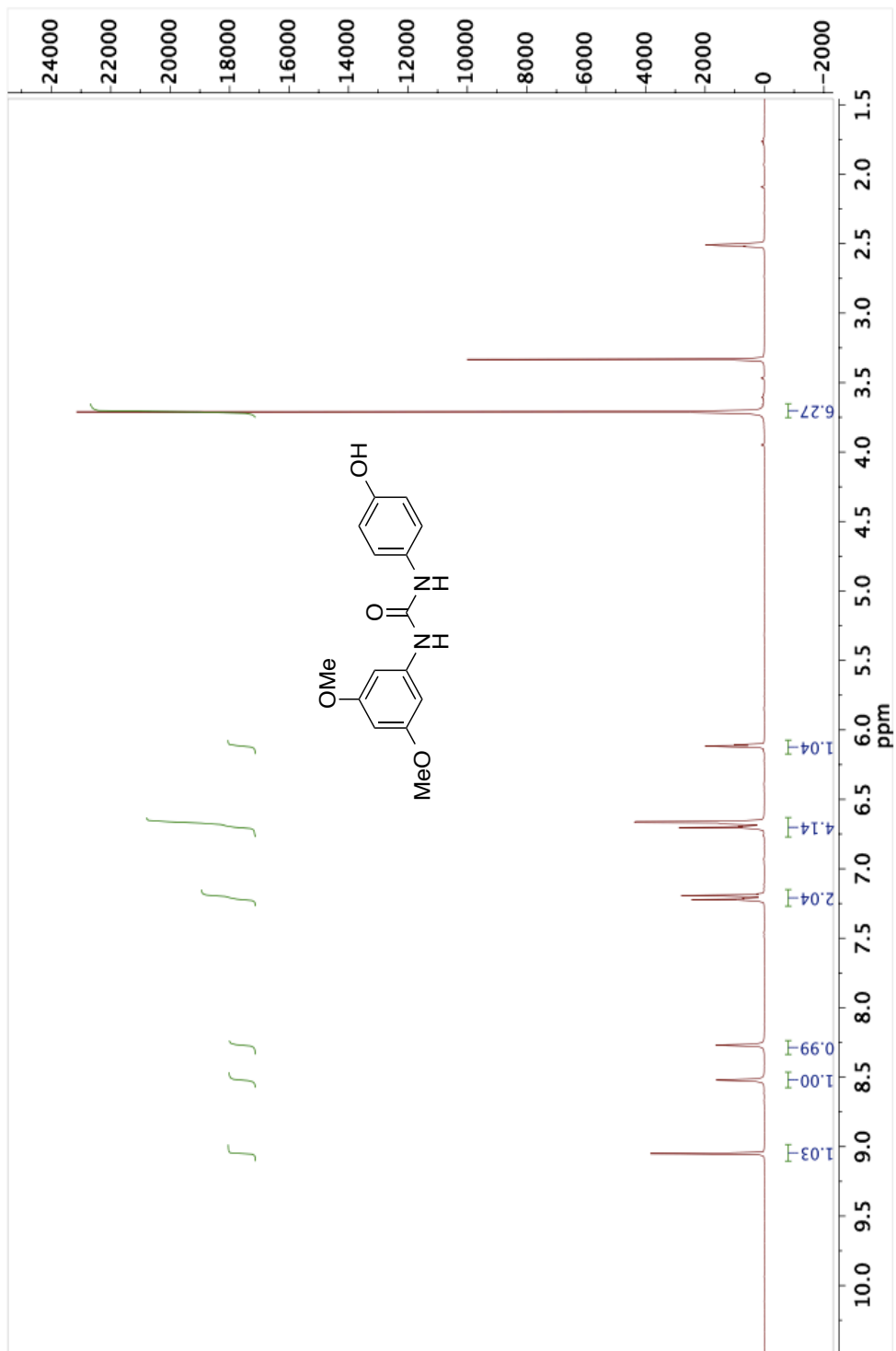


Figure 6.13. ^1H NMR (300 MHz, DMSO-d_6) of **3**.

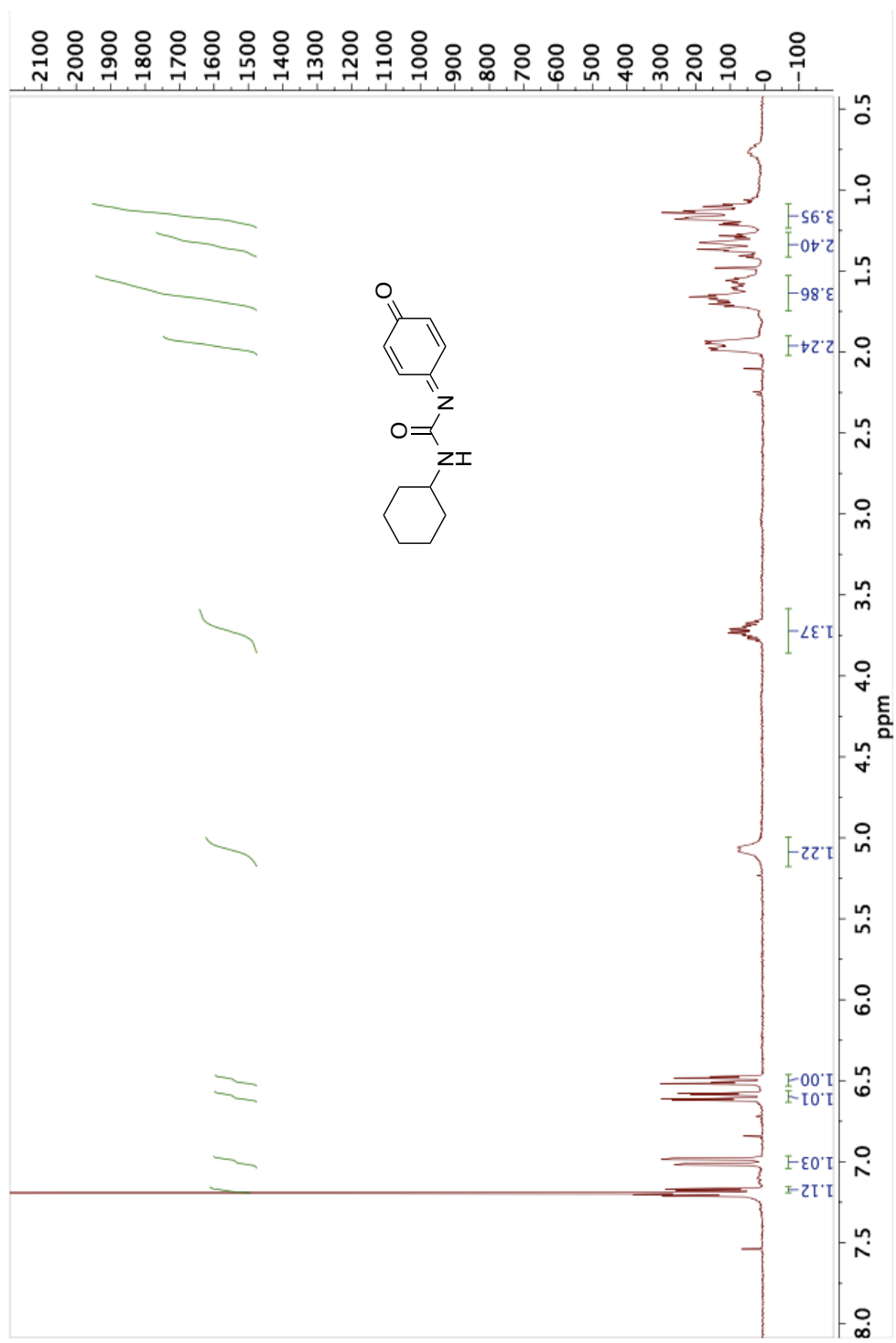


Figure 6.14. ^1H NMR (300 MHz, DMSO-d_6) of **5b**.

INTENTIONALLY BLANK PAGE

MANUSCRIPT – VII

Unpublished Results

Investigations into the Ring-Opening Polymerization of Aliphatic Lactones

Kurt V. Fastnacht, Danielle Coderre, Thomas Wright and Matthew K. Kiesewetter

Chemistry, University of Rhode Island, Kingston, RI, USA

Corresponding Author: Matthew Kiesewetter, Ph.D.

Chemistry

University of Rhode Island

140 Flagg Road

Kingston, RI, 02881, USA

Email address: mkiesewetter@uri.edu

ABSTRACT

H-bonding urea or thiourea catalyst paired with a base cocatalyst have been employed for organocatalytic ring-opening polymerization (ROP) of aliphatic lactones (TOSUO, 4-MCL, 3,5-MCL and 6-MCL). 3,5-MCL and 6-MCL are mixtures of the methyl substituted regio isomers of 3 and 5-MCL and 2 and 6-MCL. Monomers were used after purification as a mixture of regioisomers. ROP were run at 2M monomer (benzene- d_6 or H_6 or acetone- d_6 or H_6) catalyzed by an H-bond donor (**1-S** or TCC at 5 mol %, **2-S** at 2.5 mol% or **3-O** at 1.67 mol%) and cocatalyst base (matched to H-bond donor mol%) initiated from benzyl alcohol (2 mol%). The reaction rates were fast, while remaining well controlled, with predictable M_n from $[M]_0/[I]_0$ and low molecular weight distributions ($M_w/M_n < 1.13$). 6-MCL only produced polymer with increased catalyst loadings. Low rates and control resulted for the polymerization of 6-MCL. Variation of the substituent along with its position on the monomer resulted in different reaction rates. The relative rates of ROP for functionalized ϵ -caprolactone (4-MCL, 3,5-MCL, 6-MCL, and TOSUO) by H-bonding organic catalysts have been evaluated and a mechanistic reasoning discussed. Random copolymers with low dispersities were synthesized. A series of copolymers of CL and 3,5-MCL were produced and evaluated using TGA and DSC.

INTRODUCTION

The production of aliphatic polyesters are of interest due to their biodegradability and biocompatibility for potential applications within the medical¹⁻⁴ and material fields.⁵⁻⁷ These materials are typically synthesized through polycondensation reactions, but the need for more controlled reactions has led to the ring-opening polymerization (ROP) of cyclic esters using metal catalysts. These catalysts have shown good control over molecular weight (M_n) and molecular weight distribution (M_w/M_n). For example, Breteler, using a chiral salen AlO*i*Pr complex was able to produce P-6-MCL with M_w/M_n of 1.04.⁸ The polymerization of other methyl substituted ϵ -caprolactones (ϵ -CL) have been identified as well, with moderate control over M_w/M_n (1.12 – 2.8).⁸⁻¹⁵ In an effort to avoid metal catalysts, some have resorted to enzymatic catalysts for ROP of cyclic esters.¹⁶⁻²² Enzymatic catalysts however, are plagued by poor solubility, long reaction times and low conversions. Several lipases have been employed for the polymerization of the aliphatic monomer 4-MCL in the monomer bulk at 60°C,²³ but were slow and did not yield high conversions (< 35% conversion after 10 days). 1,4,8-trioaspiro[4.6]-9-undecanone (TOSUO) has also been evaluated using metal catalysts.²⁴⁻²⁸ TOSUO is of particular interest due to the ease of post polymerization modification due to the ketal component within the backbone.

As an alternative to metal and enzymatic catalysts, the ROP of aliphatic lactones using H-bond donating (thio)urea catalysts has the potential to be fast, controlled and free of metal contamination. Here in, we report on the (co)polymerizations of TOSUO and methyl functionalized ϵ -caprolactone monomers (4-MCL, 3,5-MCL and 6-MCL) using H-bond donating (thio)ureas and base cocatalysts.

EXPERIMENTAL SECTION

General Considerations. All manipulations were performed in an MBRAUN stainless steel glovebox equipped with a gas purification system or using schlenk technique under a nitrogen atmosphere. All chemicals were purchased from Fisher Scientific and used as received unless stated otherwise. Tetrahydrofuran and dichloromethane were dried on an Innovative Technologies solvent purification system with alumina columns and nitrogen working gas. Benzene- d_6 and acetone- d_6 were purchased from Cambridge Isotope Laboratories and distilled from CaH_2 under a nitrogen atmosphere. ϵ -caprolactone (CL; 99%) and benzyl alcohol were distilled from CaH_2 under reduced pressure. 4-methylcyclohexanone was purchased from Frontier Scientific. 3-methylcyclohexanone, 7-methyl-1,5,7-triazabicyclo[4,4,0]dec-5-ene (MTBD), 1,5,7-triazabicyclo[4.4.0]dec-5-ene (TBD), 3,4,4'-trichlorocarbanilide (TCC) and 1,8-diazabicyclo[5.4.0]undec-7-ene (DBU) were purchased from TCI. 2-*tert*-butylimino-2-diethylamino-1,3-dimethylperhydro-1,3,2-diazaphosphorine (BEMP) was purchased from Acros. The H-bond donors **1-S**, **2-S** and **3-O** were prepared according to published procedures.²⁹ Monomers were synthesized according to published procedures.^{10,30} NMR spectra were performed on Bruker Avance III 300 MHz or 400 MHz spectrometers. Size exclusion chromatography (SEC) was performed at 40 °C using dichloromethane eluent on an Agilent Infinity GPC system equipped with three Agilent PLGel columns 7.5 mm \times 300 mm (5 μm , pore sizes: 50, 10³, 10⁴ Å). M_n and M_w/M_n were determined versus PS standards (162 g/mol-526 kg/mol, Polymer Laboratories).

Example 3,5-MCL Polymerization Experiment. A 7 mL vial was charged with **3-O** (14.2 mg, 0.0155 mmol), MTBD (2.34 mg, 0.0155 mmol), benzyl alcohol (1.98 mg,

0.0187 mmol) and C_6D_6 (234 μ L). In a second 7 mL vial, 3,5-MCL (0.120 g, 0.936 mmol) was dissolved in C_6D_6 (234 μ L). The contents of the second vial were transferred to the first via pipette and stirred until homogenous, approximately 10 seconds. The contents were transferred to an NMR tube via pipette, and the reaction was monitored by 1H NMR. The reaction was quenched using benzoic acid (11.4 mg, 0.0936 mmol). Polymer was precipitated with the addition of hexanes. Supernatant was decanted and solid P-3-MCL and 5 was dried in vacuo. Yield: 98%, $M_n = 11,000$, $M_w/M_n = 1.13$.

Example Copolymerization Experiment. A 7 mL vial was charged with **3-O** (15.1 mg, 0.0166 mmol), MTBD (2.45 mg, 0.0166 mmol), benzyl alcohol (2.18 mg, 0.0200 mmol) and C_6D_6 (250 μ L). In a second 7 mL vial, TOSUO (86 mg, 0.500 mmol) and CL (57 mg, 0.500 mmol) were dissolved in C_6D_6 (250 μ L). The contents of vial 2 were transferred to the first via pipette and stirred until homogenous, approximately 5 seconds. The contents were transferred to an NMR tube via pipette, and the reaction was monitored by 1H NMR. The reaction was quenched using benzoic acid (12.1 mg, 0.100 mmol). Polymer was precipitated with the addition of hexanes. Supernatant was decanted and solid polymer was dried in vacuo, 97% yield $M_n = 7,300$, $M_w/M_n = 1.09$.

RESULTS AND DISCUSSION

Monomer synthesis was done using published procedures.^{9,22,31} The regioselectivity of the oxidation reaction is dictated by the stability of the expanding ring transition state.³¹ This produces a ratio of regio-isomers from 2 and 3-methylcyclohexanone of approximately 9:1 for 6-MCL:2-MCL and 1:1 for 5-MCL:3-MCL. 2 and 6-MCL will be referred to as 6-MCL due to the mixture being predominately 6-MCL. For added confusion, 3 and 5-MCL mixtures will be referred to as 3,5-MCL (Figure 7.1). The oxidation of 4-methylcyclohexanone only gives a single regio-isomer. The ratios obtained for each monomer were determined via ¹H NMR and are in agreement with other reports.^{9,22,31} Monomers were used after purification as a mixture of regioisomers. Conversions discussed below are of the total monomer concentration; the regioisomers could not be resolved during ROP (Figure 7.2).

The ROP of functionalized ϵ -caprolactones (TOSUO, 4-MCL, 6-MCL and 3,5-MCL) were screened with various H-bond donors and base cocatalysts (Figure 7.1). Reaction progression was monitored using ¹H NMR and quenched with solutions of benzoic acid in DCM. ROP were run at 2M monomer (benzene-*d*₆ or H₆ or acetone-*d*₆ or H₆) catalyzed by an H-bond donor (**1-S** or TCC at 5, **2-S** at 2.5 or **3-O** at 1.67 mol%) and cocatalyst base (matched to H-bond donor mol%) and initiated from benzyl alcohol (2 mol%). All polymerizations show a first order consumption of monomer (Figures 7.3-11). Resulting polymers were analyzed for molecular weights using gel permeation chromatography.

The ROP of TOSUO was conducted using a series of H-bond donating catalysts in benzene. All catalysts examined produced PTOSUO within 24hrs with high

conversions, while still remaining well controlled (Table 7.1). The fastest of which, **3-O**/BEMP, produced P-TOSUO to 97% conversion in just 3 minutes, while remaining well controlled ($M_n = 9300$ g/mol, $M_w/M_n = 1.07$). **3-O** was evaluated with two other strong bases, DBU and MTBD. However, both displayed reduced activity relative to BEMP (Table 7.1, entries 4 & 7). Interestingly, the rate of ROP of TOSUO by **3-O**/MTBD is comparable to that of the un-functionalized CL (Table 7.1, entries 1 & 4).²⁹ Previous reports for the ROP of lactones have suggested enhanced kinetics when prepared in polar solvent.³² As an alternative solvent, acetone was evaluated for the cocatalyst pair **3-O**/MTBD. The ROP resulted in a decrease in reaction time from 30 to 18 minutes, while remaining moderately controlled (Table 7.1, entry 8). In polar solvents (thio)ureas favor formation of an imidate species via proton transfer from (thio)urea to base. The increase in reaction kinetics is attributed to the more active imidate species (Figure 7.12).³²⁻³⁴ A comparative run of TOSUO catalyzed by TBD was completed in 146 minutes but is considerably less controlled (Table 7.1, entry 9). The ROP of TOSUO with $AlOiPr$ complexes result in reduced rates and control.²⁴⁻²⁸ Reaction times are typically hours long with M_w/M_n values > 1.2 .

The ROP of methyl substituted ϵ -CL (3,5-MCL, 6-MCL and 4-MCL) monomers were also studied. The first of which, 3,5-MCL, was subjected to the same H-bond donor screen in benzene, but only with MTBD as base cocatalyst. The **3-O**/MTBD cocatalyst pair produced the fastest conversion with 98% in 180 minutes (Table 7.1, entry 12). The ROP of 3,5-MCL shows less control for all H-bond donors when compared to both ϵ -CL and TOSUO. Interestingly, the most active cocatalyst pair, **3-O**/MTBD, was also the most controlled. Again, a change of solvent to acetone was examined using **3-O**/MTBD

and produced P-3,5-MCL at a much faster reaction rate. A decrease in time from 180 to 111 minutes was observed, which did not come at expense of reaction control ($M_n = 10,500$, $M_w/M_n = 1.13$). The ROP of 3,5-MCL with **3-O**/MTBD was compared with TBD in acetone. The TBD catalyzed reaction saw a great reduction in both rate and control with 93% conversion in 1,437 minutes and an M_w/M_n of 2.67.

Due to similar rates seen with TOSUO and 3,5-MCL, **3-O**/MTBD was the only catalyst pair employed for the ROP of 4-MCL (Table 7.1, entries 18 and 19). The reaction reached 91% conversion in 149 minutes, and remained well controlled ($M_n = 8800$, $M_w/M_n = 1.08$). Under the same reaction conditions in acetone- d_6 , the reaction reached 93% conversion in 113 minutes, with an M_n of 8,400 and an M_w/M_n of 1.13. The ROP conducted in acetone produced increased reaction rates. Unlike TOSUO and 3,5-MCL in acetone, 4-MCL decreased slightly in reaction control. Polymerization of 4-MCL has been done previously with both metal and lipase catalysts. The lipases were very inactive, with the fastest only seeing 35% conversion after ten days at 60°C in the monomer bulk.²³ An AlO*t*Pr complex was much more reactive, seeing 96% conversion in 6 hours at 90°C ($M_n = 11,900$, $M_w/M_n = 1.25$). The **3-O**/MTBD is much faster and retains control of the reaction, all under mild conditions.

6-MCL was subjected to all H-bonding catalysts with MTBD under normal catalyst loadings in but yielded no polymer after long periods of monitoring (>15hrs). A switch to the more active cocatalyst pair **3-O**/BEMP was also unsuccessful in producing ROP. A bulk polymerization at 110°C was attempted, but again did not yield polymer. However, an increased cocatalyst loading to 10 mol% for **3-O**/BEMP in acetone was successful with 96% conversion in 70 hours. This reaction was not well controlled with

an M_n of 1,000g/mol and an M_w/M_n of 2.22. The comparative run with TBD reached 78% conversion in 267 hours. TBD exhibited slightly better control with an M_n of 2,600 and an M_w/M_n of 1.47. Metal based catalysts (Mg, Sn, Al) have shown to open 6-MCL much faster and remain well controlled relative to either TBD or **3-O**/MTBD, with reaction times as low as 2 hrs and M_w/M_n as low as 1.04.⁹⁻¹³

Copolymerizations of TOSUO and CL were produced using **3-O**/MTBD in benzene. The polymerization reaction proceeded with both monomers opening at similar rates, indicating the formation of a random copolymer (Figure 7.13). Conversions of 99 and 95% were obtained in 30 minutes for TOSUO and CL respectively, yielding a polymer of M_n 7,300 and M_w/M_n of 1.09. The polymerization of 6-MCL with CL using **3-O**/BEMP in acetone created a random copolymer with little incorporation of 6-MCL. At 190 minutes, CL and 6-MCL reached 95 and 10% conversion respectively. However, at 90 minutes, CL was converted to 83% while 6-MCL was lagging at a mere 3%. This indicates a majority chain of CL with little incorporation of 6-MCL. After 4 more days of monitoring 6-MCL only reached 30% conversion. A copolymer between 3,5 and 6-MCL catalyzed by **3-O**/BEMP in acetone was attempted, but again 6-MCL only converted 24% in 24 hrs. 3,5-MCL reached 94% within the same period.

A series of copolymers of ϵ -CL with 25, 50 or 75% 3,5-MCL were prepared for thermal analysis. Polymerizations were run using **3-O**/MTBD in benzene, and all copolymerizations were completed within 90 minutes with high control ($M_w/M_n < 1.09$). Copolymerizations and thermal analysis of these copolymers have been done previously with AlO_iPr ; however, due to drastic differences in rate constants for CL (25°C) and 3,5-MCL (0°C) of 243 and 13.8 min^{-1} respectively, gradient block copolymers formed.¹⁵ 1H

NMR for the copolymerization of CL with 3,5-MCL using **3-O**/MTBD indicate simultaneous conversion and completion, producing a random copolymer (Figure 7.14).

Copolymers of 3,5-MCL and ϵ -CL along with their homopolymers were evaluated using both TGA and DSC. Polymers were dialyzed prior to analysis. It should be noted that the homopolymer of CL is solid, but the incorporation of 25% 3,5-MCL reduces crystallinity, and the polymer becomes a viscous liquid. TGA analysis of the series of polymers indicated a variety of decomposition onsets (Table 7.2). The individual polymers of 3,5-MCL and CL gave onsets of 326 and 296°C respectively. Copolymers of CL with 25, 50 or 75% 3,5-MCL decomposed at 345, 300 and 342°C respectively. The DSC of CL shows a T_g at 53°C, and the incorporation of 25% 3,5-MCL decreases the T_g to 26.4°C, indicative of a shift towards an amorphous structure (Figure 7.15 and 7.16). The copolymers of CL with 50 or 75% 3,5-MCL, along with 3,5-MCL alone did not indicate a T_g ; however, interpretation of the DSC is limited due to the noise present of copolymers of > 50% 3,5-MCL. This suggests highly amorphous character. These results are consistent with the previously described copolymers.¹⁵

Mechanistic Discussion: ROP conducted in benzene is suggested to go through an H-bonding mechanism, where an H-bond donor and base cocatalyst activate monomer and alcohol/chain end respectively. In acetone, the formation of an imidate through proton transfer from (thio)urea to base becomes the active catalyst (Figure 7.12). Although each monomer is a derivative of the 7-membered ring ϵ -CL, the observed rates for each functionalized monomer differ relative to its substitution. Under the same reaction conditions CL, 3,5-MCL, 4-MCL and TOSUO catalyzed by **3-O**/MTBD in benzene have rate constants of 0.1052, 0.0205, 0.0164 and 0.1151 min⁻¹ respectively.

Under the same reaction conditions, 6-MCL did not show any conversion over the period monitored (> 15 hrs).

The lack of difference in reaction rate between ϵ -CL and TOSUO indicates little steric or electronic inhibition from the ketal present in the γ -position. The comparable reaction rate of TOSUO with CL would suggest substitution with 2 carbons of separation between the substituent on either side of the reactive functional group (ester) does not affect the rate of reaction. However, perhaps counter intuitively, the switch from the bulkier 1,3-dioxalane to a methyl substantially decreases the reaction rate (k_{obs} TOSUO = 0.1151 min^{-1} , 4-MCL = 0.0164 min^{-1}). Also, the observed rate of 4-MCL is lower than that of 3,5-MCL (0.0205 min^{-1}), which contains methyl substitution closer to the ester (β and δ vs. γ).

To understand the variation in rate constants for functionalized CL monomers, a series of binding experiments were conducted. Equilibrium constants (K_{eq} , Scheme 7.1) between TOSUO, 3,5-MCL, 6-MCL and ϵ -CL to **1-S** were calculated to be 14.1, 14.8, 18.9 and 42 M^{-1} respectively, using ^1H NMR titration experiments.³⁵ The high K_{eq} value of CL indicates stronger binding for the un-substituted ring. However, the rate constant of ϵ -CL is similar to TOSUO. Also TOSUO, 3,5-MCL and 6-MCL have similar K_{eq} , yet 3,5-MCL and 6-MCL have rate constants much smaller than TOSUO. Previous reports have indicated similar inconsistencies between rate and binding values, albeit between H-bond donors and base cocatalysts, suggesting stronger binding does not indicate faster reaction rates.³⁶

The drastic reduction in activity of 6-MCL versus the other methyl substitutions led us to several experiments to identify the problem. First, binding

experiments between MTBD and both n-butanol and 2-butanol, which represent the propagating chain ends of both ϵ -CL and 6-MCL respectively. The alcohols and base were mixed 1:1 and compared to a reference using ^1H NMR. The hydroxyl protons of n-butanol and 2-butanol shifted up field 0.33 and 0.37 ppm respectively. A difference of 0.04 ppm does not suggest significantly greater binding to either a primary or secondary alcohol. Next, a simple ROP of 6-MCL experiment catalyzed by **3-O**/MTBD (1.67 mol% each) with 50% initiator was done to identify the source of slow kinetics. The reaction proceeded to 40% conversion after 2 hrs of reaction time. If monomer conversion reached 50% almost instantaneously, then initiation would not be a problem. These results suggest steric inhibition of the incoming nucleophile on the congested ester. It is likely that after initiation from the primary alcohol initiator, propagation from a secondary alcohol becomes even more difficult resulting in no reactivity under normal reaction conditions. Also, 6-MCL contains both regio-isomers 2 and 6-MCL. It is possible one might polymerize faster relative to the other. However, the lack of conversion indicates the H-bond/base systems are indiscriminate of either isomer.

CONCLUSION

H-bond donating catalysts have been successfully employed for the ROP of several aliphatic lactones derived from ϵ -CL. All monomers examined saw the fastest reaction rates with **3-O**/base. All monomers examined saw increased reaction rates and control versus either metal or enzymatic catalysts (except 6-MCL). 6-MCL proved to be difficult to open and needed high catalyst loadings and the strong phosphazene base cocatalyst BEMP. TOSUO, 3,5-MCL and 4-MCL were all reported to have fast reaction times to full conversion (< 3hrs) while still remaining well controlled (< 1.13). Polymerizations done in acetone were faster and more controlled than their benzene counterparts. Our mechanistic data suggests dissimilar kinetics due to the steric effects between the substituents and the incoming nucleophile. Position substitution on the lactone is not the sole determining factor of reaction rate.

Copolymerizations between CL and 3,5-MCL created random copolymers at fast rates with predictable M_n from $[M]_0/[I]$ and low M_w/M_n . The physical observations paired with the lack of a melting temperature within the range evaluated using DSC, suggested the creation of an amorphous polymer with the incorporation of 25% or greater of 3,5-MCL to CL. The TGA indicated similar decomposition temperatures regardless of the copolymer ratio. This is likely a result of the amorphous character of the copolymers.

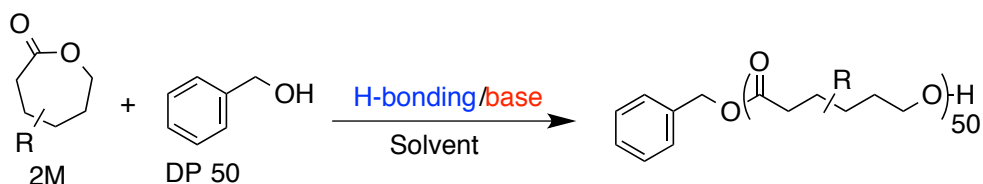
LIST OF REFERENCES

- (1) Kutikov, A. B.; Song, J. *ACS Biomater. Sci. Eng.* **2015**, *1* (7), 463–480.
- (2) Davenport Huyer, L.; Zhang, B.; Korolj, A.; Montgomery, M.; Drecun, S.; Conant, G.; Zhao, Y.; Reis, L.; Radisic, M. *ACS Biomater. Sci. Eng.* **2016**, *2* (5), 780–788.
- (3) Vert, M. *Biomacromolecules* **2005**, *6* (2), 538–546.
- (4) Van Horn, B. A.; Davis, L. L.; Nicolau, S. E.; Burry, E. E.; Bailey, V. O.; Guerra, F. D.; Alexis, F.; Whitehead, D. C. *J. Polym. Sci. Part A Polym. Chem.* **2017**, *55* (5), 787–793.
- (5) C. K. Ober; S. Z. D. Cheng; P. T. Hammond, et al. *Macromolecules* **2009**, *42* (2), 465–471.
- (6) Hedrick, J. L.; Magbitang, T.; Connor, E. F.; Glauser, T.; Volksen, W.; Hawker, C. J.; Lee, V. Y.; Miller, R. D. *Chem. - A Eur. J.* **2002**, *8* (15), 3308–3319.
- (7) Feig, V. R.; Tran, H.; Bao, Z. *ACS Cent. Sci.* **2018**, *4* (3), 337–348.
- (8) Ten Breteler, M.; Zhong, Z.; Dijkstra, P. J.; Palmans, A. R. A.; Peeters, J.; Feijen, J. *J. Polym. Sci. Part A Polym. Chem.* **2007**, *45*, 429–436.
- (9) Martello, M. T.; Hillmyer, M. A. *Macromolecules* **2011**, *44* (21), 8537–8545.
- (10) Petersen, S. R.; Wilson, J. A.; Becker, M. L. *Macromolecules* **2018**, *51*, 6202–6208.
- (11) Moughton, A. O.; Sagawa, T.; Gramlich, W. M.; Seo, M.; Lodge, T. P.; Hillmyer, M. A. *Polym. Chem.* **2013**, *4* (1), 166–173.
- (12) Wilson, J. A.; Hopkins, S. A.; Wright, P. M.; Dove, A. P. *Biomacromolecules* **2015**, *16* (10), 3191–3200.
- (13) Macdonald, J. P.; Sidera, M.; Fletcher, S. P.; Shaver, M. P. *Eur. Polym. J.* **2016**,

74, 287–295.

- (14) van As, B. A. C.; Chan, D. K.; Kivitt, P. J. J.; Palmans, A. R. A.; Meijer, E. W. *Tetrahedron Asymmetry* **2007**, *18* (6), 787–790.
- (15) Vion, J. M.; Jérôme, R.; Teyssié, P.; Aubin, M.; Prud'homme, R. E. *Macromolecules* **1986**, *19* (7), 1828–1838.
- (16) Bisht, K. S.; Henderson, L. A.; Gross, R. A.; Kaplan, D. L.; Swift, G. *Macromolecules* **1997**, *30* (9), 2705–2711.
- (17) Heise, A.; Duxbury, C. J.; Palmans, A. R. A. In *Handbook of Ring-Opening Polymerization*; Dubois, P., Coulembier, O., Raquez, J.-M., Eds.; Wiley-VCH: Federal Republic of Germany, 2009; pp 379–394.
- (18) Varma, I. K.; Albertsson, A. C.; Rajkhowa, R.; Srivastava, R. K. *Prog. Polym. Sci.* **2005**, *30* (10), 949–981.
- (19) Kobayashi, S.; Makino, A. *Chem. Rev.* **2009**, *109* (11), 5288–5353.
- (20) Albertsson, A. C.; Srivastava, R. K. *Adv. Drug Deliv. Rev.* **2008**, *60* (9), 1077–1093.
- (21) Kadokawa, J.; Kobayashi, S. *Curr. Opin. Chem. Biol.* **2010**, *14* (2), 145–153.
- (22) Peeters, J.; Palmans, A. R. A.; Veld, M.; Scheijen, F.; Heise, A.; Meijer, E. W. *Biomacromolecules* **2004**, *5* (5), 1862–1868.
- (23) Serata, N.; Yanagi, C.; Kunugi, S. *Biocatal. Biotransformation* **2002**, *20* (2), 111–116.
- (24) Tian, D.; Dubois, P.; Jérôme, R. *Macromolecules* **1997**, *30* (9), 2575–2581.
- (25) Tian, D.; Halleux, O.; Dubois, P.; Jerome, R.; Sobry, R.; Van den Bossche, G. *Macromolecules* **1998**, *31* (3), 924–927.

- (26) Tian, D.; Dubois, P.; Jérôme, R. *Macromolecules* **1997**, *30* (7), 1947–1954.
- (27) Tian, D.; Dubois, P.; Grandfils, C.; Jérôme, R. *Macromolecules* **1997**, *30* (3), 406–409.
- (28) Tian, D.; Dubois, P.; Jérôme, R. *Macromol. Symp.* **1998**, *130*, 217–227.
- (29) Fastnacht, K. V.; Spink, S. S.; Dharmaratne, N. U.; Pothupitiya, J. U.; Datta, P. P.; Kiesewetter, E. T.; Kiesewetter, M. K. *ACS Macro Lett.* **2016**, *5* (8), 982–986.
- (30) Nicolau, S. E.; Davis, L. L.; Duncan, C. C.; Olsen, T. R.; Alexis, F.; Whitehead, D. C.; Van Horn, B. A. *J. Polym. Sci. Part A Polym. Chem.* **2015**, *53* (20), 2421–2430.
- (31) Itoh, Y.; Yamanaka, M.; Mikami, K. *J. Org. Chem.* **2013**, *78* (1), 146–153.
- (32) Dharmaratne, N. U.; Pothupitiya, J. U.; Bannin, T. J.; Kazakov, O. I.; Kiesewetter, M. K. *ACS Macro Lett.* **2017**, *6* (4), 421–425.
- (33) Lin, B.; Waymouth, R. M. R. M. *J. Am. Chem. Soc.* **2017**, *139* (4), 1645–1652.
- (34) Zhang, X.; Jones, G. O.; Hedrick, J. L.; Waymouth, R. M. R. M. *Nat. Chem.* **2016**, *8* (11), 1047–1053.
- (35) Lohmeijer, B. G. G.; Pratt, R. C. R. C.; Leibfarth, F.; Logan, J. W.; Long, D. a.; Dove, A. P.; Nederberg, F.; Choi, J.; Wade, C. G.; Waymouth, R. M. R. M.; Hedrick, J. L. *Macromolecules* **2006**, *39* (25), 8574–8583.
- (36) Kazakov, O. I.; Kiesewetter, M. K. *Macromolecules* **2015**, *48* (17), 6121–6126.

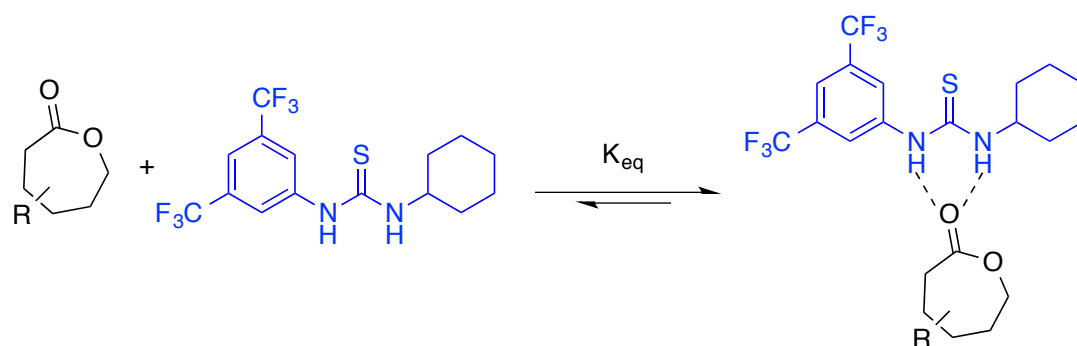


Entry	Monomer	Donor	Base	Solvent	Time (min)	Conv. ^a	M_n (g/mol) ^b	M_w/M_n ^b
1	CL	3-O	MTBD	C_6D_6	26	97	7,900	1.05
2	TOSUO	1-S	MTBD	C_6D_6	186 hrs	82	n/a	n/a
3	TOSUO	2-S	MTBD	C_6D_6	18 hrs	92	10,600	1.15
4	TOSUO	3-O	MTBD	C_6D_6	30	97	10,600	1.08
5 ^c	TOSUO	3-O	BEMP	C_6H_6	3	97	9,300	1.07
6	TOSUO	TCC	MTBD	C_6D_6	102	93	9,300	1.17
7	TOSUO	3-O	DBU	C_6D_6	224	93	9,400	1.06
8 ^c	TOSUO	3-O	MTBD	acetone	18	97	9,200	1.13
9	TOSUO	n/a	TBD	acetone- d_6	146	93	6,300	2.26
10	3,5-MCL	1-S	MTBD	C_6D_6	120 hrs	91	9,000	1.18
11	3,5-MCL	2-S	MTBD	C_6D_6	24 hrs	88	8,700	1.206
12	3,5-MCL	3-O	MTBD	C_6D_6	180	98	8,800	1.13
13	3,5-MCL	TCC	MTBD	C_6D_6	691	95	8,800	1.33
14	3,5-MCL	3-O	MTBD	acetone- d_6	111	97	10,500	1.13
15	3,5-MCL	n/a	TBD	acetone- d_6	24 hrs	93	6,200	2.67
16	6-MCL	3-O	MTBD	acetone- d_6	70 hrs	96	1,000	2.22
17	6-MCL	n/a	TBD	acetone- d_6	267 hrs	78	2,600	1.47
18	4-MCL	3-O	MTBD	C_6D_6	149	91	8,800	1.08
19	4-MCL	3-O	MTBD	acetone- d_6	113	93	8,400	1.13

Table 7.1. Cocatalysts for the ROP of functionalized ϵ -Caprolactone. Cocatalyst TCC, **1-S**, **2-S**, **3-O** at 5, 5, 2.5 and 1.67 mol% respectively, cocatalyst base mol% matched to H-bond donor. a. Monomer conversion was monitored via 1H NMR. b. M_n and M_w/M_n were determined by GPC (CH_2Cl_2) vs polystyrene standards. c. Aliquots were taken due to rapid turnover.

Polymer (% 3,5-MCL)	TGA Decomposition Onset (°C)
PCL	296
CL : 3,5-MCL (25)	342
CL : 3,5-MCL (50)	300
CL : 3,5-MCL (75)	345
3,5-MCL	326
4-MCL	323

Table 7.2. Decomposition onset temperatures for homo and copolymers. TGA conditions: Sample size ~7 mg were placed in aluminum pans. Start at 20°C, ramp to 100°C at 20°C, hold for 10 minutes, ramp 2°C/min to 425°C and hold for 5 minutes. N₂ gas flow rate of 10 mL/min. Polymer samples were purified by dialysis prior to use.



Scheme 7.1. Example equilibrium reaction illustrating binding between H-bond donor and monomer.

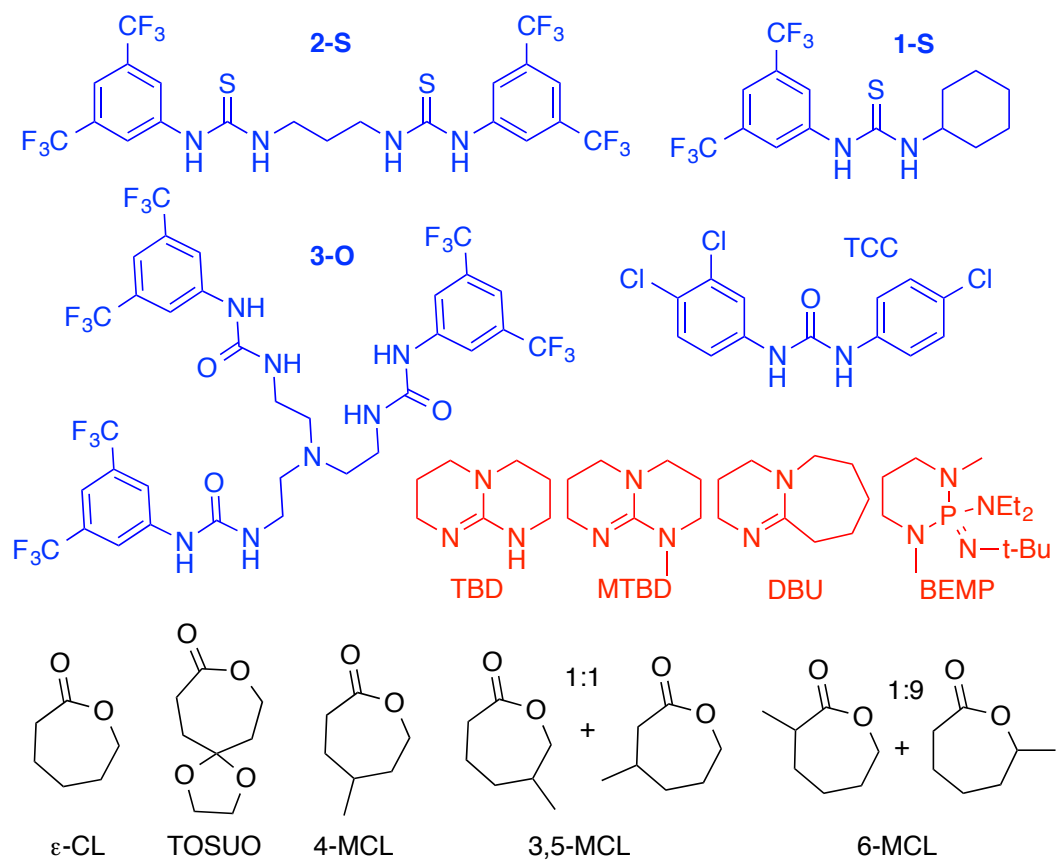


Figure 7.1. Dual catalyst species consisting of an H-bond donor and base cocatalyst used for the ROP of functionalized ϵ -Caprolactone.

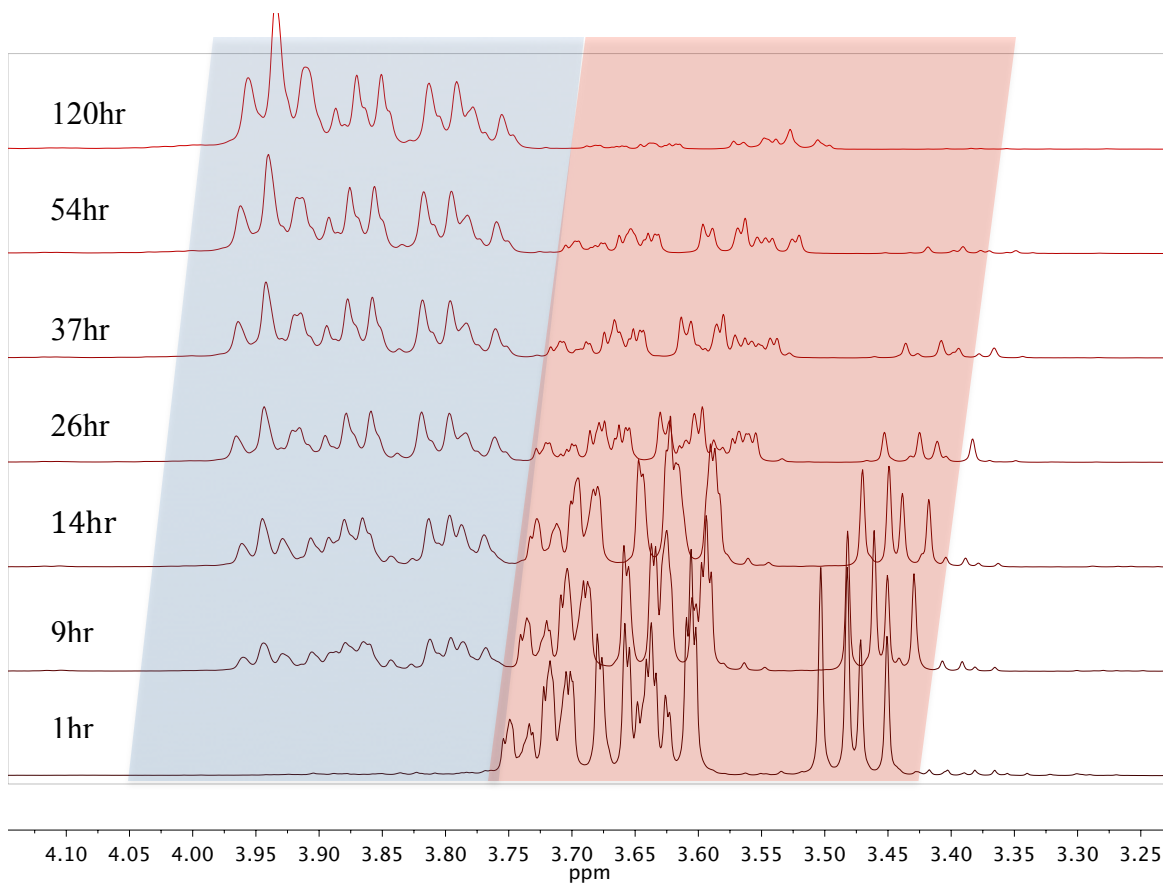


Figure 7.2. Example ¹H NMR (300 MHz, CDCl₃) of 3,5-MCL monomer (red), conversion to polymer (blue). 3,5-MCL (120 mg, 0.963 mmol), catalyzed by **1-S** (17.3 mg, 0.0468 mmol) and MTBD (7.15 mg, 0.0468 mmol) from benzyl alcohol (1.98 mg, 0.0187 mmol) in C₆D₆.

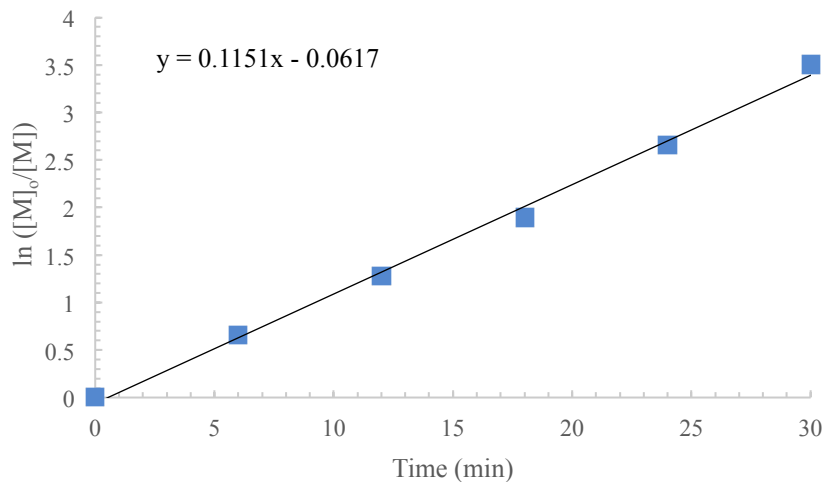


Figure 7.3. First order evolution of [TOSUO] versus time for the **3-O**/MTBD (0.0145 mmol each) cocatalyzed ROP of TOSUO (2M, 0.871 mmol) from benzyl alcohol (0.017 mmol) in C₆D₆.

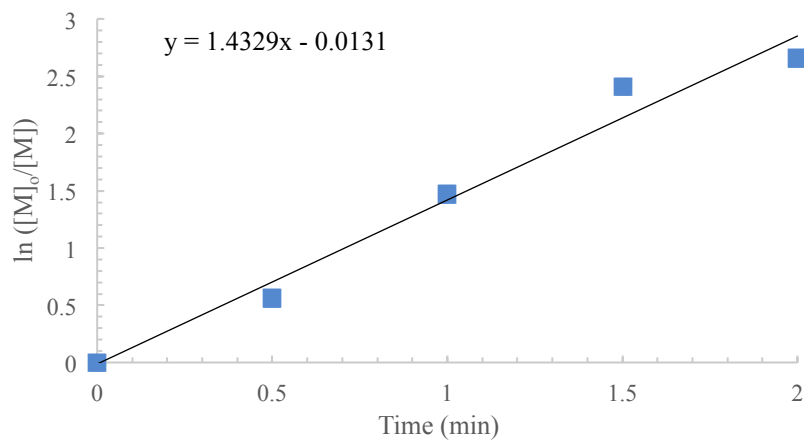


Figure 7.4. First order evolution of [TOSUO] versus time for the **3-O**/BEMP (0.0145 mmol each) cocatalyzed ROP of TOSUO (2M, 0.871 mmol) from benzyl alcohol (0.017 mmol) in C₆D₆.

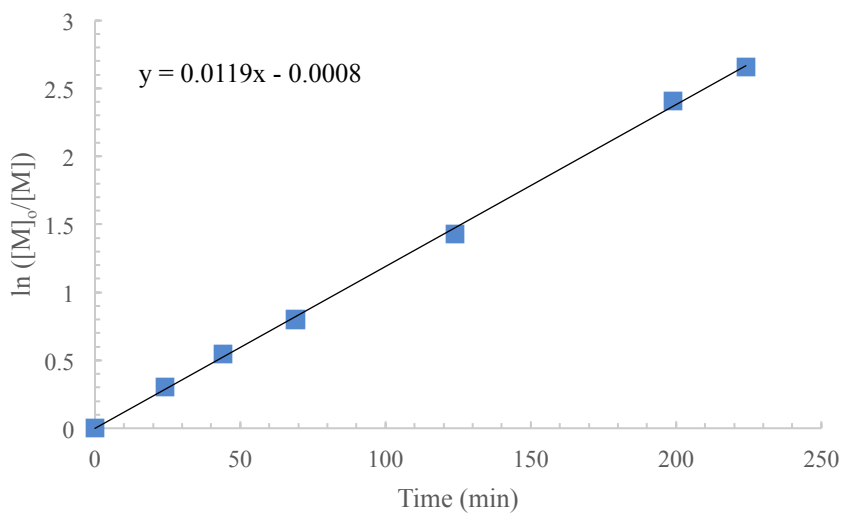


Figure 7.5. First order evolution of [TOSUO] versus time for the **3-O**/DBU (0.0145 mmol each) cocatalyzed ROP of TOSUO (2M, 0.871 mmol) from benzyl alcohol (0.017 mmol) in C₆D₆.

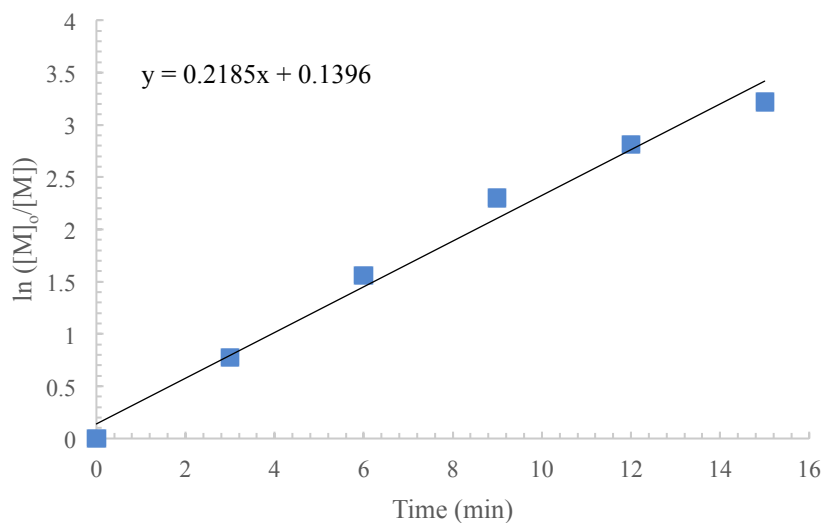


Figure 7.6. First order evolution of [TOSUO] versus time for the **3-O**/MTBD (0.0145 mmol each) cocatalyzed ROP of TOSUO (2M, 0.871 mmol) from benzyl alcohol (0.017 mmol) in acetone-*d*₆.

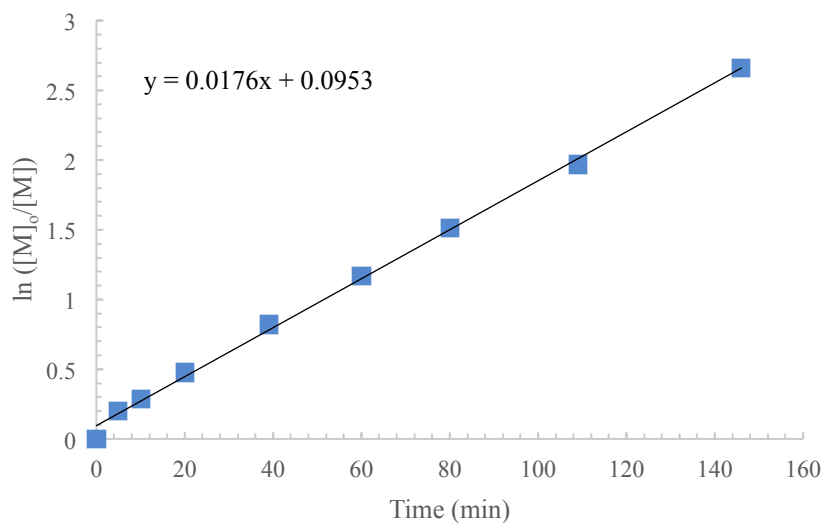


Figure 7.7. First order evolution of [TOSUO] versus time for the TBD (0.0436 mmol each) catalyzed ROP of TOSUO (2M, 0.871 mmol) from benzyl alcohol (0.017) mmol) in acetone- d_6 .

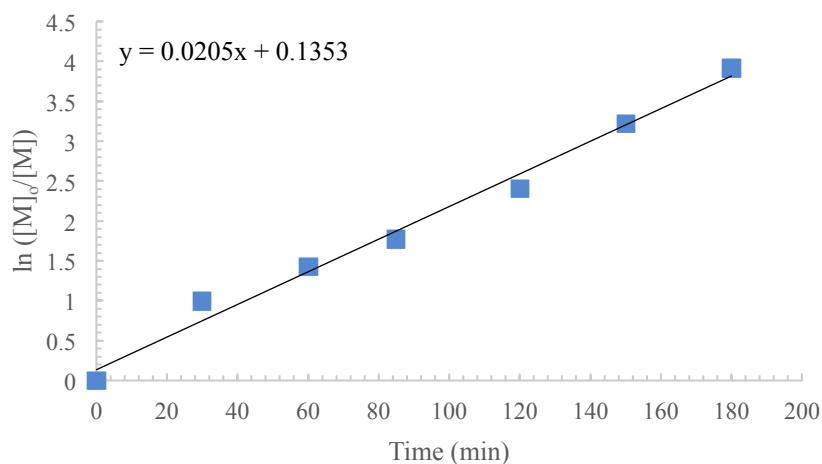


Figure 7.8. First order evolution of [3,5-MCL] versus time for the **3-O**/MTBD (0.0155 mmol each) cocatalyzed ROP of 3,5-MCL (2M, 0.936 mmol) from benzyl alcohol (0.019) mmol) in C_6D_6 .

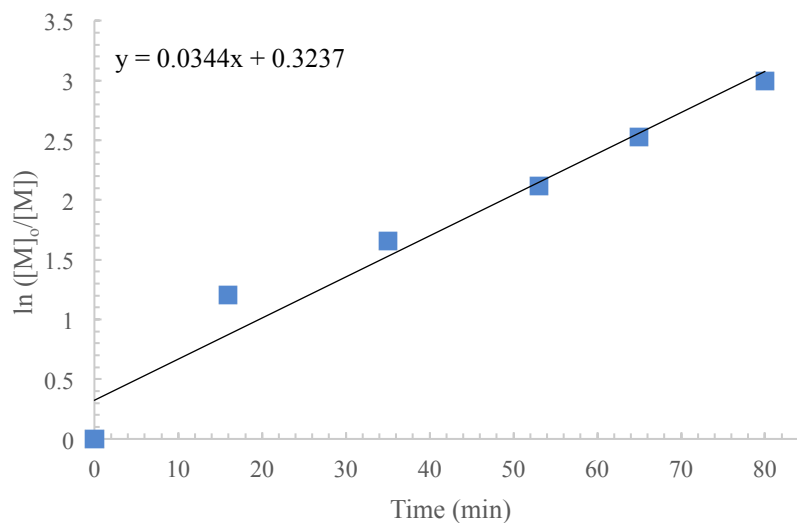


Figure 7.9. First order evolution of [3,5-MCL] versus time for the **3-O**/MTBD (0.0155 mmol each) cocatalyzed ROP of 3,5-MCL (2M, 0.936 mmol) from benzyl alcohol (0.019) mmol) in acetone- d_6 .

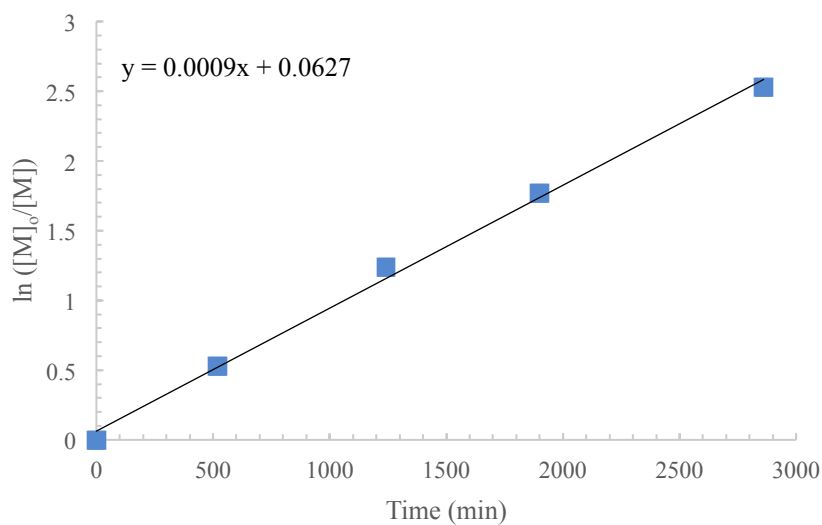


Figure 7.10. First order evolution of [6-MCL] versus time for the **3-O**/BEMP (0.0963 mmol each) cocatalyzed ROP of 6-MCL (2M, 0.936 mmol) from benzyl alcohol (0.019) mmol) in acetone- d_6 .

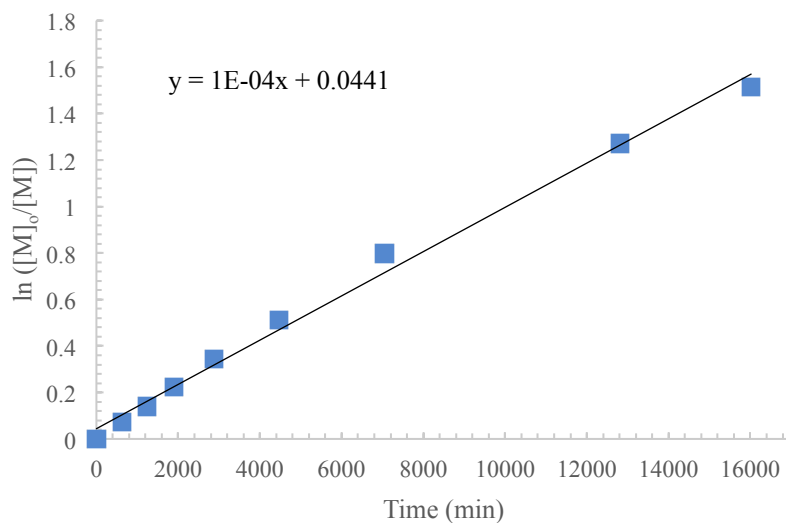


Figure 7.11. First order evolution of [6-MCL] versus time for the TBD (0.0468 mmol each) catalyzed ROP of [6-MCL] (2M, 0.936 mmol) from benzyl alcohol (0.019 mmol) in acetone- d_6 .

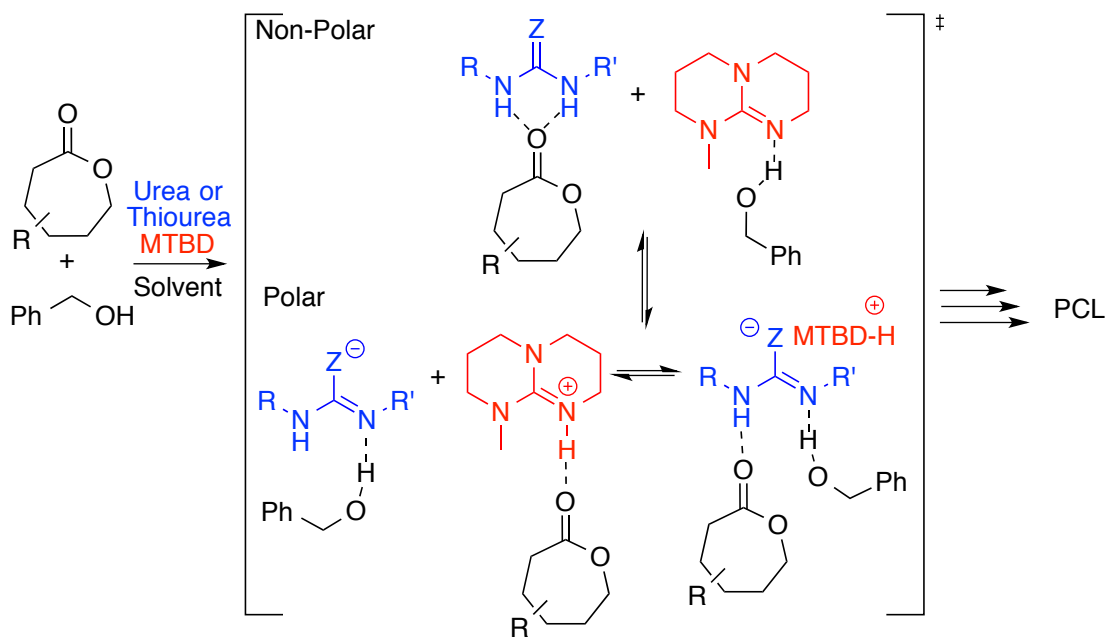


Figure 7.12. The H-bonding and imidate mediated ROP of cyclic esters.

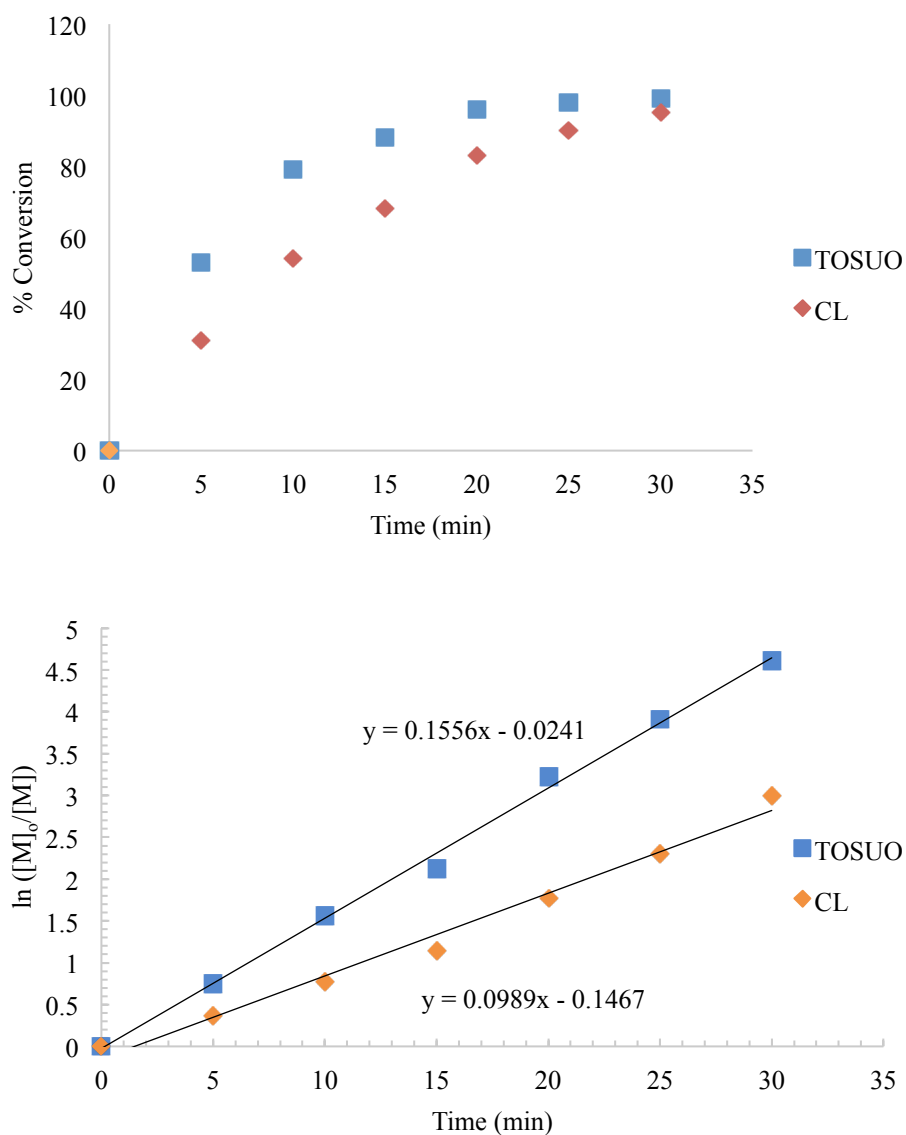


Figure 7.13. Conversion vs time (top) and first order evolution (bottom) of [TOSUO] and [CL] versus time for the **3-O**/MTBD (0.0166 mmol each) cocatalyzed ROP of TOSUO and CL (2M, 0.50 mmol each) from benzyl alcohol (0.02 mmol) in C_6D_6 .

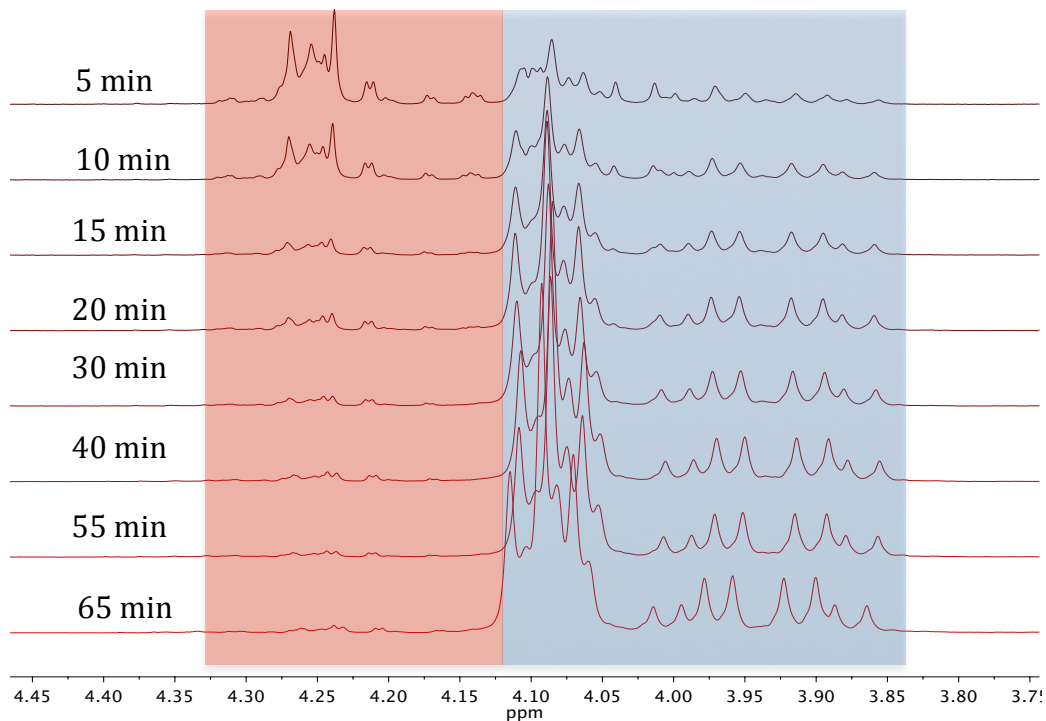


Figure 7.14. ¹H NMR (300 MHz, CDCl₃). Random copolymerization of CL and 3,5-MCL. CL (57.0 mg, 0.50 mmol) and 3,5-MCL (64.0 mg, 0.50 mmol) cocatalyzed by **3-O**/MTBD (15.1 / 2.45 mg, 0.0166 mmol each) from benzyl alcohol (2.18 mg, 0.02 mmol) in C₆H₆. Distinguishing between the individual monomer resonances is not possible. However, integration over the ranges for both monomer (red) and polymer (blue) resonances separately allows for the calculation of conversions.

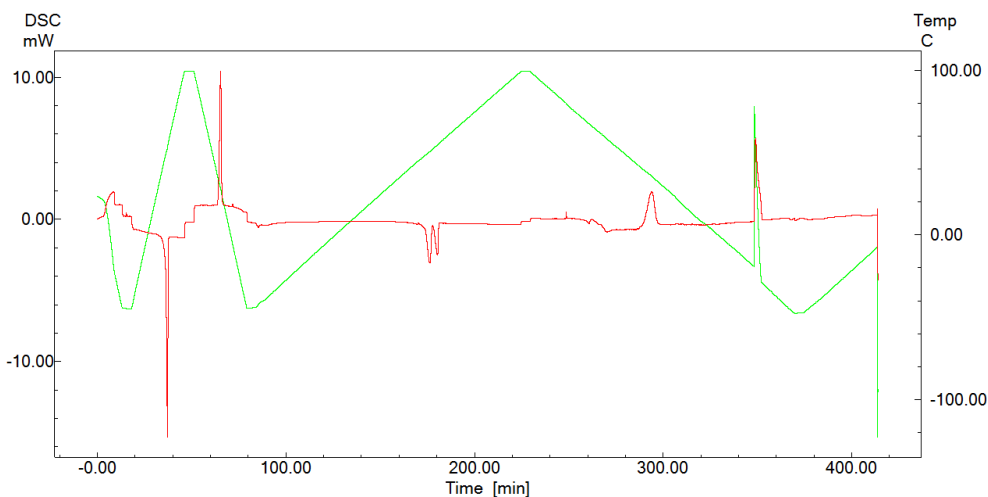


Figure 7.15. DSC of PCL ($M_n = 8,800$; $M_w/M_n = 1.08$). Temp program: start 25°C, cool to -40°C at 5°C/min, heat to 100°C at 5°C/min, cool to -40 at 5°C/min, heat to 100°C at 1°C/min, cool to -40°C at 1°C/min. Green line shows temperature program and the red line is the thermal response.

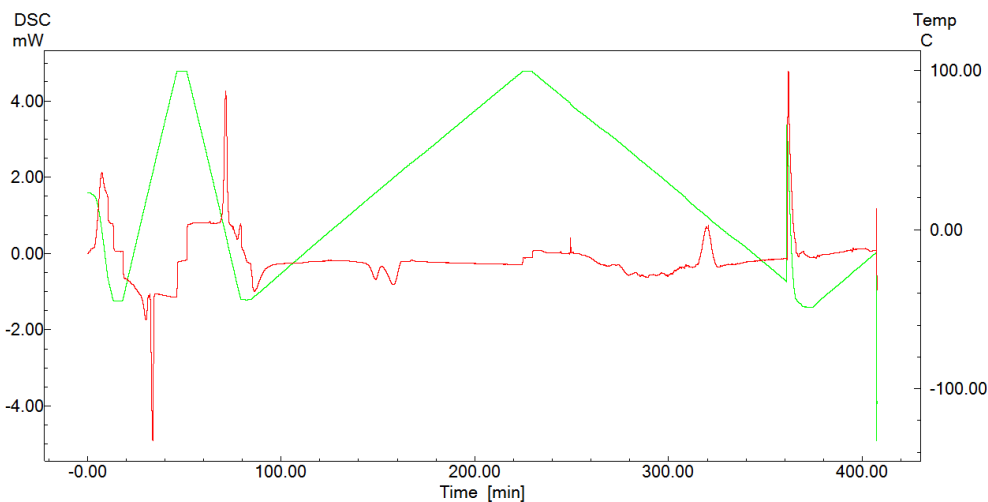


Figure 7.16. DSC of copolymer of 3,5-MCL and CL (25% 3,5-MCL) ($M_n = 10,500$; $M_w/M_n = 1.07$). Temp program: start 25°C, cool to -40°C at 5°C/min, heat to 100°C at 5°C/min, cool to -40 at 5°C/min, heat to 100°C at 1°C/min, cool to -40°C at 1°C/min. Green line shows temperature program and the red line is the thermal response.